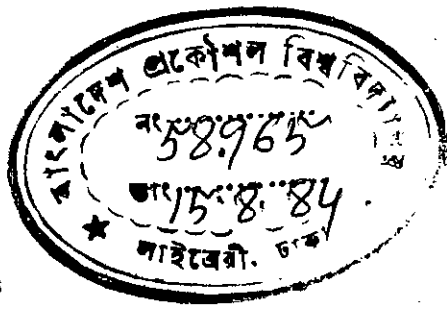


OPTIMUM DESIGN OF INTZE TANKS AND SUPPORTING
TOWERS USING FINITE ELEMENTS



A Thesis
by
MD. NURUL HUDA

Submitted to the Department of Civil Engineering,
Bangladesh University of Engineering & Technology, Dhaka,
in partial fulfilment of the requirements for the degree
of
MASTER OF SCIENCE IN CIVIL ENGINEERING



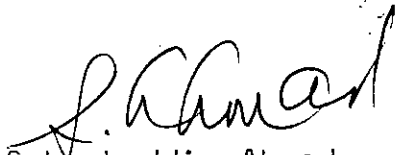
July, 1984

OPTIMUM DESIGN OF INTZE TANKS AND SUPPORTING
TOWERS USING FINITE ELEMENTS

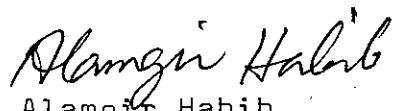
A Thesis
by
MD. NURUL HUDA

Approved as to style and content by:


Chairman of
the Committee


Dr. Sohrabuddin Ahmad
Professor,
Dept. of Civil Engineering, BUET.

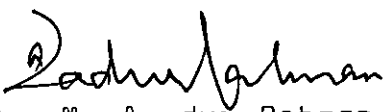
Member


Dr. Alamgir Habib
Professor and Head,
Dept. of Civil Engineering, BUET.


Member


Dr. Md. Alee Murtuza
Professor,
Dept. of Civil Engineering, BUET.

Member


Dr. M. Azadir Rahman
Associate Professor,
Dept. of Civil Engineering, BUET.

Member
External


Dr. M. Wahhajuddin
Associate Professor,
Dept. of Mechanical Engineering,
BUET.

July, 1984.



To my parents



CERTIFICATE OF RESEARCH

Certified that the work presented in this thesis is the result of the investigation carried out by the candidate under the supervision of Dr. Sohrabuddin Ahmad at the Department of Civil Engineering, BUET, Dhaka.



Md. Nurul Huda
Candidate

S. Ahmad
Supervisor

DECLARATION

I do hereby declare that neither this thesis nor any part thereof has been submitted or is being concurrently submitted in candidature for any degree at any other university.

Md. Nuzul Huda

Candidate

ACKNOWLEDGEMENT

The author expresses his indebtedness to Dr. Sohrabuddin Ahmad, Professor of Civil Engineering, under whose supervision this research was carried out. Without his constant guidance and invaluable suggestions at every stage, this work could not possibly have materialised.

Profound gratitude is expressed to Dr. M. Azadur Rahman and Dr. Sohrabuddin Ahmad for providing the author with the valuable Finite Element programs that were the main tools in the research.

Grateful thanks are offered to Dr. M. Shamim-uz-Zaman, for supplying the author the design calculations of an Intze tank being constructed in Bangladesh.

The author expresses his deep gratitude to Dr. Alamgir Habib, Professor and Head, Dept. of Civil Engineering for his continuous advice and encouragement in course of the research.

Sincerest thanks are expressed to Professor J.R.Choudhury, Dean of the Faculty of Civil Engineering, who inspired the author with his valuable suggestions and frequent enquiries regarding the progress of the work, in addition to the timely help he extended to the author in connection with the use of computer facilities in his capacity as Director of the Computer Center, BUET.

Heartiest thanks are expressed to Mr. M.A. Malek for typing the thesis with extreme care and to Mr. Shahiduddin for drawing the figures.

ABSTRACT

Intze tanks are widely used in this country and other parts of the world as large - capacity overhead water-reservoirs. From the point of view of structural efficiency and economy the Intze tanks are found to be preferable to other types of water-towers for a wide spectrum of capacities. Unfortunately, however, the design of such an important structure have not yet been rationalised. In fact, the conventional methods of analysis of the Intze tanks and the supporting towers are so approximate and in some cases so contradictory that designers often get lost as to which method to follow. It was mainly to resolve this problem that the author has been prompted to undertake this research work. As part of the investigation, therefore, the author studied the conventional methods, discussed them in some detail to bring out their differences, illustrating each method with a case study. The same problems were then analysed by available Finite Element programs using axi-symmetric shell elements for the tank and space frame elements for the tower. The results of Finite Element analysis clearly indicate that the conventional methods often lead to uneconomical designs in some respects and what may, in fact, be fatal to unsafe designs in other respects. Thus it is advisable that more sophisticated methods, such as Finite Element analysis should be adopted whenever possible, for the analysis of Intze tanks to make the design safe and economical.

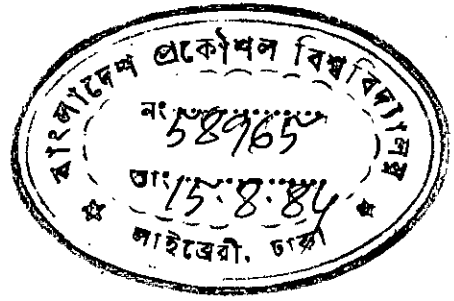
CONTENTS

	Page
Certificate of Research	iv
Declaration	v
Acknowledgement	vi
Abstract	vii
Contents	viii
Chapter 1 INTRODUCTION	
1.1 Introduction	1
1.2 The Intze Tank	2
1.3 Analysis of Intze Tanks: Shortcomings of Conventional Methods	4
1.4 Objective of the Research	6
1.5 Scope of the Research	6
Chapter 2 CONVENTIONAL ANALYSIS OF INTZE TANKS	
2.1 Introduction	8
2.2 General Discussion of Conventional Methods of Analysis	9
2.3 The Assumptions, Outline and Discussion of the Membrane Analysis	13
2.3.1 The Top Dome	13
2.3.2 The Top Ring Beam	16
2.3.3 The Cylindrical Wall	16
2.3.4 The Bottom Ring Beam	18
2.3.5 The Conical Wall	19
2.3.6 The Bottom Dome	21
2.3.7 The Bottom Circular Beam	22
2.4 Case Studies	25
2.4.1 Case Study 1	25
2.4.2 Case Study 2	30
2.4.3 Case Study 3	33
2.4.4 Case Study 4	36
Chapter 3 CONVENTIONAL ANALYSIS OF THE SUPPORTING TOWER	
3.1 Introduction	39
3.2 Conventional Methods of Analysis	40

	Page
3.2.1 Jai Krishna and Jain's Method	40
3.2.2 Sushil Kumar's Method	44
3.2.3 Gray and Manning's Method	46
3.3 Case Studies	55
3.3.1 Case Study 1	55
3.3.2 Case Study 2	59
3.3.3 Case Study 3	62
3.3.4 Case Study 4	65
 Chapter 4 FINITE ELEMENT ANALYSIS OF THE INTZE TANK	
4.1 Introduction	70
4.2 The Finite Element Program	71
4.3 Finite Element Idealisation of the Intze Tank	74
4.4 Graphical Representation of Results	83
4.5 Comparison of Design Stresses Obtained by Conventional Methods and Finite Element Method at Critical Sections	128
4.6 Economy of Designs Based on Finite Element Analysis	133
4.7 Analysis for Wind Load	134
4.8 Discussion	146
4.8.1 The Top Dome	146
4.8.2 The Top Ring Beam	147
4.8.3 The Cylindrical Wall	147
4.8.4 The Bottom Ring Beam	150
4.8.5 The Conical Wall	151
4.8.6 The Bottom Circular Beam	152
4.8.7 The Bottom Dome	152
 Chapter 5 SPACE FRAME ANALYSIS OF THE TOWER	
5.1 Introduction	154
5.2 The Space-Frame Program	154
5.3 Case Studies	156
5.3.1 Case Study 1	156
5.3.2 Case Study 2	167
5.3.3 Case Study 3	170
5.3.4 Case Study 4	173

	Page
5.4 Study of Parameters	179
5.4.1 Distribution of Horizontal Force to the Columns at Their Top	180
5.4.2 Orientation of Column Section	180
5.4.3 Batter of Columns	189
5.4.4 Stiffness of Braces	192
Chapter 6 CONCLUSION	
6.1 Findings from the Investigation	196
6.1.1 Introduction	196
6.1.2 Conclusions from the Analysis of the Tank	197
6.1.3 Conclusions from the Analysis of the Tower	198
6.2 Scope for Further Research	199
References	201

CHAPTER 1
INTRODUCTION



1.1 Introduction

Reinforced concrete overhead water tanks are widely used as service reservoirs in water supply systems and for other purposes requiring elevated sources of water. The size of the tank depends on the quantity of water to be stored, the height on the pressure-head required and the shape generally on economy. Of course other considerations such as architectural demand or specific conditions of a site often influence the geometry.

Water towers are usually constructed in a wide variety of shapes. Gray and Manning⁽¹⁾ illustrate several types that include cylindrical, conical, polygonal or rectangular tanks having one or more compartments and supported on columns, shafts or a combination of both. The shape of the tank largely affects the structural design and the cost of construction. Therefore, to find out the most economical design, the structural engineer may have to try a few alternatives within the latitudes of his choice. The final selection would then be based on the estimated total cost comprising the costs of concrete, reinforcement and shuttering for the different alternatives.

The geometrical shape leading to the least surface-area of the tank seldom gives the most economical solution, but is always a useful guideline towards the best shape. Also the design of the tank generally affects the cost of the

supporting tower and the foundations. Thus the cheapest tank may not necessarily result in the cheapest complete tower. However, as regards the preliminary choice of shape, an important observation is that different shapes prove to be economical in different capacity ranges. For capacities below 50,000 gallons, cylindrical or rectangular tanks with flat bottom and roof seem to be economical, while the Intze tanks are found to be preferable for a wide spectrum of capacities ranging from 50,000 to about 400,000 gallons. For capacities above that, prestressed concrete tanks or flat floor rectangular tanks might be more economical.

1.2 The Intze Tank

As stated earlier, the Intze tanks are found to be more economical than other types of overhead water tanks for a wide range of capacities. An Intze tank essentially consists of several axi-symmetric shells namely, the top dome, the cylindrical wall, the conical dome and the bottom spherical dome with three ring beams inserted at the junctions as shown in Fig. 1.1. The economy of the Intze tanks results mainly from their efficient container shape as explained below.

It is found that, for storing large volume of water, an elevated circular tank with a flat floor-slab supported on a mesh of beams develops large bending moments in the floor-slab calling for its excessive thickness, since tension cracks must be avoided to ensure a leak-proof design.

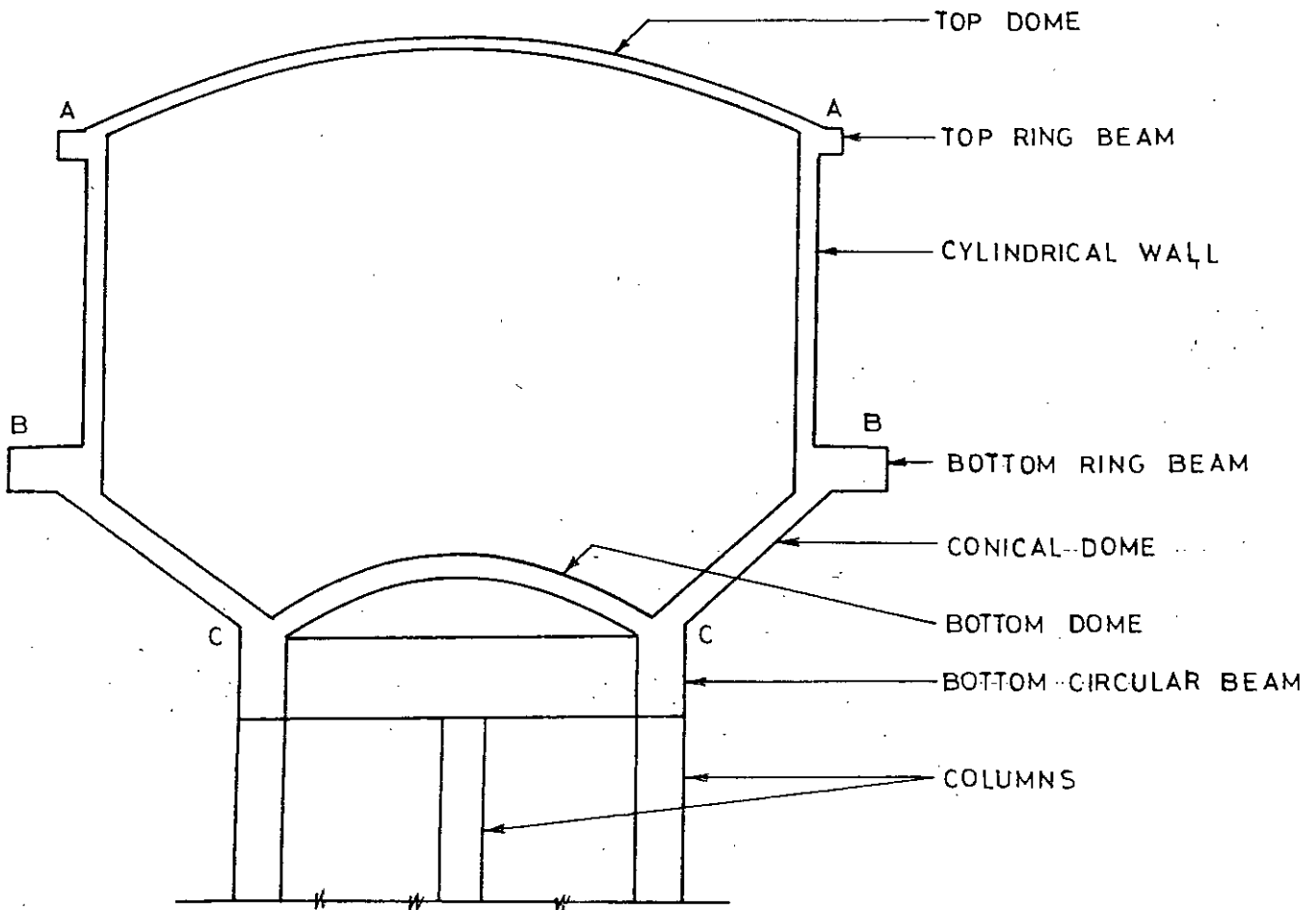


Fig. 1.1 Vertical section of an Intze tank showing various parts.

Moreover, the complex arrangement of beams and columns raises the cost of shuttering and makes the analysis difficult and less accurate. Domes prove to be an economical alternative in such circumstances. Domes with small rise generally adopted in such cases develop only compressive stresses in them (except perhaps near the edges) and are thus water-tight. The required thickness of the dome is small and this results in considerable saving of material. A similar saving may also be attained by making the bottom conical. The Intze tank, which employs a combination of cone and dome as its floor, is a further improvement over the simple domed-floor. It is supposed to be so proportioned that the inward and outward horizontal thrusts on the bottom circular beam at the junction of the cone and the bottom dome approximately balance each other. In short the interaction between various shells and ring beams of the Intze tank helps produce an efficient structural shape that consumes less material and thus makes the tank economical.

1.3 Analysis of Intze Tanks: Shortcomings of Conventional Methods

The fundamental philosophy of the Intze tank geometry is to take advantage of the membrane action of shells to resist a major proportion of the loads while keeping the bending action within the threshold of insignificance. However, it is difficult to assess the actual emancipation of the two actions mainly due to the uncertain boundary conditions imposed by the ring beams and the inevitable

complications that ensue when compatibility is considered. As such, for trouble-shooting, most of the conventional methods entirely neglect the bending stresses and suggest a pure membrane analysis for the shells while the ring beams are designed for hoop forces arising out of membrane action of shells. The implications are quite significant. The ring beams and component shells are in general over-designed for membrane forces while inadequate provision of flexural reinforcements in the shells especially at their edges tend to considerably reduce the factor of safety. And the only conventional method⁽²⁾ that suggests a secondary analysis for the effects of continuity is rarely followed by designers due to the complicated and laborious procedure of the secondary analysis. Moreover, even if this endeavour is undertaken, there still remains considerable controversy over the accuracy of the analysis. While deferring further and more elaborate discussion of the conventional methods to Chapter 2, it may be stated here that the conventional analysis of Intze tanks results in underdesign somewhere and overdesign elsewhere.

As regards the analysis and design of the supporting tower by conventional methods similar observations hold good as would be apparent from the discussion presented in Chapter 3. In short it can be said that although the Intze tanks are more economical compared to other types of overhead water tanks their economy might be further improved if the design is based on a more rational analysis.

1.4 Objective of the Research

With the advent of modern digital computers, Finite Element method^{(3),(4)} using numerical integration has emerged as a powerful tool doing real wonders in solving highly complex problems in structural engineering and other fields with enormous speed and accuracy. Realising the importance of optimum design of Intze tanks in the context of their vast use in Bangladesh, and considering the availability of a well-documented Finite Element program⁽⁵⁾ for analysis of axi-symmetric shell structures, a space-frame program⁽⁶⁾ for analysis of towers and lastly a powerful IBM-370 computer in BUET, the author was inspired to undertake this research project aimed at optimum design of Intze tanks and supporting towers. The objective of the research is to rationalise the design of Intze tanks and supporting towers using Finite Element analysis, thereby making the structure safe and economical.

1.5 Scope of the Research

As part of the literature survey, this work first presents a brief outline of the conventional methods of analysis of Intze tanks and supporting towers, illustrated with appropriate case studies, in the two chapters that follow. Next, the results of Finite Element analysis of the illustrated cases mentioned above are presented in graphical form and then tabulated along with the results of conventional analysis for direct comparison. The tank dimensions are

then suitably modified and then the new stress conditions are also plotted for the modified sections to check the adequacy of the modified dimensions.

The towers illustrating conventional analysis are similarly analysed by Finite Element method presenting the results in graphical and tabular forms. Some parameters affecting the design of the tower are also studied.

Finally, on the basis of the results of this investigation, conclusions are drawn and suggestions for improvement in the design of the structural components of the tank and the tower are made.

CHAPTER 2

CONVENTIONAL ANALYSIS OF INTZE TANKS

2.1 Introduction

This chapter presents a brief but comprehensive discussion of the conventional methods of analysis of Intze tanks critically discussing the simplifying assumptions made for the sake of analysis and identifying the points of uncertainties and weaknesses. Three methods are considered for discussion here which are due to the following authors:

1. Jai Krishna and Jain⁽²⁾
2. Gray and Manning⁽¹⁾
3. Sushil Kumar⁽⁷⁾

The above methods are more or less complete by themselves. It may be possible to conceive of some other methods for analysis of the component shells of the Intze tank using shell theories⁽⁸⁾. However in any method, whatsoever, the primary concern would be proper assumption of boundary conditions for the shells. This poses a difficult problem, since the amount of restraint exerted by the stiffening ring-beams at the junctions is anything but apparent. As a consequence, it becomes necessary, for the sake of analysis, to make certain simplifying assumptions that may not be fully justified. Needless to say, the three methods, referred to above, are not free from such limitations. These methods are, however, very popular among practitioners in this and neighbouring countries. As such these three methods

have been selected as representative conventional methods for discussion. Three case studies, one for each method, are included at the end of this chapter. An additional design example (case study 4) is also included here in order to reflect the important features of standard design practice.

2.2 General Discussion of Conventional Methods of Analysis

The conventional methods of analysis of Intze tanks, mentioned in the preceding article, can be divided into two categories.

Methods belonging to the first category suggest a simple membrane analysis for the component shells, the ring beams being supposed to carry the thrusts arising out of membrane actions of the shells (Fig. 2.1). These methods do not consider the question of compatibility of displacements and rotations at the junctions and neglect the bending stresses in the shells. The methods due to Sushil Kumar and Gray and Manning fall under this category. In fact, these two methods are almost identical save and except one point of discord regarding the meridional moment at the bottom of the conical dome. While Sushil Kumar assumes that there is no such moment at all (as would happen if pure membrane action prevailed), Gray and Manning recommend designing the bottom of the conical dome for a restraint moment that would occur at the bottom of a circular tank having the same diameter as the bottom of the cone and the same height as the

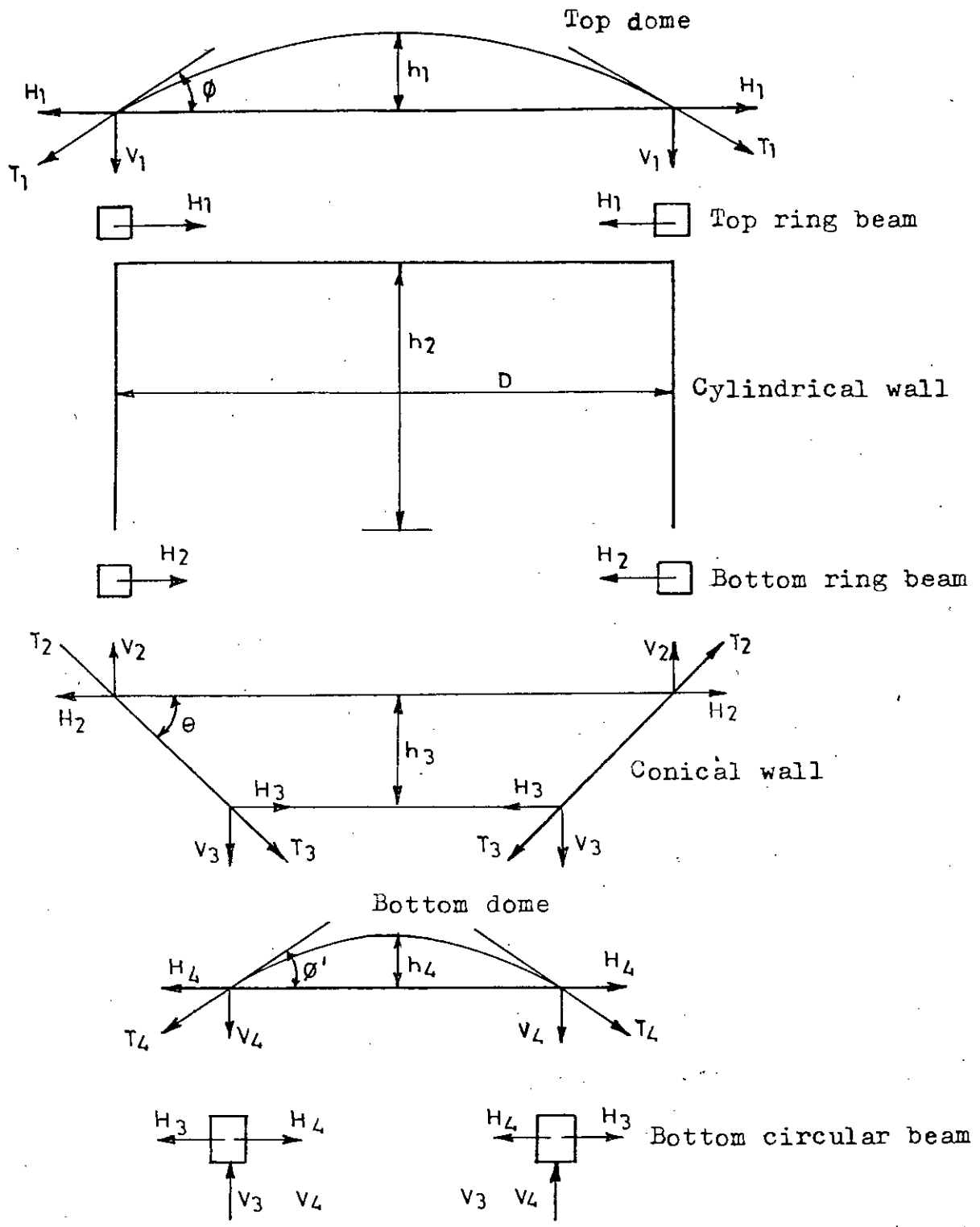
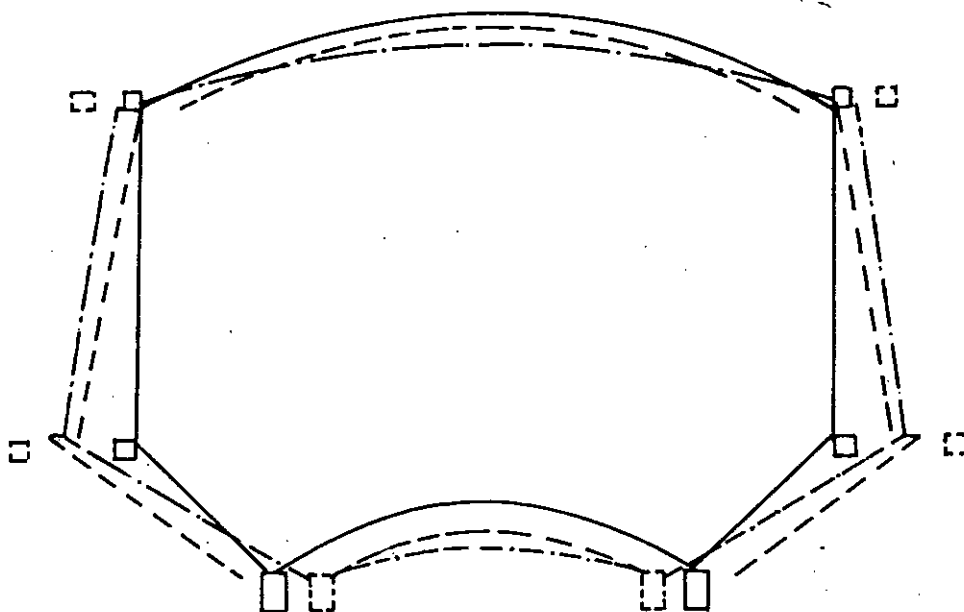


Fig. 2.1 Meridional membrane forces and their components.

depth of water at this level. In all other respects the two methods are indistinguishable and although in some cases the expressions for stress resultants may appear to be different, simple trigonometrical transformations coupled with consideration of geometry quickly reveal their equivalence.

The other method due to Jai Krishna and Jain belong to the second category where the analysis of the Intze tank is performed in two phases. In Phase-I a membrane analysis is carried out using the same principle and formulae as the methods of category 1, while, in Phase-II, a secondary analysis is proposed for the effects of continuity. In the first phase actual loads are applied on the shells and boundary conditions are applied in such a manner as to ensure that only membrane stresses occur. These stresses are obviously not the actual values and also the boundary displacements and rotations of the shells and ring beams are incompatible (Fig. 2.2). Thus, the continuity analysis is essential for establishing compatibility and to obtain correct stresses. For this step it is essential to define the relationships between edge loadings and resulting edge displacements. These relationships are obtained on the basis of shell bending theories. Compatibility equations are then set up for each junction with the actual edge forces as unknowns. These are linear simultaneous equations and can be solved to obtain the secondary stresses. For each junction two equations are needed, one ensuring compatibility of



- (Firm line) = Undeformed shape
 (Dotted line) = Independent shell deformation
 — - - (Chain line) = Deformation maintaining continuity.

Fig. 2.2 Continuity of displacements.

rotation and the other that of horizontal displacement. Continuity of vertical displacement is automatically satisfied. Solving these equations for unknown edge forces, the final stress resultants such as the meridional moment, hoop tension and meridional thrust can be calculated. It is assumed that the shells are thin and the effect of one junction does not propagate to the next junction. It is also implied that the shells meet each other at the centres of ring-beams. Unfortunately, however, the above analysis

for effects of continuity involves tedious calculations and hence, more or less, impracticable. Of course a computer program developed for the purpose by Jain and Singh⁽⁹⁾ might prove to be useful.

It is reported that this method was further generalised by Arya⁽¹⁰⁾ for the case of axi-symmetric shell structures by providing non-dimensional values in the form of numerical tables for stiffnesses and membrane displacements. These values are claimed to be more accurate and applicable to shells with uniformly varying thickness as well⁽¹¹⁾.

2.3 The Assumptions, Outline and Discussion of the Membrane Analysis

A brief outline of the membrane analysis is now presented, to give a clear concept of the procedure usually adopted for the analysis of different parts of the Intze tank. The assumptions made implicitly or explicitly to arrive at the working formulae are stated and discussed to bring out the drawbacks of analysing the Intze tanks by the membrane theory of shells.

2.3.1 The Top Dome

Assumptions: (i) The dome is hinged along its edge A, the joint between the top dome and the top ring beam, but is restrained from radial displacement (Fig. 2.3).

(ii) Membrane action prevails in the shell and edge disturbances are negligible.

Referring to Fig. 2.3, let

R = Radius of top dome

h = Rise of the dome

D = Diameter of the tank

ϕ = Semi-central angle of the dome

w = Total vertical load per unit area of dome surface.

The expressions for meridional membrane force N_ϕ and circumferential membrane force N_θ (hoop-force) in the dome, as used by the three methods, are presented below in tabular form.

<u>Method</u>	<u>N_ϕ</u>	<u>N_θ</u>
a) Sushil Kumar	$wR(1-\cos \phi)/\sin^2 \phi$	$wR\left(\frac{\cos^2 \phi + \cos \phi - 1}{1 + \cos \phi}\right)$
b) Gray & Manning	$2\pi Rhw/(\pi D \sin \phi)$	$wR\left(\cos \phi - \frac{1}{1 + \cos \phi}\right)$
c) Jai and Jain	$3wR/(1+\cos \phi)$	not determined in membrane analysis.

Discussion: The assumption that there is no rotational restraint at joint A is incorrect. In fact, the Phase-II analysis of Jai and Jain shows the existence of some sagging moment at joint A tending to close the angle A (tension on outer face). The other assumption that radial displacement is completely restrained is also far from being true. Thus, although the above expressions give compressive values of N_θ for $\phi < 51^\circ 48'$, continuity analysis shows development of hoop tension near the edge of the dome. The actual stress

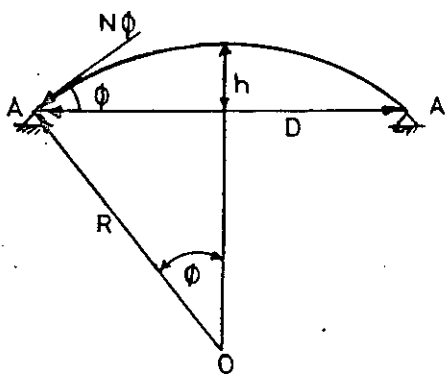


Fig. 2.3

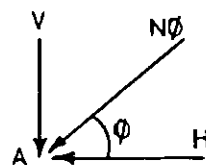


Fig. 2.4

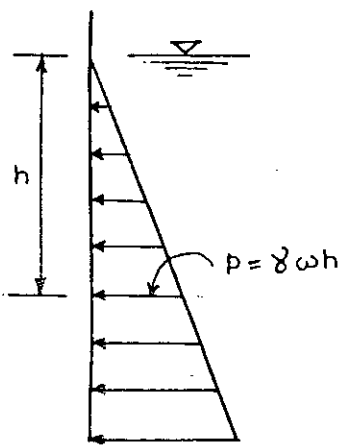
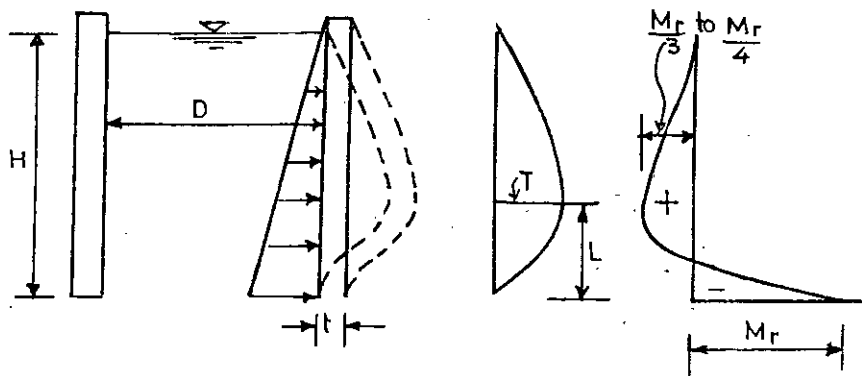


Fig. 2.5



(a) Cylindrical tank with monolithic floor slab.

(b) Hoop force (c) BM diagram.

Fig. 2.6

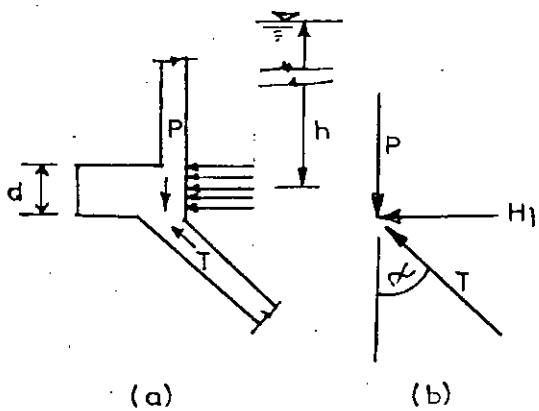


Fig. 2.7

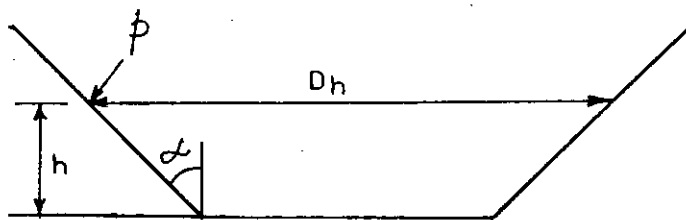


Fig. 2.8

condition can be revealed only by a rational analysis such as that of the Finite Element method.

2.3.2 The Top Ring Beam

Assumption: This ring beam at joint A resists the horizontal component of the meridional thrust N_ϕ from the top dome (Fig. 2.4) through hoop action.

Thus hoop force, $T_\theta = HD/2$; where $H = N_\phi \cos \phi$, and $D =$ diameter of the tank.

Discussion: The above formula clearly gives an over-estimate of the hoop force in the top ring beam, because in deriving this formula compatibility of displacements at joint A has not been considered. It is easy to guess that in the process of maintaining continuity of radial displacement in the vicinity of joint A, the adjacent portions of the top dome and the cylindrical wall would carry a considerable share of the hoop force.

2.3.3 The Cylindrical Wall

Assumptions: (i) The cylindrical wall is flexible in the vertical direction and has no restraint against rotation or radial displacement at either end. This assumption dismisses the possibility of development of any restraint moment at the base of the wall.

(ii) The fluid pressure against the wall is resisted entirely by hoop action, the hoop tension at any level of the wall being directly proportional to the hydrostatic pressure at that level.

Thus, at any depth h below water level (Fig. 2.5) the hoop tension is given by $N_{\theta} = \gamma_w hD/2$, where D = diameter of tank, and γ_w = density of water.

Discussion: The assumption that there is no restraint moment at the base of the cylindrical wall needs careful investigation. Because due to lack of confidence in the above assumption, designers tend to provide enormous flexural reinforcements for meridional moment calculated by using Reissner's⁽¹²⁾ theory for a cylindrical wall cantilevering off the base, while providing for hoop tension given by the above formula. It may be noted here that Reissner's theory, as simplified by Carpenter, gives the following formulae for calculating the bending moment at the base and the position and magnitude of maximum circumferential tension (Fig. 2.6), where the coefficients F and K are given in Table 2.1.

$$\text{Restraint moment, } M_r = F\gamma_w H^3,$$

$$\text{Maximum hoop tension, } N_{\theta} = \gamma_w HD(1-K)/2, \text{ and}$$

$$\text{Position of maximum hoop tension, } L = KH.$$

Obviously, the maximum hoop tension and maximum restraint moment cannot occur simultaneously at the base. In fact, if the bottom were free, the hoop tension would be maximum with zero restraint moment; on the other hand, if the bottom were fixed, the hoop tension would be zero with maximum restraint moment. In case of a partial restraint, as appears to be the situation at the base of the cylindrical wall in an Intze tank, the magnitude of the hoop tension and restraint moment would depend on the actual effective restraint and could be

TABLE 2.1

Coeffs. H/t → H/D ↓	F				K			
	10	20	30	40	10	20	30	40
0.2	0.046	0.028	0.022	0.015	0.65	0.50	0.45	0.40
0.3	0.032	0.019	0.014	0.010	0.55	0.43	0.38	0.33
0.4	0.024	0.014	0.010	0.007	0.50	0.39	0.35	0.30
0.5	0.020	0.012	0.009	0.006	0.45	0.37	0.32	0.27
1.0	0.012	0.006	0.005	0.003	0.37	0.28	0.24	0.21
2.0	0.006	0.004	0.003	0.002	0.30	0.22	0.19	0.16
4.0	0.004	0.002	0.001	0.001	0.27	0.20	0.17	0.14

determined only by a rational analysis such as that of the Finite Element method.

2.3.4 The Bottom Ring Beam

Assumption: This ring beam introduced at the junction of the cylindrical wall and the conical dome is supposed to carry, in addition to the fluid pressure against its inner surface, the entire horizontal component of the inclined meridional thrust of the conical dome below it through hoop action.

Let T be the meridional thrust of the conical dome, the vertical component of which must balance the total vertical load (say P) at the top of the cone, then its horizontal component would be (Fig. 2.7), $H_1 = T \sin \alpha = P \tan \alpha$. Also fluid pressure, $H_2 = \gamma_w h d$. Thus hoop tension in the

ring beam comes out to be $T_{\theta} = HD/2$, where $H = H_1 + H_2$.

Discussion: Apparently the above procedure for calculating the hoop force in the bottom ring beam seems to be reasonable, but since the exact stress distribution in the region is not known, it would be wise to wait until a Finite Element analysis reveals the mystery, before making a final comment.

2.3.5 The Conical Wall

Assumptions: (i) There is no meridional moment in the wall.

(ii) The radial movement is unrestrained at either end of the wall.

The above assumptions lead to the following formula for hoop tension N_{θ} at any height h above the base of the cone (Fig. 2.8).

$$N_{\theta} = (p/\cos \alpha + q \tan \alpha) \times D_h/2, \text{ where,}$$

D_h = diameter of the cone at any height h ,

p = hydrostatic pressure at this level,

q = self-wt. of the wall per unit area, and

α = inclination of the wall with the vertical.

Discussion: The above formula gives a fairly constant value of the hoop tension N_{θ} throughout the cone. This is quite illogical, since it violates the very noble design concept of the truncated-cone-and-dome floor according to which the inward and outward thrusts on the circular beam at the junction of the cone and the bottom dome should approximately balance. This would mean negligible radial

movement of the circular beam and therefore considering continuity of radial displacement, the hoop tension in the cone should gradually vanish towards its lower end. It may be noted here that the Phase-II analysis of Jai and Jain actually shows such a trend.

The other assumption that bending moment in the cone is zero is also untrue. Because the weights of water over the cone and the bottom dome tend to cause rotations of the circular beam, in opposite directions so that the resultant rotation of the beam would be negligible in a well-proportioned design. As such the circular beam may be looked upon as a fixed support giving rise to restraint moments on its either side i.e. both in the cone and in the bottom dome. Perhaps induced by such a consideration, Gray and Manning recommend designing the bottom of the conical dome for a restraint moment that would occur at the base of a circular tank having the same diameter as the bottom of the cone and the same height as the depth of water at this level and that can be calculated using Reissner's theory (Art. 2.3.3). In fact, out of the three methods mentioned in Art. 2.1, only Sushil Kumar completely neglects this restraint moment, while both Gray & Manning as well as Jai & Jain take into account this moment calculated in some way or other. Jai and Jain obtains the restraint moment from Phase-II analysis for effects of continuity.

2.3.6 The Bottom Dome

Assumptions: (i) The dome is hinged along the periphery.
(ii) Pure membrane state of stress exists throughout.

Accordingly the meridional thrust N_ϕ at the edge is given by a formula similar to the one for top dome,

$$N_\phi = W / (2\pi R \sin^2 \phi), \text{ where,}$$

W = total wt. of the dome and the water resting directly above it.

R = Radius of the dome

ϕ = Semi-central angle (Fig. 2.9).

Discussion: The assumption (i) neglects the meridional restraint moment. But, as discussed in Art. 2.3.5, some undetermined restraint moment exists at the edge. Phase-II analysis of Jai and Jain gives similar indication.

The membrane analysis does not worry about the hoop stress which is assumed to be compressive. But any outward movement of the circular beam may cause tensile hoop stresses near the edge of the bottom dome under certain conditions. These points would be studied through Finite Element analysis for a rational design.

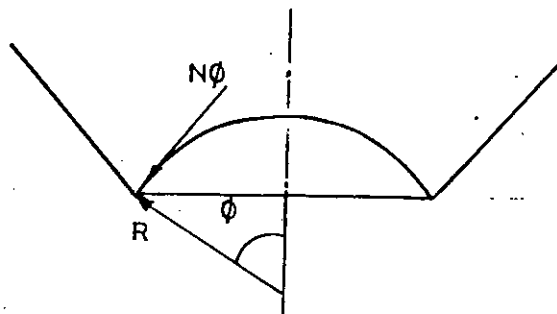


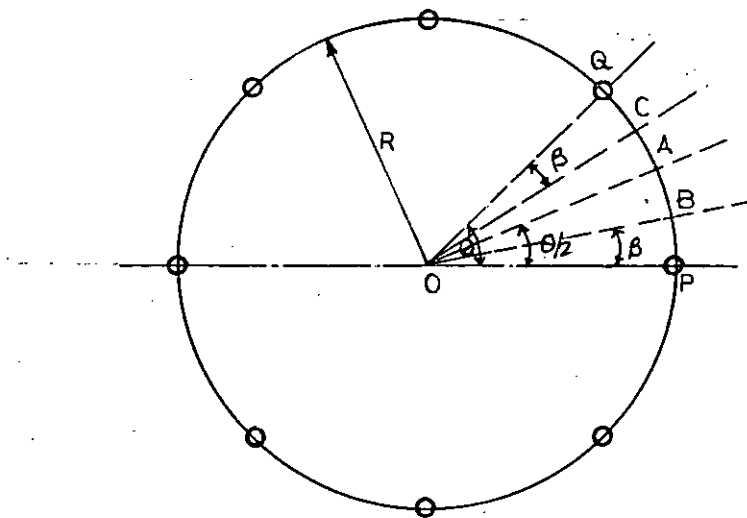
Fig. 2.9

2.3.7 The Bottom Circular Beam

The function, behaviour, and design concept of the bottom circular beam are totally different from those of other parts of the Intze tank. Instead of having a continuous support, as is the case with all other components, the circular beam is supported only at some discrete points along its periphery by a number of equidistant columns (Fig. 2.10).

As such the circular beam is subjected to bending moments, torsion and shear for which the following assumptions hold good:

- (i) Shear force and torsion are zero at mid-span
- (ii) Torsion is zero at supports.



- A = Section of max. +ve BM
- B, C = Section of max. twisting mom.
- P, Q = Section of max. -ve BM and max. shear force.

Fig. 2.10

Hence the beam is to be designed for

- (i) Maximum shear force and -ve bending moments at supports.
- (ii) Maximum +ve bending moments at mid-span and
- (iii) Maximum torsion at points of contraflexure.

The formulae for finding out the maximum bending and twisting moments are given below (7).

- (i) Max. -ve BM at support = $K_1 WR^2\theta$ (θ in radians)
- (ii) Max. +ve BM at midspan = $K_2 WR^2\theta$ "
- (iii) Max. twisting moment at
point of contraflexure = $K_3 WR^2\theta$ "

The values of the coefficients K_1 , K_2 , K_3 and the angles θ and β for different numbers of columns are given in Table 2.2, and

R = Radius of the circle of columns

W = Vertical load (including self-wt.) per unit length of the periphery.

TABLE 2.2

No. of cols n	θ	K_1	K_2	K_3	β
4	90°	0.137	0.070	0.021	$19\frac{1}{4}^\circ$
5	72°	0.108	0.054	0.014	$15\frac{1}{4}^\circ$
6	60°	0.089	0.045	0.009	$12\frac{3}{4}^\circ$
7	$51\frac{3}{7}^\circ$	0.077	0.037	0.007	$10\frac{3}{4}^\circ$
8	45°	0.066	0.030	0.005	$9\frac{1}{2}^\circ$
9	40°	0.060	0.027	0.004	$8\frac{1}{2}^\circ$
10	36°	0.054	0.023	0.003	$7\frac{1}{2}^\circ$

Discussion: The Finite Element analysis of the Intze tank using axi-symmetric thick-shell elements is unable to provide any information regarding the moments etc. in the circular beam. This is a limitation of the use of axi-symmetric shell elements. Hence no discussion of the above analysis would be possible in the light of Finite Element analysis. However, the circular beam will be considered as straight bracings in the space frame analysis that may throw some light on the magnitudes of the moments and shears in the beam.

2.4 Case Studies

Some four examples of Intze tank design are presented here to illustrate the usual design practices so far discussed. The same tanks are analysed by the Finite Element method using axi-symmetric shell elements program, the results being presented in tabular/graphical form in Chapter 4.

Details of calculation of the design examples are available in the corresponding references and hence omitted here. Only the final stresses and reinforcements are quoted here. The physical dimensions of the tanks are shown in figures.

2.4.1 Case Study 1

This design example is taken from "Plain and Reinforced Concrete" by Jai Krishna & Jain⁽²⁾. Figures here are in FPS units but the source data were in SI units. The analysis is carried out in two phases:

- i) Phase-I, the Membrane Analysis
- ii) Phase-II, the Continuity Analysis.

Whenever the results of Phase-I and Phase-II happen to be different, the values given in Phase-II are to be considered for design.

Design Criteria:

Capacity of the tank = 118,200 gallons (Imperial)

Live load + coating on top dome = 23.20 psf

f'_c (M ₂₀₀ grade concrete)	= 2,850 psi
f_c (in compression)	= 1,000 psi
f_{cs} (in shear)	= 100 psi
f_{ct} (direct tension)	= 170 psi
f_{ct} (flexural tension)	= 240 psi
f_s (in contact with water)	= 14,000 psi
f_s (in other places)	= 18,000 psi
Maxm. nominal reinf.	= 0.3%

Tank dimensions are shown in Fig. 2.11.

Notations:

N_ϕ	= Meridional membrane force (lbs/ft) (Tension = +ve)
N_θ	= Circumferential membrane force " (" ")
T_θ	= Total hoopforce (lbs) in ring beams(" ")
M_ϕ	= Meridional moment (lb-ft/ft) (Tension outside = +ve)
A_s	= Steel area in ² /ft or in ²

The stress-resultants are shown in Table 2.3.

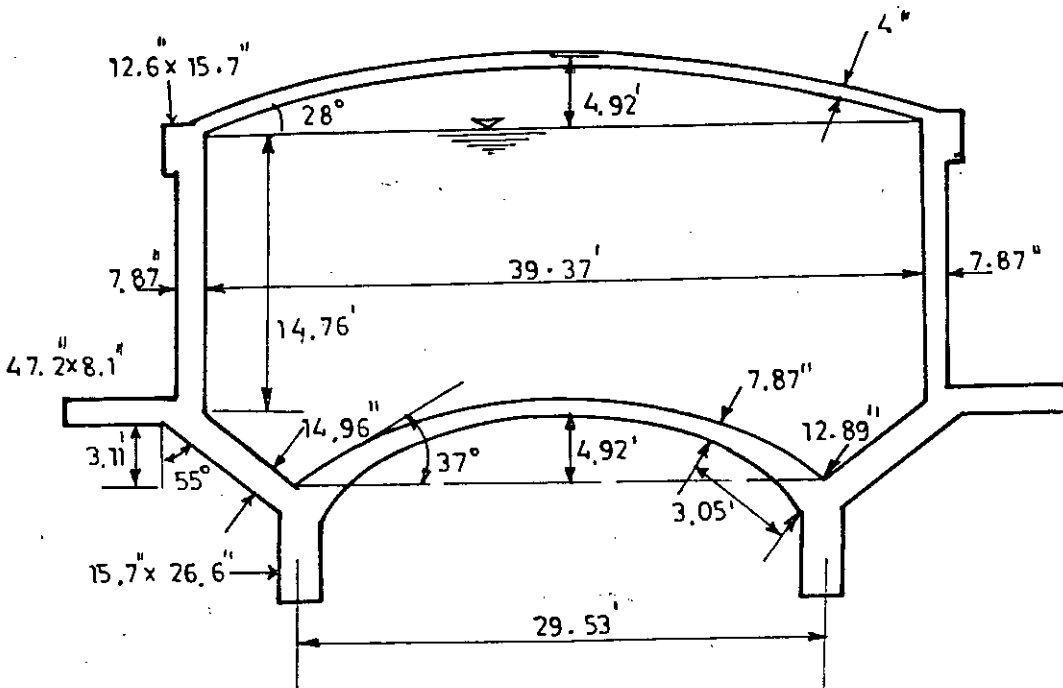


Fig. 2.11 Physical dimensions of the tank of case study 1.

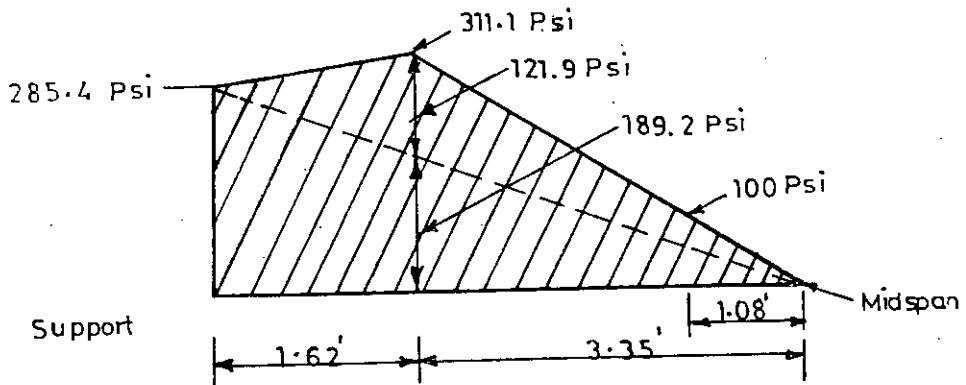


Fig. 2.12 Shear stress diagram for bottom circular beam.

TABLE 2.3

Stress-resultants of Case Study-1

Location		Stress-resultant	Phase-I	Phase-II	A_s
Top dome edge		N_ϕ	-1,592.5	-1,592.5	0.144
		N_θ	---	2,204.0	0.157
		M_ϕ	0.0	330.7	0.10
Top ring beam		T_θ	27,645.5	9,259.3	0.66
Cylindrical wall	Top	N_θ	0.0	4,414.8	0.32
		M_ϕ	0.0	327.4	0.264
	Bottom	N_θ	18,142.9	18,008.5	1.29
		M_ϕ	0.0	1,510.1	0.264
Bottom ring beam		T_θ	86,555.5	85,232.7	6.09
Conical wall	Top	N_θ	36,809.9	34,202.7	2.44
		M_ϕ	0.0	1,366.8	0.50
	Bottom	N_ϕ	-18,680.5	-18,680.5	0.50
		N_θ	33,127.6	-151.9	2.44
		M_ϕ	0.0	7,458.1	0.50
Bottom dome edge		N_ϕ	-13,370.0	-13,372.0	0.264
		N_θ	---	-80.0	0.264
		M_ϕ	0.0	-5,216.0	0.45

Bottom circular beam:

Vertical load on the beam, $w = 19,138.1$ lbs/ft.

-ve $M = 216,271.6$ ft-lbs (at support)

+ve $M = 108,135.8$ " (at mid-span)

Twisting moment, $M_t = 16,384.2$ ft-lbs (at $\beta = 9\frac{1}{2}^\circ$)

Shear force, $SF = 95,017.6$ lbs (at column face)

-ve $A_s = 5.58$ in² at top & bottom each

+ve $A_s = 5.58$ in² at bottom

Stirrups are calculated on the basis of the shear stress diagram shown in Fig. 2.12.

Total quantity of material required is estimated as follows:

Reinforcement volume, $V_s = 55.45$ cft

= 12.13 tons

Concrete volume, $V_c = 3,669.4$ cft

= 245.7 tons

N.B. 20% may be added, for contingency, to the material volumes estimated.

2.4.2 Case Study 2

This design example illustrates the method suggested by Gray & Manning⁽¹⁾.

Design Criteria:

Capacity of the tank = 250,000 gallons (40,000 cft)

LL + coating on top dome = 40 psf

Weight of lantern = 3,000 lbs

f'_c = 3,000 psi

f_c (direct compression) = 1,000 psi

f_{ct} (direct tension) = 200 psi

f_s (not in contact with water) = 18,000 psi

f_s (in contact with water) = 14,000 psi

n (modular ratio) = 10

Nominal reinforcement = 0.3%

Notations used are as in case study-1

The physical dimensions are calculated on the basis of Fig. 2.13, and shown in Fig. 2.14. The stress-resultants are shown in Table 2.4.

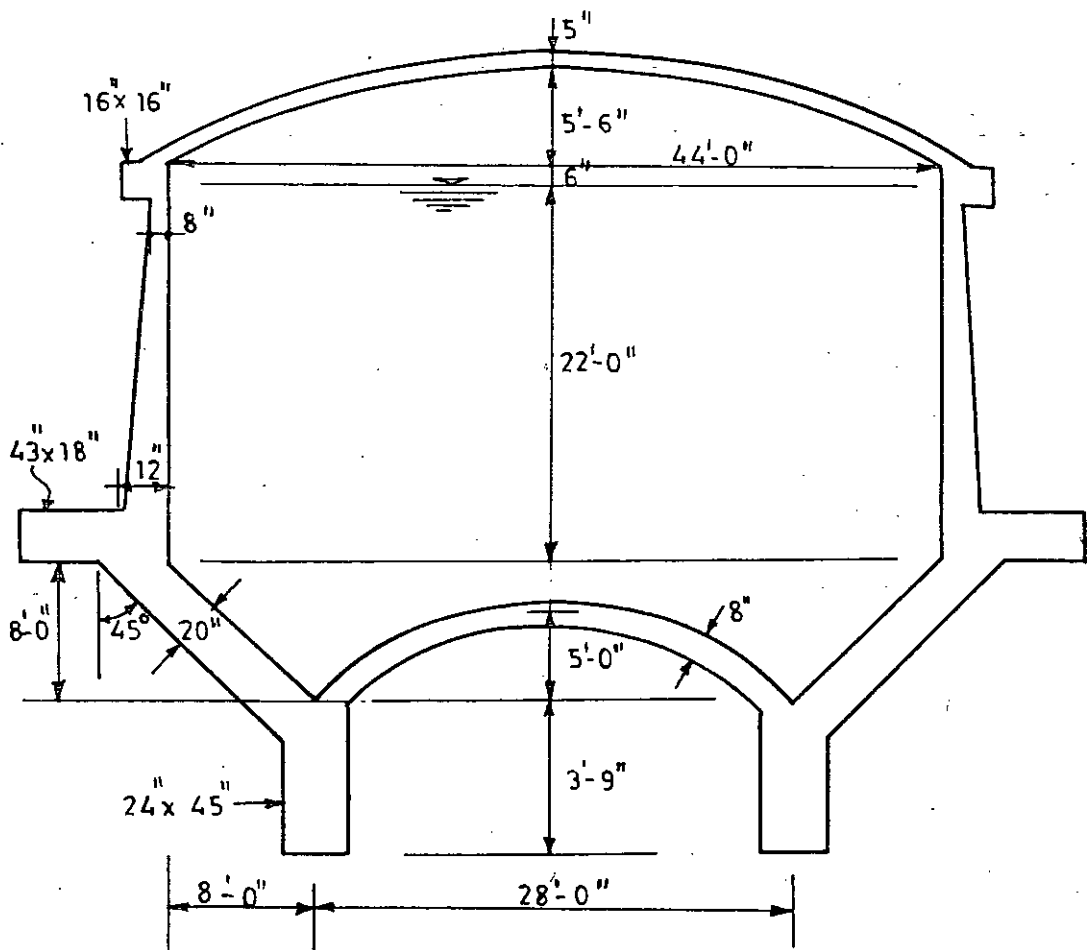
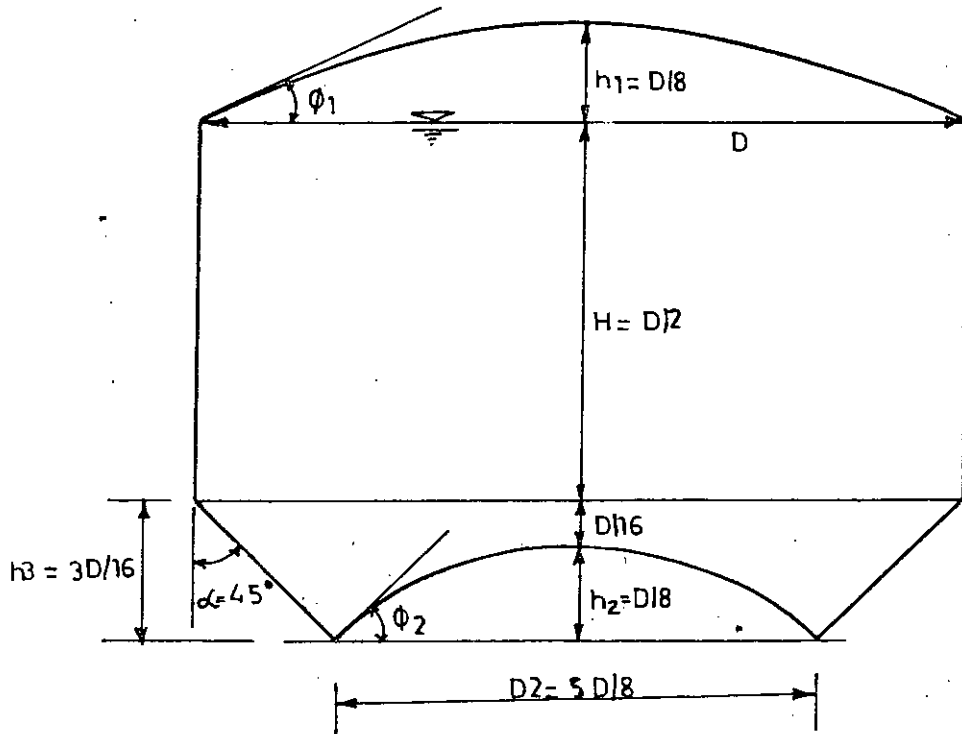


TABLE 2.4

Stress resultants of Case study 2

Location		Stress resultants		A_s
		Symbols	Values	
Top dome edge		N_ϕ	-2,595.4	0.18
		N_θ	-1,616.7	0.18
Top ring beam		T_θ	51,048.1	3.65
Cylindrical wall	Top	N_θ	0.0	0.67
	Bottom	N_ϕ	-3,967.0	0.43
N_θ		28,187.5	2.01	
Bottom ring beam		T_θ	153,469.1	10.96
Conical wall	Top	N_θ	48,280.0	3.45
	Bottom	N_ϕ	-54,873.5	0.72
		N_θ	40,623.0	2.90
M_ϕ	-13,027.5	0.72		
Bottom dome		N_ϕ	-19,013.0	0.288

Bottom circular beam

Total vertical load on the beam, $w = 52,445.0$ lbs/ft.- ve $M = 532,837.0$ ft-lbs, - ve $A_s = 13.2$ in²+ ve $M = 242,198.0$ " + ve $A_s = 6.0$ in²Twisting mom. M_t (at $\beta = 9\frac{1}{2}^\circ$) = 40,366.0 ft-lbs.

SF (at column face) = 282,831.0 lbs.

2.4.3 Case Study 3

This design example is quoted from "Treasure of R.C.C. Designs" by Sushil Kumar⁽⁷⁾. Figures mentioned here have been obtained by unit conversion from SI to FPS system.

Design Criteria:

Capacity	= 223,600 gallons
LL + coating	= 30.7 psf
f'_c (M200 grade concrete)	= 2,850 psi
f_c (compression)	= 1,000 psi
f_{ct} (direct tension)	= 170 psi
f_{ct} (flexure)	= 240 psi
f_s	= 14,000 psi
n (modular ratio)	= 13
Nominal reinforcement	= 0.3% (maximum)
j	= 0.841
k	= 0.476
R	= 200 psi

The final physical dimensions of the tank are shown in Fig. 2.16, however, the relative dimensions suggested by the author⁽⁷⁾, in general, are as in Fig. 2.15.

The stress-resultants are shown in Table 2.5.

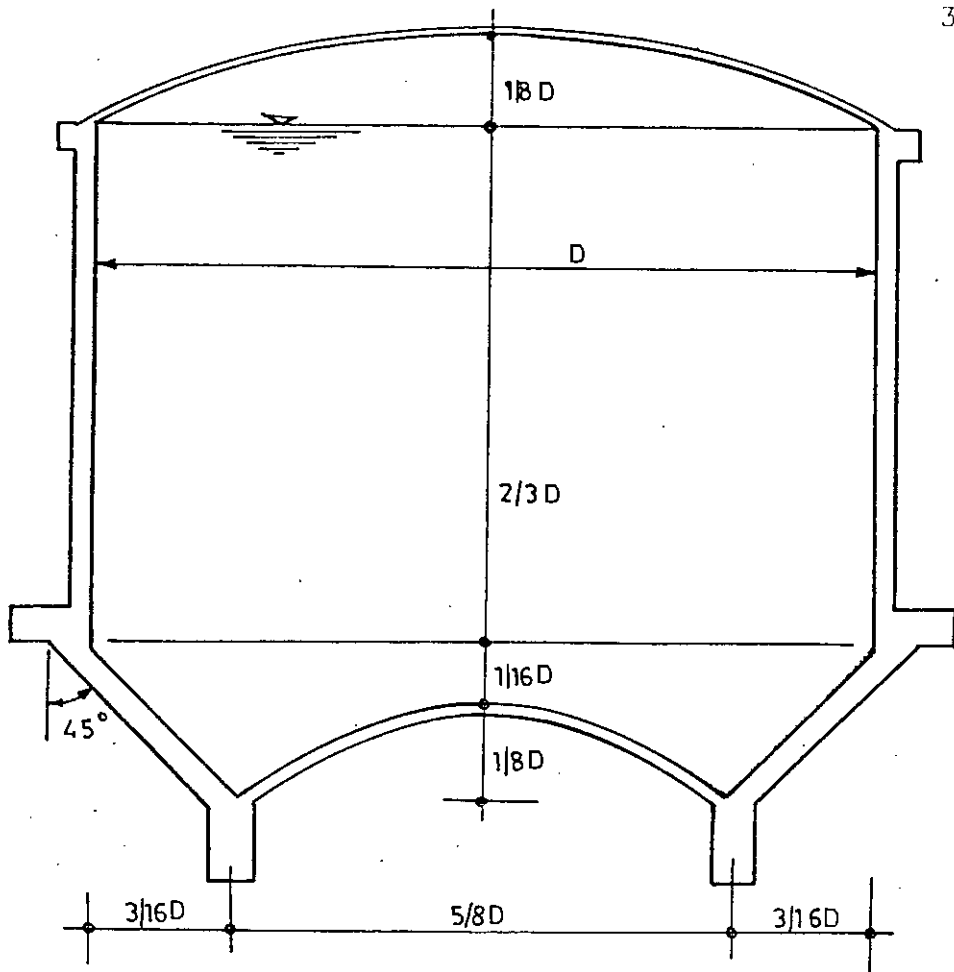


Fig. 2.15 Suggested relative dimensions.

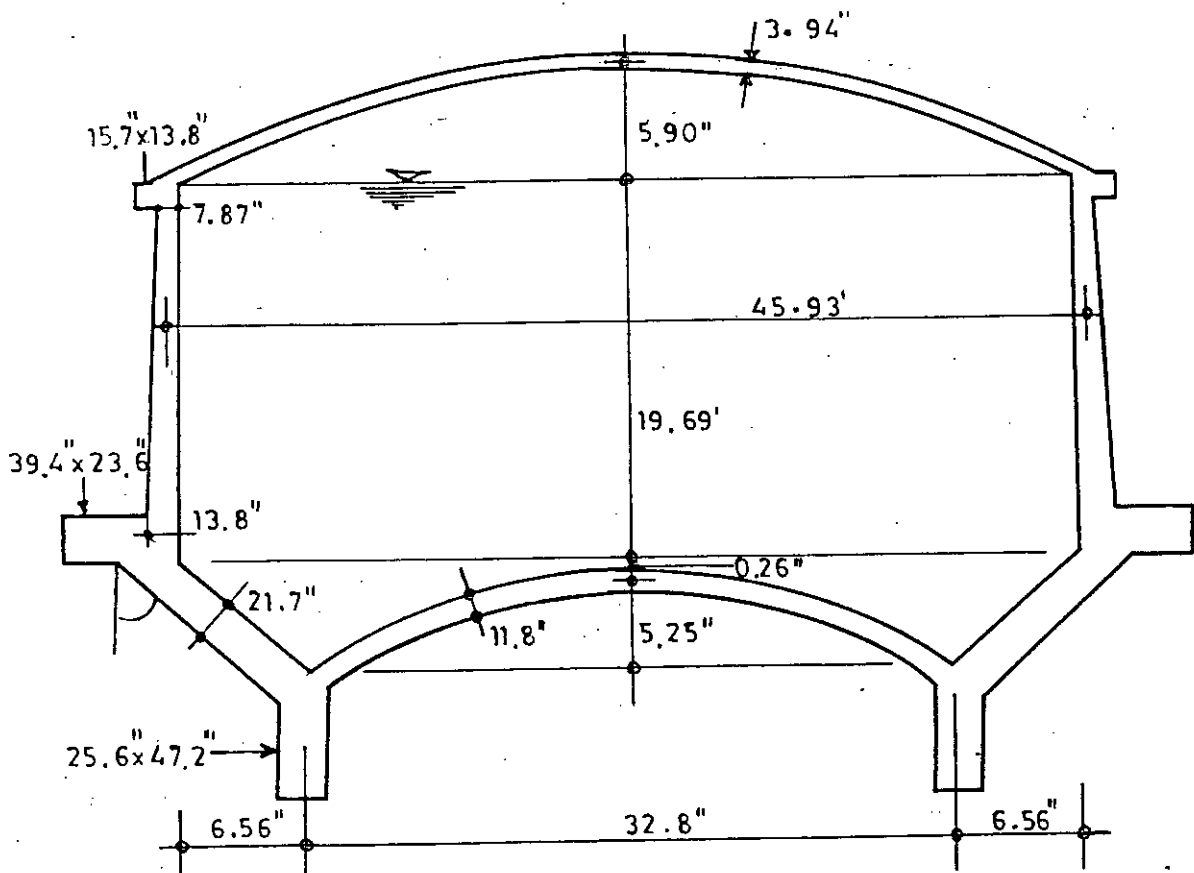


Fig. 2.16 Physical dimensions of the tank of case study 3.

TABLE 2.5
Stress resultants of case study 3

Location	Stress-resultants		A_s
	Symbols	Values	
Top dome edge	N_ϕ	-2,040.9	Nominal
	N_θ	-1,905.4	Nominal
Top ring beam	T_θ	40,432.0	2.84
Top of cylindrical wall	N_ϕ	-1,209.4	Nominal
Bottom of cylindrical wall	N_ϕ	-3,454.1	Nominal
	N_θ	28,222.2	2.02
Bottom ring beam	T_θ	168,210.0	12.02
Top of conical wall	N_ϕ	-6,876.4	Nominal
	N_θ	51,223.0	3.66
Bottom of conical wall	N_ϕ	-30,910.0	Nominal
	N_θ	45,373.9	3.66
Bottom dome edge	N_ϕ	-22,040.0	-
	N_θ	-9473.0	-

2.4.4 Case Study 4

This is a practical design example. The design of this tank has been collected from a consultancy report⁽¹²⁾ of the Civil Engineering Department of BUET. To some extent the design follows the method of Sushil Kumar⁽⁷⁾ but at the same time provides considerable flexural reinforcement for apprehended meridional moments in the shells. The objective of including this design case is to shed light on the precautionary measures usually adopted by designers of Intze tanks to account for the uncertainties, since exact behaviour of the structure is yet to be established. The flexural reinforcements provided add considerably to the cost of the structure and hence the utility of such reinforcement should be investigated. In passing, it may be mentioned here that it would be apparent from a rational analysis of the structure by Finite Element method (in Chapter 4) that while moderate flexural reinforcement is a real need somewhere, it amounts to sheer wastage elsewhere.

Design Conditions:

Capacity of the tank	= 151,700 gallons
Live load + coating on top dome	= 20 psi
Concrete strength f'_c	= 2,500 psi
f_c (in contact with water)	= 750 psi
f_c (elsewhere)	= 1,125 psi
f_{ct} (direct tension)	= 150 psi
f_s (in contact with water)	= 12,000 psi

f_s (elsewhere)	= 18,000 psi
n (modular ratio)	= 10
Nominal reinforcement	= 0.25%
Height of tank above G.L.	= 70'
Wind pressure	= 30 psf
Earthquake force	= 9% of total weight

The final physical dimensions of the tank are shown in Fig. 2.17, and the stress-resultants are shown in Table 2.6.

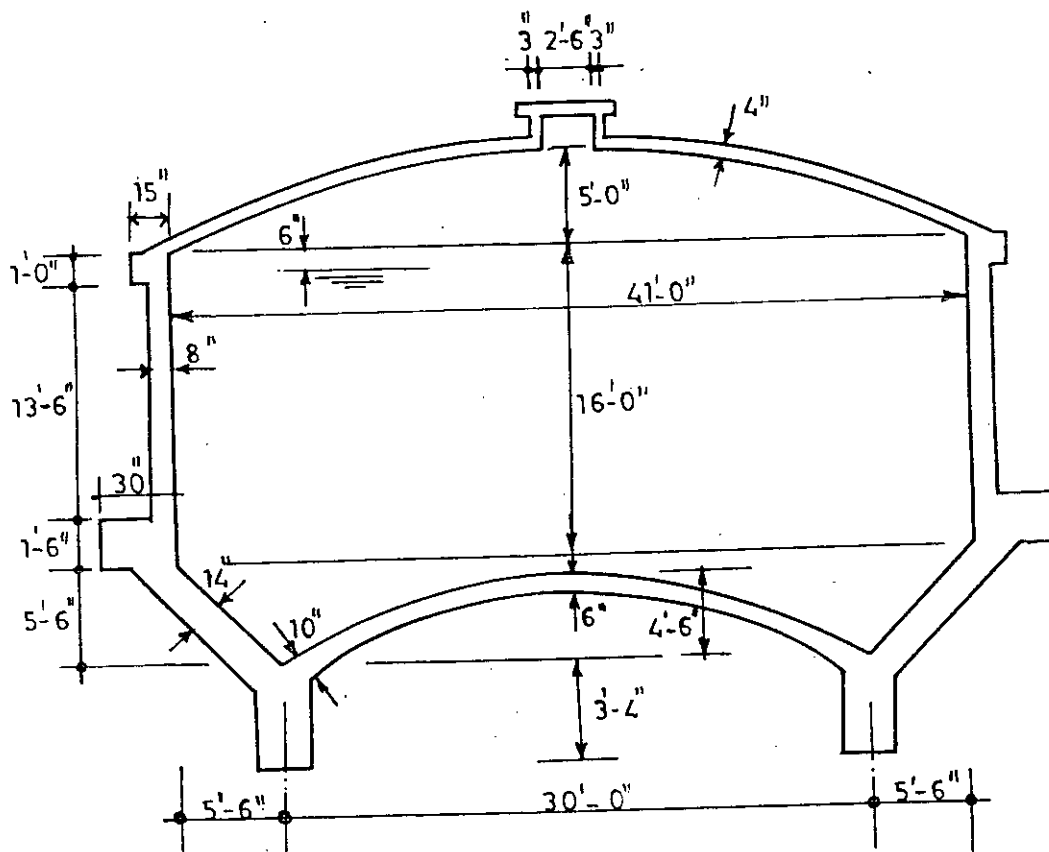


Fig. 2.17 Physical dimensions of the tank of case study 4.

TABLE 2.6

Stress resultants of case study 4

Location	Stress-resultants		A_s
	Symbols	Values	
Top dome edge	N_ϕ	-165.0	Nominal
Top ring beam	T_θ	30,012.0	1.67
Top of cylindrical wall	N_ϕ	-947.6	Nominal
Bottom of cylindrical wall	N_ϕ	-2,297.6	Nominal
	N_θ	9,865.0	0.822
	M_ϕ	-2,915.0	0.51
Bottom ring beam	T_θ	87,039.0	7.25
Top of conical wall	N_ϕ	-4,048.0	-
	N_θ	27,550.0	2.3
	M_ϕ	-5,918.0	0.50
Bottom of conical wall	N_ϕ	-18,365.0	-
	N_θ	27,550.0	2.3
	M_ϕ	-5,918.0	0.50
Bottom dome edge	N_ϕ	-17,682.7	Nominal

CHAPTER 3

CONVENTIONAL ANALYSIS OF THE SUPPORTING TOWER

3.1 Introduction

The most common form of the Intze tank staging consists of a circle of columns connected by several layers of straight bracings monolithically cast with the columns. The bottom circular beam of the tank atop the circle of columns transmits the loads of the tank to the columns and also acts as the uppermost bracing of the tower. Usually the columns are symmetrically placed along the circumference and are of the same sectional area so that they receive equal shares of the vertical load of the tank. However, the columns are also subjected to lateral forces due to wind or earthquake acting on both the tank and the tower. These lateral forces induce bending moments, shear and axial forces in the columns and bracings. Sometimes the columns are slightly battered to improve their efficiency in resisting lateral forces.

The whole problem is statically indeterminate and calls for a space frame analysis of the tower that could be performed only with the aid of a computer. However, to make the analysis practicable in absence of computer facilities a few conventional methods have been evolved by different authors on the basis of certain assumptions that allow a sort of plane frame analysis of the tower. Some of these methods are discussed in this chapter and illustrated with case studies. It will be seen that the conventional methods differ considerably in their approach and give widely different

results. It is difficult to say which method is more rational unless a rigorous investigation with computer aided space-frame analysis reveals the mystery. And it is very much desirable to establish a rational and reliable method of analysis to make the design safe and economical.

3.2 Conventional Methods of Analysis

Three methods of analysis of the tower are briefly outlined in the following sub-articles. The methods are due to the following authors:

- (i) Jai Krishna and Jain⁽²⁾
- (ii) Sushil Kumar⁽⁷⁾
- (iii) Gray and Manning⁽¹⁾

The assumptions made in each method are also mentioned and each method is illustrated by a case-study.

3.2.1 Jai Krishna and Jain's Method

(a) Analysis of columns:

Assumptions: (i) The gravity load of the tower including the weight of water is equally distributed among all the columns. (ii) The axial forces induced in the columns by the lateral forces due to wind or earthquake may be calculated by considering the whole tower to be a single vertical cantilever beam with its section built up with the columns spaced apart. (iii) The columns develop points of inflection at mid-heights of each panel i.e. at points x, y, z in Fig. 3.1.

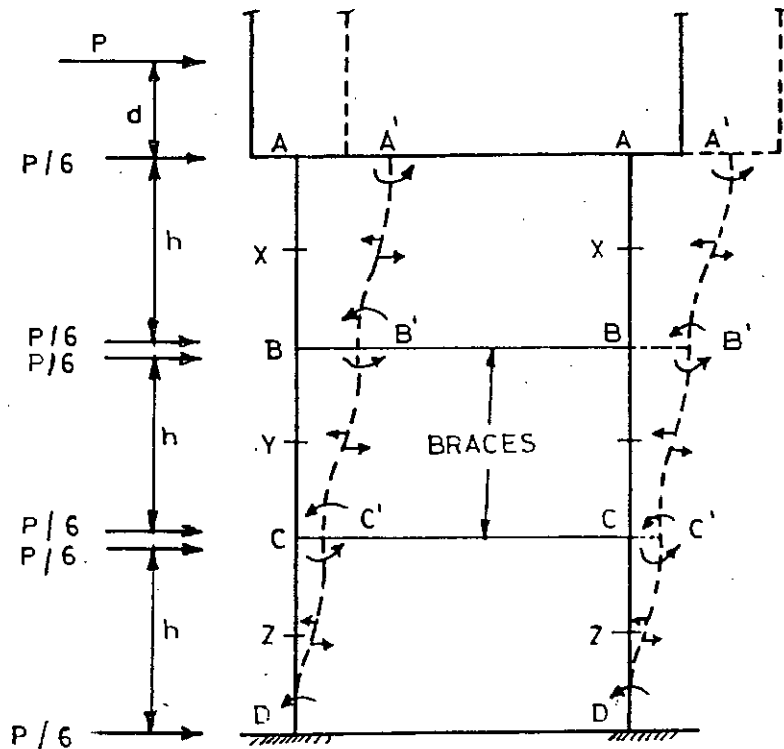


Fig. 3.1 Deflection of tower under wind load.

Let there be n columns in a tower ($n \geq 6$) located symmetrically on a circle of mean diameter D . Let the sectional area of each column be a . The total sectional area of the cantilever beam is thus nxa and the section can be considered to be a ring of mean diameter D and equivalent thickness $t = na/(\pi D)$ as shown in Fig. 3.2. Thus moment of inertia of the beam section is $naD^2/8$.

If m be the bending moment in the cantilever beam, then the axial force in a column C making an angle θ with bending axis is $4m \sin \theta / (\pi D)$. Thus axial force (due to wind) on columns lying on the bending axis is zero, while that on columns farthest from bending axis is $4m/(\pi D)$ and is tensile on windward side and compressive on leeward side. At the bottom panel where m is maximum, this axial force is also maximum. The shear force in column C is $SF = 2Q \cos^2 \theta / n$, where Q is the total shear force at mid-height of any panel.

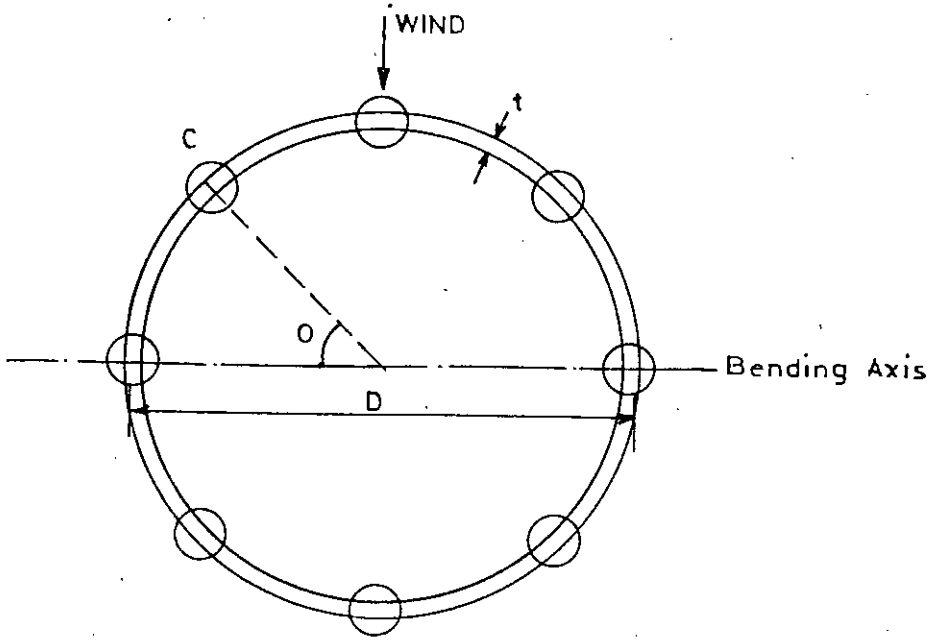


Fig. 3.2 Equivalent beam section.

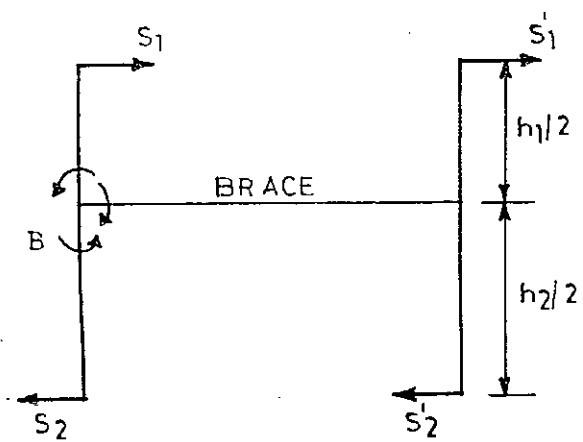


Fig. 3.3

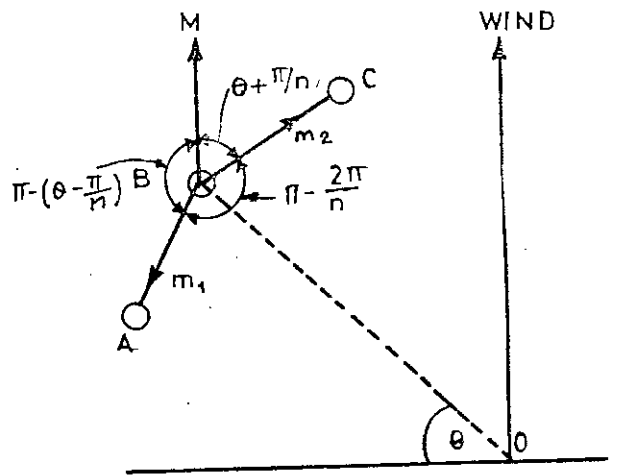


Fig. 3.4

Thus at columns farthest from bending axis $SF = 0$. While at columns on the bending axis shear force is maximum, i.e. $SF = 2Q/n$.

The bending moment at the top and bottom of each panel is given by $BM = SF \times h/2$, where h is the clear panel height. Obviously BM is maximum at the bottom panel where SF is maximum. Thus at panel zz in Fig. 3.1, $Q = P_1 + 5P/6$.

$$\text{Hence, } SF_{\max} = (P_1 + 5P/6) \times 2/n,$$

$$\text{and } BM_{\max} = SF_{\max} \times h/2.$$

For maximum axial force, $m = P_1(d+2.5h) + 6.5Ph/6$.

(b) Analysis of bracings:

At every junction of columns and bracings, the columns impose a moment on the joint. Fig. 3.3 shows the shear force in columns on either side of a brace. The moment imposed at joint B is $S_1h_1/2 + S_2h_2/2$, clockwise. This joint moment has to be resisted by the two braces meeting at the joint. Thus the braces are subjected to bending moment and twisting moment at each joint. The bending moment in the brace about the vertical axis of its section is almost zero and even the twisting moment is negligible. Thus the braces bear the joint moment mostly by developing bending moment about the horizontal axis of its section. These moments in the braces can be calculated by considering statical equilibrium of moments at the joint.

Considering the joint B in Fig. 3.4 where the joint moment is M , the hogging moments m_1 and m_2 set up in the braces AB and BC meeting at B balance the joint moment. Thus, from Fig. 3.4,

$$m_1/\sin(\theta + \pi/n) = m_2/\sin(\theta - \pi/n) = M/\sin(2\pi/n),$$

where $M = (Q_1 h_1 + Q_2 h_2) \cos^2 \theta / n$, Q and h denoting the shear force and height of panel for the panels above and below the brace.

$$\text{On simplification, } m_1 = \frac{Q_1 h_1 + Q_2 h_2}{n \sin(2\pi/n)} \cos^2 \theta \sin(\theta + \pi/n)$$

$$m_2 = \frac{Q_1 h_1 + Q_2 h_2}{n \sin(2\pi/n)} \cos^2 \theta \sin(\theta - \pi/n)$$

From these expressions value of θ for maximum moment can be calculated.

Shear force in brace AB of length a is given by

$$\text{SF}_{\text{brace}} = \frac{Q_1 h_1 + Q_2 h_2}{na \sin(2\pi/n)} \{ \cos^2 \theta \sin(\theta + \pi/n) - \cos^2(\theta - 2\pi/n) \\ \times \sin(\theta - 3\pi/n) \}$$

For maximum value of shear force, $Q = \pi/n$, i.e. wind blowing parallel to the brace.

The twisting moment in the braces may be taken as about 5% of the bending moment.

3.2.2. Sushil Kumar's Method

(a) Analysis of columns:

Assumptions: (i) The total vertical load of the tank and the

tower is equally divided among the columns. Thus if W be the total vertical load and n be the number of columns, then load per column $P_d = W/n$.

(ii) The vertical force in any column due to lateral forces of wind or earthquake is proportional to the distance of the column from the neutral axis.

Thus $P_w = M_w r / \Sigma r^2$, where

M_w = moment due to wind at a given level,

r = distance of any column from neutral axis,

Σr^2 = sum of squares of the distances of all the columns from neutral axis.

Thus axial force due to wind is zero in columns lying on the neutral axis and maximum in columns farthest from neutral axis, being tensile on windward side and compressive on leeward side.

The maximum axial force can also be calculated by the formula $P_w = 2M_w / (nR) = 4M_w / (nD)$, the same formula as in Jai and Jain's method.

(iii) The shear force in any column is equal to the total horizontal force at the level considered divided by the number of columns.

(iv) The points of inflection occur at mid-heights of the panels between bracings so that the maximum bending moment in a column at the top or bottom of any panel is given by

$$BM = 1/2 \times \text{horizontal shear at that panel} \times \text{panel height.}$$

The shear force and bending moment obtained by this method for columns on bending axis are only half of those obtained by Jai & Jain's method.

(b) Analysis of bracing:

Assumptions: (i) Maximum bending moment occurs in a brace QR when wind blows perpendicular to the adjacent brace PQ, as in Fig. 3.5.

(ii) Shear force in bracing = $\frac{2 \times \text{moment}}{\text{length of bracing}}$

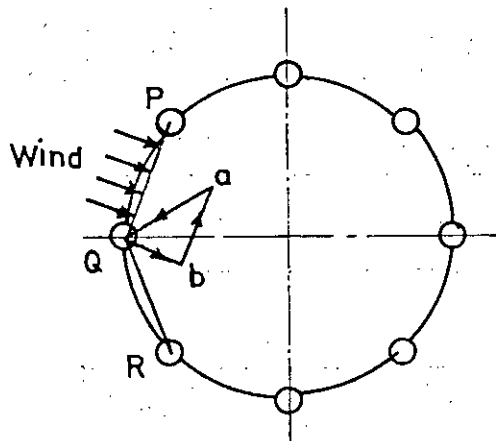


Fig. 3.5

3.2.3 Gray and Manning's Method

(a) Analysis of columns:

In reference (1), the authors suggest approximate methods of analysis of polygonal braced towers for three different cases, namely:

- (a) with columns hinged at the footings,
- (b) with columns fixed at the footings, and

(c) with columns braced horizontally and fixed at the footings, the braces being chords of the circle on which the columns are situated.

In case (a), illustrated in Fig. 3.6(a), the wind moment is equal to Ph and the axial load due to the wind is V_r in the outermost column and is in direct proportion in the interior columns as follows:

$$V_b = V_r \times b/r, \quad V_a = V_r \times a/r, \quad V_o = 0$$

Since the columns are hinged at the footings the values of V_r etc., are obtained as follows by equating Ph and the moment of resistance, M_R .

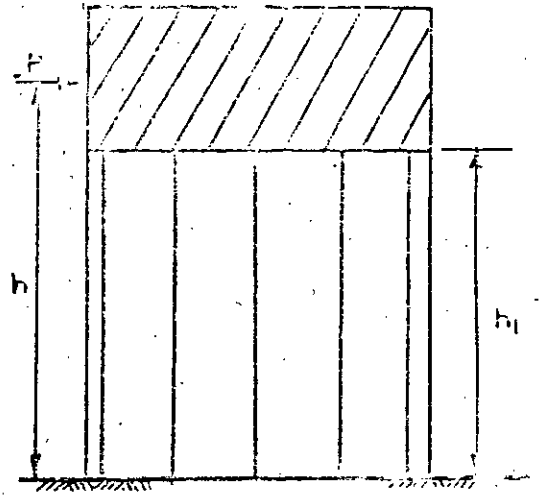
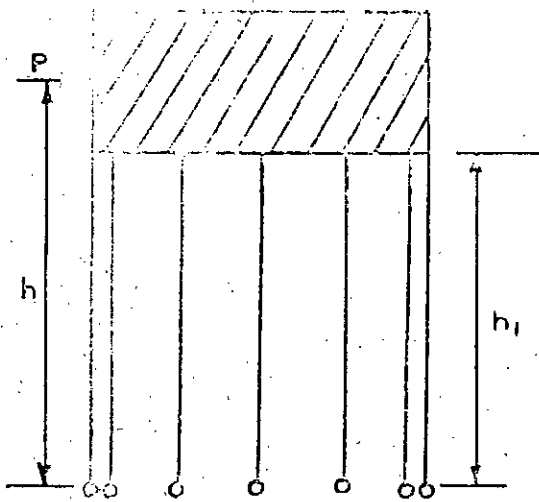
$$\begin{aligned} Ph = M_R &= 2V_r \cdot r + 4 V_b \cdot b + 4 V_a \cdot a \\ &= 2V_r/r (r^2 + 2b^2 + 2a^2) \end{aligned}$$

In general terms when each column is considered $Ph = V_r/r \cdot \Sigma a^2$.

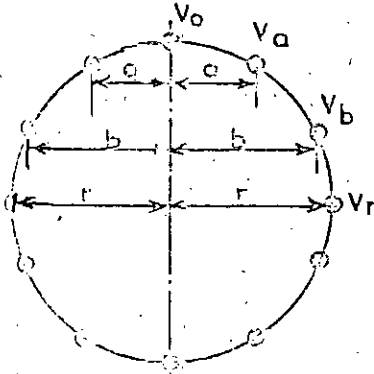
This expression gives the value of V_r , etc. The horizontal shear is assumed to be equally divided between the columns. The bending moment at the top of each column = $P/n \cdot h_1$, where n = the number of columns.

In case (b) with columns fixed at the footings, as in Fig. 3.6(b), if n = the number of columns, the resisting moment will include the sum of the moments at the bases of the separate columns. The value of the latter is

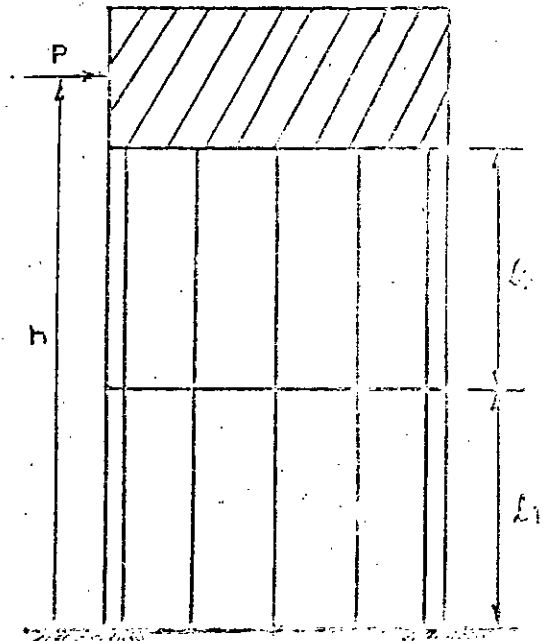
$$n \cdot P/n \cdot h_1/2 = Ph_1/2.$$



(b)



(a)



(c)

Fig. 3.6

Then $Ph = Ph_1/2 + V_T/r \cdot \Sigma a^2$, from which V_T etc. are found.

In case (c), with horizontal braces introduced, as in Fig. 3.6(c), the calculations are similar to those in case (b), but l_1, l_2 etc. takes the place previously occupied by h_1 , but the effectiveness of the braces must be considered.

In each case, the columns must be designed for three conditions:

- (i) Direct load due to weight of the structure and contents of the container.
- (ii) Direct load and bending moment due to wind combined with direct load as in condition (i).
- (iii) Effects of wind as in condition (ii), combined with direct load due to weight of structure only i.e. considering the tank empty.

All columns must be designed for the most severe conditions, since, the wind may blow from any direction.

(b) Effectiveness of braces:

The braces at columns V_T are practically at right angles to the direction of the wind force; therefore their resistance to bending is of no aid in stiffening these columns, and the stiffness of the windward and leeward columns V_T will depend mainly upon the torsional stiffness of the braces, which should, therefore, be provided with suitable reinforcement. For the shear to be divided equally

among the columns, the torsional resistance required of each of the two braces is quite large and an inadmissibly large brace would be required to provide such resistance. Further the torsional resistance available is only differential since the two columns adjacent to each column V_r are also tending to twist the brace in the same direction as is column V_r . Therefore the assumption of equal shear on each column is quite inadmissible in the case of twelve or more or even eight columns.

In the case of six or four columns, braces between adjacent columns are much more effective than is the case with greater numbers and the condition of "equal shear" is more likely to be obtained. It can be shown that in general the moment of resistance M_B required for the brace is $P l / (2 \sin \pi/n \cdot \Sigma I)$, where n is the number of columns. If the columns are circular, octagonal or square, then each column will have approximately the same moment of inertia about the plane of bending and then the foregoing expression becomes, $M_B = P l / (2n \sin \pi/n)$. Thus if $n = 6$, $M_B = P l / 6$, which is twice the bending moment on the column. For $n = 12$, $M_B = P l / 6.22$ which is about three times the bending moment on the column and an inordinately large brace might be required. It may be noted that for $n = 12$, the column shears in columns V_r , V_b , V_a and V_o may be assumed to be in the ratio $1:4/3:5/3:2 = 3:4:5:6$. Then maximum column shear would be in column V_o and $= P/9$ and column moment $= P l / 18$. In general, however, the columns on bending axis

may be regarded twice as effective as others so that for n columns, the maximum column shear = $2P/(n+2)$ and maximum column moment = $P_1/(n+2)$. For $n = 12$, column moment = $P_1/14$, for example.

(c) Columns other than circular or polygonal:

It is not strictly legitimate to divide the bending moment due to the wind between the columns in proportion to their flexural rigidities (EI/l) or their moments of inertia except when the latter are calculated for each column about an axis perpendicular to the direction of the wind. The method is only justified when the column sections are circular and have the same moments of inertia about all axes through the centre. An inspection of Fig. 3.7 a section through a tower, will show how an error arises if the moment of inertia is calculated about an axis through the middle of column A and parallel to its short side and if the same value is taken for the moments of inertia of columns B, C, etc.

(d) Inclined columns:

As a rule the columns are only slightly battered, and it is then sufficiently accurate to treat the structure as if the columns were vertical as shown by dotted lines in Fig. 3.8. The direct column load due to wind moment is not greatly changed by the splay. However, a simple correction may be applied by increasing the column load by the

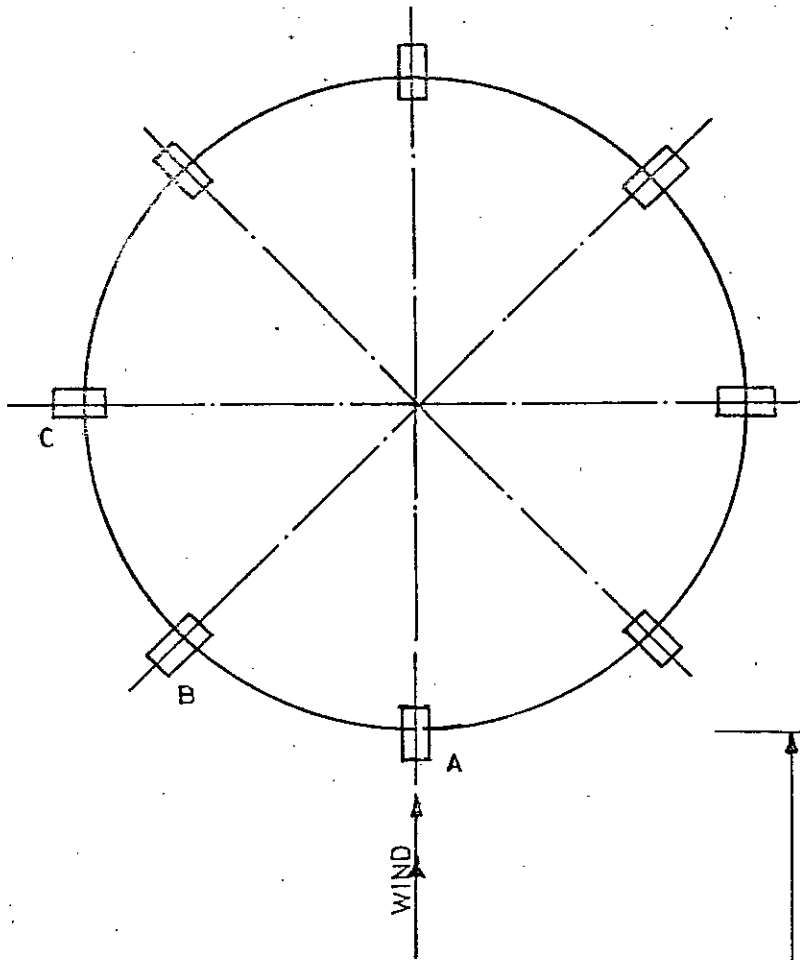


Fig. 3.7

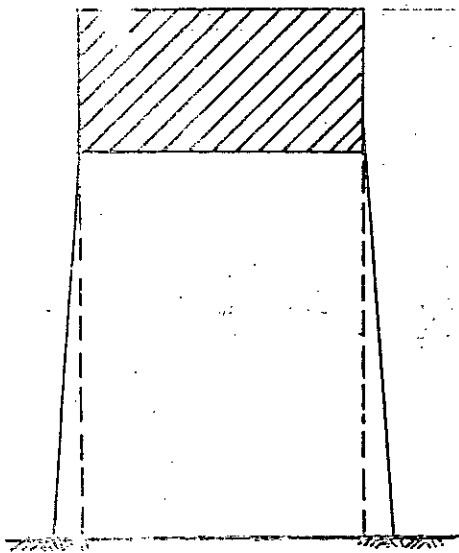


Fig. 3.8

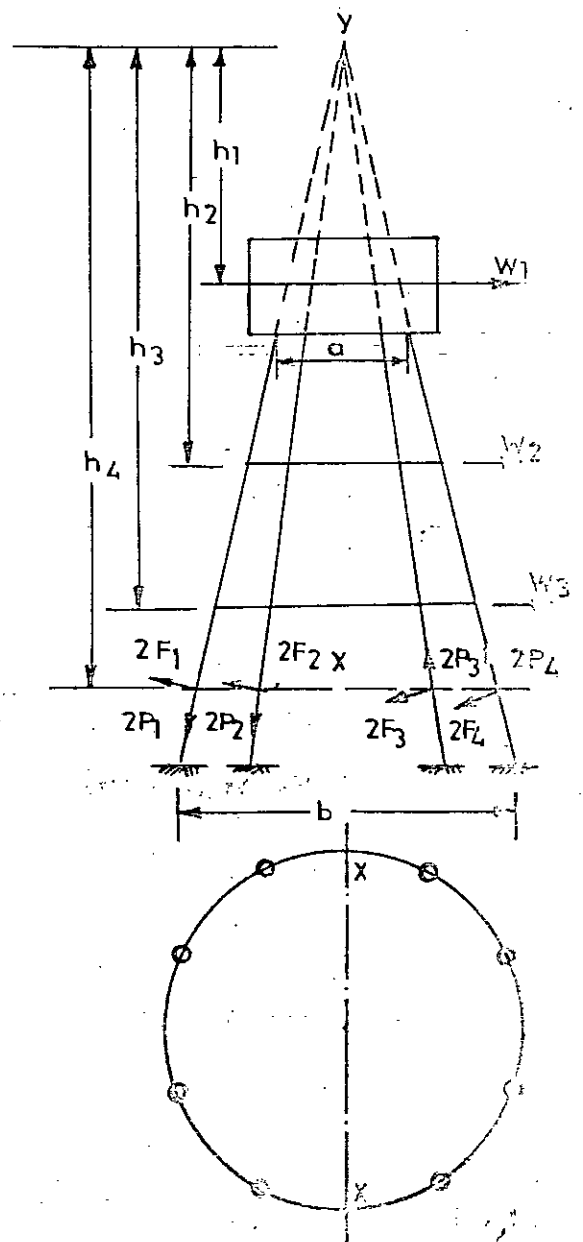


Fig. 3.9

factor $\text{Sec } \theta$, where θ is the angle which the column makes with the vertical. The direct dead load etc., on the columns must also include this factor. The bending moments on the columns due to flexure will be identical with those obtained for vertical columns.

(e) Greatly inclined columns:

Fig. 3.9 shows a water-tower supported on eight battered columns. All the columns have the same batter and if their centre-lines are produced upwards they meet in a point Y. In theory the analysis of deflections, where the columns vary in slope in any elevation and where the braces are of different lengths and often inclined to the direction of the wind, becomes impracticably complicated. For simplicity, it is assumed that the points of contraflexure in the columns occur half-way between the braces. It is also assumed that the columns are circular or octagonal in cross-section so that they are equally stiff in all directions; this is only approximately true if they are square.

The wind load on the tank is W_1 and the wind loads on the legs and braces are W_2 and W_3 and are assumed to be concentrated on the lines of the braces. If P_1, P_2, P_3 and P_4 are the direct thrusts on the columns and F_1, F_2, F_3 and F_4 are the shearing forces, it is not possible to find P_1, P_2, P_3 and P_4 merely by taking moments about axis X as the shearing forces do not pass through axis X. But as the lines of action of P_1, P_2, P_3 , and P_4 all pass through Y, taking moments about Y:

$$W_1 h_1 + W_2 h_2 + W_3 h_3 + W_4 h_4 = \text{sum of moments of } F_1, F_2, F_3 \text{ and } F_4 \approx 2 (F_1 + F_2 + F_3 + F_4) h_4$$

If the batter on the columns is not more than 1 in 6 it may be assumed (although this is not strictly correct) that $F_1 = F_2 = F_3 = F_4$. It may also be assumed that the values of P_1 etc. vary directly as their distances from axis X. With eight columns this makes P_2 equal to about 0.42 P_1 , etc. Since F_1, F_2 etc. are known, taking moments about X, the values of P_1, P_2 etc. can be determined. If the columns are rectangular in cross-section and the depth is equal to twice the breadth, it may be assumed that $F_1 = 4F_2$ and $F_4 = 4F_3$.

3.3 Case Studies

The conventional methods of analysis of the supporting tower of Intze tanks discussed in the preceding article are illustrated with design examples in the following sub-articles. Details of calculation are omitted for the sake of brevity. In some cases the figures quoted have been obtained by unit conversion from MKS system to FPS system.

3.3.1 Case Study 1

This example quoted from reference (2) presents the analysis and design of the supporting tower for the Intze tank of case study-1 in Chapter 2 and illustrates the method of Jai Krishna and Jain.

Design Features:

Height of tower above G.L.	= 42.65' (Fig. 3.10)
Depth of foundation below G.L.	= 2.46'
No. of columns	= 8
No. of layers of bracings	= 3
Diameter of column circle	= 29.53'
Wt. of tank	= 5,233 ^k
Wt. of water	= 1,216.9 ^k
Effective wind pressure	= 20.48 psf
Assumed column size	= 19.69" diameter
Assumed bracing section	= 9.84"x14.57"

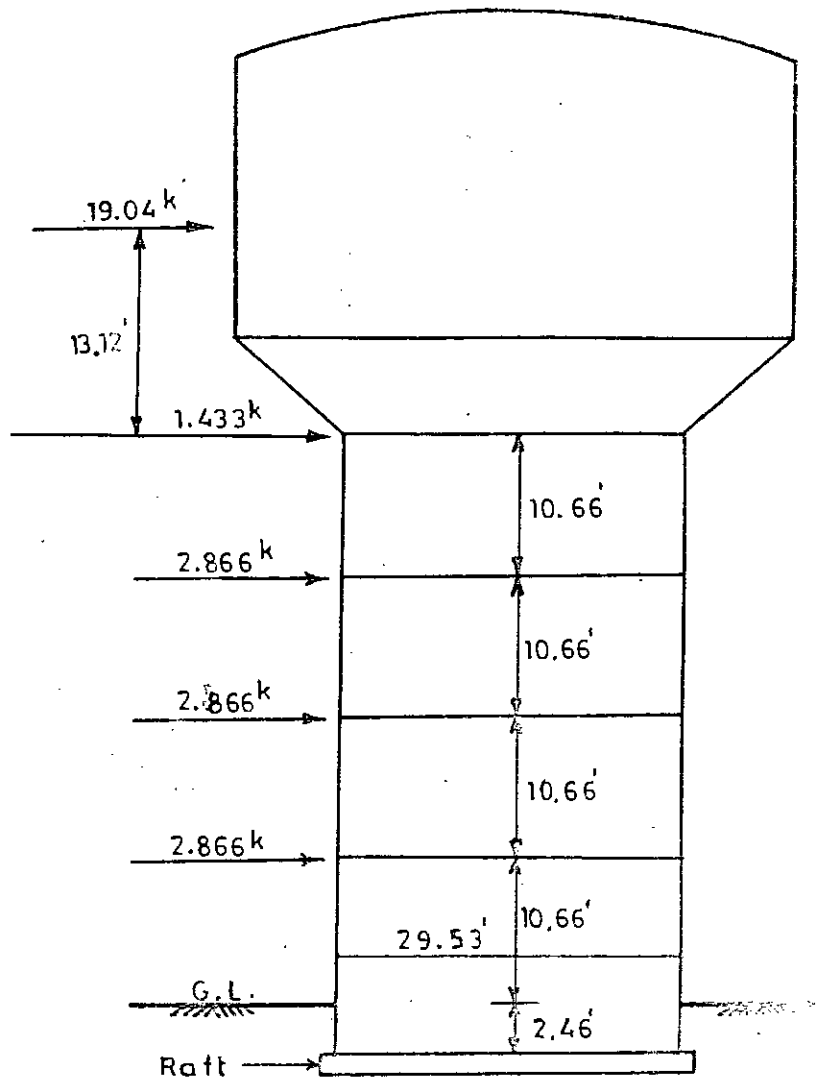


Fig. 3.10 Wind forces on the tower of case study 1.

Design of Columns:

The critical sections for design of columns are the lower ends of the bottom panel.

Total horizontal force due to wind, $Q = 29.071^k$

Moment of wind forces about the mid-height

of bottom panel $M = 1,187.28^k$

Axial force per column due to dead load and water

$= 69.82^k$ (for tank)

$+ 152.12^k$ (for water)

$+ 20.28^k$ (for tower)

$= 242.22^k$

Leeward Column:

Axial force due to wind $= 20.13^k$

∴ Total axial force $= 262.35^k$

Shear force and bending moment are zero.

Column on bending axis:

Axial force for wind $= 0.0$

∴ Total axial force $= 242.22^k$

Shear force (due to wind) $= 7.266^k$

Bending moment (" ") $= 47.68^k$

Assumed reinforcement $= 23.20 \text{ in}^2$

Effective sectional area $= 421.9 \text{ in}^2$

Effective moment of inertia $= 10,943 \text{ in}^4$

For leeward column: concrete stress = 621.8 psi safe.

For column on bending axis:

Direct stress = 573.2 psi

Bending stress = 514.9 psi

Since $33\frac{1}{3}\%$ overstressing is allowed when wind effect is considered, therefore,

$$\frac{573.2}{\frac{4}{3} \times 900} + \frac{514.9}{\frac{4}{3} \times 1,000} = 0.864 < 1 \quad \therefore \text{safe.}$$

Design of Bracings:

Maximum moment = 68.35^k

(For calculation procedure see Art. 3.2.1)

Maximum twisting moment = 3.42^k

Maximum shear force = 13.27^k

Assumed steel ratio = 0.021

With $33\frac{1}{3}\%$ overstressing allowed, $R = 240$ psi

$d_{reqd} = 13.1$ " O.K. Area of steel = 2.73 in^2 at top

and bottom each

Shear stress = 119.5 psi

Torsional shear stress = 125.9 psi.

3.3.2 Case Study 2

This example is taken from reference (1) to illustrate the method of analysis of towers suggested by Gray and Manning.

Design conditions:

Height of tower = 40' (Fig. 3.11)

No. of columns = 12

No. of layers of bracings = 1

Diameter of column circle = 40'

Weight of water = 1,476^k

Total horizontal wind force = 24^k acting as shown
in Fig. 3.11

Assumed column section = 18" square

Assumed bracing section = 12"x16"

Design of columns:

Load per column when tank is empty = 57^k

Load per column when tank is full = 180^k

Maximum shear per column due to wind = $\frac{24 \times 2}{12 + 2} = 3.43^k$

Maximum moment at column end = 34.3^{k'}

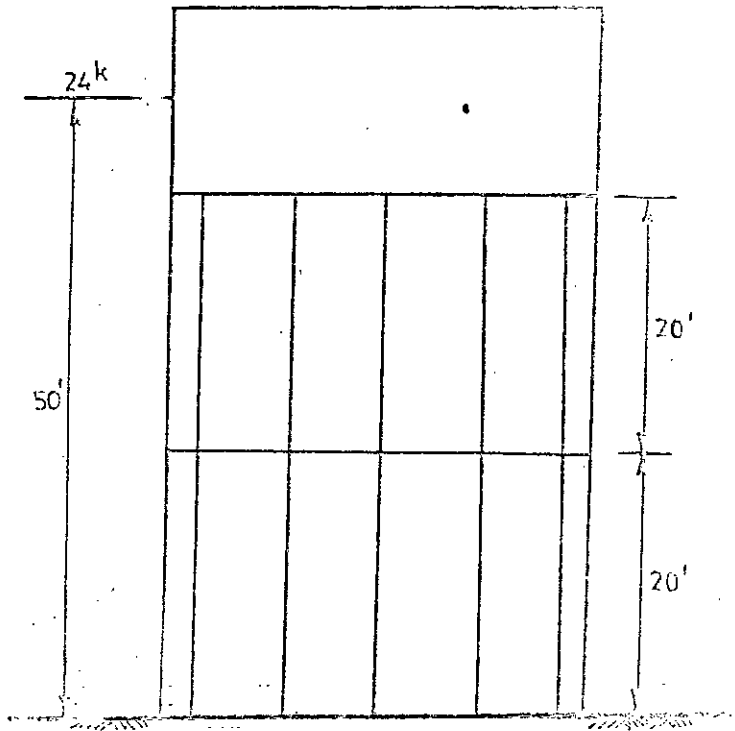
For columns farthest from NA. max. moment = $\frac{24}{12} \times 10 = 20^k$

Axial force in column farthest from NA due to wind
= 8.11^k

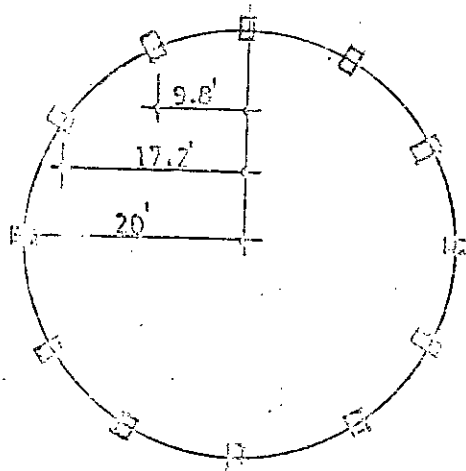
Assuming $A_s = 4.9 \text{ in}^2$ (4 # 10 bars),

equivalent area of column = $324 + 14 \times 4.9 = 392 \text{ in}^2$

and equivalent section modulus = 1348 in³



(a)



(b)

Fig. 3.11 Section and elevation of the tower of case study.

∴ Combined stresses are: when tank full,

$$\begin{aligned}
 \text{in leeward column} &= \frac{180,000 + 8,110}{392} \pm \frac{20.0 \times 12,000}{1,348} \\
 &= 480 \pm 178 \\
 &= + 658 \text{ or } + 302 \\
 \text{in windward column} &= \frac{18,000 - 8,110}{392} \pm 178 \\
 &= 438 \pm 178 \text{ psi} \\
 &= + 616 \text{ or } + 260 \text{ psi} \\
 \text{in columns on NA} &= \frac{180,000}{392} \pm \frac{34.3 \times 12,000}{1,348} \\
 &= 459 \pm 305 \\
 &= + 764 \text{ or } + 154 \text{ psi}
 \end{aligned}$$

When tank empty,

$$\begin{aligned}
 \text{in leeward column} &= \frac{570,000 + 8,110}{392} \pm 178 \\
 &= + 344 \text{ or } -12 \text{ psi (NB:-ve = tension)} \\
 \text{in wind ward column} &= \frac{57,000 - 8,110}{392} \pm 178 \\
 &= + 303 \text{ or } -53 \text{ psi} \\
 \text{in columns or NA} &= \frac{57,000}{392} \pm 305 \\
 &= + 450 \text{ or } - 161 \text{ psi}
 \end{aligned}$$

∴ All the stresses are safe both in compression and tension ($f_{ct} = 200 \text{ psi}$)

Design of braces:

Moment in brace is taken to be the same as the column moment i.e = $34.3^k'$

∴ Shear force in brace = $6,86^k$ (assuming brace length=10')

Using 4 # 9 bars, stress in steel = $\frac{34,300}{1.99 \times 13} = 15,900 \text{ psi}$

Shearing stress in brace = $\frac{6,860}{12 \times 0.9 \times 14.5} = 144 \text{ psi}$

Use $3/8" \phi @ 6" \text{ c/c}$.

3.3.3 Case Study 3

This example is quoted from reference⁽⁷⁾ to illustrate the method of Sushil Kumar for analysis of the supporting tower of Intze tank. Here the tank loads considered are those of case study-3 of Chapter-2.

Design features:

Height of the tower = 49.2' (Fig. 3.12)

No. of columns = 8

No. of layers of bracings = 3

Diameter of column circle = 32.8'

Diameter of tank = 45.93'

Weight of tank = 1,178.57^k

Weight of water = 2,313.49^k

Effective wind pressure = 21.5 psf

Assumed column section = 25.6" dia

Assumed bracing section = 19.69"x19.69"

Design of columns:

The columns are designed for the maximum axial force and moment at the base of the columns. Total horizontal force due to wind, $Q = 45.1^k$

Shear force per column = 5.638^k

Moment of wind forces about the base of the tower = 2,189.6^{k'}

Axial force per column due to dead load and water

= 147.32^k (for wt. of tank)

+ 289.19^k (for wt. of water)

+ $\frac{39.86^k}{476.37^k}$ (for wt. of columns and bracings)

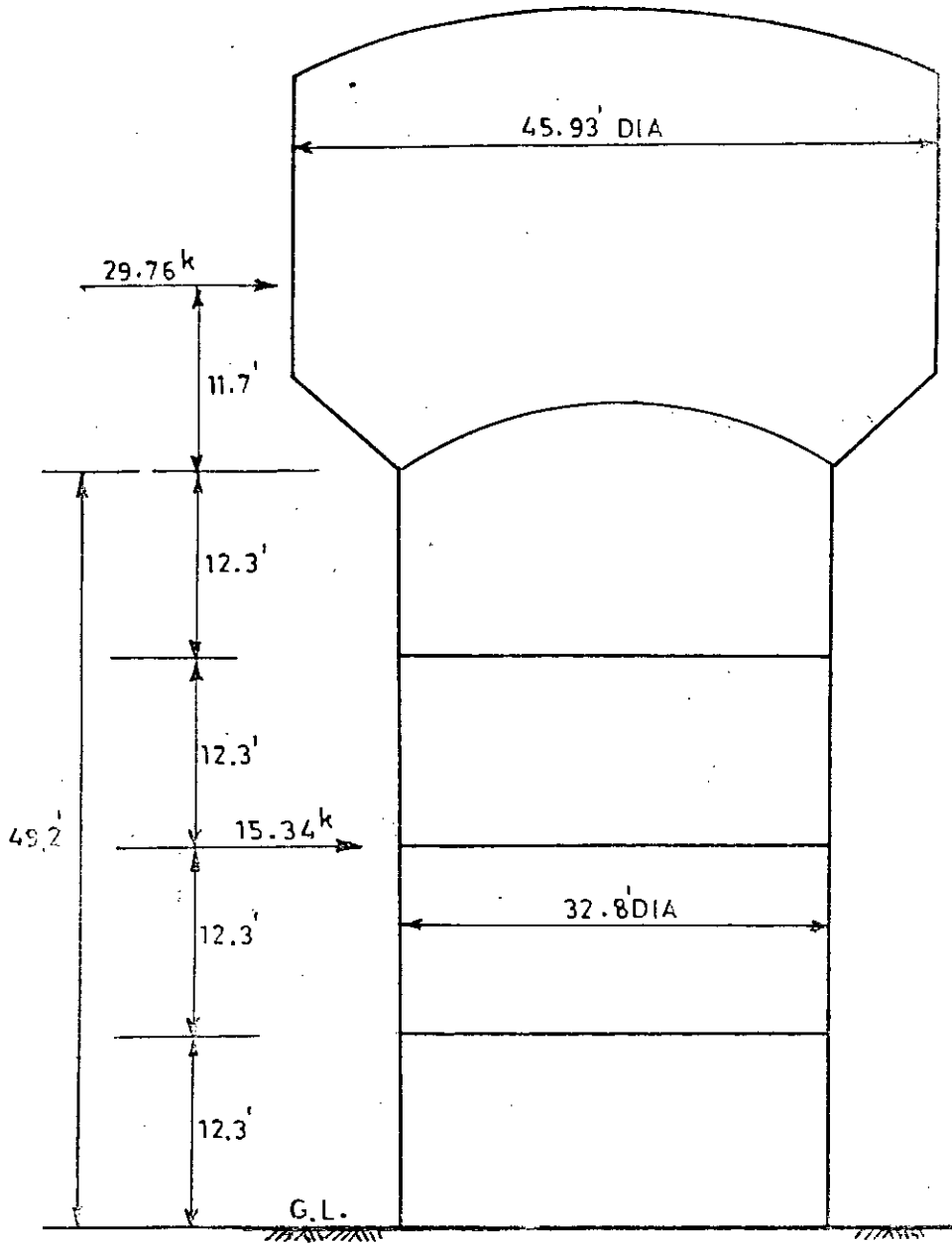


Fig. 3.12 Wind forces on the tower of case study 3.

Leeward column:

$$\text{Axial force due to wind} = 33.37^k$$

$$\text{Total maximum axial force} = 509.74^k$$

$$\text{Maximum BM in column} = 31.83^{k'}$$

Columns on bending axis:

$$\text{Axial force due to wind} = 0.0$$

$$\text{Total maximum axial force} = 476.37^k$$

$$\text{Maximum BM in column} = 31.83^{k'}$$

The columns on bending axis are not critical for design.

For leeward column, assumed steel area = 9.97 in^2

Equivalent area of column = 634 in^2

Equivalent moment of inertia = $27,700 \text{ in}^4$

Maximum stress in concrete:

$$\text{Due to direct load} = 803.6 \text{ psi}$$

$$\text{Due to bending} = 176.4 \text{ psi}$$

With 33% overstressing allowed while considering wind effect,

$$\frac{803.6}{710 \times 1.33} + \frac{176.4}{1,000 \times 1.33} = 0.984 < 1, \text{ safe.}$$

Design of bracings:

$$\text{Maximum moment} = 89.83^{k'}$$

$$\text{Moment of resistance of bracing} = 93.8^{k'} \quad \text{O.K.}$$

$$\text{Area of steel reqd.} = 3.44 \text{ in}^2$$

$$\text{Area used} = 3.8 \text{ in}^2 \text{ on each face (top \& bottom),}$$

Since reversal of wind direction will reverse the sign of BM.

$$\text{Maximum shear force} = 14.37^k, \quad \text{Shear stress} = 46.4 \text{ psi}$$

Provide nominal stirrups (8 mm ϕ @ 35 mm c/c).

3.3.4 Case Study 4

The design of the supporting tower for the Intze tank of case study-4 in Chapter 2 due to BRTC⁽¹²⁾ is considered in this case study. In addition to wind load this example also considers earthquake force on the tower.

Design features:

Height of tower = 70' (Fig. 3.13)

No. of columns = 8

Size of column = 18"x30"

No. of layers of bracings = 6

Size of bracing = 15"x31"

Columns battered in the ratio of 1:11

Diameter of column circle at bottom = 42.1'

Wt. of tank = 724^k

Wt. of water = 1,500^k

Effective wind pressure = 24 psf on tank body

" " " = 30 psf on tower.

Earthquake force = 9% of (wt. of tank + 1/3rd wt. of tower)
at midheight of tank.

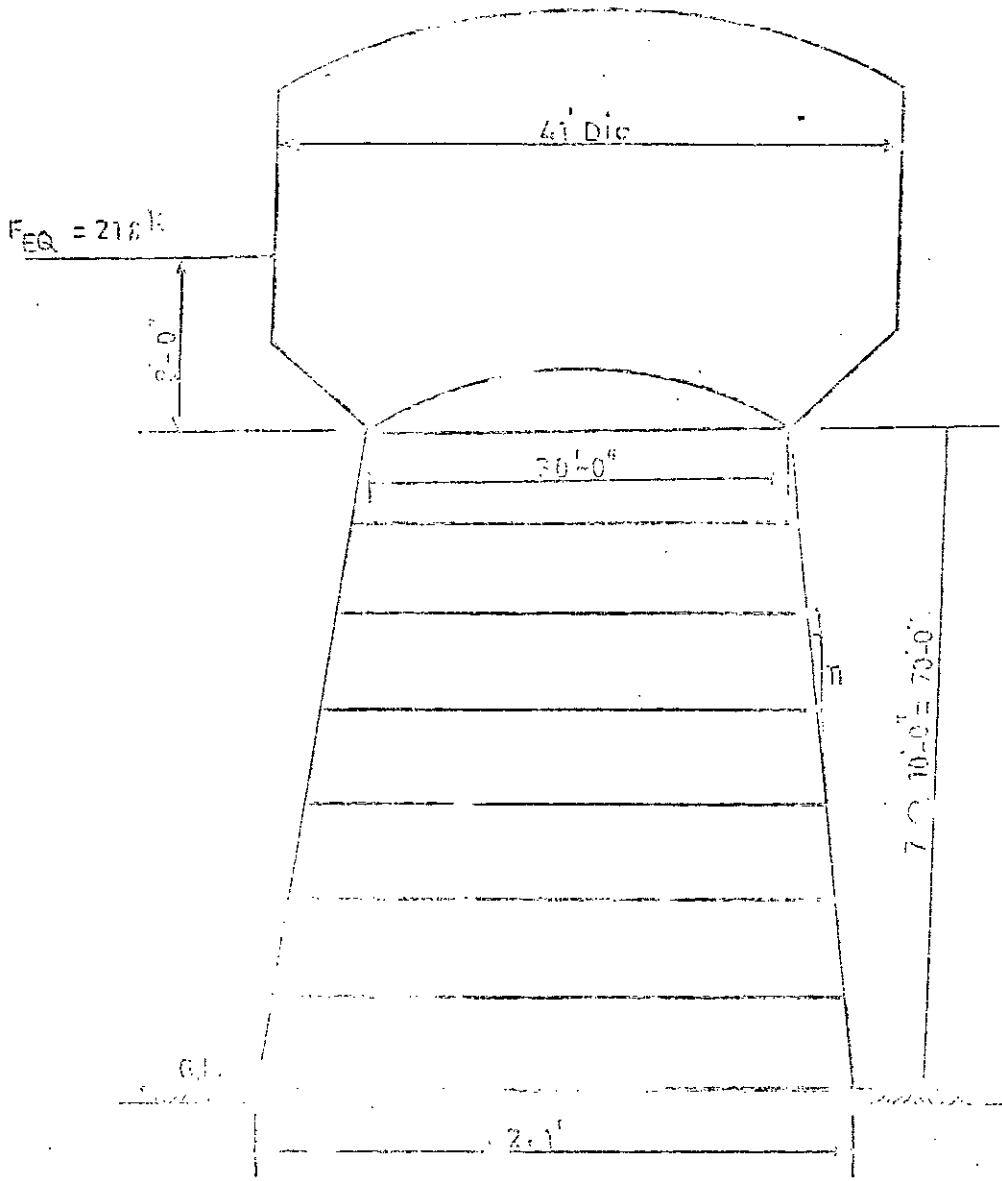
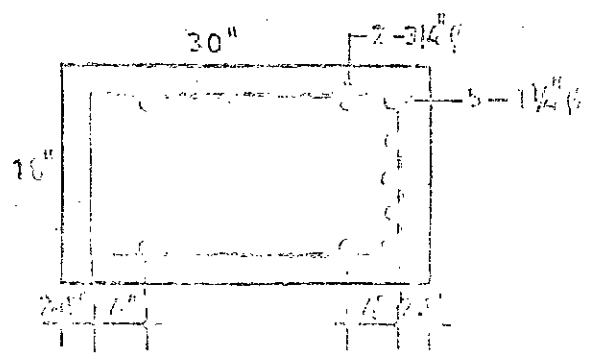


Fig. 3.13 Earthquake force on the tower of case study 4.



Design of columns

Axial force per column due to tank = 90.5^k

" " " due to water = 187.5^k

" " " due to wt. of tower = 71.0^k

Total axial force per column = 349^k

Wind force = 72^k (total)

Earthquake force = $0.09 (2224 + \frac{1}{3} \times 568) = 218^k > 72^k$

∴ Earthquake governs.

Horizontal shear per column = 27.25^k

Moment in column = $27.25 \times 5 = 136.25^k'$

Earthquake force is assumed to act at a height of 78' from G.L.

Moment of earthquake force about the base of tower = $17004^k'$

Maxm. axial force on farthest column = $\pm 201^k$ (from bending axis)

For empty tank E.Q. force = 82^k

Moment about base = $6412^k'$

Max. axial force on farthest column = $\pm 76^k$

Thus for tank full of water, $P_{col.} = 349 \pm 201 = 550^k$ or 148^k

$M_{col.} = 136^k'$

For empty tank $P_{col.} = 161.5 \pm 76 = 237.5^k$
or 85.5^k

$M_{col.} = 51^k'$

The most severe load case for design gives

$$P_{col.} = 550^k, M_{col.} = 136^k'$$

Assumed reinforcement = 10 # 10 bars + 4 # 6 bars (Fig. 3.14)

$$P = 0.2125 f_c' A_g + 0.85 A_s f_s$$

$$= 0.2125 \times 2.5 \times 540 + 0.85 \times 14.06 \times 18$$

$$= 502^k > 349^k; \text{ O.K. for dead load.}$$

$$\text{when earthquake acts: } m = \frac{f_y}{.85f'_c} = \frac{40}{.85 \times 2.5} = 18.82$$

$$p_g = \frac{14.06}{540} = 0.026$$

$$p_g m = 0.49, n = 9$$

$$S = I/C = 4978 \text{ in}^3$$

with 33% overstressing allowed when earthquake acts,

$$f'_c = 3325 \text{ psi}, f'_s = 23940 \text{ psi}$$

$$F_a = 0.34 (1 + p_g m) f'_c = 1.684 \text{ ksi}$$

$$f_a = \frac{P}{A_g} = \frac{550}{540} = 1.0185 \text{ ksi}$$

$$f_b = \frac{136 \times 12}{4978} = 0.328 \text{ ksi.}$$

$$\begin{aligned} \therefore \frac{f_a}{F_a} + \frac{f_b}{F_b} &= \frac{1.0185}{1.684} + \frac{0.328}{4 \times 1.496} \\ &= 0.605 + 0.219 \\ &= 0.824 < 1 \quad \text{O.k.} \end{aligned}$$

Design of bracings:

$$\begin{aligned} \text{Moment in bracing} &= \frac{\text{Col. moment}}{\sin 22 \frac{1}{2}^\circ} \\ &= \frac{136.25}{\sin 22 \frac{1}{2}^\circ} \\ &= 365 \text{ k'} \end{aligned}$$

$$\text{Bracing shear (for top bracing)} = 61 \text{ k}$$

$$\begin{aligned} \text{Resisting moment} &= \frac{189 \times 15 \times 27^2}{12000} \times 1.33 \text{ (33\% overstressing allowed)} \\ &= 229 \text{ k'} \end{aligned}$$

$$M_1 = 229 \text{ k'} , \quad M_2 = 136 \text{ k'}$$

$$A_{s1} = 4.89 \text{ in}^2$$

$$f'_s = 2 f_s \frac{d-d'/d}{1-k} = 16000 \text{ psi}$$

$$A_{s2} = 2.78 \text{ in}^2 , \quad \text{Total } A_s = 7.67 \text{ in}^2$$

Use 7 # 10 bars. Shear stress, $v = 150.6 \text{ psi}$

$$v' = 150.6 - 55 \times 1.33$$

$$= 78 \text{ psi}$$

$$\text{Spacing} = \frac{44 \times 16000}{78 \times 15} = 6" \text{ c/c}$$

use 4 legged $3/8" \phi$ stirrups @ $5.5" \text{ c/c}$.

CHAPTER 4

FINITE ELEMENT ANALYSIS OF THE INTZE TANK

4.1 Introduction

A Finite Element program⁽⁵⁾ for the analysis of axi-symmetric shell structures subjected to symmetric or non-symmetric loads has been adapted and used for the analysis of Intze tanks for the following load cases:

- 1) Gravity (self-wt.), considered symmetric
- 2) Hydrostatic pressure " symmetric
- 3) Wind load " non-symmetric.

The design examples presented in the case studies in Chapter 2 have been analysed by the Finite Element method, first with the original dimensions and then with dimensions modified on the basis of the stress conditions depicted in the first analysis. The results of both the cases are shown graphically in Art. 4.4 for all the case studies. Direct comparison of numerical values of stresses at critical sections obtained by conventional and Finite Element analysis are made in Art. 4.5. The graphical plots include displaced shape for original dimensions, meridional membrane force (N_{ϕ}), circumferential membrane force (N_{θ}) and meridional moment (M_{ϕ}) for gravity, hydrostatic pressure and combined effect of gravity and hydrostatic pressure for original and modified dimensions. In some cases individual plots for gravity and hydrostatic pressure have been omitted in view of the fact that the design stresses are governed almost exclusively by the combined effect.

The effect of wind load on the tank body has been studied for case study 4 only and the results are presented and discussed towards the end of this chapter (Art. 4.7).

4.2 The Finite Element Program

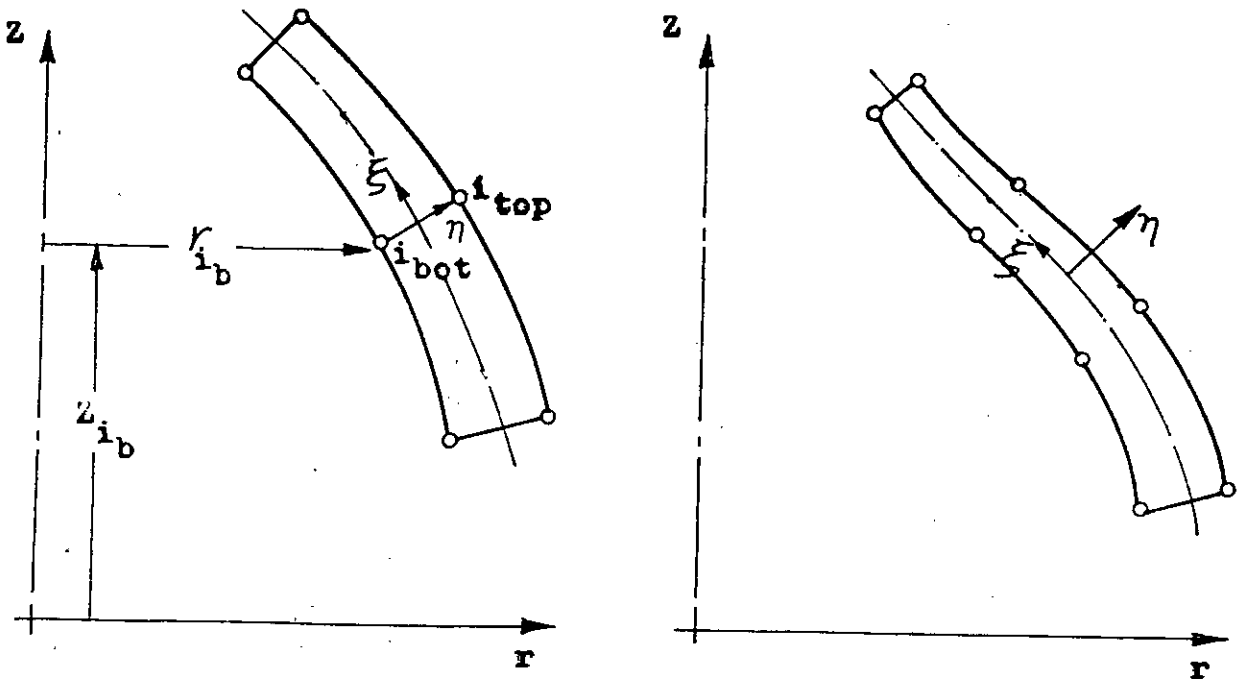
Ahmad⁽⁵⁾ developed a very general Finite Element computer program for analysis of axi-symmetric shell structure. The author has adapted the same program with considerable modifications and additions for analysis of Intze tanks. The modifications were made for the following reasons:

- i) Due to its highly general nature the original program needed large volume of input data, the preparation and punching of which was tedious. To overcome this difficulty a subroutine was written to generate the necessary data for Intze tanks with minimal input and feed them into the main program as and when necessary.
- ii) In the original program the output for stresses was in global co-ordinates which could not be conveniently used for design. As such modifications were made to obtain the stress resultants N_ϕ , N_θ and M_ϕ directly from the computer, considering their direct use in design.
- iii) The original program required that all the load cases have the same number of Fourier harmonics. However, as in Intze tanks, the gravity load and hydrostatic pressure are symmetric they require only one harmonic (i.e. zero-th harmonic) for analysis; whereas the wind load being non-

symmetric requires a number of Fourier harmonics for accurate representation. Considering these facts the program was modified in such a manner that the analysis is carried out in a single harmonic for gravity and hydrostatic pressure while that for wind load is carried out in as many harmonics as desired. The flexibility of the original program had to be sacrificed to some extent to attain this specific goal.

The subroutine for data generation is so written as to allow for nonuniform thickness of the shells. The cylindrical shell and the conical dome are assumed to have thicknesses that vary linearly from top to bottom, while the top and bottom domes may have thicknesses that vary from element to element at different rates. Slight modification would be required if it is desired to use stepped variation in thickness of the shells especially for the cylindrical wall.

The output of the program is the nodal displacements in the ascending order of the nodes for every right hand side (load case). However, it has been modified to offer choice between nodal points and Gauss integrating points for stress calculations. It has been observed that the stresses at Gauss points follow a more smooth curve than those at nodal points do, although the overall trend and magnitudes are practically the same. Another flexibility is that the user may opt for parabolic elements with one mid-side node or cubic elements with two mid-side nodes (Figs. 4.1 and 4.2). Using Fourier analysis the non-symmetric



(a) Parabolic

(b) Cubic

Fig. 4.1 Geometry of Element.

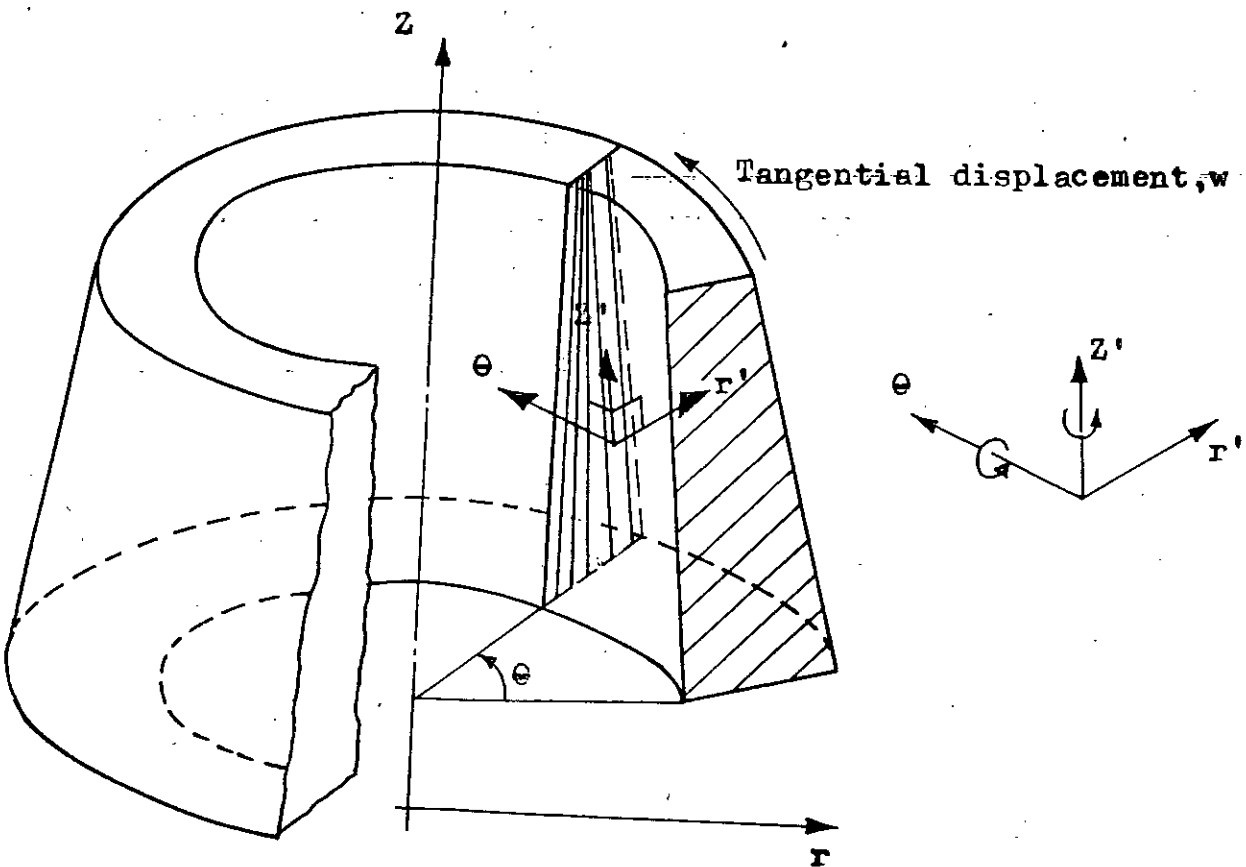


Fig. 4.2 Local coordinates and Nodal degrees of freedom.

load (due to wind) acting on the axisymmetric shell is replaced by a set of harmonics

and each harmonic is treated separately. Thus the loads are prescribed circumferentially by:

$$\begin{bmatrix} R \\ Z \\ T \end{bmatrix} = \begin{bmatrix} \Sigma R_n \cos n\theta \\ \Sigma Z_n \cos n\theta \\ \Sigma T_n \sin n\theta \end{bmatrix}$$

where R , Z and T are the radial, axial and circumferential components of loads respectively. The load amplitude R_n , Z_n or T_n for the n -th harmonic is defined as the maximum intensity per radian.

The displacements and stresses are calculated independently for each harmonic and the results are automatically superimposed to give the final effects of the loading at every node. If they vary circumferentially, the final results are calculated at a specified number of sections along the circumferential direction and the results are printed for every point indicated by its angular distance from the reference diameter ($\theta = 0$). As the results are symmetric about this diameter only half of the shell needs to be taken into consideration.

4.3 Finite Element Idealisation of the Intze Tank

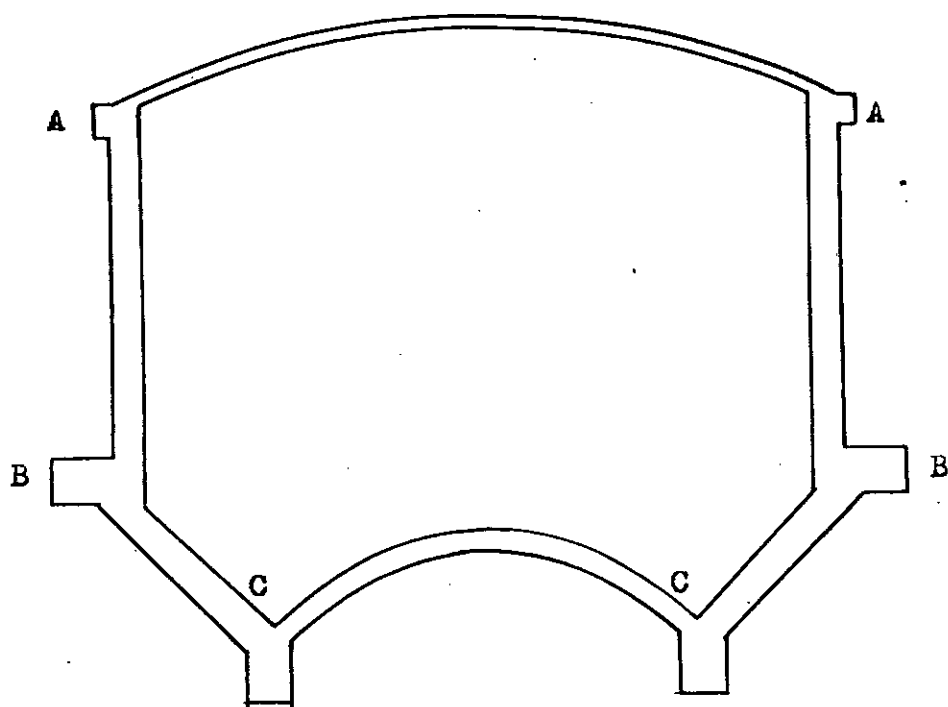
For Finite Element analysis, the Intze tank is represented by a chain of unbranched axis-symmetric shell elements placed end to end. In fact, a theoretical limitation of the

above program is that it cannot deal with branching and, as such, it becomes necessary to make some idealisations especially at the junctions where the shells meet the ring beams. The following assumptions are made:

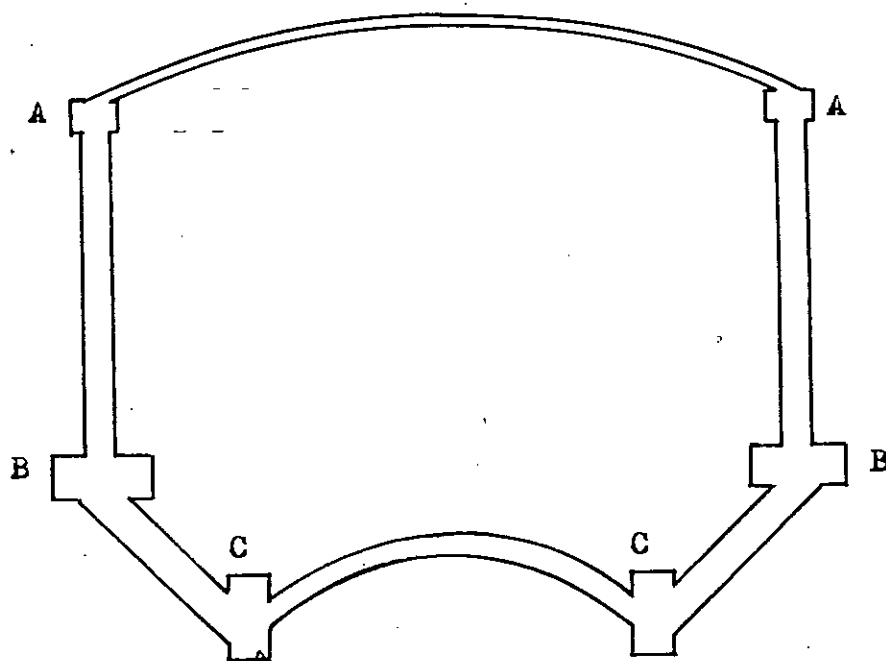
- (i) The shells meet the ring-beams in such a manner that the mid-surface of each shell coincides with that of the ring-beam at the junction (Fig.4.3).
- (ii) The ring-beams are treated as parts of shells with large thickness.
- (iii) The bottom circular beam atop the circle of columns is assumed to have zero vertical displacement throughout although it is supported only at the columns.

As regards the first assumption it may be noted here that even the conventional methods make this assumption either implicitly or explicitly. On the other hand the conventional methods also utilise the third assumption for analysis of the cone and the bottom dome above the bottom circular beam. The circular beam itself is, however, analysed assuming discrete supports. In the Finite Element analysis, using axi-symmetric shell elements, the assumption (iii) leaves no scope for calculating the moments, shears etc. in the circular beam. For the design of this beam, therefore, recourse is taken to conventional analysis.

To examine the justifiability of assumption (i), let us consider the free body diagrams of joint A for actual and idealised conditions (Fig. 4.4).



(a) Actual shape



(b) Idealised shape

Fig. 4.3 Idealisation of Intze tank.

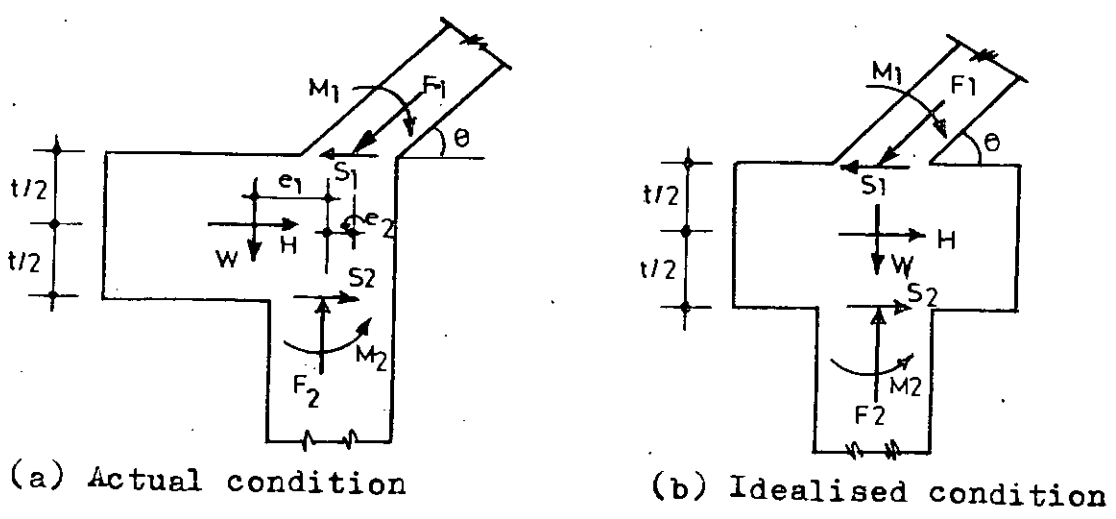


Fig. 4.4 Free body diagrams of joint A.

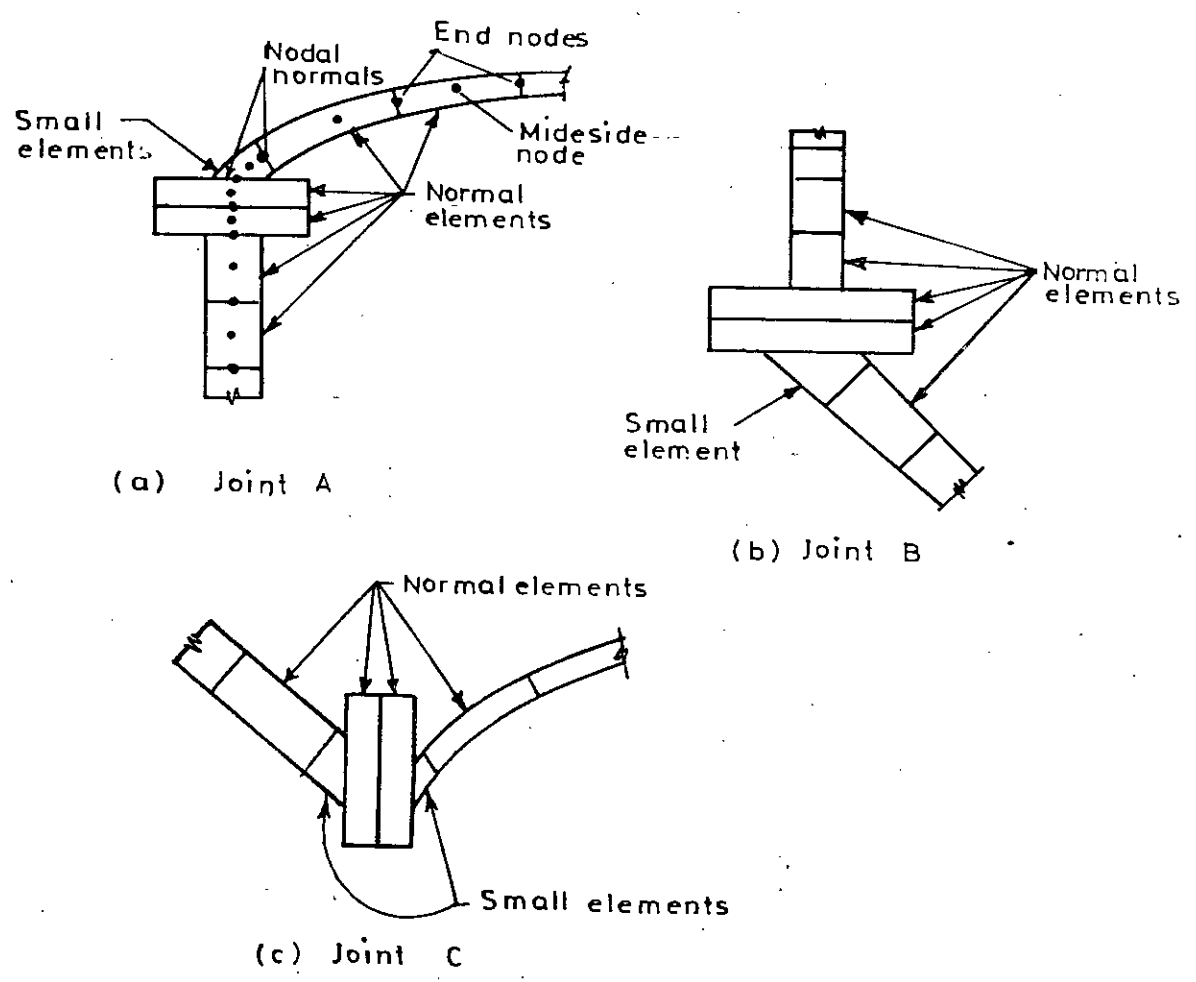


Fig. 4.5 Treatment of junctions.

The top dome may exert a meridional force F_1 , a shear force S_1 and a moment M_1 on the ring beam A at the point where it meets the ring beam. Similarly, the reactions of the cylindrical wall may be taken as F_2 , S_2 and M_2 respectively. The self-wt. W of the ring beam acts vertically downwards through its C.G. and H is the radial force due to hoop tension in the ring beam.

Summing forces in the vertical and horizontal directions we find in both the cases:

$$F_2 = W + F_1 \sin \theta$$

$$H = (S_1 - S_2) + F_1 \cos \theta$$

The vertical forces causing compression on horizontal sections of the ring-beam are of little concern. Whereas, it is seen that the radial force H , which causes hoop tension in the ring-beam and is the main parameter in the design of the ring-beam, remains practically the same in both the cases, since shifting the position of the ring beam laterally does not affect the magnitudes of F_1 , S_1 or S_2 .

If the value of H remains unchanged in the two cases, the hoop tension in the ring beam also remains practically the same; because, the change of diameter of the ring beam due to the small lateral movement is negligible compared to its actual diameter.

The rotational effect of the moments M_1 and M_2 and the shear forces S_1 and S_2 about the C.G. of the ring-beam is the same in both the cases. However, the rotation caused

by the forces F_1 and F_2 about the θ -axis passing through the c.g. of the ring beam is slightly different in the two cases. The rotation of the ring beam is, however, of little importance so long as the design of the ring beam itself is concerned. But the real effect will be in the value of M_2 and this point needs clarification.

In Fig. 4.4a,

$$M_2 = M_1 + H \cdot t/2 - (S_1 + F_1 \cos \theta)t - W e_1 + F_1 \sin \theta e_2$$

while in Fig. 4.4b,

$$M_2 = M_1 + H \cdot t/2 - (S_1 + F_1 \cos \theta)t$$

Assuming that the values of M_1 , H , S_1 and F_1 remain the same in both the cases we get

$$\Delta M_2 = W \cdot e_1 - (F_1 \sin \theta) e_2$$

It can be seen that $e_2 \ll e_1$

while on the other hand it can be guessed that $F_1 \gg W$.

As a result ΔM_2 tends to be negligible.

However, in some cases it may be that $e_2 = 0$, then

ΔM_2 will be equal to $W \cdot e_1$ which may be regarded as the net error in M_2 due to idealisation.

Similarly the effect of idealisation at joints B and C may be studied.

Finally, it is deemed necessary to present a little discussion regarding the division of the structure into elements and the special treatment of the junctions or kinks. The program has some limitation in dealing effectively with

sharp kinks. It requires that the nodal normal, the coordinate direction η , be approximately normal to the middle surface. Near the junctions the shapes of the elements become odd due to lack of continuity of slopes of the middle surfaces of the two elements on the two sides of the junction. To overcome this difficulty, the technique most commonly adopted is to keep the elements near the junction small compared to other normal elements (Fig. 4.5). This limits the odd element behaviour to a small zone near the kink which is then neglected during plotting the stresses and the trend of the curves outside the odd element is continued upto the joint. However, in this regard it must be noted here that this technique has been established to be reasonable by using it in simple cases where the actual deflected shape or stress pattern is known by exact theoretical analysis. This means that the behaviour of odd element is contained in those elements and so long as those elements are kept very small, their performance does not affect the overall behaviour of the structure. However, a different technique has been developed in eliminating the undesirable behaviour of the odd elements (Fig. 4.6). This new technique has been tested in simple cases and is found to be in excellent conformity with exact values. Both the techniques have been applied to the Intze tank and it has been observed that the two methods practically coincide everywhere except near the junctions.

The new technique is illustrated in Fig. 4.6 as applied to joint A. Comparing Figs. 4.6(a) with 4.6(b), it is observed

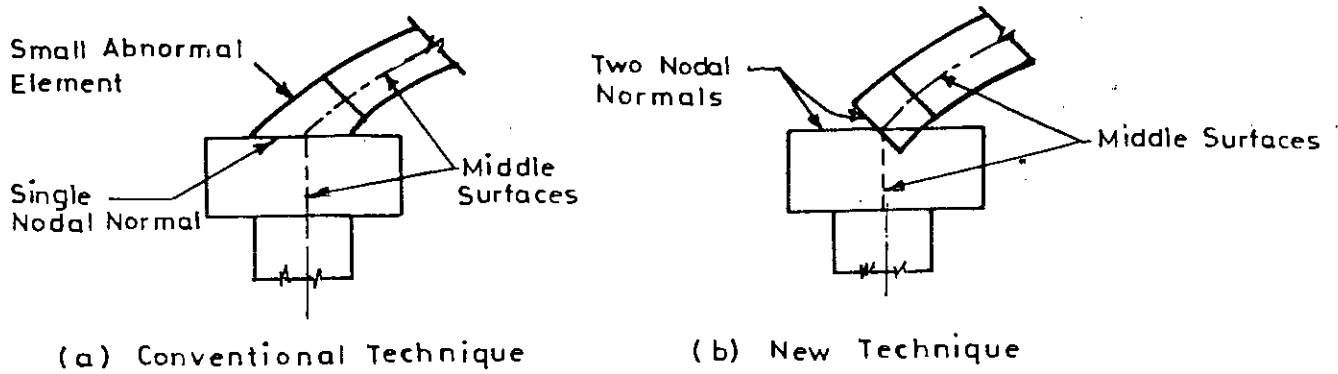


Fig. 4.6 Idealisation of joint A by two different approaches.

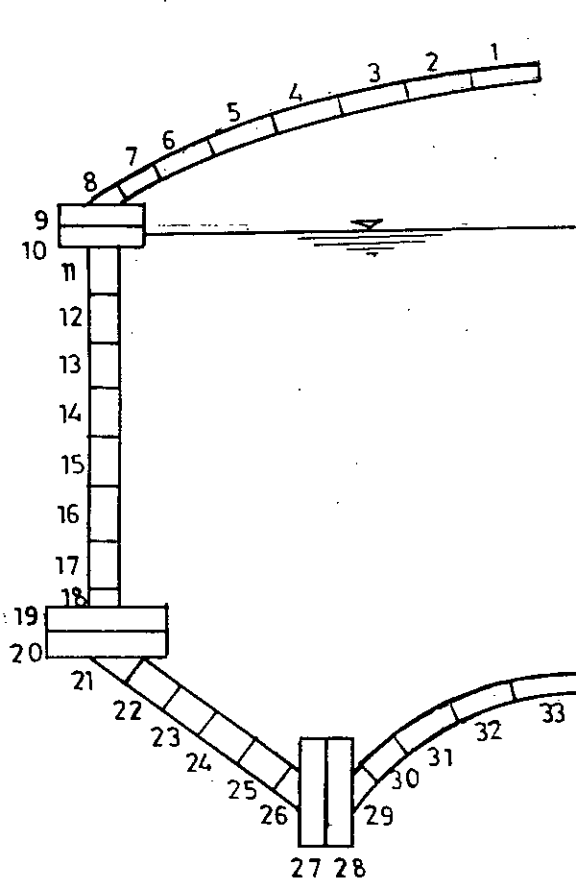


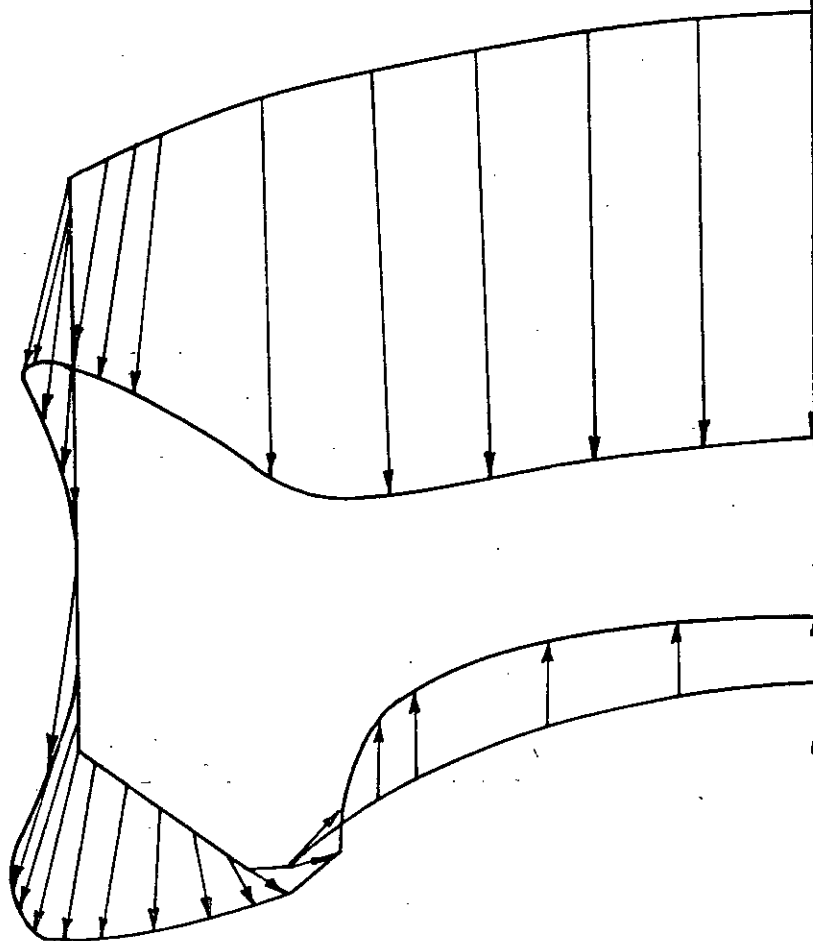
Fig. 4.7 Idealised section of the Intze tank showing division into 33 elements.

that, in the new technique, two nodal normals are erected at the node i where the middle surfaces of the adjacent elements have different slopes. This makes the nodal normal of each element perpendicular to its middle surface at the node. This idealisation practically amounts to removing a small quantity of material from one side of the middle surface and adding it to the other side so that the odd shaped element now assumes a normal shape. At first sight, this process may appear to be awkward and unrealistic, but consideration of strain energy for bending will reveal that shifting a small quantity of material from tension side to compression side or vice versa does not change the total quantity of strain energy so long as the behaviour of the material is linearly elastic. Since the finite element formulation is based on the minimisation of strain energy, the above idealisation does not affect the stiffness terms, though it ensures a gentle behaviour of the element.

Fig. 4.7 shows the scheme followed in dividing the Intze tank into 33 cubic elements. All the case studies have been analysed using the same scheme.

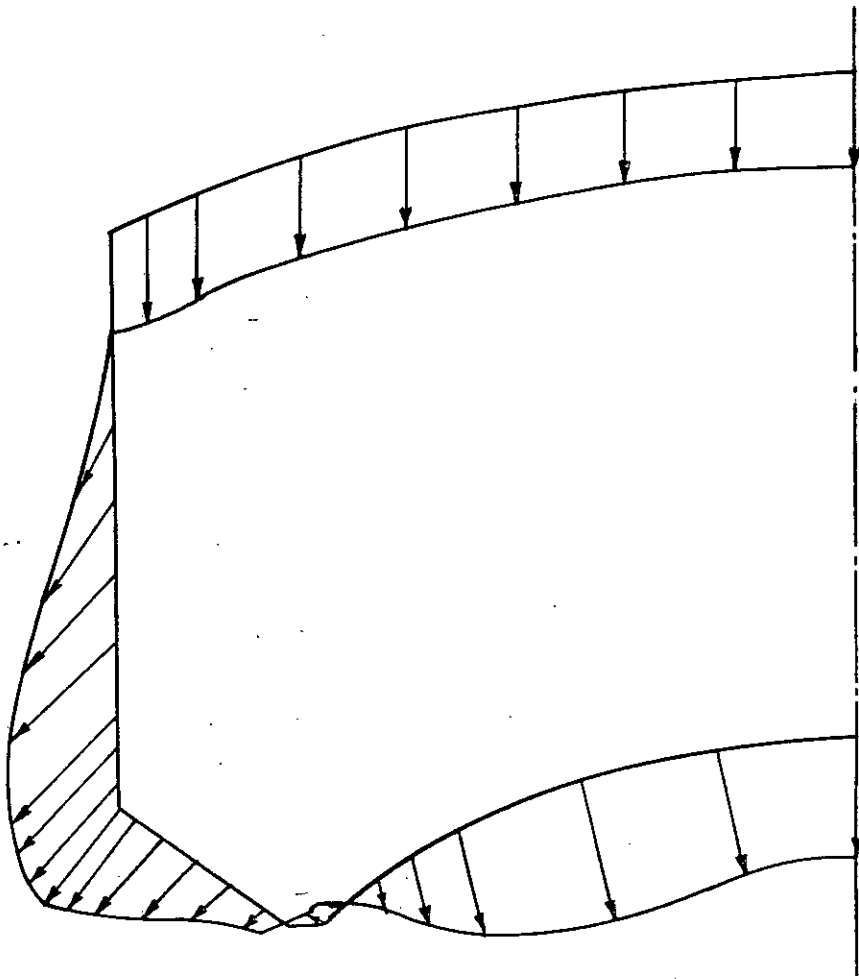
4.4 Graphical Representation of Results

The Intze tanks, considered in case studies 1 to 4 in Chapter 2, have been analysed by Finite Element method; first, with the original dimensions of the tanks, and the results are presented graphically in this article. Based on the results of the Finite Element analysis the sections of the various parts of the tanks have been suitably modified and then reanalysed. The results of reanalysis for modified dimensions are also shown graphically for each case study following the results of analysis with original dimensions. Fig. 4.8 to 4.28 represent the results of analysis for case study-1, Figs. 4.29 to 4.37 for case study-2, Figs. 4.38 to 4.46 for case study-3 and Fig. 4.47 to 4.55 for case study-4.



Scale: Dimension 1" = 64", Displacement 1" = 2×10^{-2} inch

Fig. 4.8 Displaced shape for gravity.
(Case study 1: original dimensions shown in Fig. 2.11)



Scale: Dimension 1" = 64", Displacement 1" = 2×10^{-2} inch

Fig. 4.9 Displaced shape for hydrostatic pressure.
(Case study 1: original dimensions)

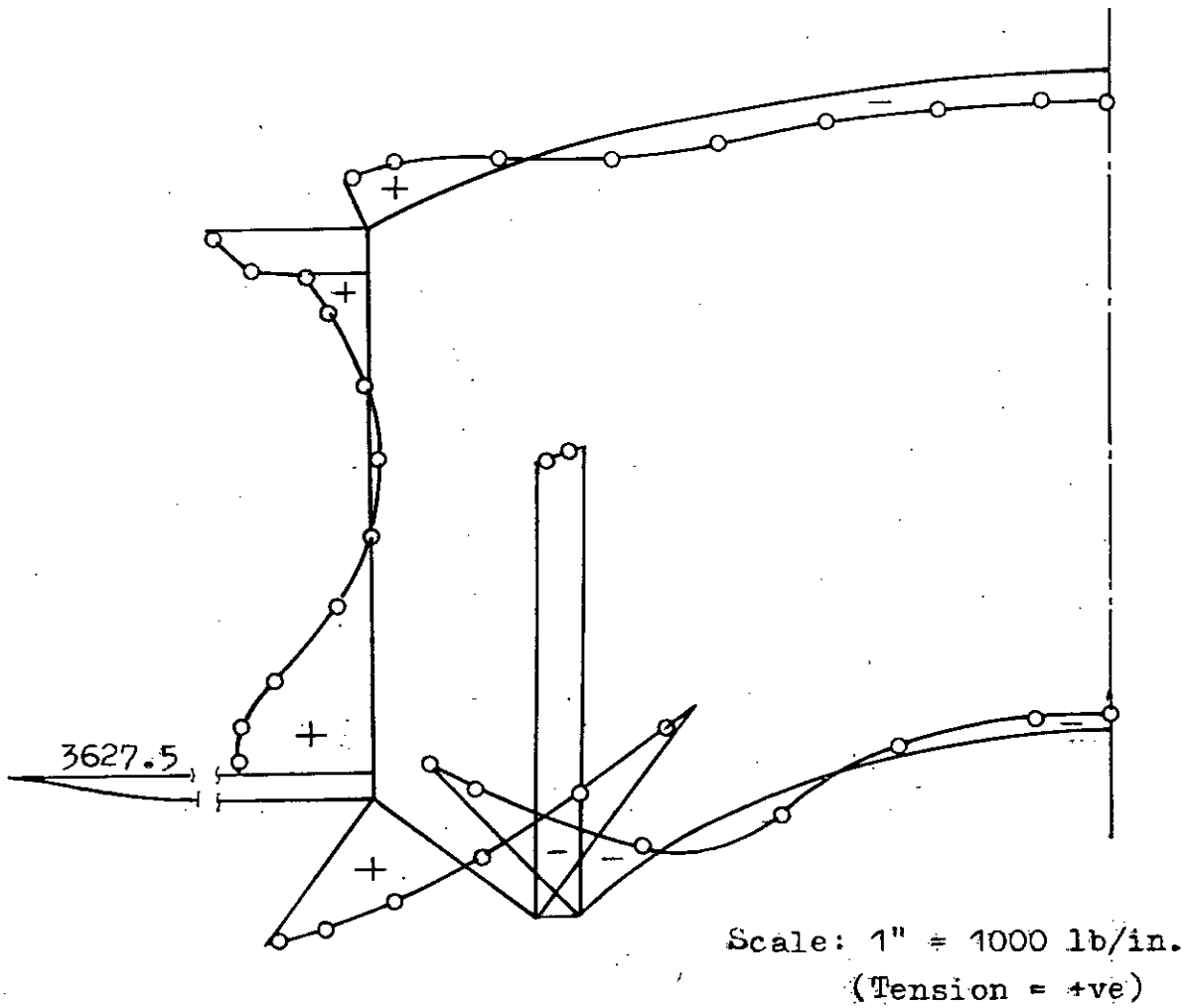


Fig. 4.10 Hoop force for gravity.
(Case study 1: original dimension)

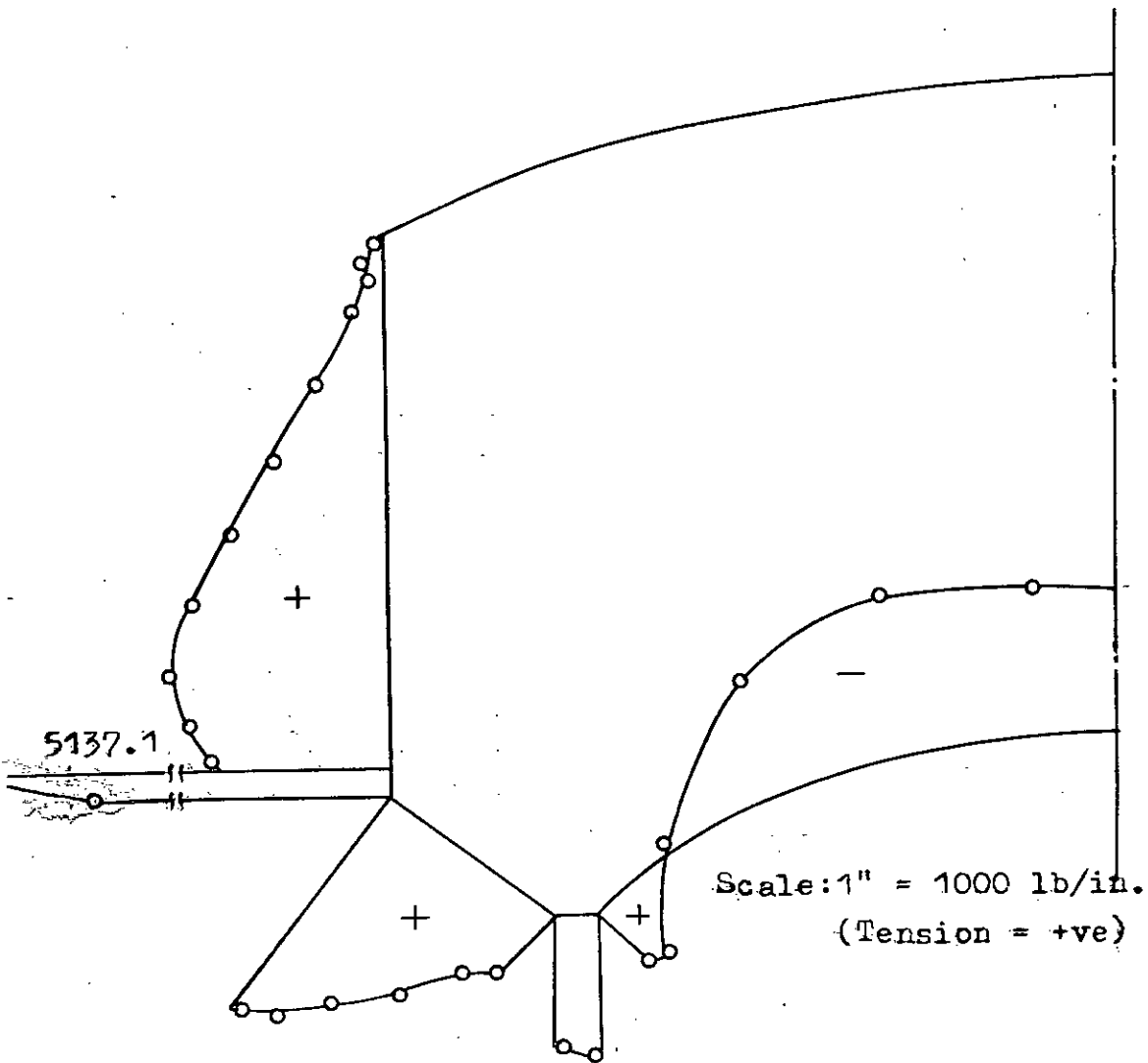


Fig. 4.11 Hoop force for hydrostatic pressure.
(Case study 1: original dimensions)

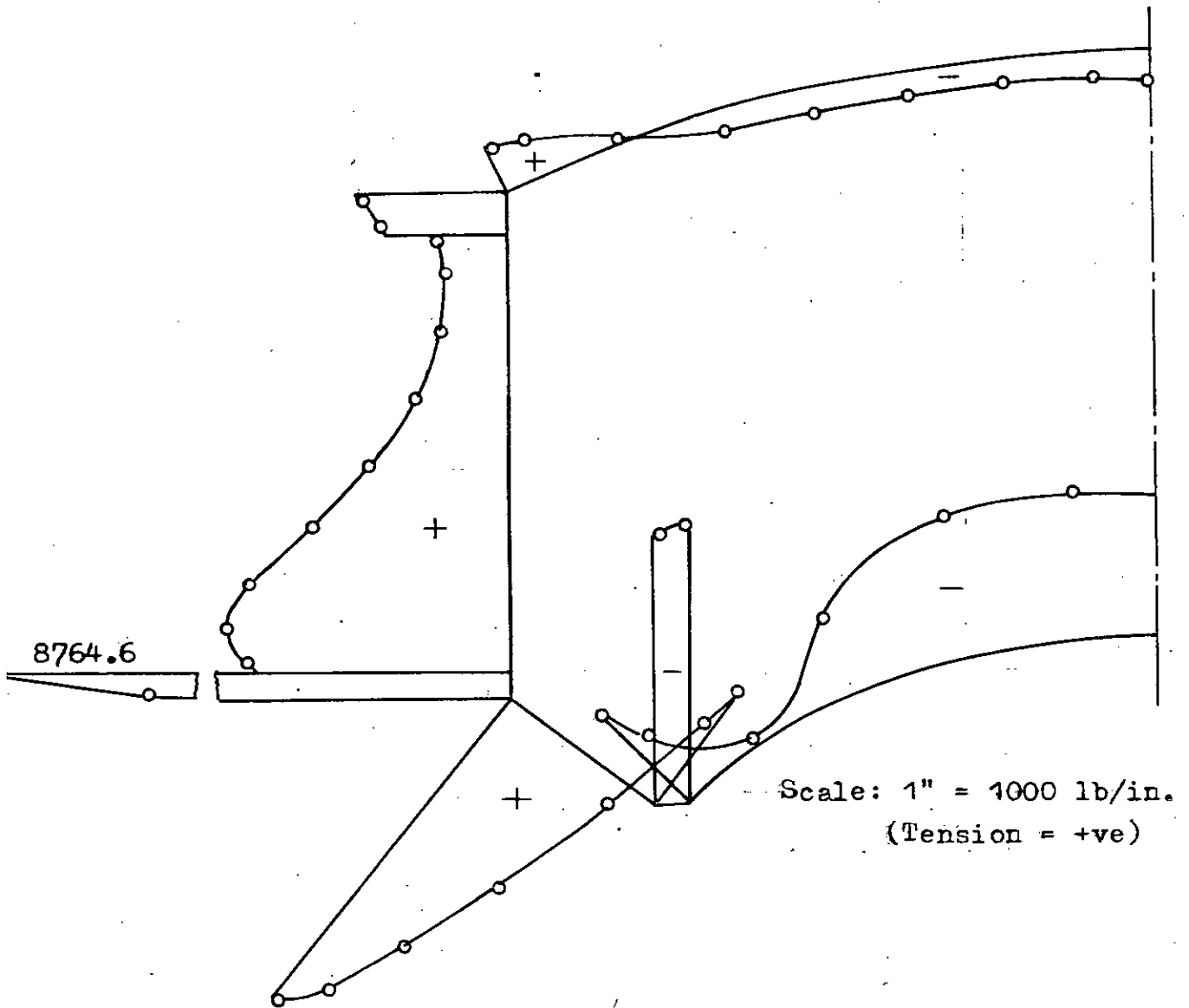
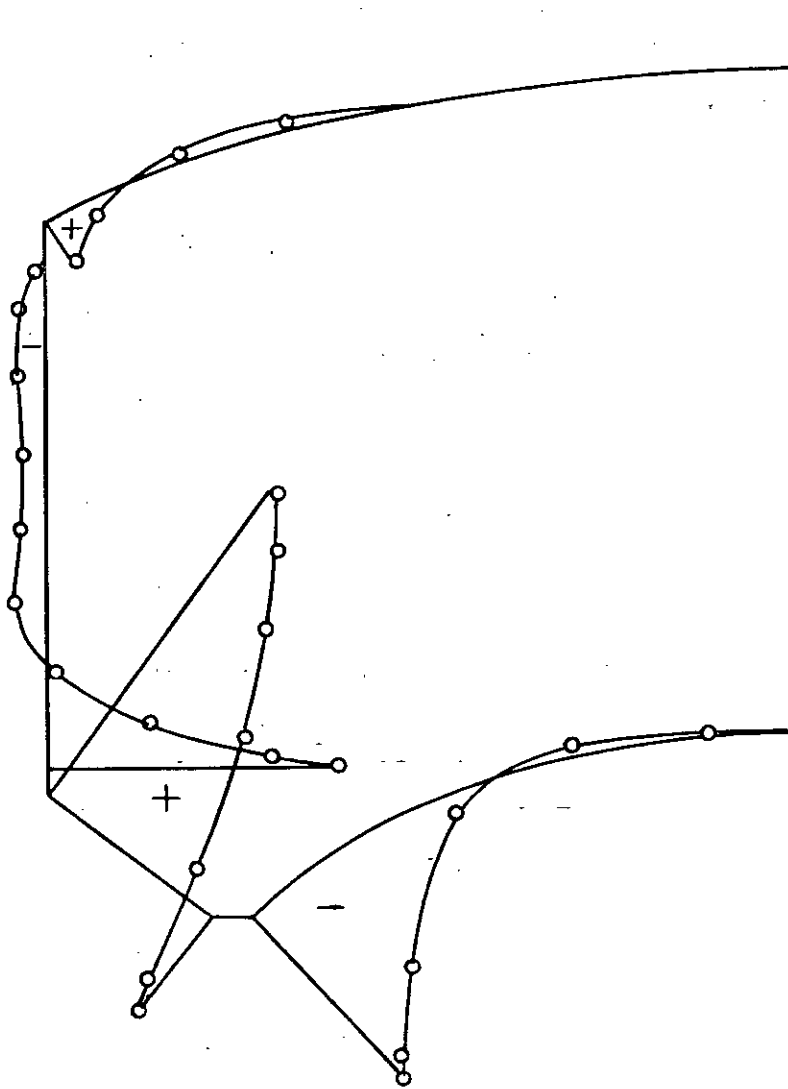


Fig. 4.12 Combined hoop force for gravity and hydrostatic pressure.
(Case study 1: original dimensions)



Scale: 1" = 2000 lb-in/in.

(Water face tension = -ve)

Fig. 4.13 Meridional moment for gravity.
(Case study 1: original dimensions)

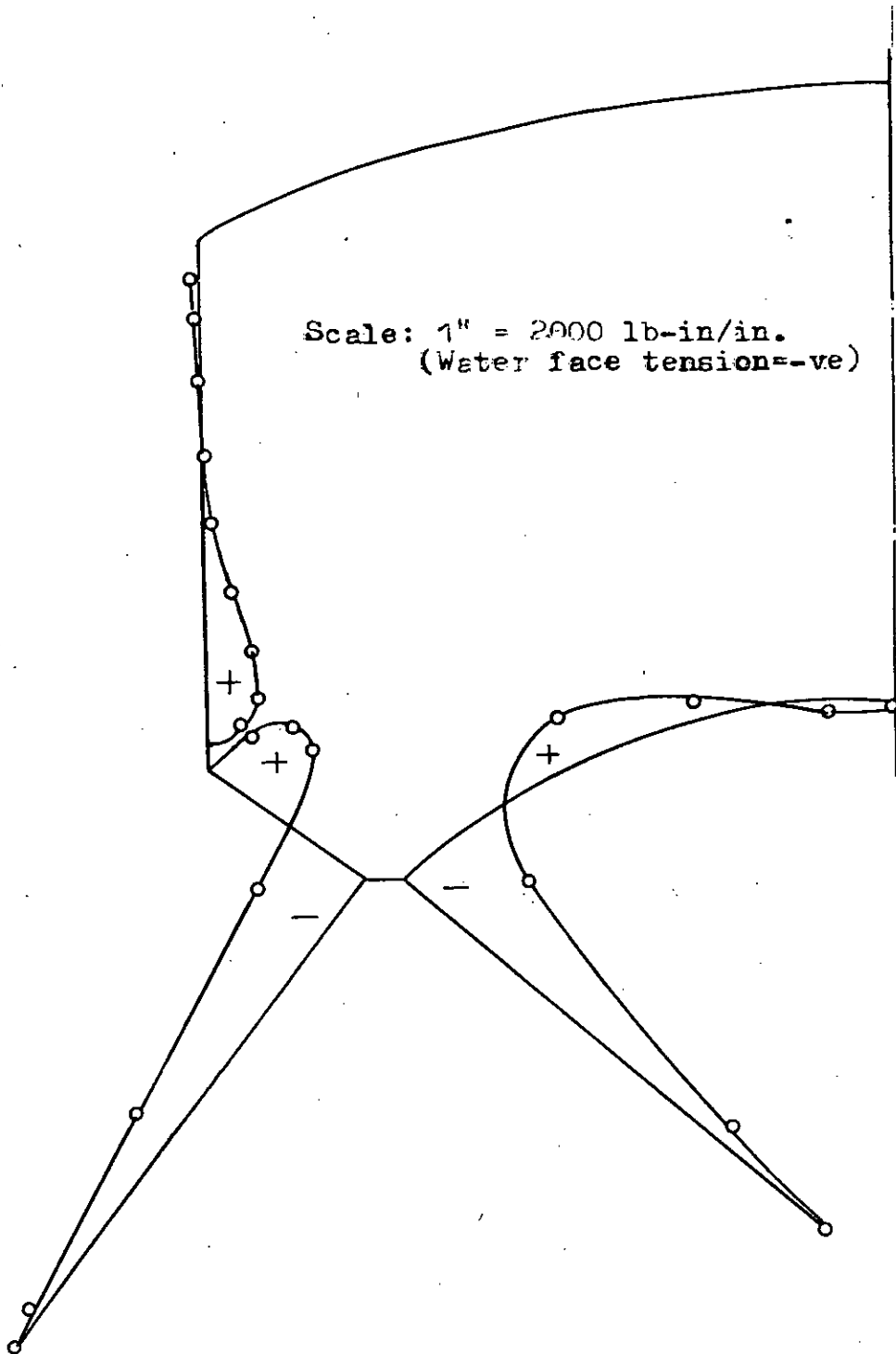


Fig. 4.14 Meridional moment for hydrostatic pressure.
(Case study 1: original dimensions)

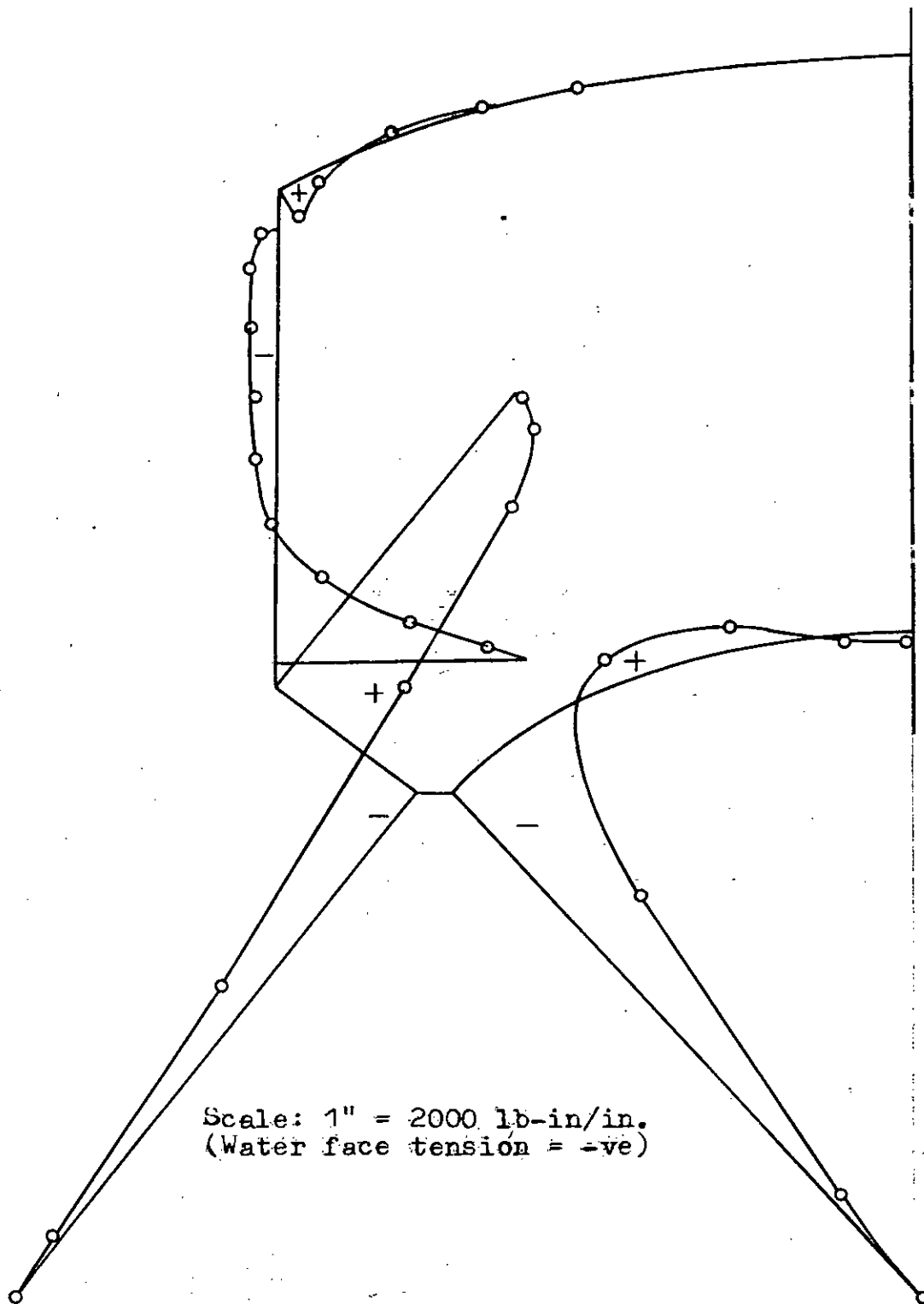


Fig. 4.15 Combined meridional moment for gravity and hydrostatic pressure.
(Case study 1: original dimensions)

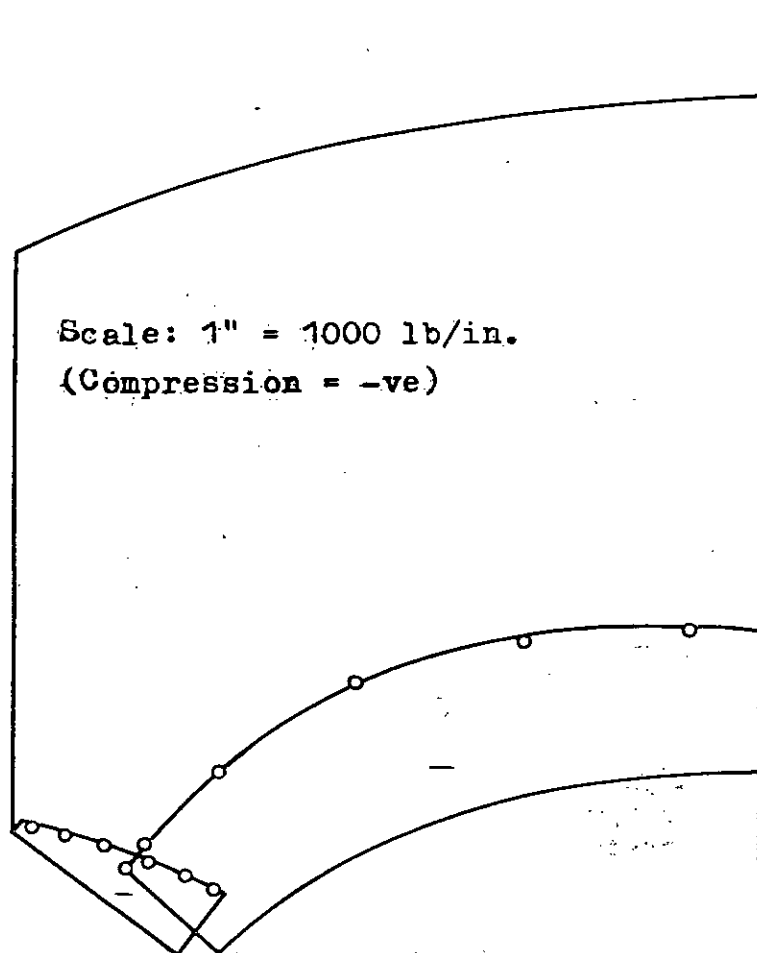


Fig. 4.16 Meridional membrane force for hydrostatic pressure.
(Case study 1: original dimensions)

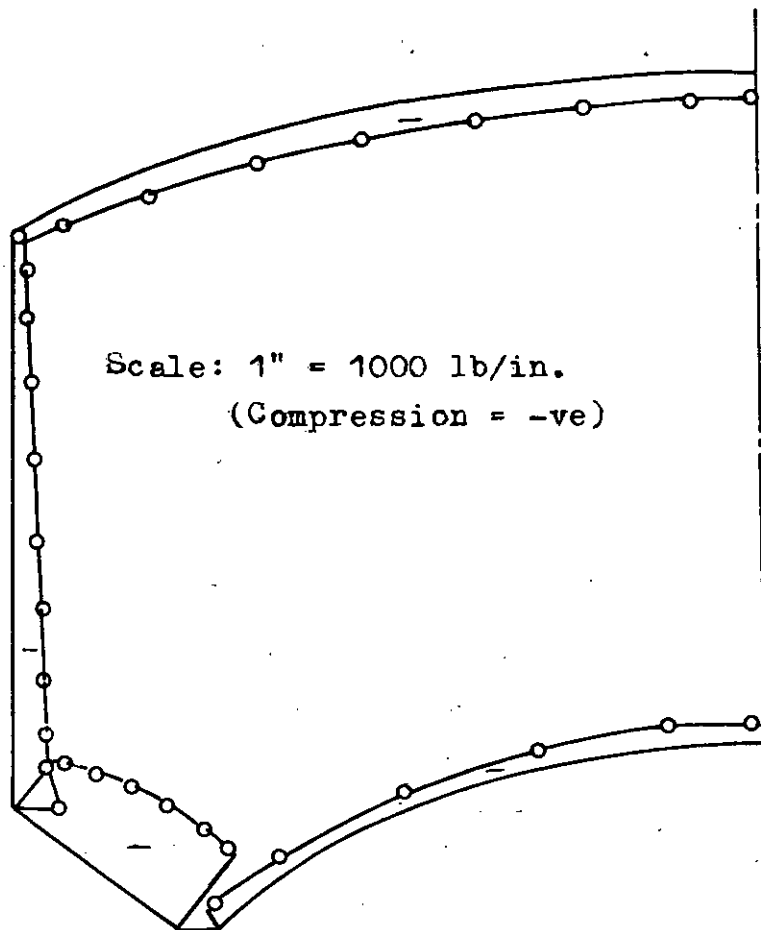


Fig. 4.17 Meridional membrane force for gravity.
(Case study 1: original dimensions)

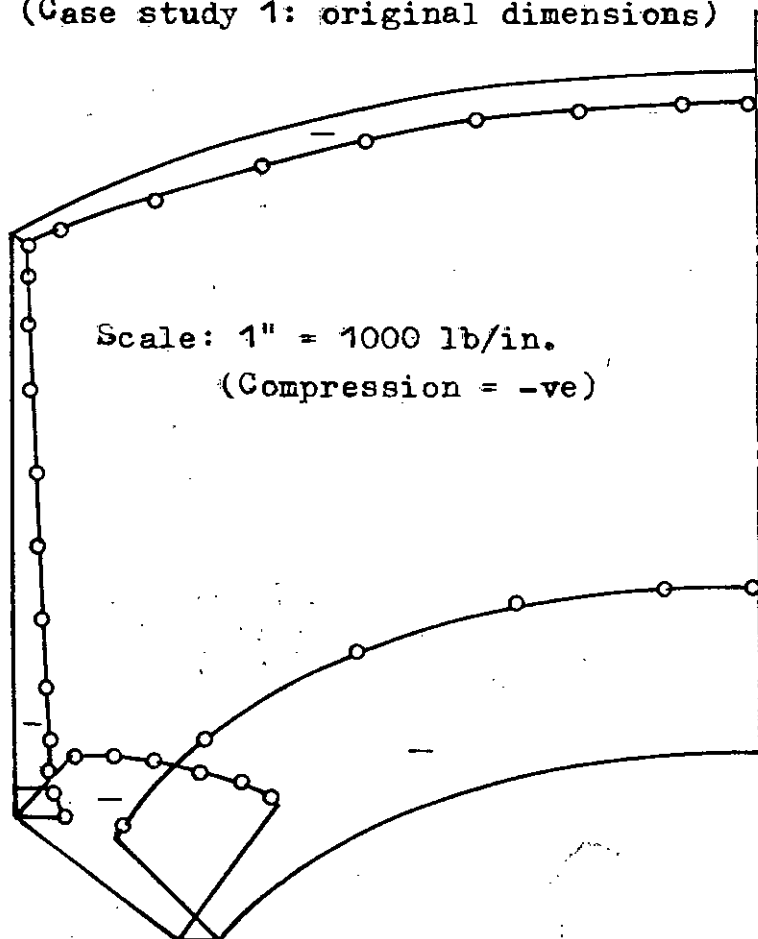
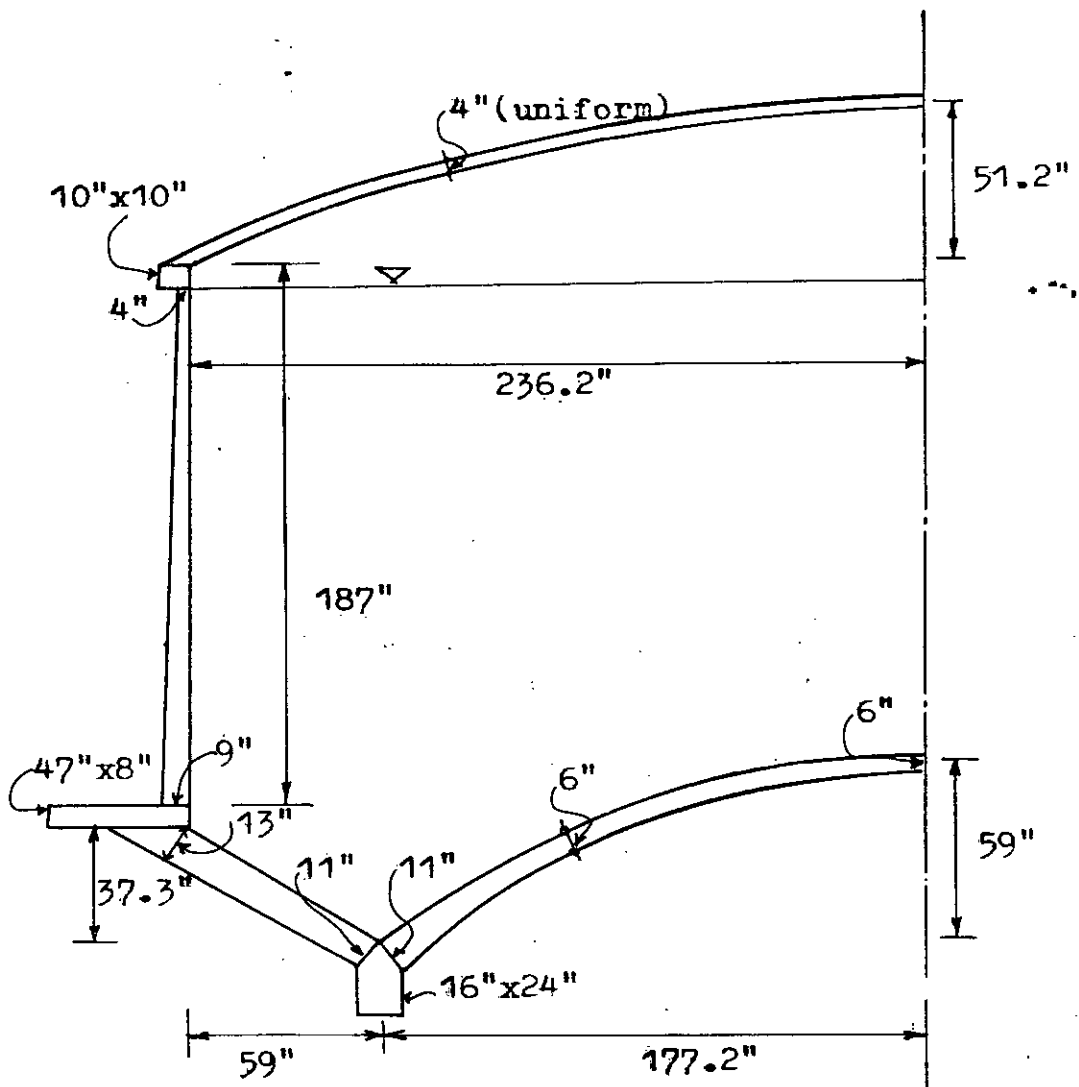


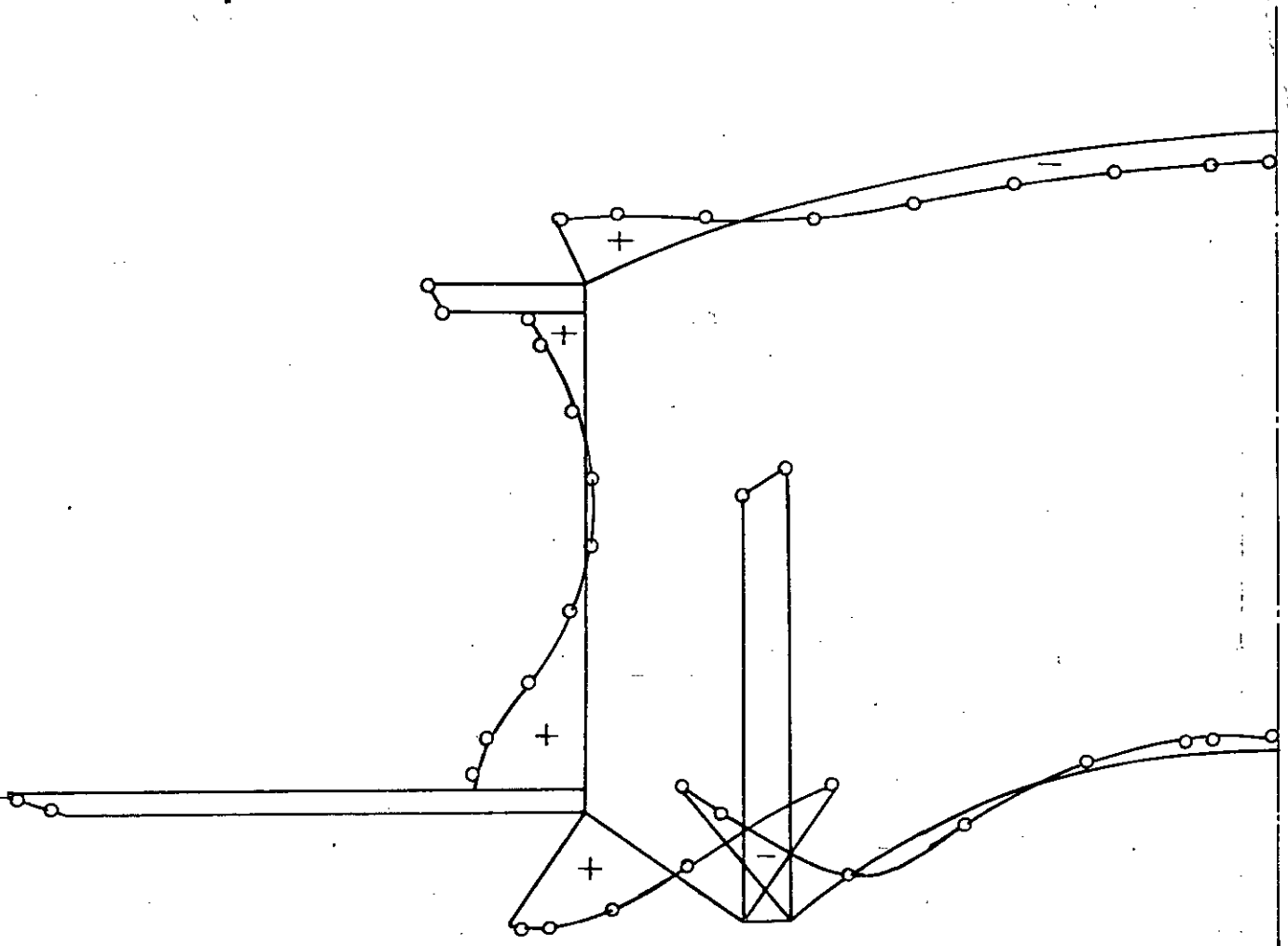
Fig. 4.18 Combined meridional membrane force for
hydrostatic pressure and gravity.
(Case study 1: original dimensions)



Scale: 1" = 64"

(Capacity = 1.18, 200 gallons)

Fig. 4.19 Section showing modified dimensions.
(Case study 1)



Scale: 1" = 1000 lb/in.
(Tension = +ve)

Fig. 4.20 Hoop force for gravity.
(Case study 1: modified dimensions)

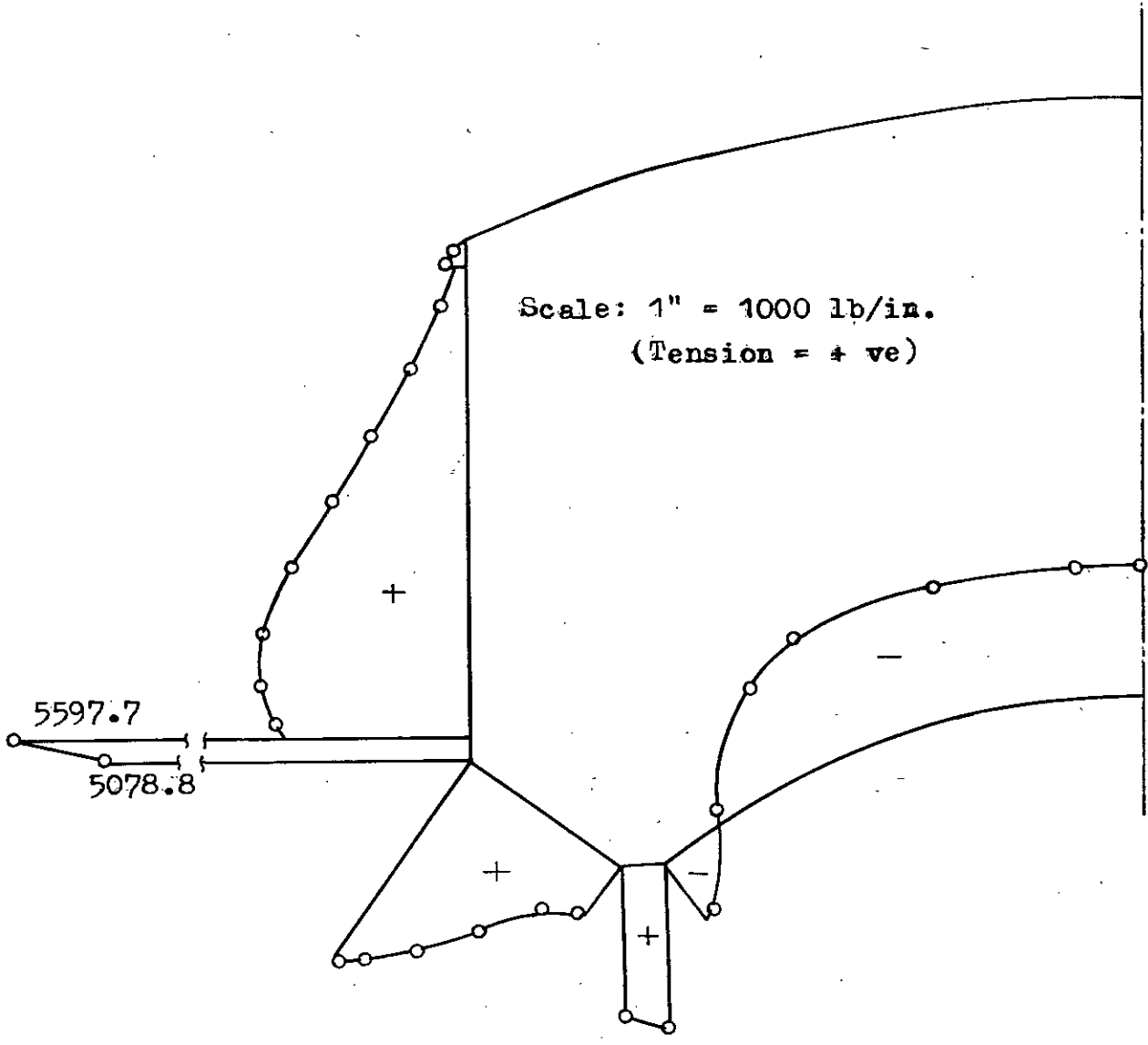


Fig. 4.21 Hoop force for hydrostatic pressure.
(Case study 1: modified dimensions)

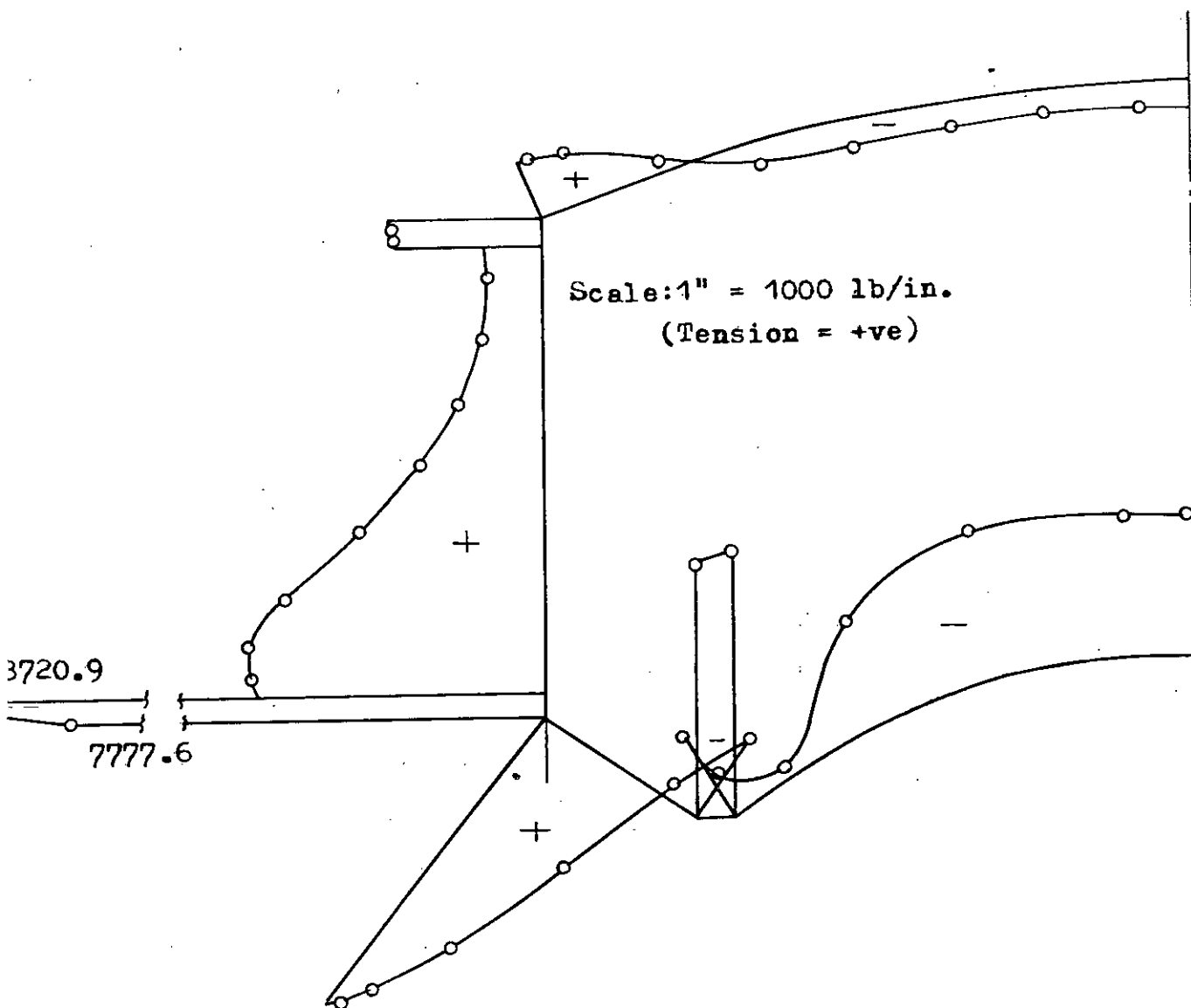


Fig. 4.22 Combined hoop force for gravity and hydrostatic pressure.
(Case study 1: modified dimensions)

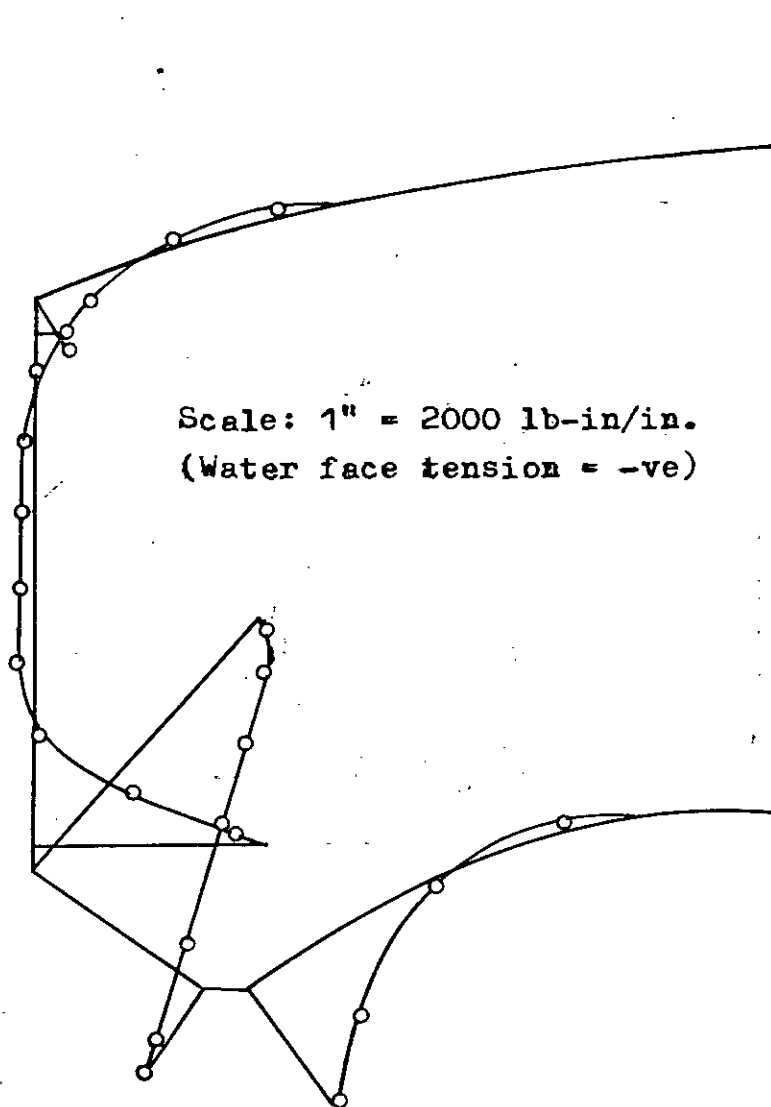


Fig. 4.23 Meridional moment for gravity.
(Case study 1: modified dimensions)

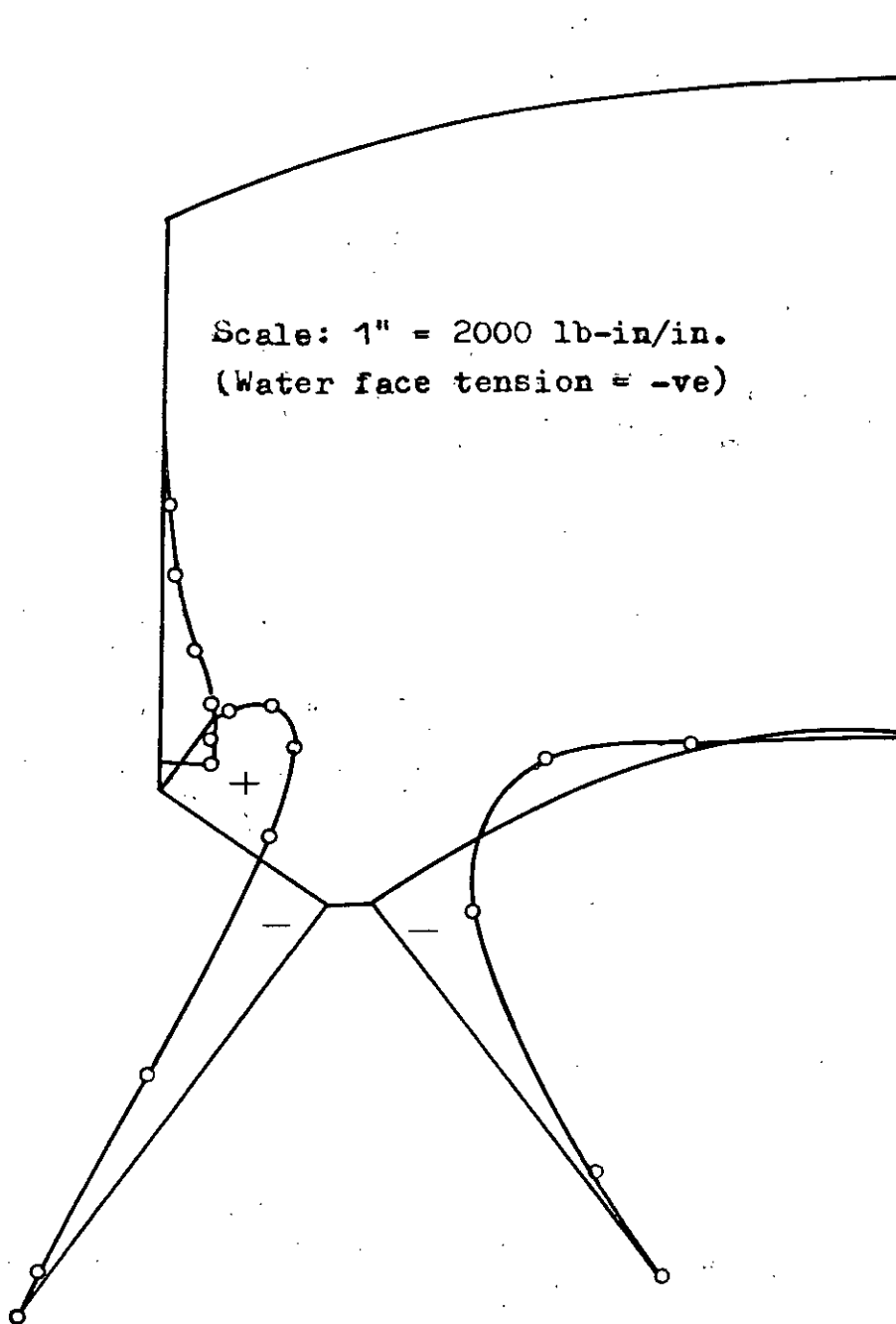


Fig. 4.24 Meridional moment for hydrostatic pressure.
(Case study 1: modified dimensions)

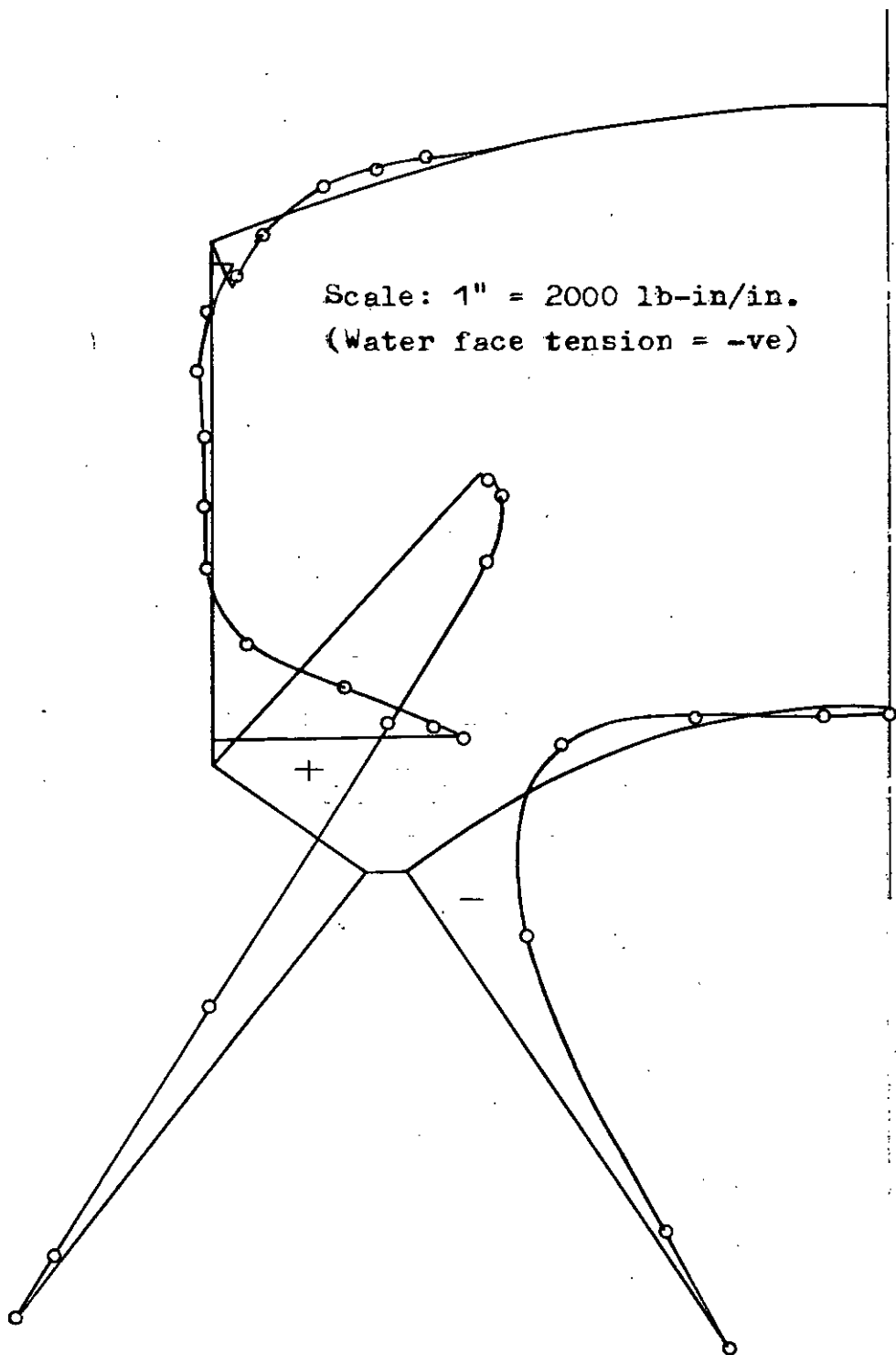


Fig. 4.25 Combined meridional moment for gravity and hydrostatic pressure.
(Case study 1: modified dimensions)

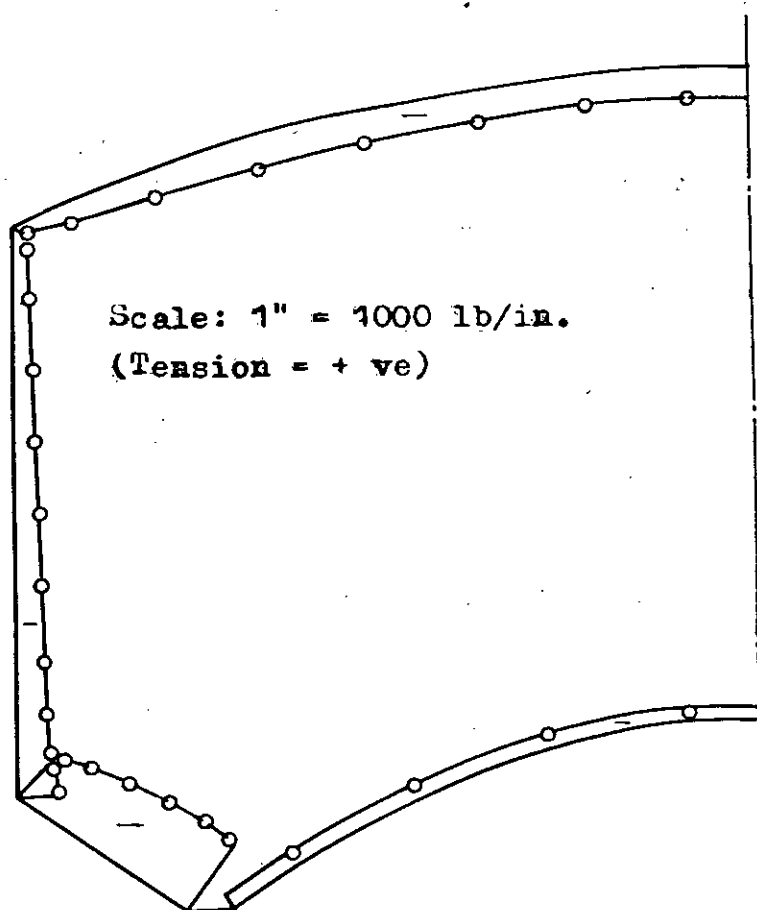


Fig. 4.26 Meridional membrane force for gravity.
(Case study 1: modified dimensions)

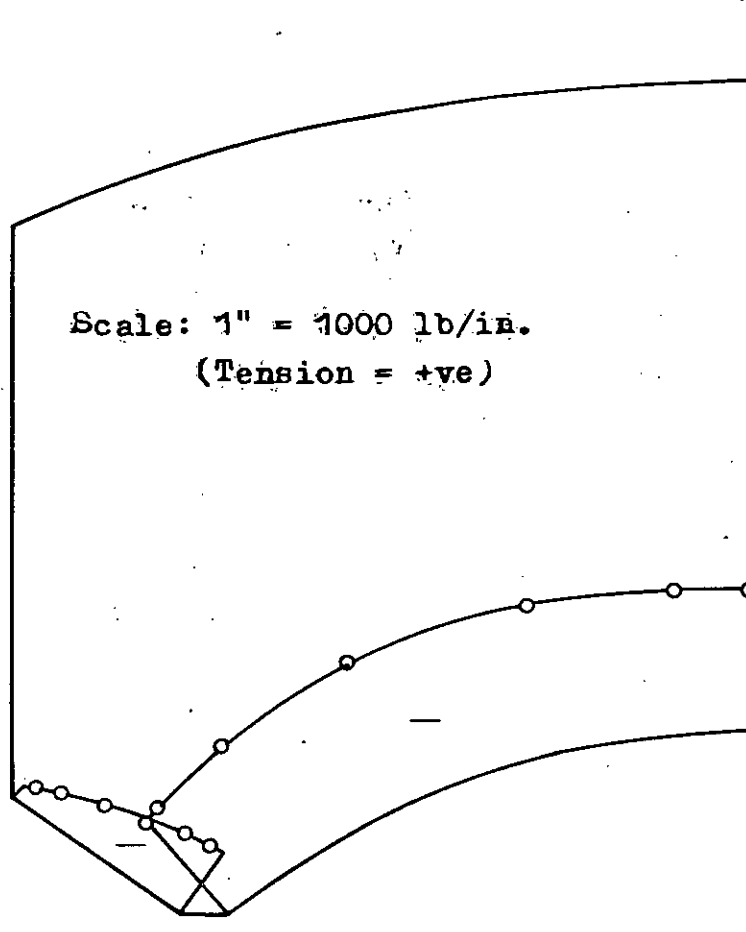


Fig. 4.27 Meridional membrane force for
Hydrostatic pressure.
(Case study 1: modified dimensions)

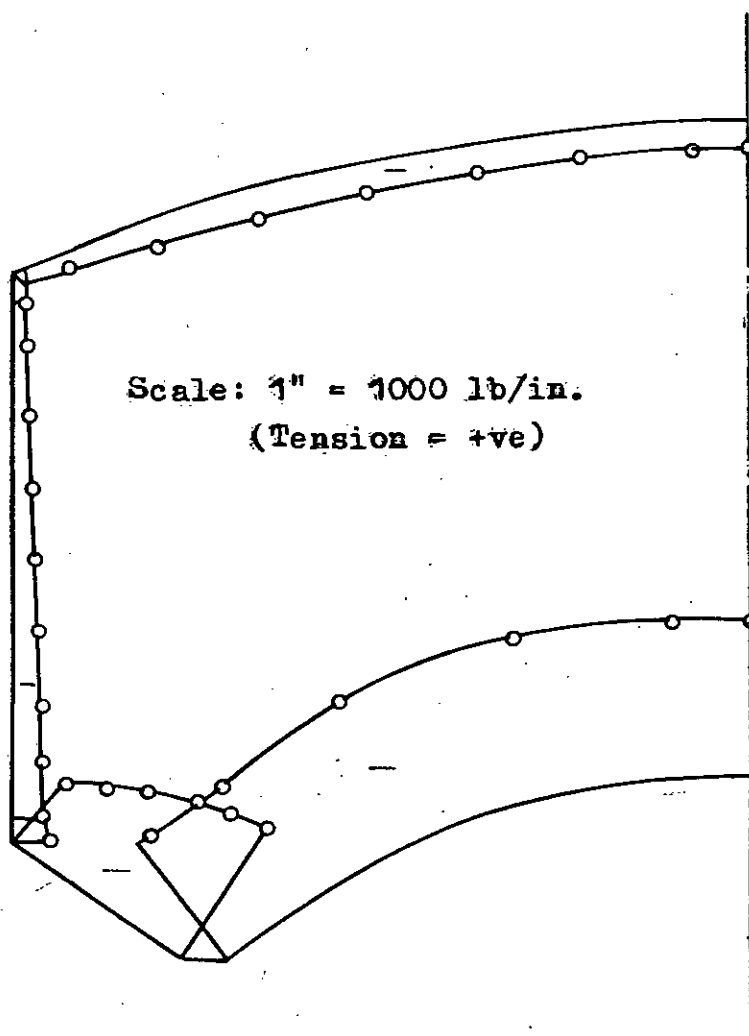


Fig. 4.28 Combined meridional membrane force for gravity and hydrostatic pressure. (Case study 1: modified dimensions)

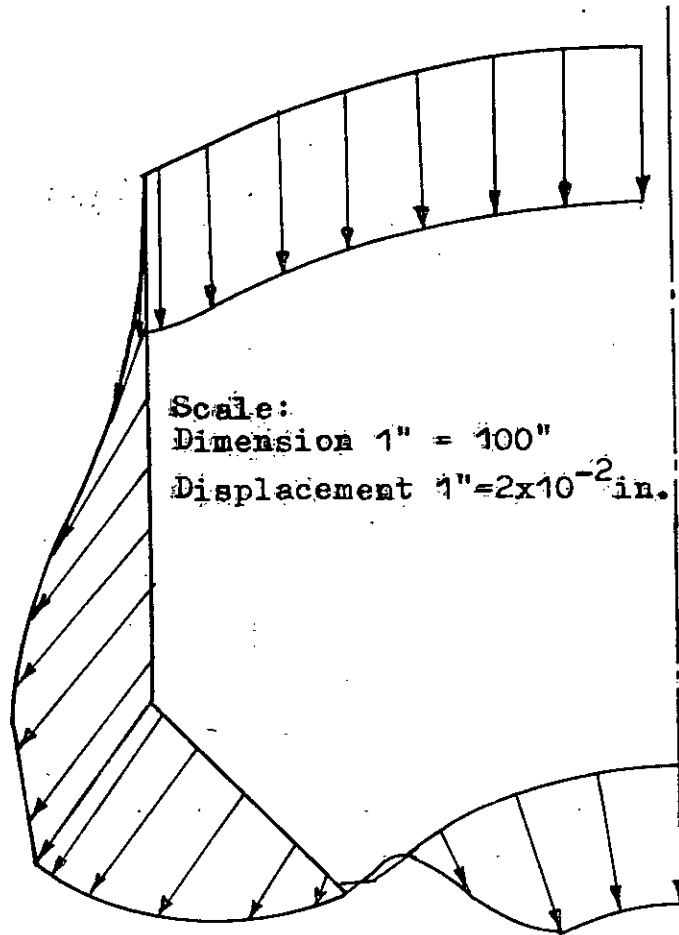


Fig. 4.29 Displaced shape for hydrostatic pressure.
(Case study 2: original dimensions vide
Fig. 2.14)

Scale:
 Dimension 1" = 100 in.
 Displacement 1" = 2×10^{-2} in.

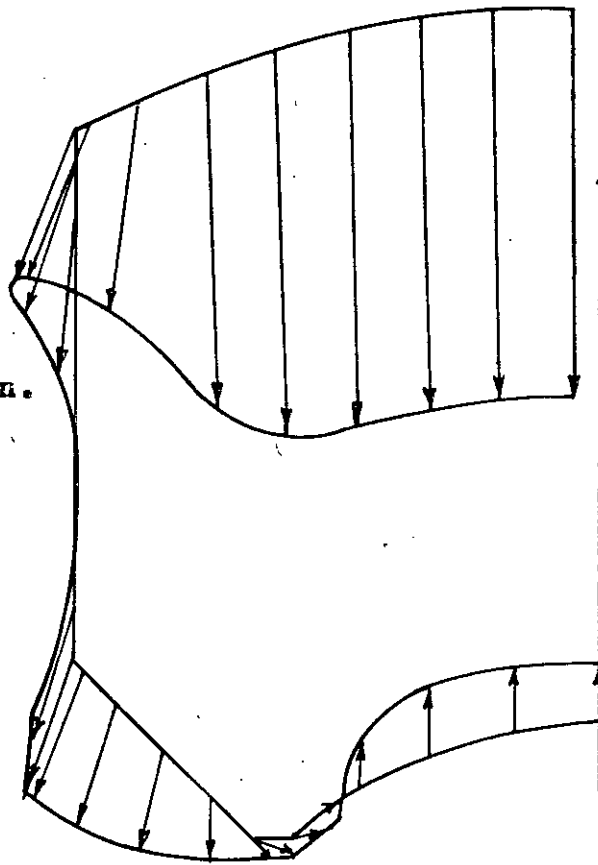


Fig. 4.30 Displaced shape for gravity.
 (Case study 2: original dimensions)

Scale: 1" = 1000 lb/in.
 (Tension = +ve)

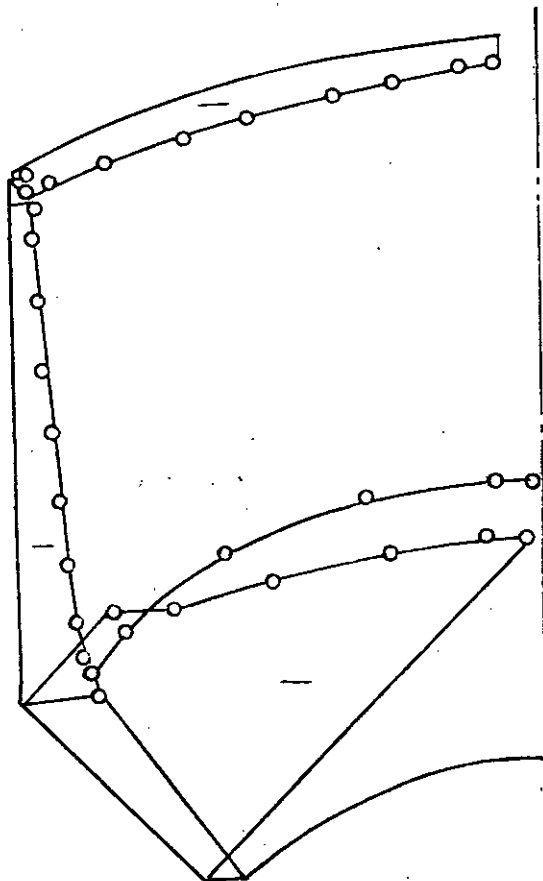


Fig. 4.31 Combined meridional membrane force for
 gravity and hydrostatic pressure.
 (Case study 2: original dimensions)

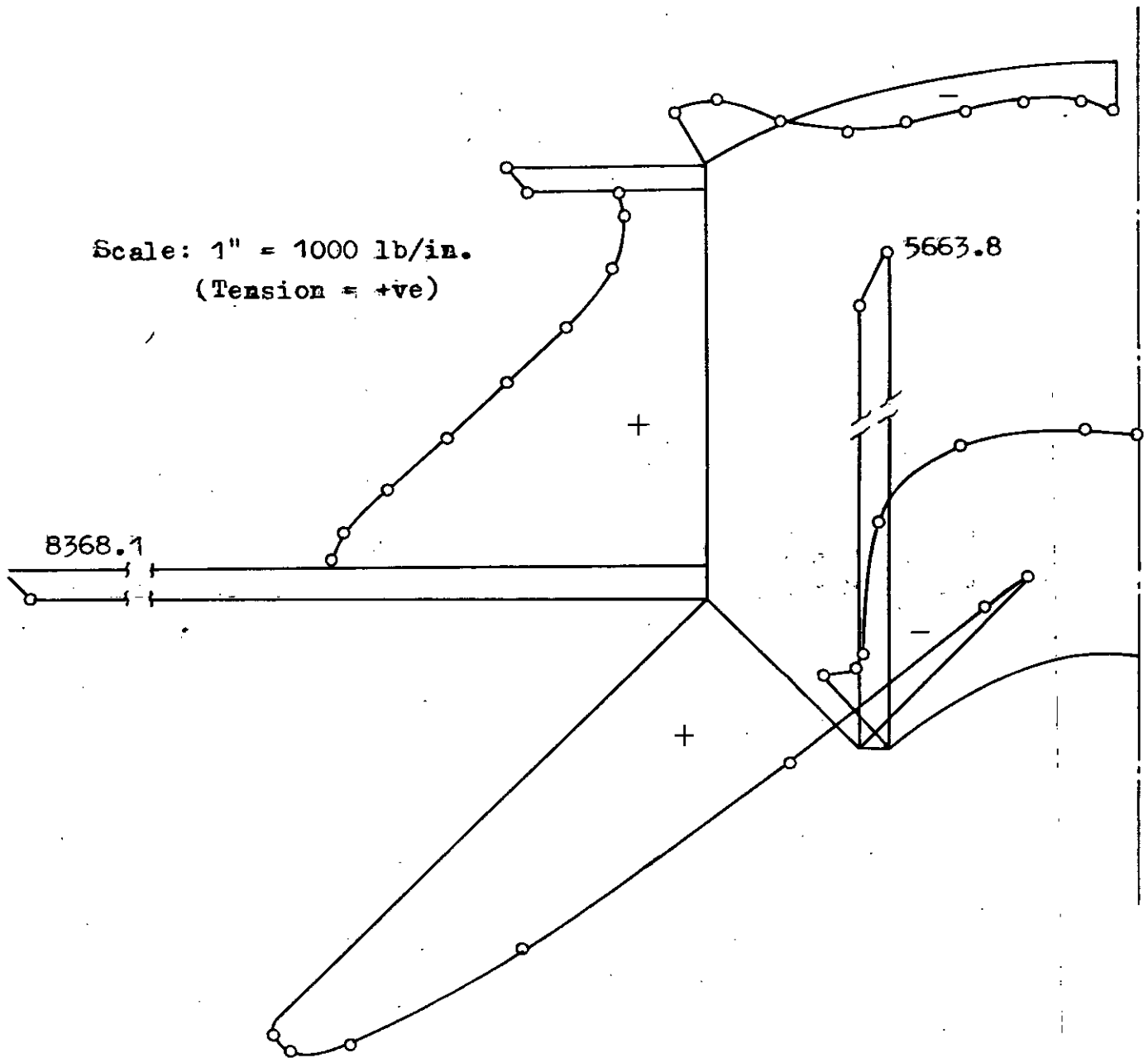


Fig. 4.32 Combined hoop force for gravity and hydrostatic pressure.
(Case study 2: original dimensions)

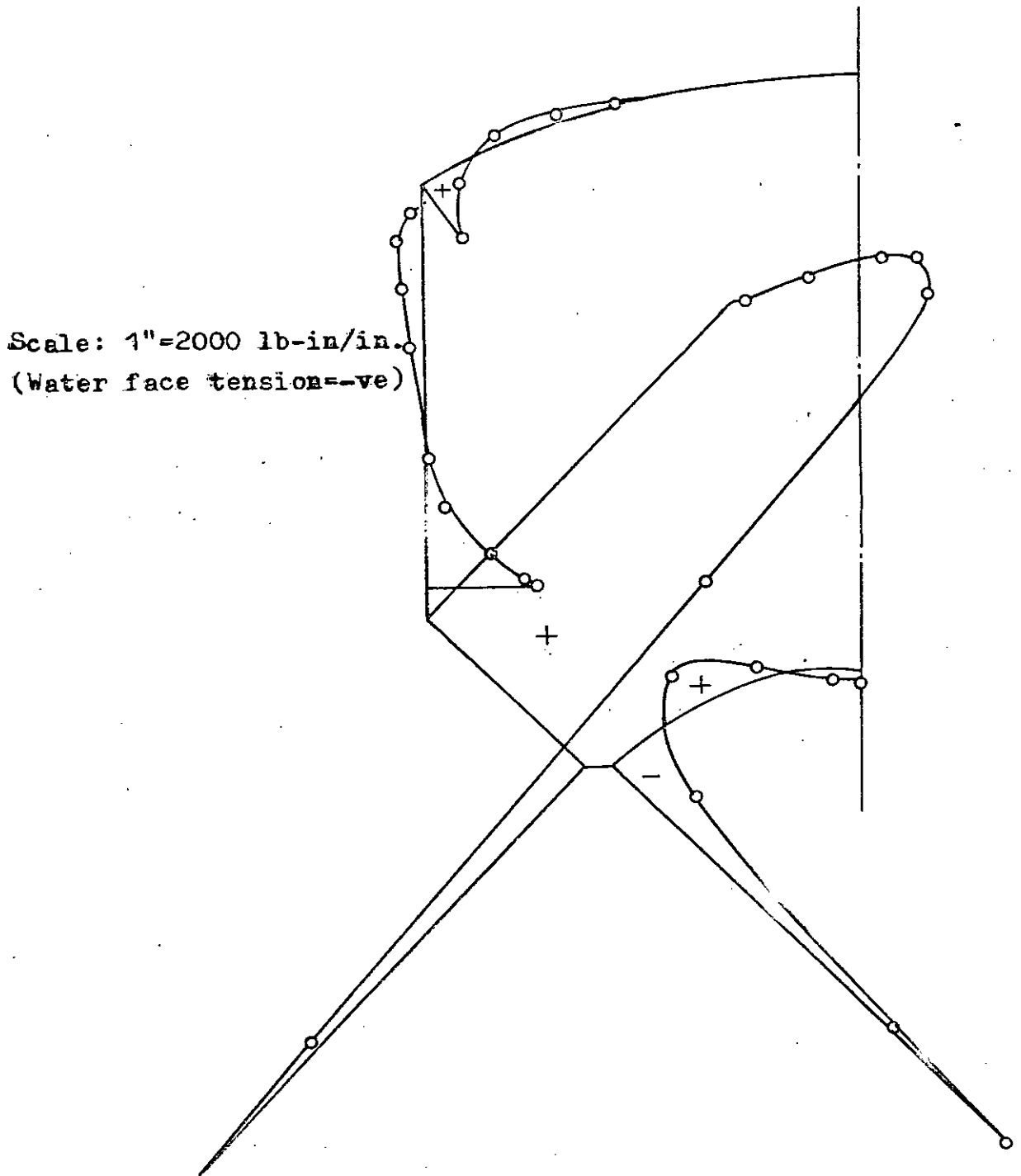
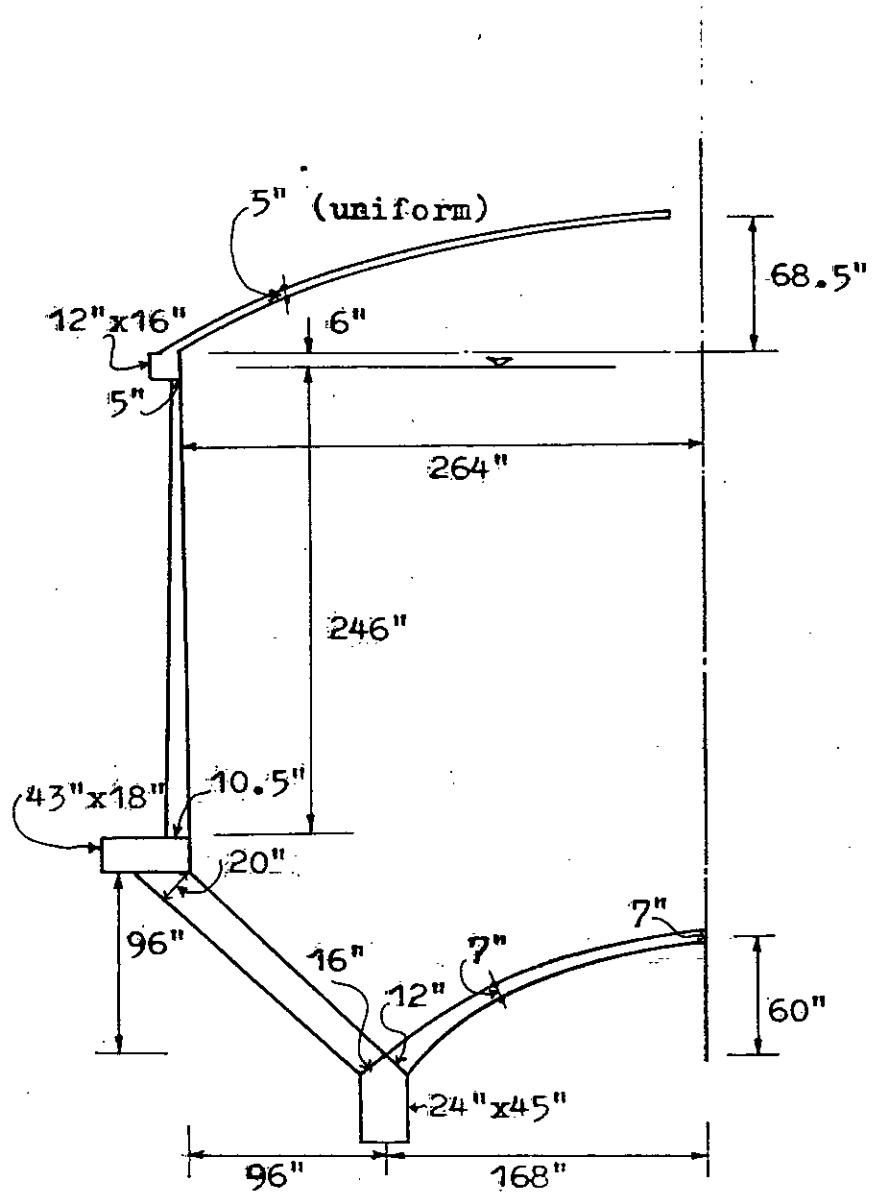
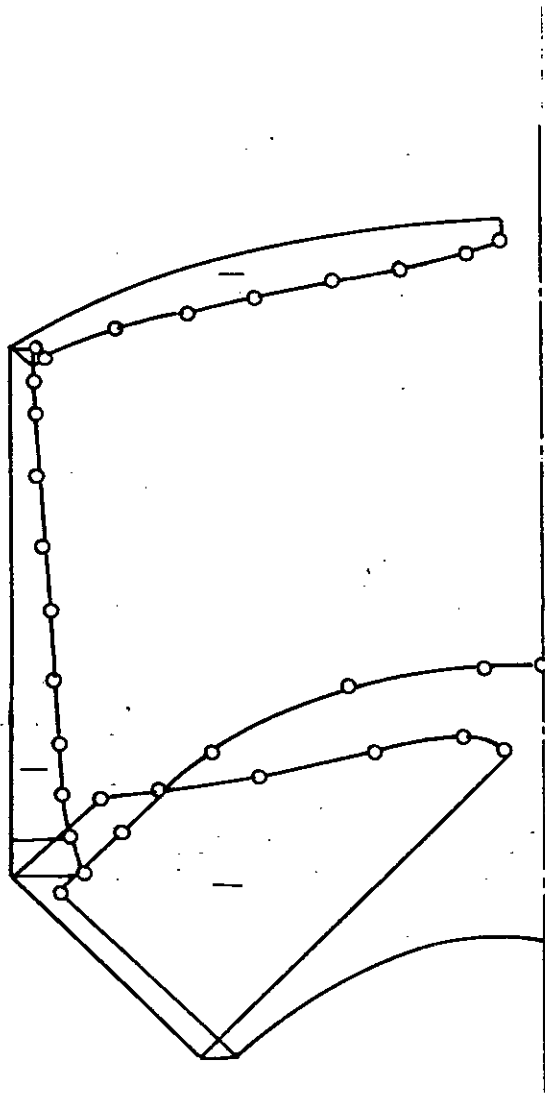


Fig. 4.33 Combined meridional moment for gravity and hydrostatic pressure.
(Case study 2: original dimensions)



Scale: 1" = 100"
 (Capacity = 250,000 gallons)

Fig. 4.34 Section showing modified dimensions.
 (Case study 2)



Scale: 1" = 1000 lb/in.
(Tension = +ve)

Fig. 4.35 Combined meridional membrane force
for gravity and hydrostatic pressure.
(Case study 2: modified dimensions)

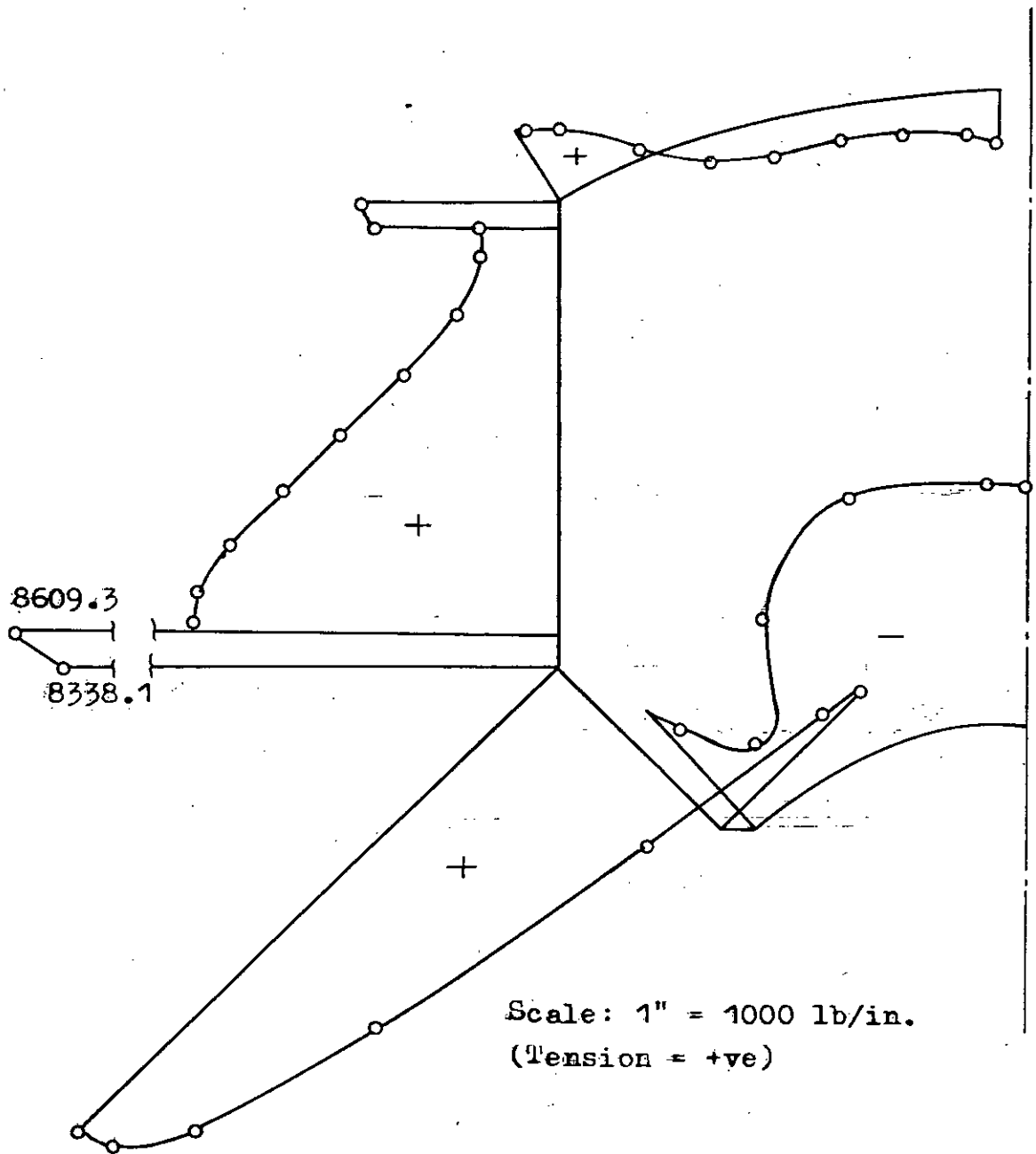


Fig. 4.36 Combined hoop force for gravity and hydrostatic pressure.
(Case study 2: modified dimensions)

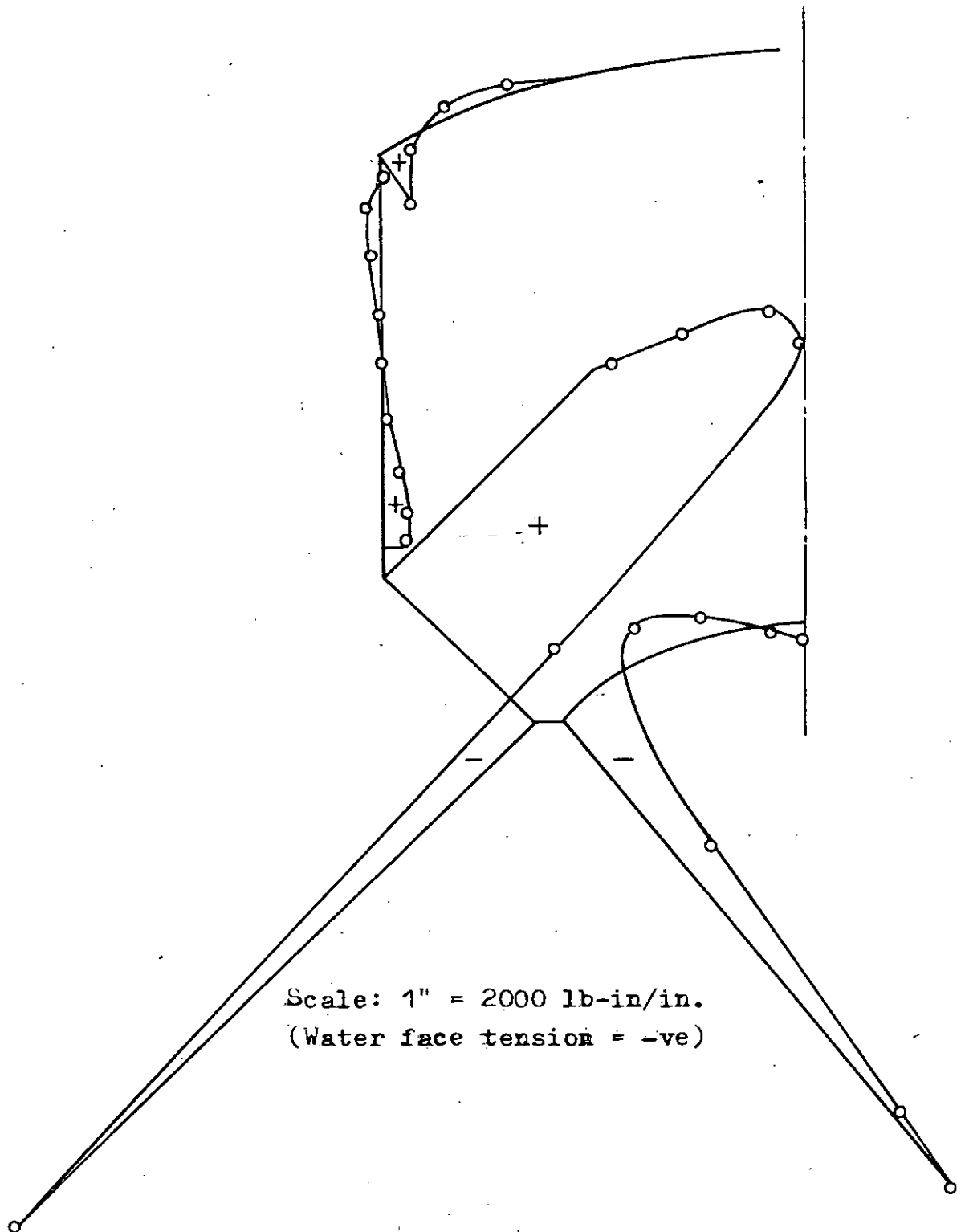
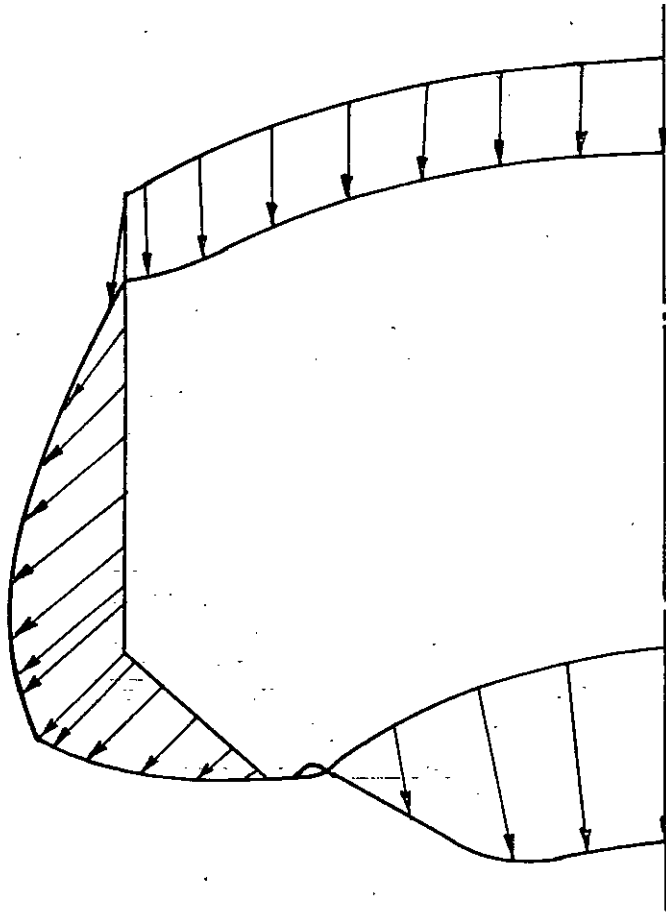


Fig. 4.37 Combined meridional moment for gravity and hydrostatic pressure.
 (Case study 2: modified dimensions)



Scale:

Dimension 1" = 100"

Displacement 1" = 2×10^{-2} inch.

Fig. 4.38 Displaced shape for hydrostatic pressure.
(Case study 3: original dimensions vide
Fig. 2.16)

Scale:
 Dimension 1"=100"
 Displacement 1"= 2×10^{-2} in.

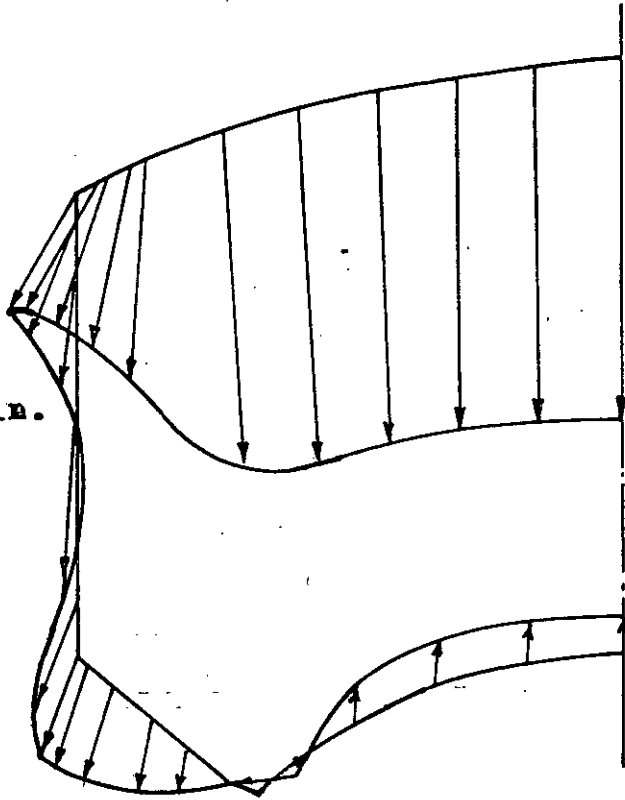


Fig. 4.39 Displaced shape for gravity.
 (Case study 3: original dimensions)

Scale: 1" = 1000 lb/in.
 (Tension = +ve)

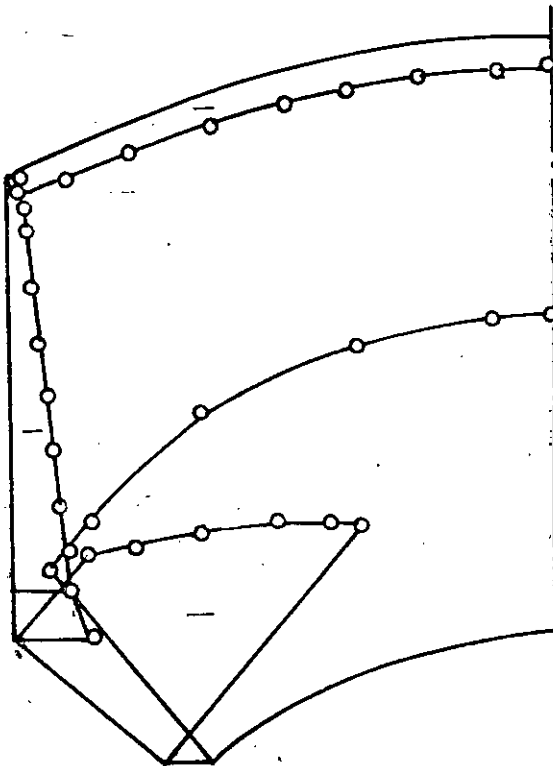


Fig. 4.40 Combined meridional membrane force for
 gravity and hydrostatic pressure.
 (Case study 3: original dimensions)

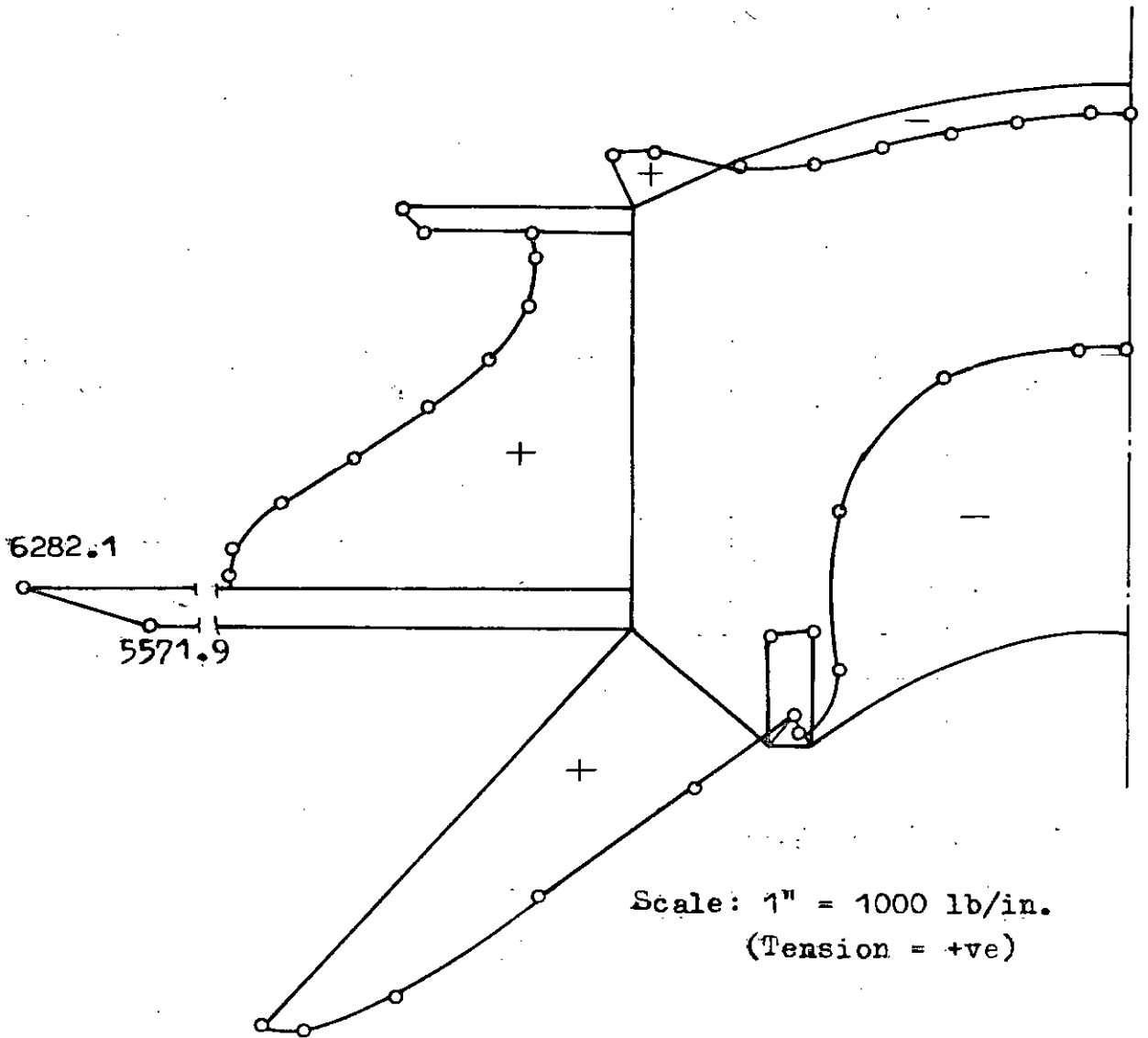
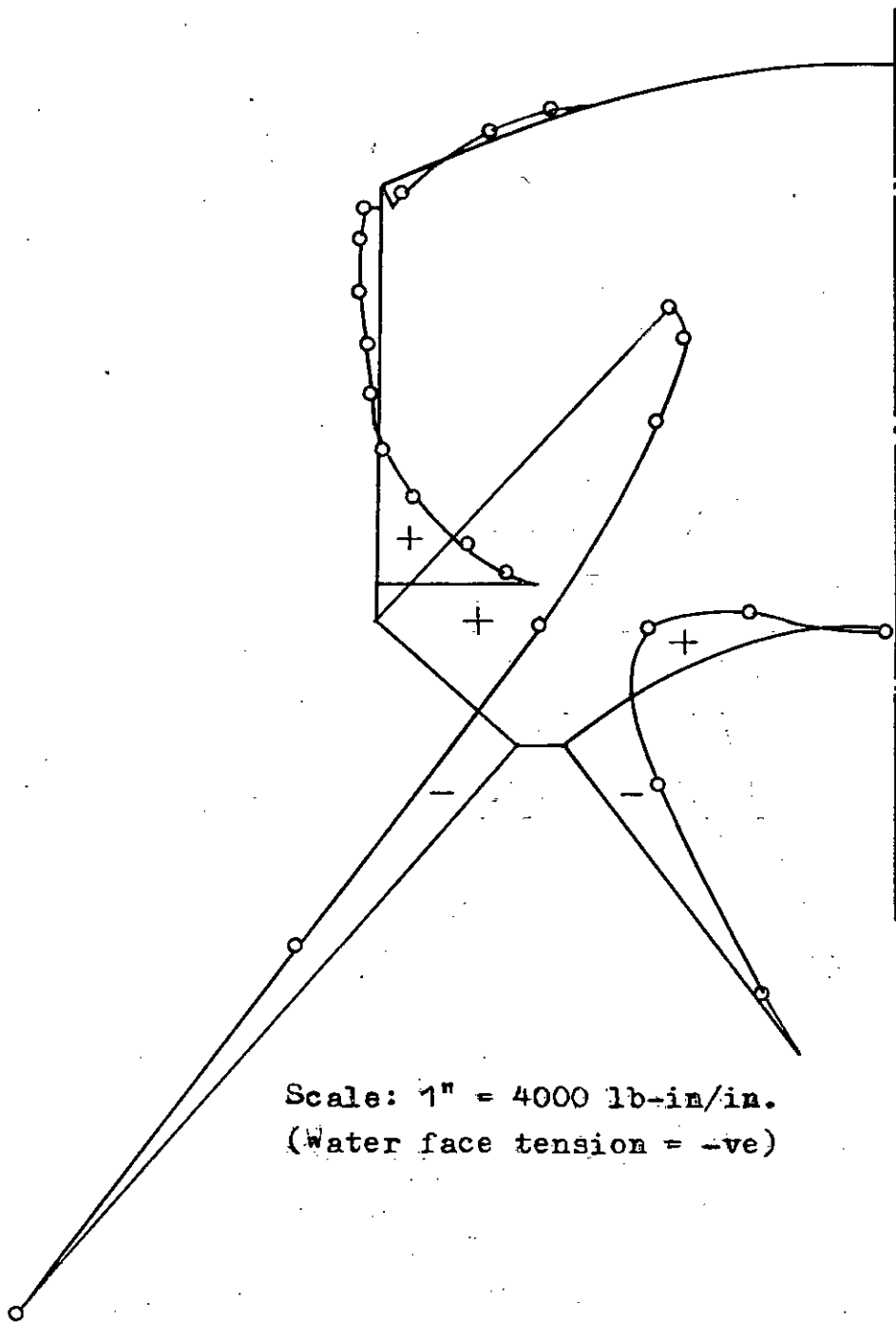


Fig. 4.41 Combined hoop force for gravity and hydrostatic pressure.
(Case study 3: original dimensions)



Scale: 1" = 4000 lb-in/in.
(Water face tension = -ve)

Fig. 4.42 Combined meridional moment for gravity and hydrostatic pressure.
(Case study 3: original dimensions)

Scale: 1" = 100"
 (Capacity=223,600 gallons)

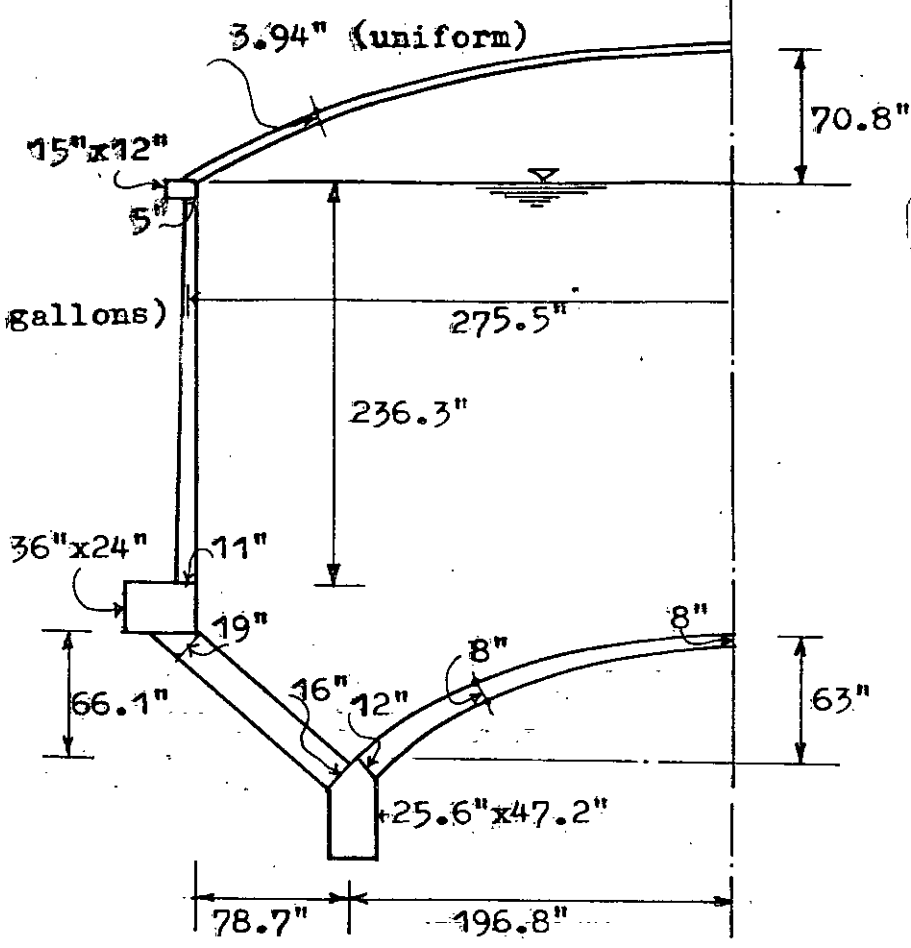


Fig. 4.43 Section showing modified dimensions.
 (Case study 3)

Scale: 1" = 1000 lb/in.
 (Tension = +ve)

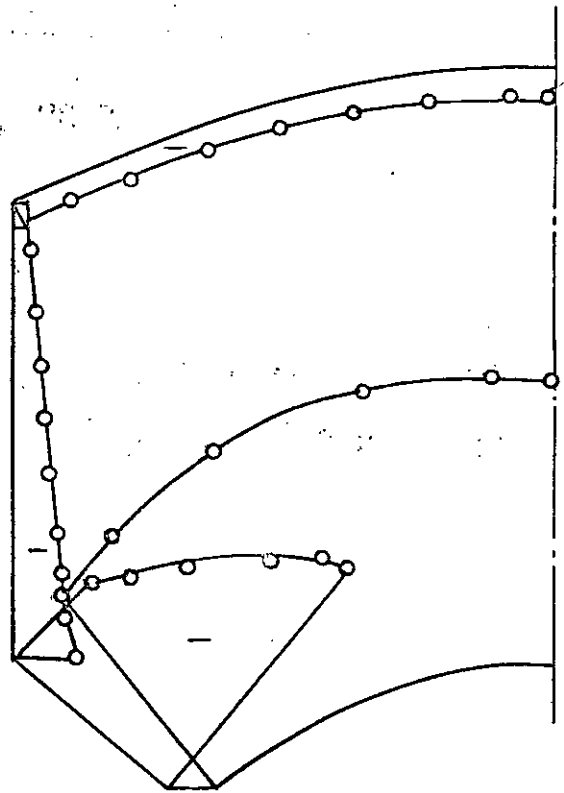


Fig. 4.44 Combined meridional membrane force for gravity and hydrostatic pressure.
 (Case study 3: modified dimensions)

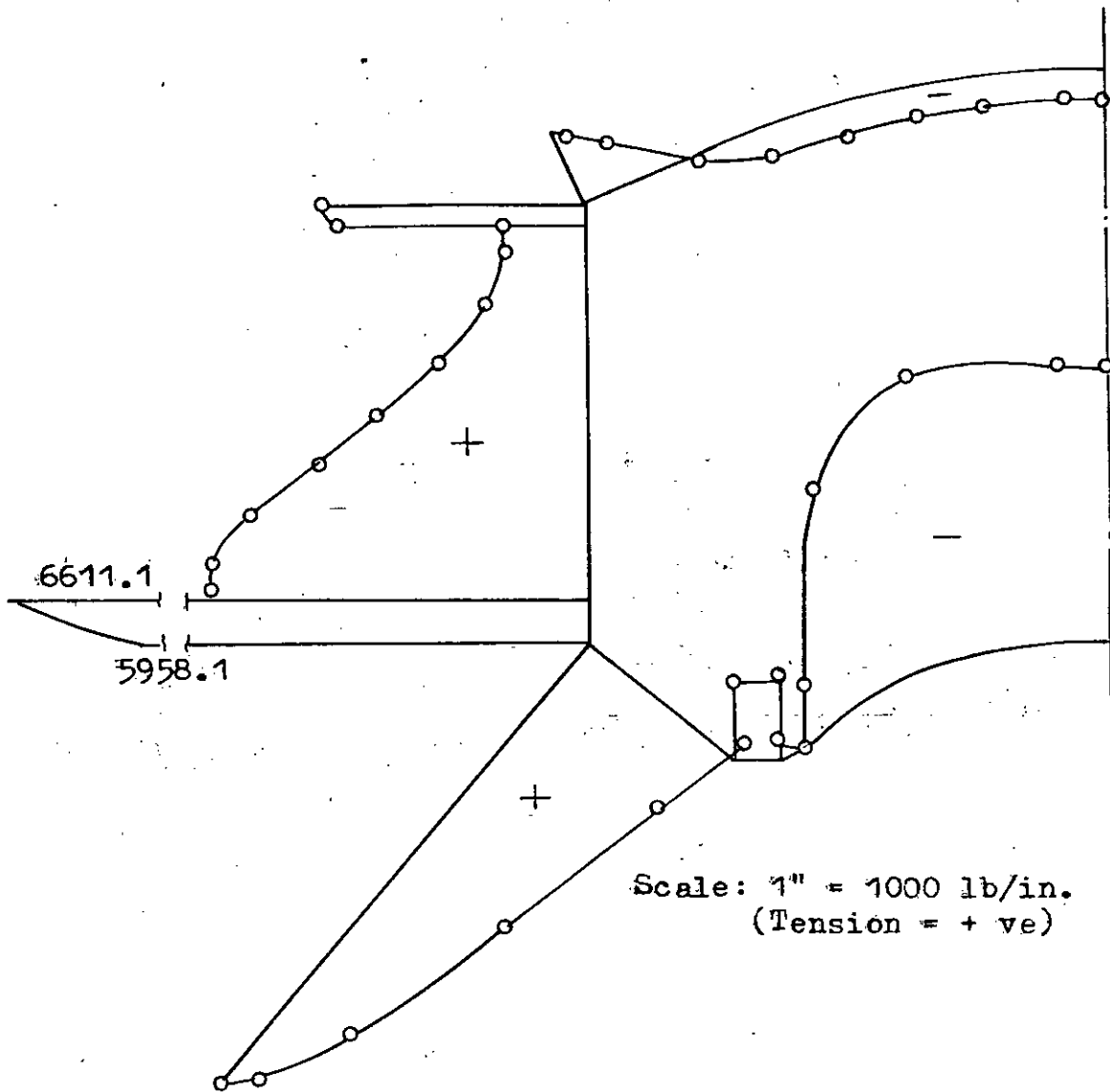


Fig. 4.45 Combined hoop force for gravity and hydrostatic pressure.
(Case study 3: modified dimensions)

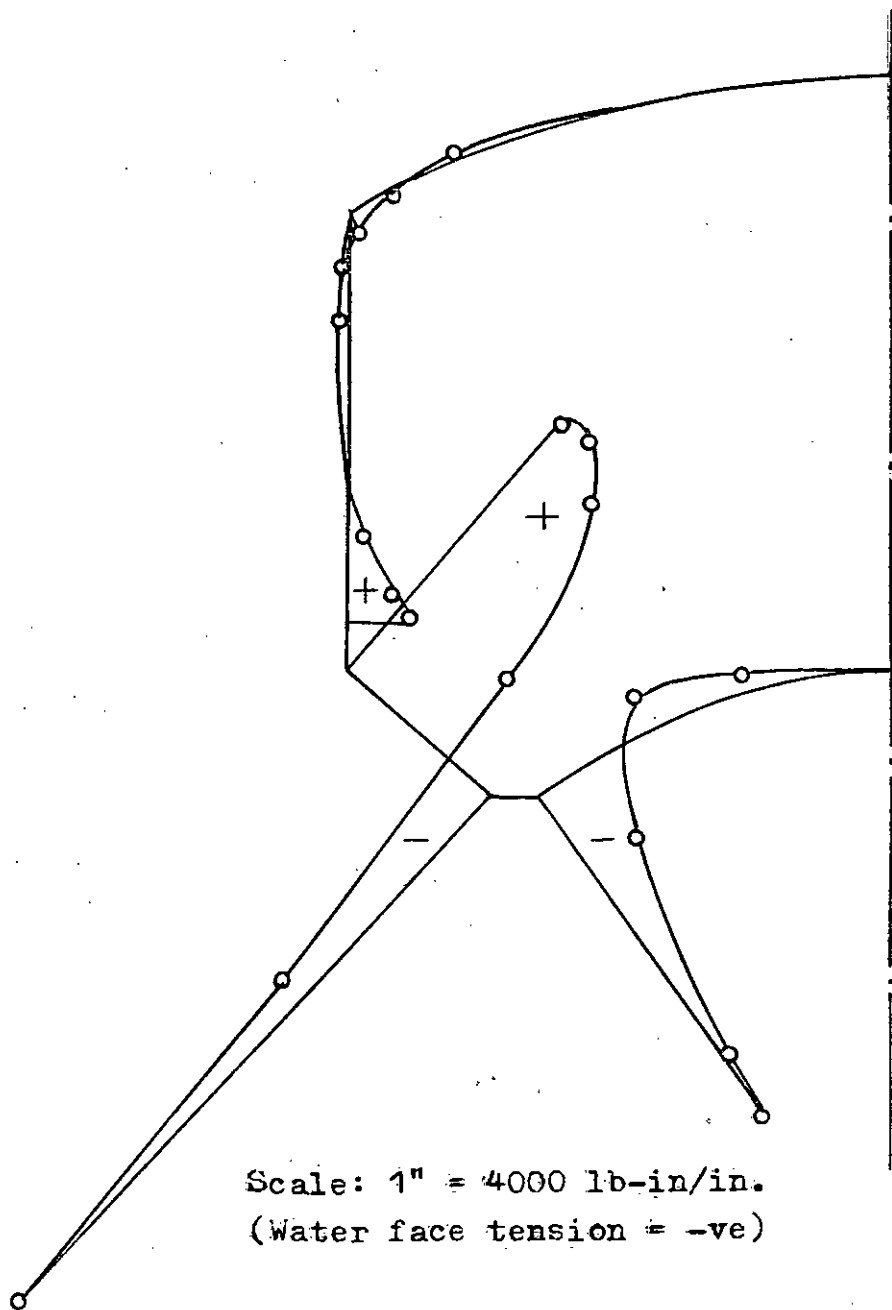


Fig. 4.46 Combined meridional moment for gravity and hydrostatic pressure. (Case study 3: modified dimensions)

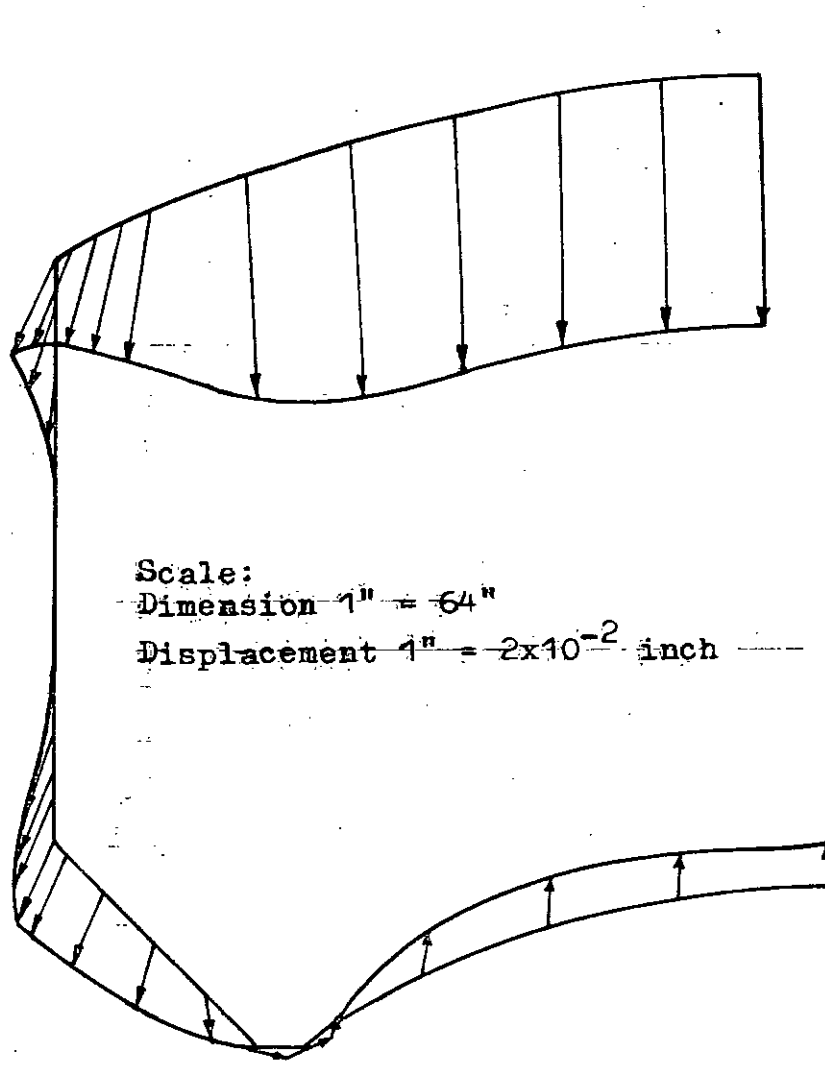


Fig. 4.47 Displaced shape for gravity.
(Case study 4: original dimensions
vide Fig. 2.17)

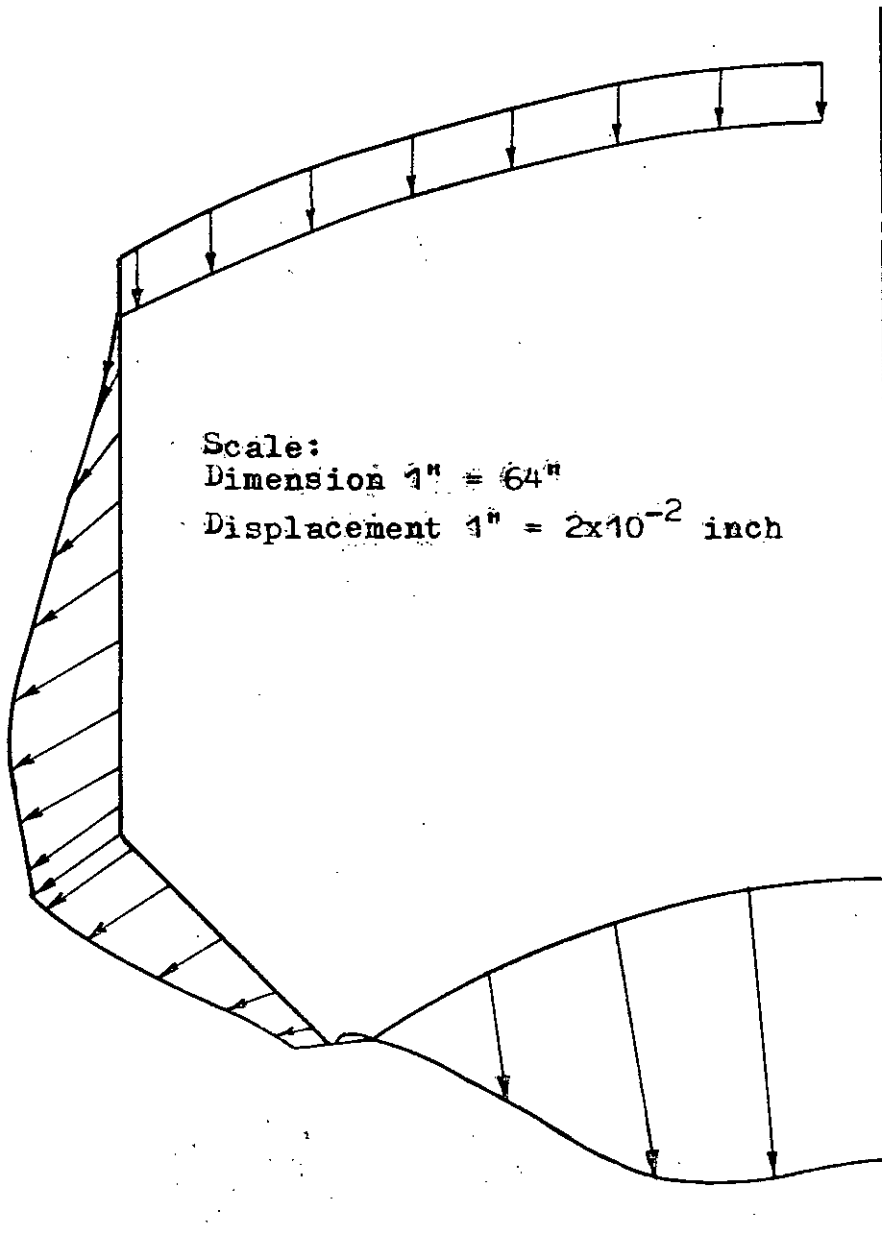


Fig. 4.48 Displaced shape for hydrostatic pressure.
(Case study 4: original dimensions)

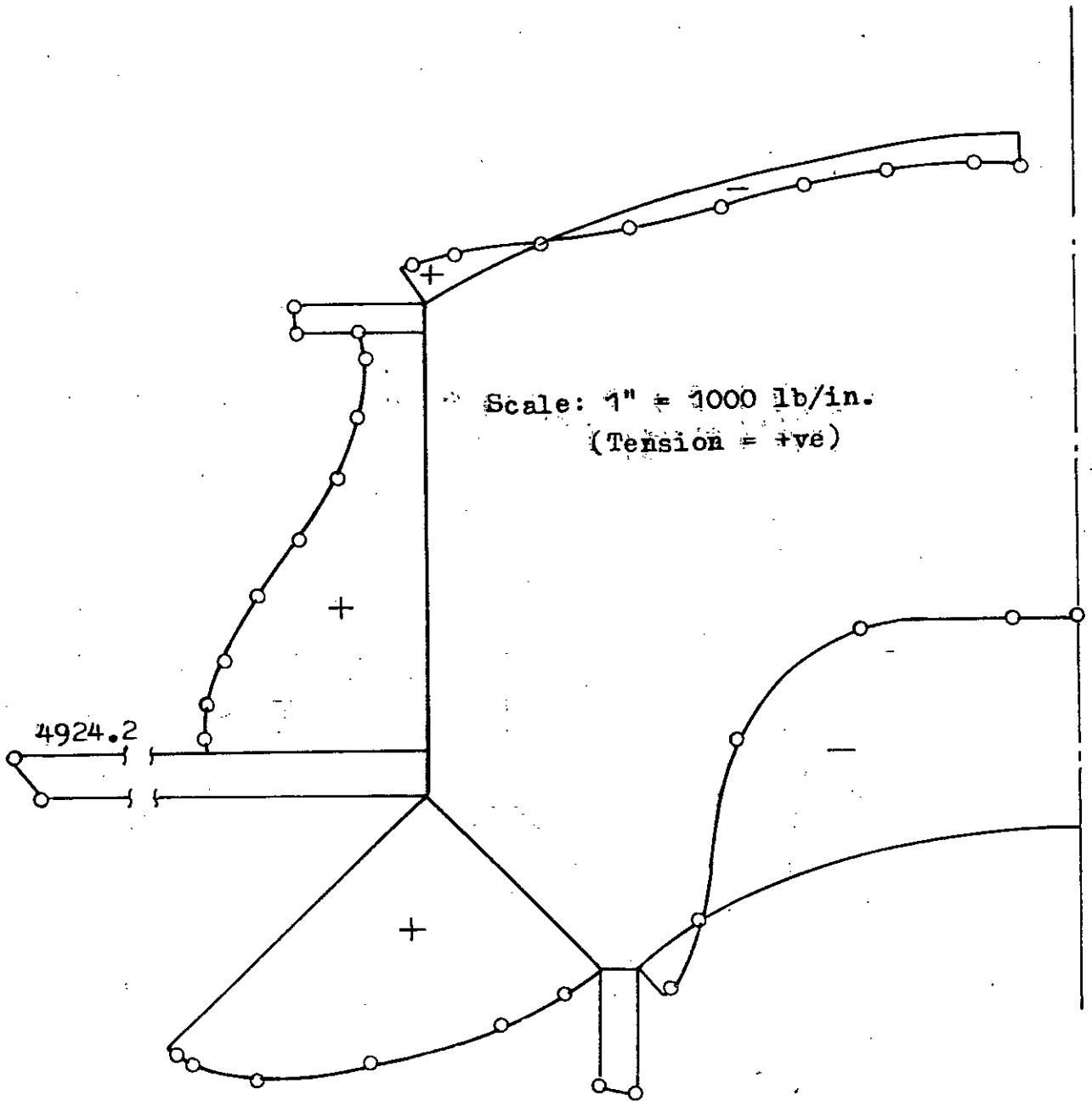


Fig. 4.49 Combined hoop force for hydrostatic pressure and gravity.
(Case study 4: original dimensions)

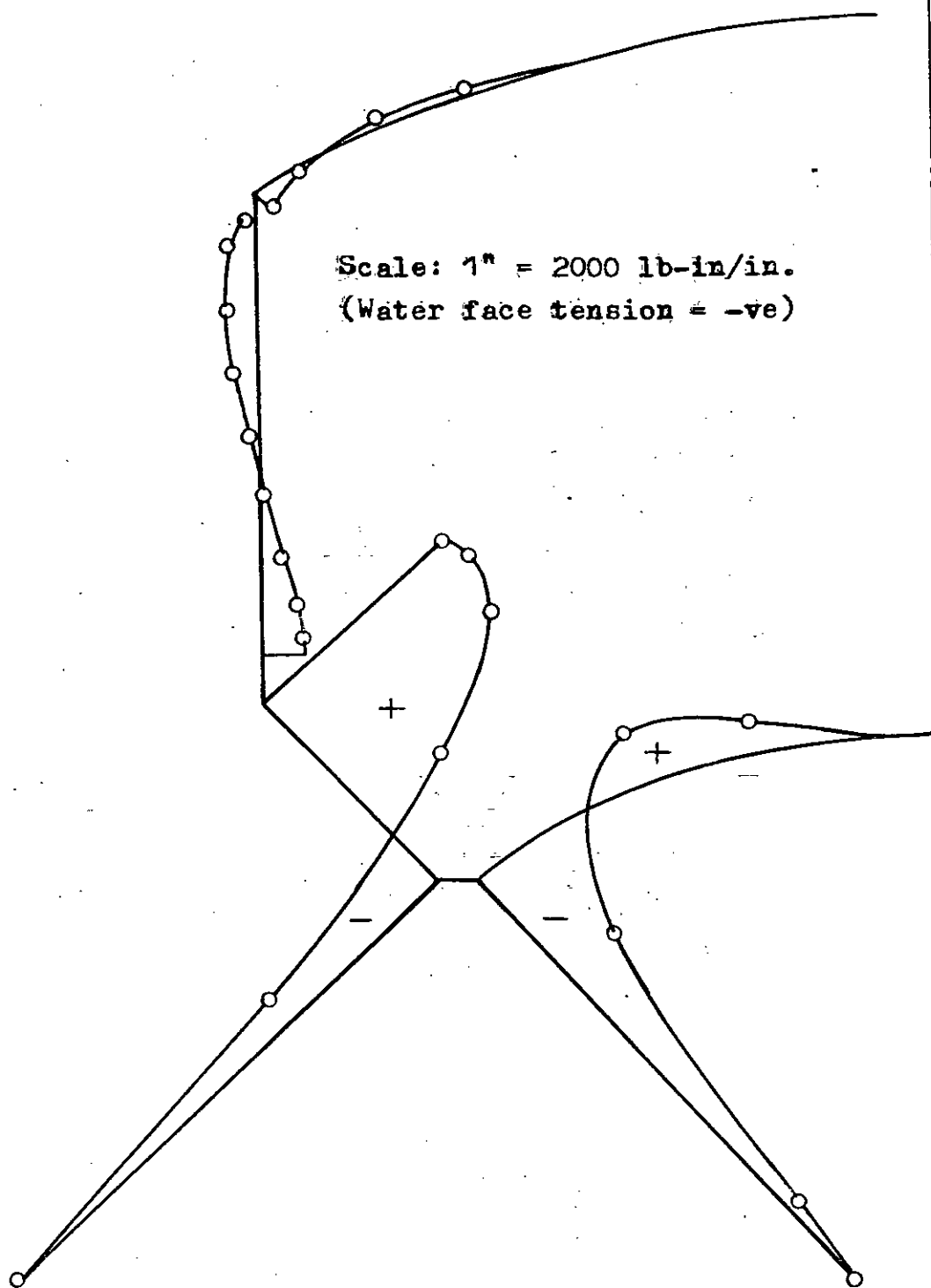


Fig. 4.50 Combined Meridional moment for gravity and hydrostatic pressure.
(Case study 4: original dimensions)

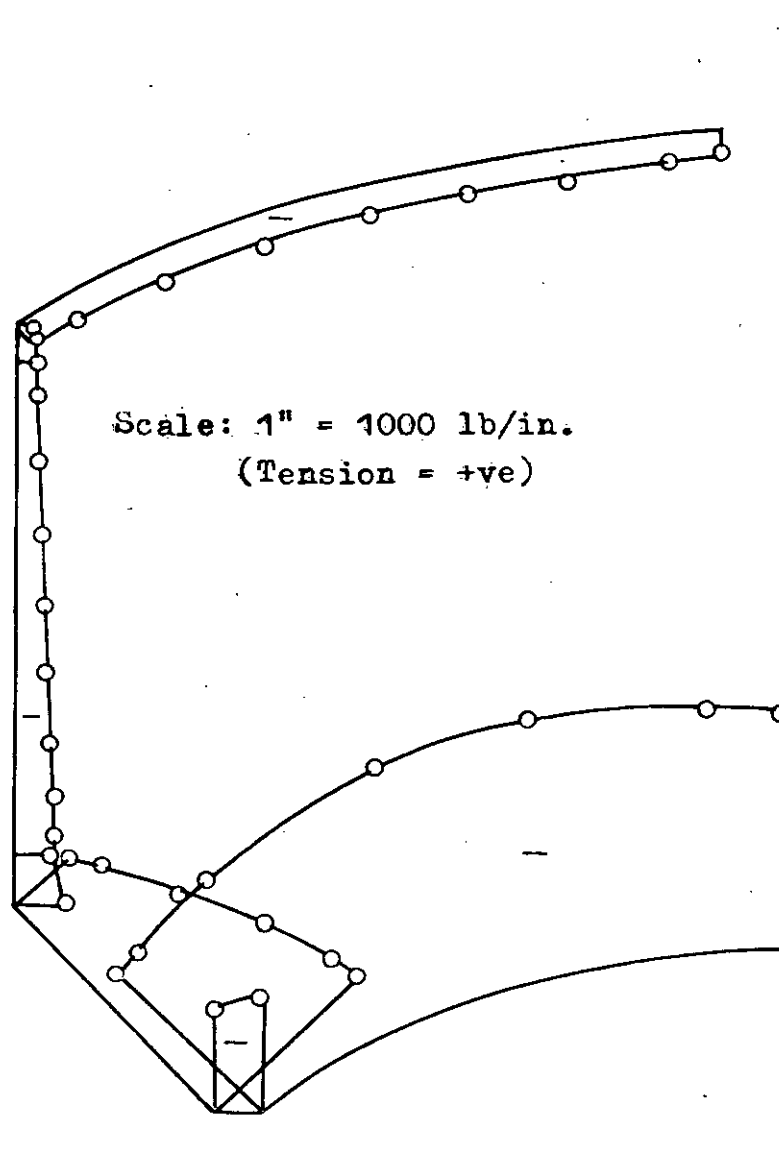
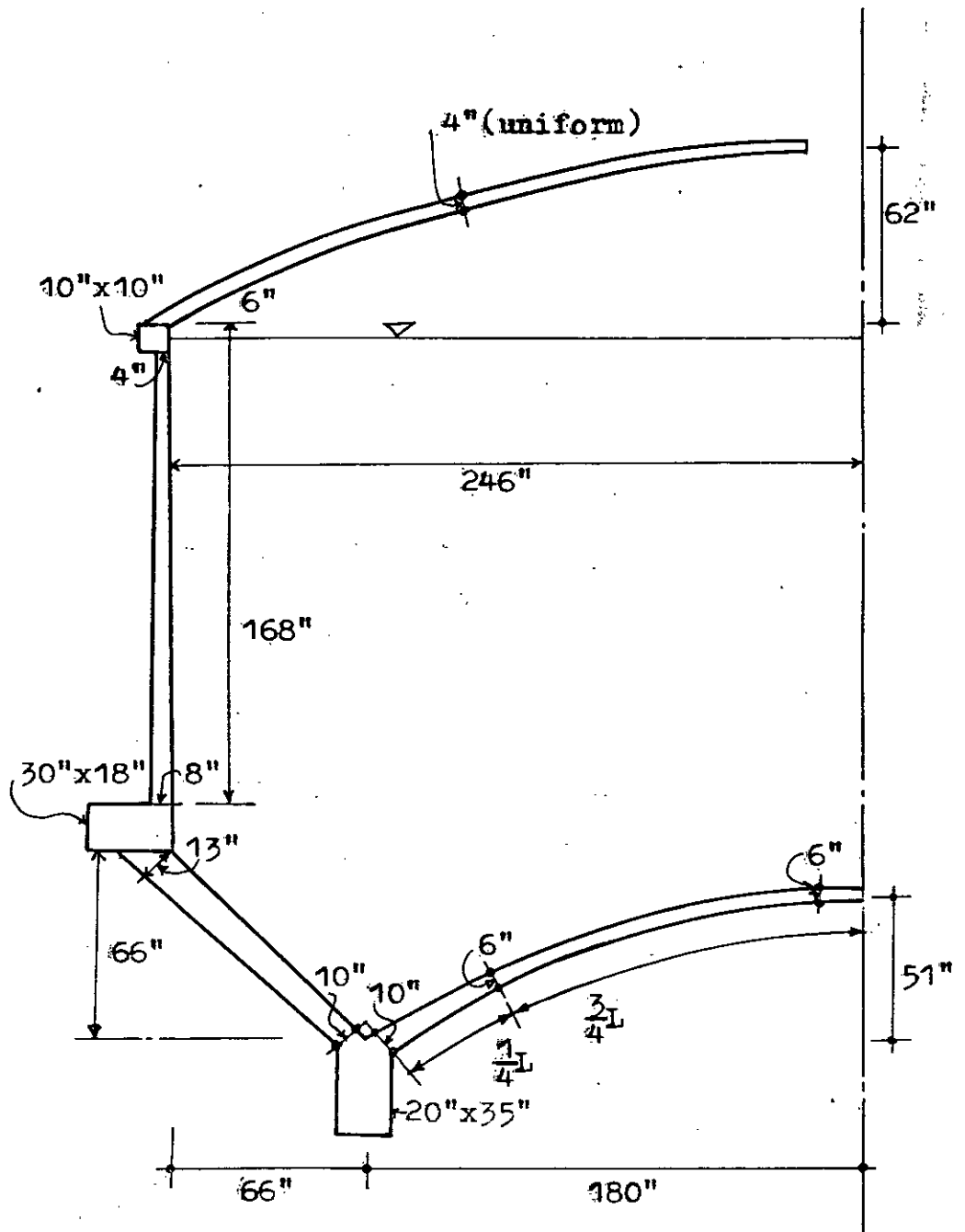


Fig. 4.51 Combined meridional membrane force for gravity and hydrostatic pressure. (Case study 4: original dimensions)



Scale: 1" = 64"

(Capacity = 1,51,700 gallons)

Fig. 4.52 Section showing modified dimensions.
(Case study 4)

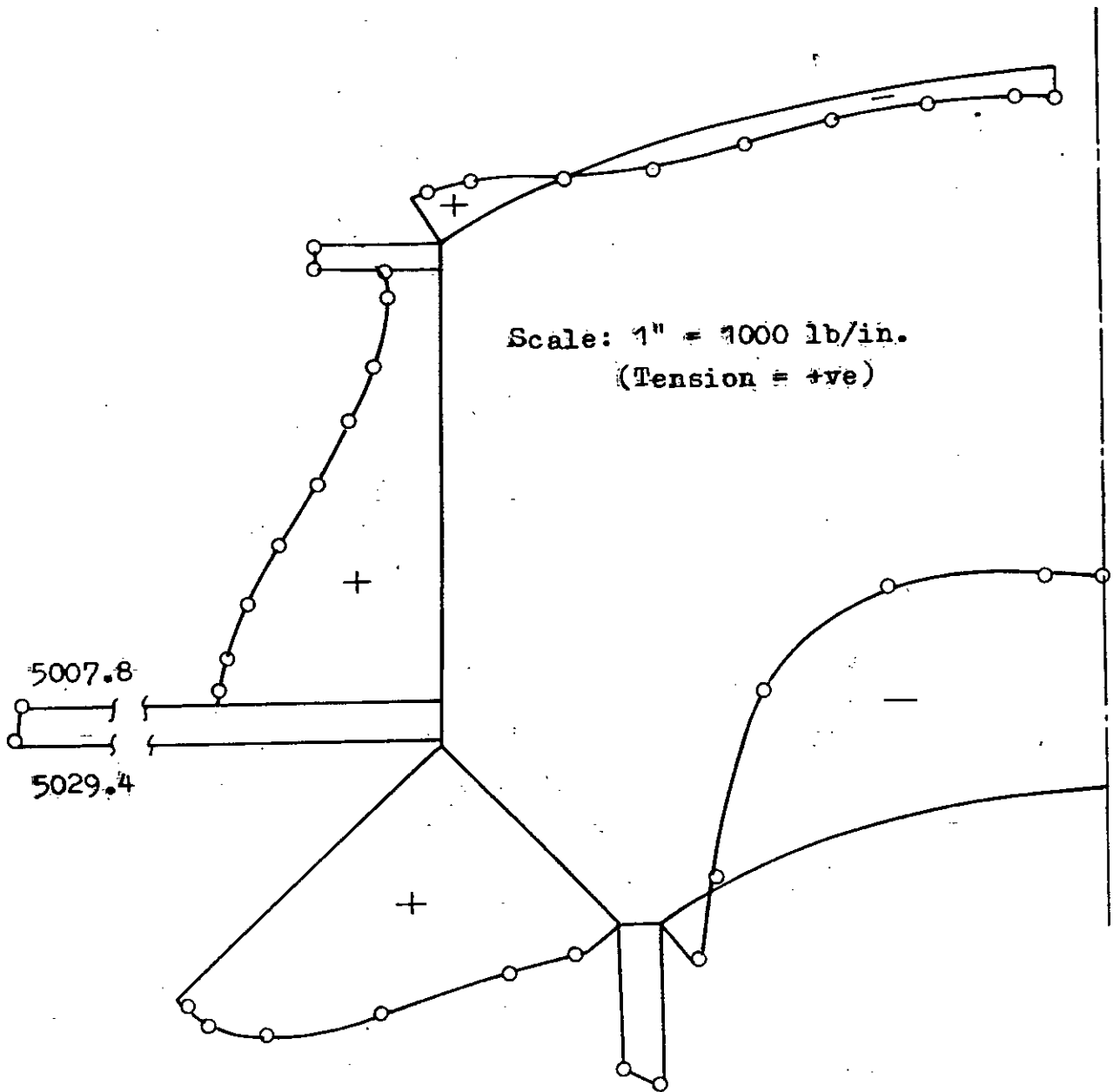


Fig. 4.53 Combined hoop force for gravity and hydrostatic pressure.
(Case study 4: modified dimensions)

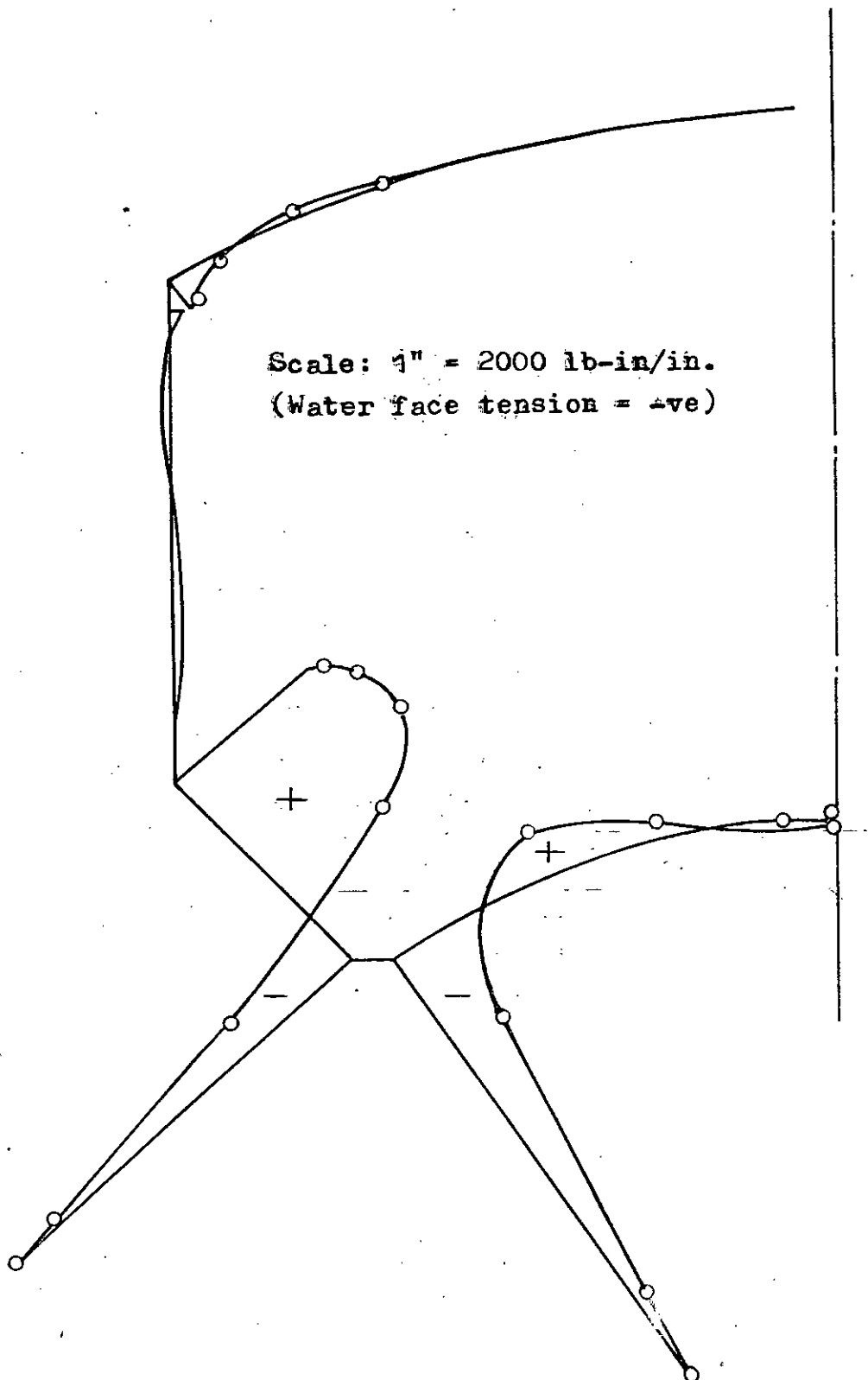


Fig. 4.54 Combined meridional moment for gravity and hydrostatic pressure.
(Case study 4: modified dimensions)

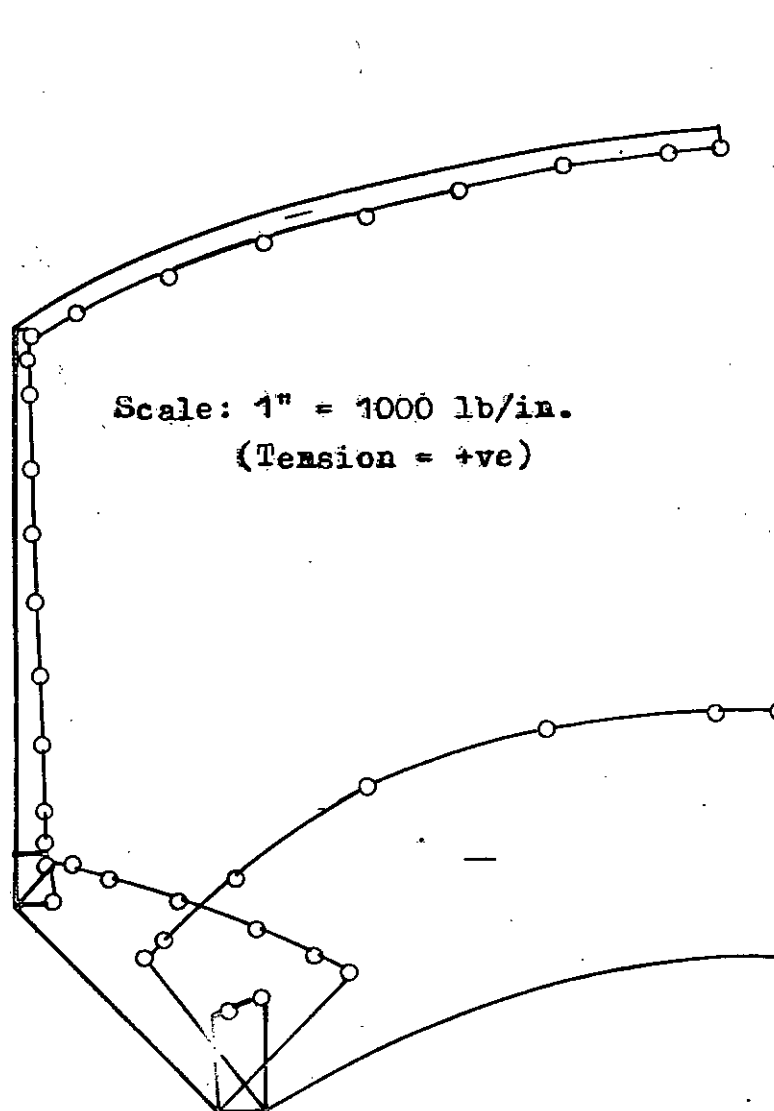


Fig. 4.55 Combined meridional membrane force for gravity and hydrostatic pressure. (Case study 4: modified dimensions)

4.5 Comparison of Design Stress Obtained by Conventional Methods and Finite Element Method at Critical Sections

In this article the results of Finite Element analysis of the Intze tanks considered in the case studies are tabulated alongside the results of conventional analysis for direct comparison of numerical values. The stresses are tabulated for the sections that are critical for design. The units and sign conventions used for the stress resultants are as follows:

Meridional membrane force, N_{ϕ}	$\frac{\text{Unit}}{\text{lbs/ft}}$	<u>Sign convention</u> Tension = +ve
Tangential membrane force or Hoop force, N_{θ}	lbs/ft	Tension = +ve
Hoop force in ring beams, T_{θ}	lbs	Tension = +ve
Meridional moment, M_{ϕ}	ft-lbs/ft	Water face tension = -ve

TABLE 4.1

Stress resultants of Case study 1

Section	Stress Resultants	Jai Krishna and Jain's Analysis	Finite Element Analysis	
			Original Dimensions	Modified dimensions
1. Top Dome Edge	N_{ϕ}	-1592.5	-1132.8	-1022.4
	N_{θ}	2204.0	3307.2	4296.0
	M_{ϕ}	330.7	513.5	569.5
2. Top Ring Beam	T_{θ}	9259.3	12351.2	8822.0
3. Top of Cylindrical Wall	N_{ϕ}	- 953.7	- 966.0	-871.2
	N_{θ}	4414.8	5144.4	4189.2
	M_{ϕ}	327.4	-223.7	110.8
4. Bottom of Cylindrical wall	N_{ϕ}	-2308.0	-2448.0	-2235.6
	N_{θ}	18008.5	17780.4	29145.6
	M_{ϕ}	1510.1	2855.8	2754.7
5. Bottom Ring Beam	T_{θ}	85232.7	65507.1	65988.1
6. Top of Conical wall	N_{ϕ}	-4718.3	-4774.8	-4746.0
	N_{θ}	34202.7	27543.6	25370.0
	M_{ϕ}	1366.8	4537.3	4473.3
7. Bottom of Conical wall	N_{ϕ}	-18680.5	-10131.6	-10026.0
	N_{θ}	- 151.9	-10635.6	-7252.8
	M_{ϕ}	- 7458.1	- 7810.4	-6312.6
8. Bottom Dome Edge	N_{ϕ}	-13372.0	- 9103.2	-9037.2
	N_{θ}	- 80.0	- 8997.6	-6926.4
	M_{ϕ}	- 5216.0	- 8275.4	-6443.2

TABLE 4.2
Stress resultants of Case study 2

Section	Stress Resultants	Gray and Manning's Analysis	Finite Element Analysis	
			Original Dimensions	Modified Dimensions
1. Top Dome Edge	N_{ϕ}	-2595.4	-1664.4	-1569.6
	N_{θ}	-1616.7	4704.0	5648.4
	M_{ϕ}	-	872.0	933.1
2. Top Ring Beam	T_{θ}	51048.1	18750.1	17626.9
3. Top of Cylindrical wall	N_{ϕ}	-1442.9	- 1510.8	-1441.2
	N_{θ}	-	6403.2	5356.8
	M_{ϕ}	-	- 157.6	38.0
4. Bottom of Cylindrical wall	N_{ϕ}	-3967.0	-4100.4	-3476.4
	N_{θ}	28187.5	27903.6	25129.2
	M_{ϕ}	-	1343.6	1446.2
5. Bottom Ring Beam	T_{θ}	153469.1	148837.2	152472.3
6. Top of conical wall	N_{ϕ}	-6750.4	-7381.2	-6690.0
	N_{θ}	48280.0	45390.0	46201.2
	M_{ϕ}	-	5542.0	3886.4
7. Bottom of conical wall	N_{ϕ}	-54873.5	-28926.0	-26929.2
	N_{θ}	40623.0	-18223.2	-13832.4
	M_{ϕ}	-13027.5	-6973.0	- 9280.0
8. Bottom circular beam	T_{θ}	-344416.5	-92686.6	-86849.6
9. Bottom dome edge	N_{ϕ}	-19013.0	-15646.8	-15458.4
	N_{θ}	-	- 8118.0	-11383.2
	M_{ϕ}	-	- 6924.9	- 7757.2

TABLE 4.3
Stress resultants of Case study 3

Section	Stress Resultants	Sushil Kumar's Analysis	Finite Element Analysis	
			Original Dimensions	Modified Dimensions
1. Top dome edge	N_{ϕ}	-2040.9	-1396.8	-1340.4
	N_{θ}	-1905.4	3945.6	4548.0
	M_{ϕ}	0.0	561.2	598.0
2. Top ring beam	T_{θ}	40432.0	16712.2	-
3. Top of cylindrical	N_{ϕ}	-1209.4	-1221.6	-1183.2
	N_{θ}	-	6710.4	5388.0
	M_{ϕ}	0.0	-217.8	49.6
4. Bottom of cylindrical wall	N_{ϕ}	-3454.1	-3726.0	-3032.4
	N_{θ}	28222.2	26534.4	24336.0
	M_{ϕ}	0.0	3382.3	1477.3
5. Bottom ring beam	T_{θ}	168210.0	139907.9	150814.8
6. Top of conical wall	N_{ϕ}	-6876.4	-7060.8	-6409.2
	N_{θ}	51223.0	36378.0	37308.0
	M_{ϕ}	0.0	9415.2	6795.6
7. Bottom of conical wall	N_{ϕ}	-30910.0	-19027.2	-17834.4
	N_{θ}	45373.9	-2958.0	-1386.0
	M_{ϕ}	0.0	-16605.9	-14600.9
8. Bottom circular beam	T_{θ}	-93695.0	-228238.4	-10619.6
9. Bottom dome edge	N_{ϕ}	-22040.0	-15535.2	-15288.0
	N_{θ}	-9473.0	-1648.8	-973.2
	M_{ϕ}	-	-8566.1	-7997.6

TABLE 4.4
Stress resultants of Case study 4

Section	Stress Resultants	Analysis by BRTC	Finite Element Analysis	
			Original dimensions	Modified dimensions
1. Top dome edge	N_{ϕ}	- 165.0	- 956.4	- 858.8
	N_{θ}	-	2582.4	3585.6
	M_{ϕ}	-	272.6	429.3
2. Top ring beam	T_{θ}	30012.0	9309.6	7543.0
3. Cylindrical wall	N_{ϕ}	- 947.6	- 862.8	- 778.8
	N_{θ}	-	4711.2	3714.0
	M_{ϕ}	-	- 131.1	75.6
4. Bottom of cylindrical wall	N_{ϕ}	-2297.6	-2220.0	-1856.4
	N_{θ}	9865.0	15778.8	15938.4
	M_{ϕ}	-2915.0	575.3	-8.4
5. Bottom ring beam	T_{θ}	87039.0	86676.3	90302.1
6. Top conical wall	N_{ϕ}	-4048.9	-4162.8	-388.0
	N_{θ}	27550.0	26232.0	26091.6
	M_{ϕ}	-5918.0	2842.2	2063.5
7. Bottom of conical wall	N_{ϕ}	-18365.0	-12698.4	-12007.2
	N_{θ}	27550.0	3105.6	3165.6
	M_{ϕ}	- 5918.0	-6756.0	-5420.8
8. Bottom dome edge	N_{ϕ}	-17682.7	-12196.8	-12070.8
	N_{θ}	-	2530.8	3553.2
	M_{ϕ}	-	-6477.5	- 6055.9

4.6 Economy of Designs Based on Finite Element Analysis

The requirement of materials and cost for designs based on conventional as well as Finite Element methods are estimated for each case study for comparison. The unit costs used are as follows:

Concrete = Tk. 60.00/cft

Steel = Tk. 15000.00/ton

Approximate calculation indicates that, for designs based on Finite Element analysis, the saving in cost attainable in different case studies are about 13% in case study 1, 14% in case study 2, 14% in case study 3 and 23% in case study 4, over the corresponding conventional methods.

4.7 Analysis for Wind Load

While the conventional methods do not provide with any means of analysing Intze tanks for wind loads, the Finite Element program is capable of dealing with the non-symmetrically applied wind load represented approximately by a number of Fourier harmonics. The analysis is carried out separately for each harmonic and the results are automatically superimposed to give the total effect.

The study for the effect of wind load on the Intze tank has been limited to case study 4 only. It is apparent from the results presented in this article that the effect of wind pressure on the Intze tank is quite insignificant compared to the stresses caused by gravity and hydrostatic pressure. The results presented here are based on a wind pressure of $q = 30$ psf (≈ 110 mph approx.) on a surface normal to the direction of wind. Since the main body of the tank is cylindrical, the pressure distribution around the circumference depends on the Reynold's number. The distribution assumed here is taken from Reference (13) by Ahmad et al and is shown in Fig. 4.56.

It has been found that about seven Fourier harmonics represent the above distribution quite accurately. The Fourier coefficients used are shown in Table 4.5. In case of a different distribution around the circumference, the Fourier coefficients will have to be recalculated. The assumed pressure distribution over the top dome is different. Since the rise of the dome is small and the maximum

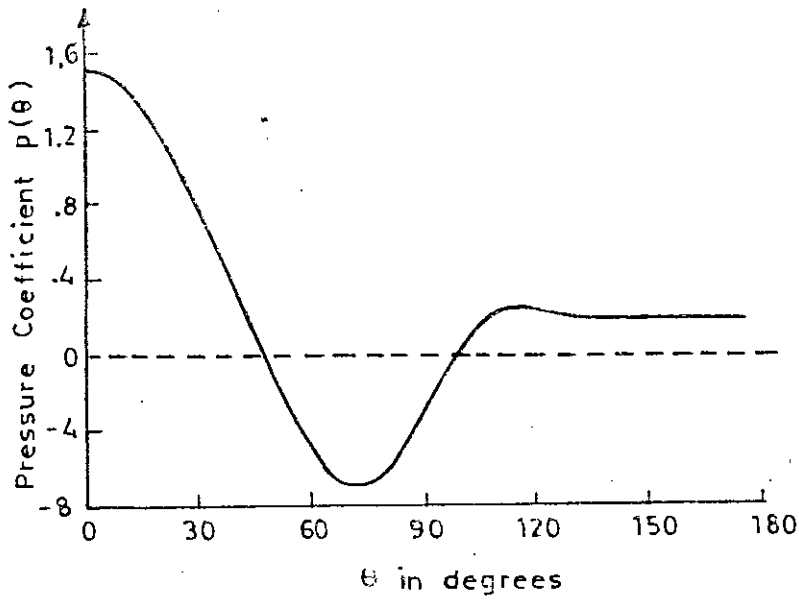


Fig. 4.56 Variation of wind pressure along the circumference of cylindrical tank.

Table 4.5 Fourier Coefficients for the pressure distribution of Fig. 4.56.

Harmonics	Coefficients
0	0.24706
1	0.31387
2	0.58763
3	0.42213
4	0.02466
5	-0.11481
6	-0.00451

inclination of a meridional section with the horizontal does not exceed 30° ; a uniform suction of $0.7q$ has been assumed all over the surface of the top dome.

The displacements and stresses have been calculated at 13 points along the semi-circle i.e. at an interval of 15° (from $\theta = 0^{\circ}$ to $\theta = 180^{\circ}$), since the distribution is symmetrical about the diameter parallel to the direction of wind. The distortion of the horizontal section is shown at four different levels and the displaced shape of the vertical section is shown for $\theta = 0^{\circ}$ and $\theta = 75^{\circ}$. The meridional moment and the hoop force are also plotted along these two vertical sections and are observed to be very insignificant. The tangential moment has been plotted for $\theta = 0^{\circ}$ only. From the distorted shape of the horizontal sections we may easily apprehend that the stresses at other sections would be further smaller and thus the plotting is unnecessary.

The results of analysis for wind load are shown in Figs. 4.57 to 4.65.

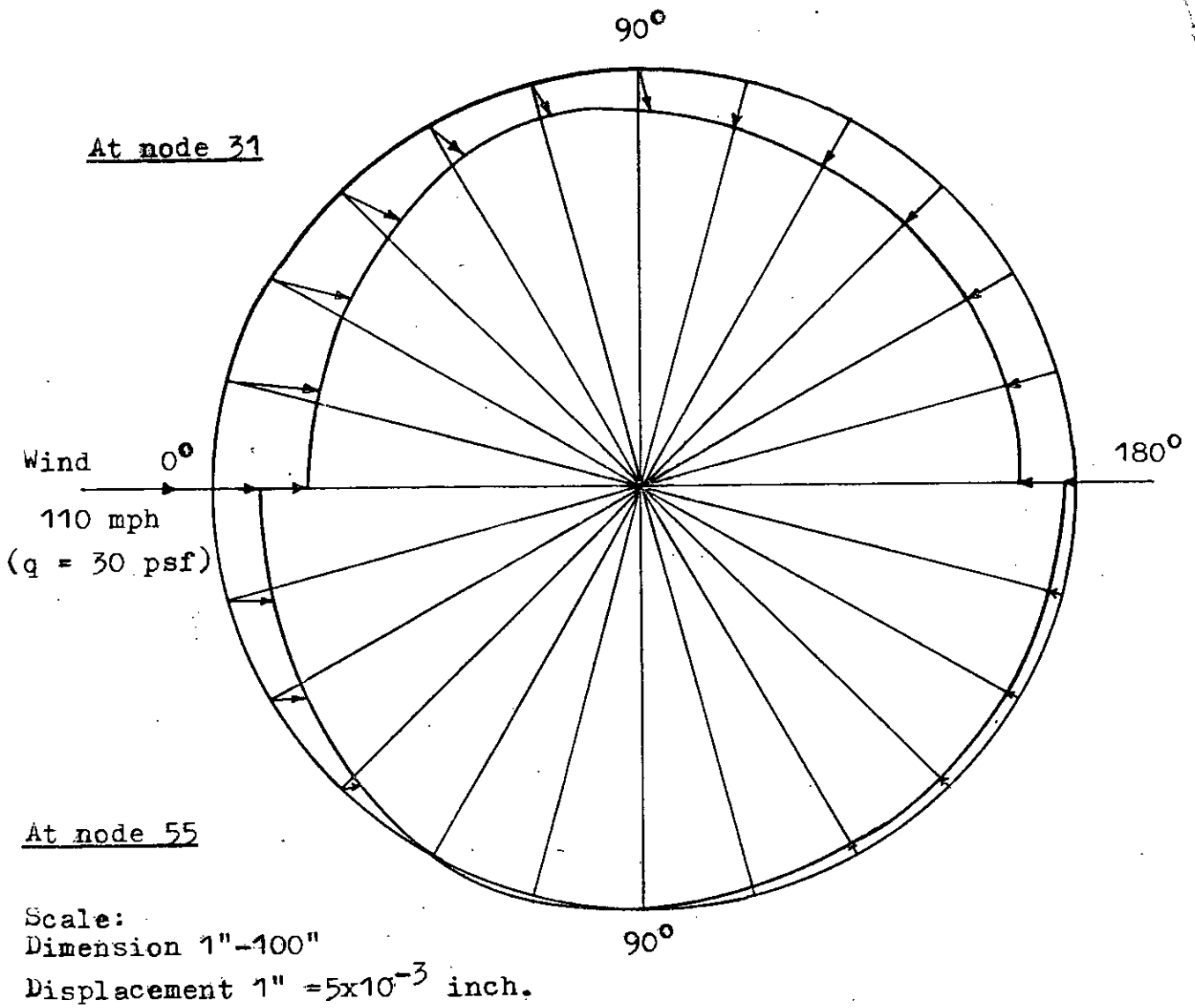


Fig. 4.57 Distortion of horizontal sections due to wind load.

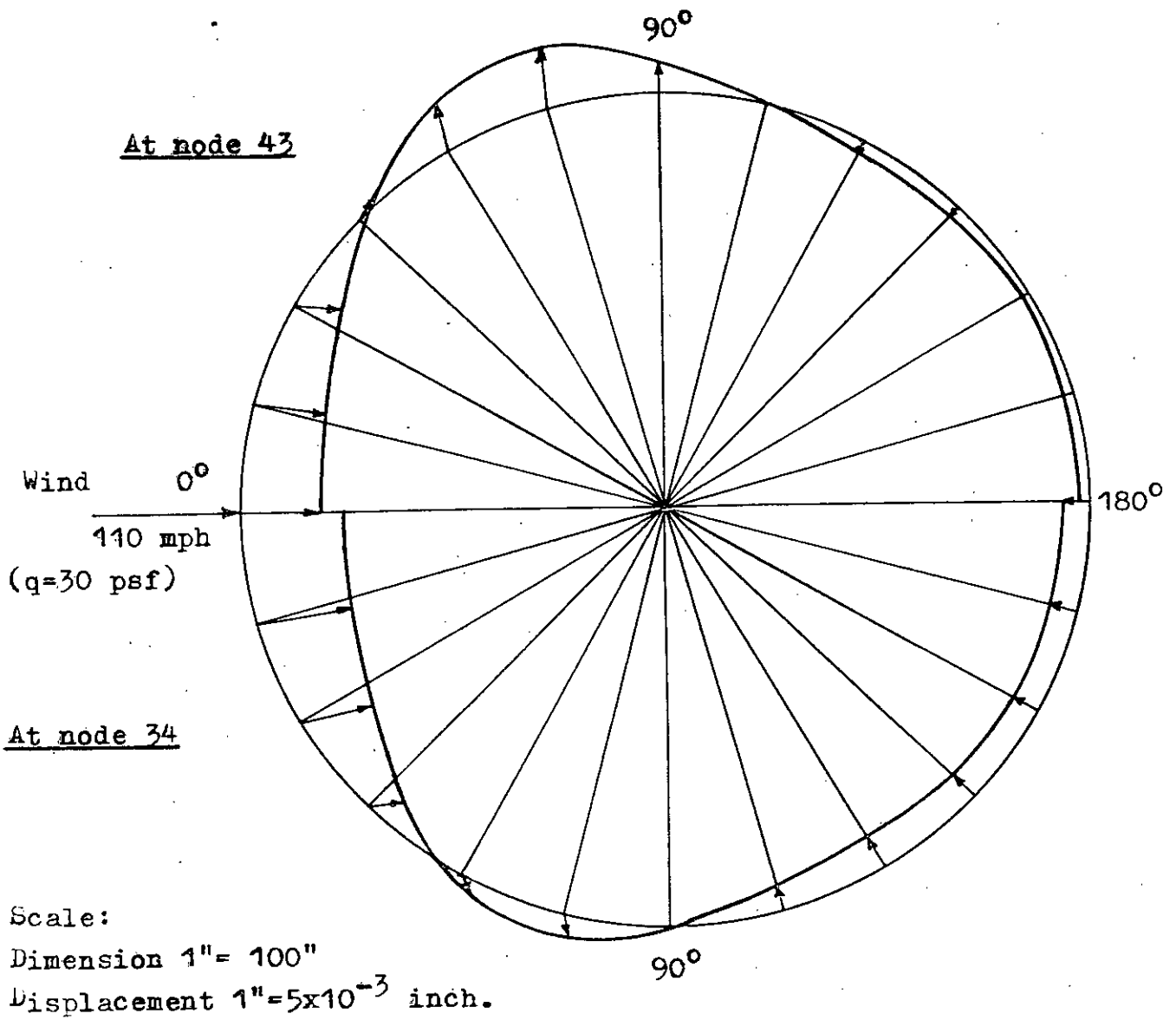


Fig. 4.58 Distortion of horizontal sections due to wind.

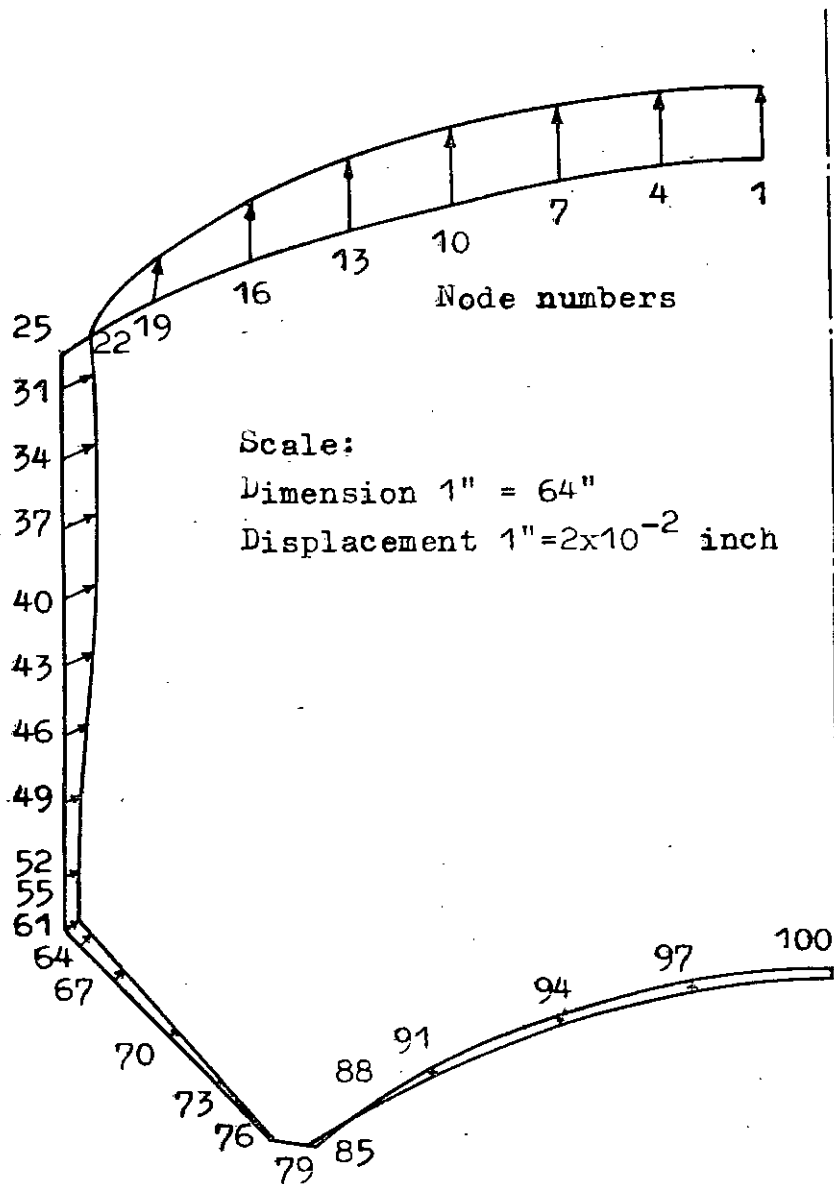


Fig. 4.59 Displaced shape for wind load at $\theta = 0^\circ$.

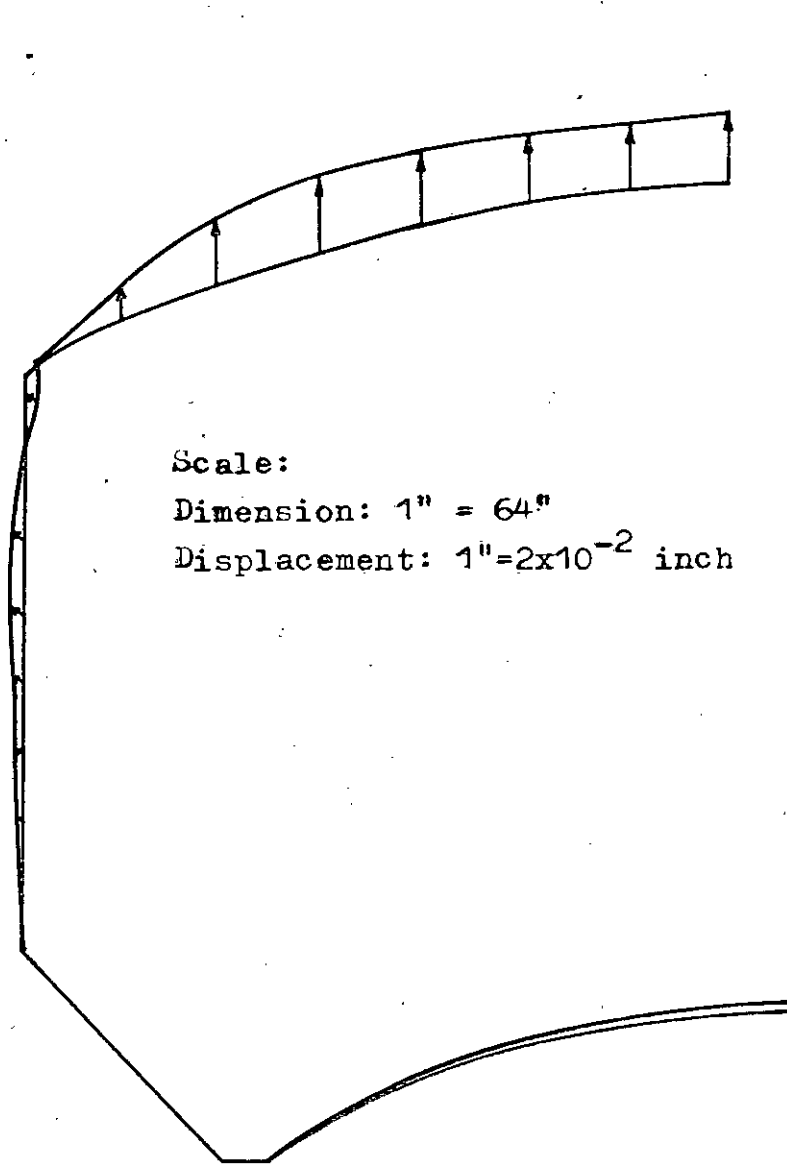


Fig. 4.60 Displaced shape for wind load
at $\theta = 75^\circ$.

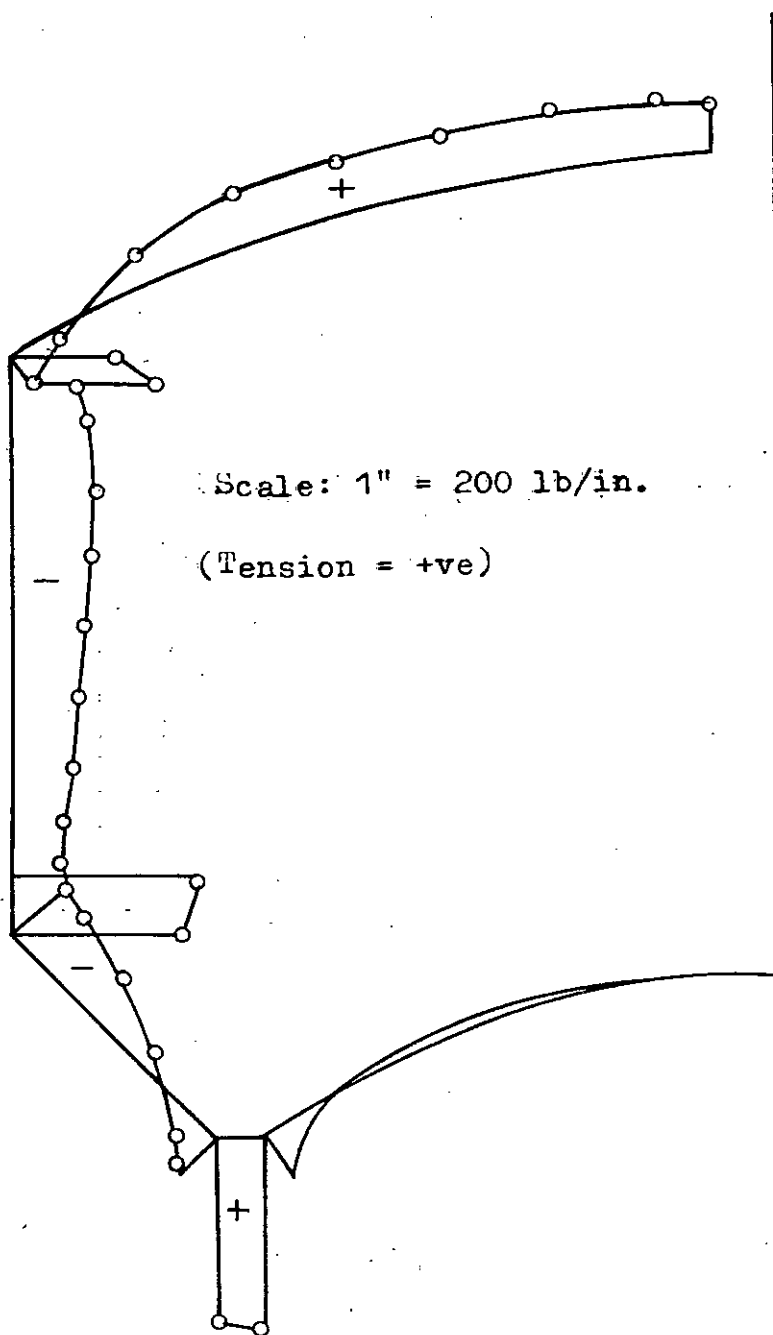


Fig. 4.61 Hoop force for wind load
at $\theta = 0^\circ$.

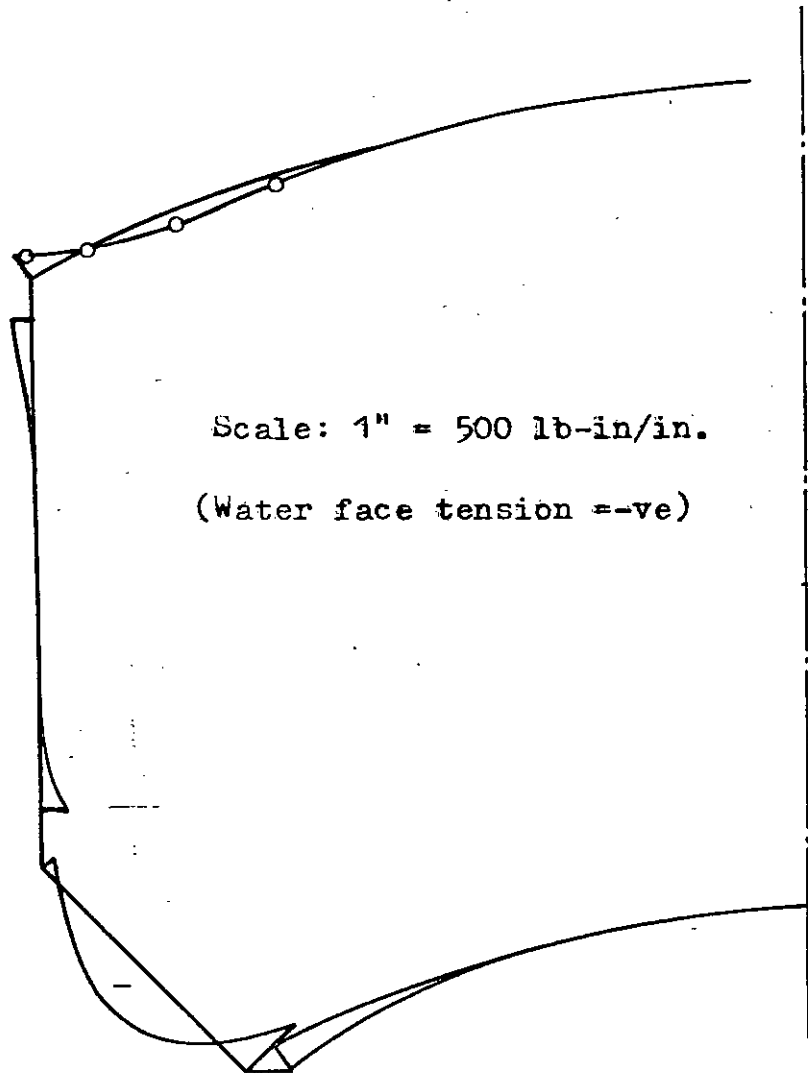


Fig. 4.62 Meridional moment for wind load
at $\theta = 0^\circ$.

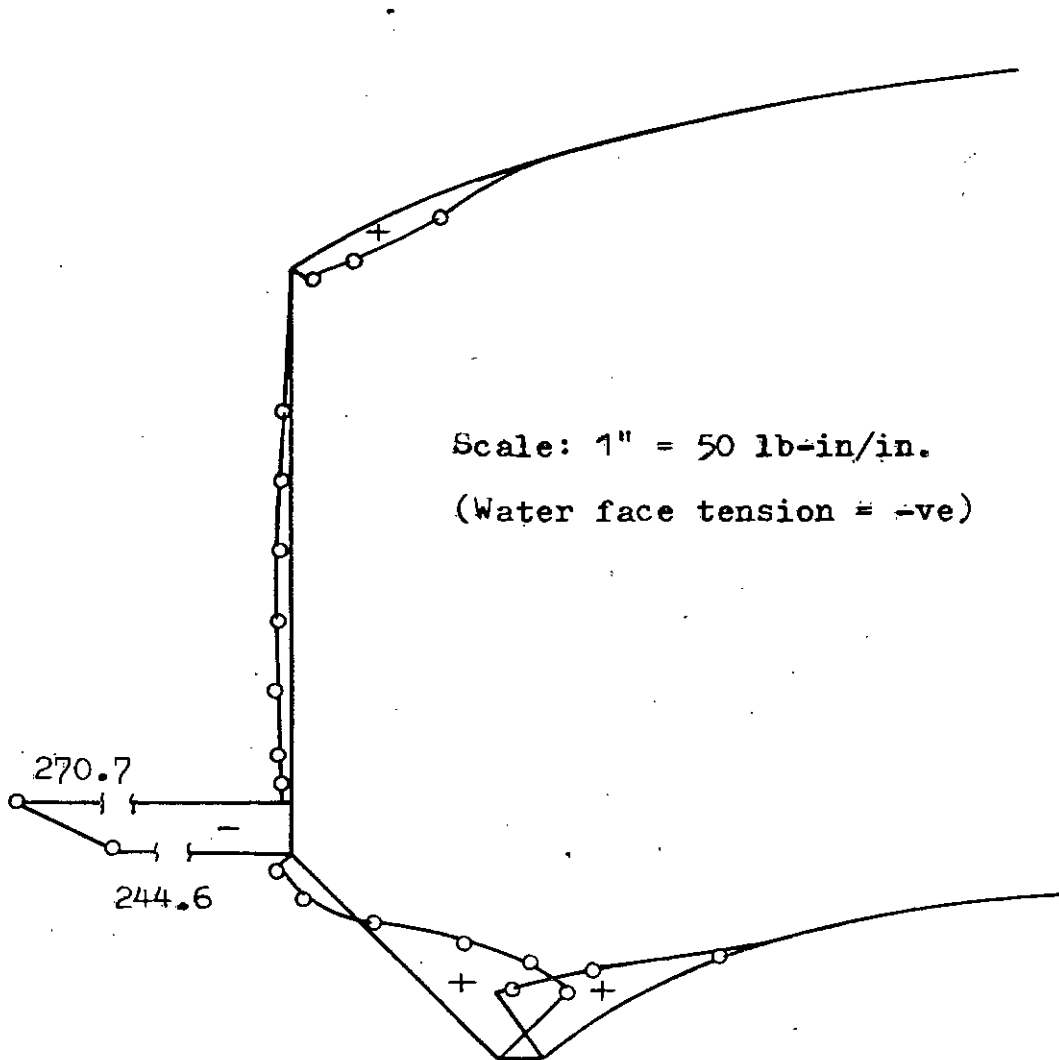


Fig. 4.63 Tangential moment for wind
at $\theta = 0^\circ$.

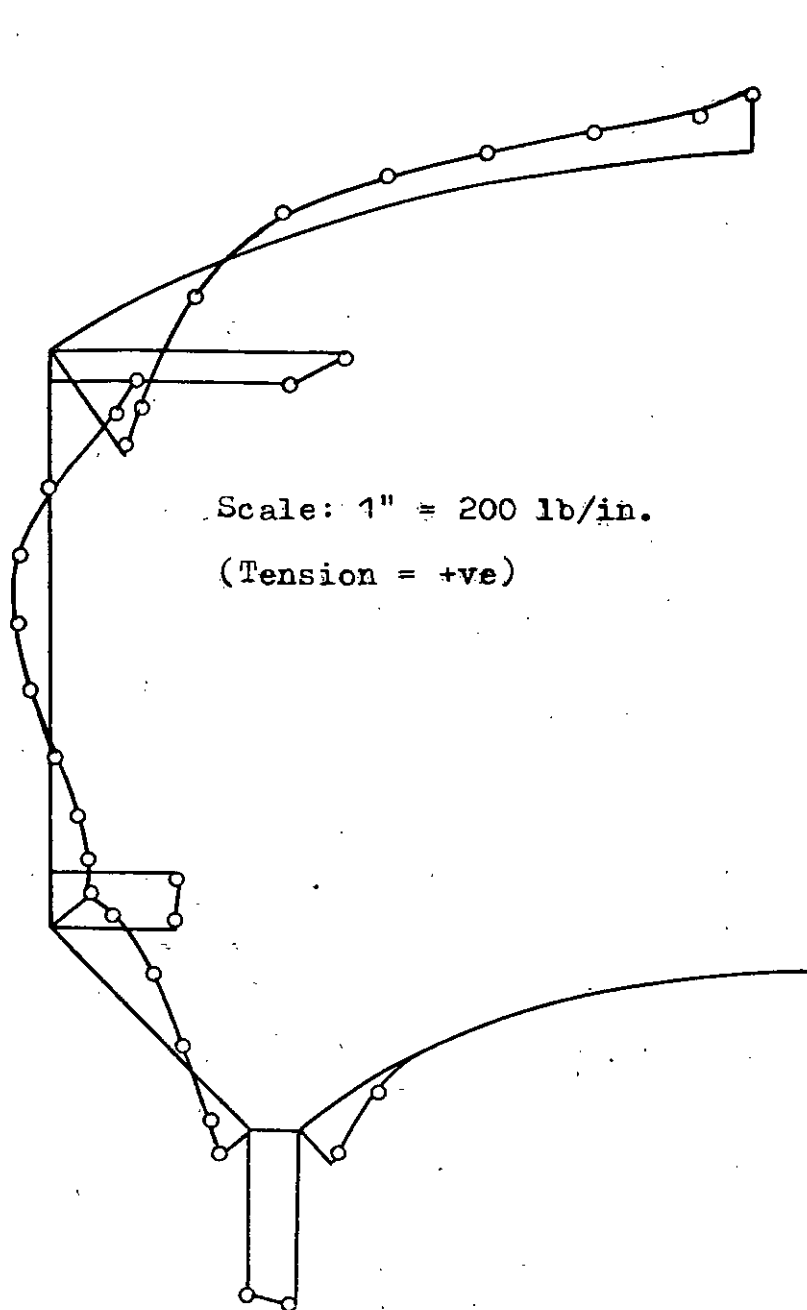


Fig. 4.64 Hoop force for wind load
at $\theta = 75^\circ$.

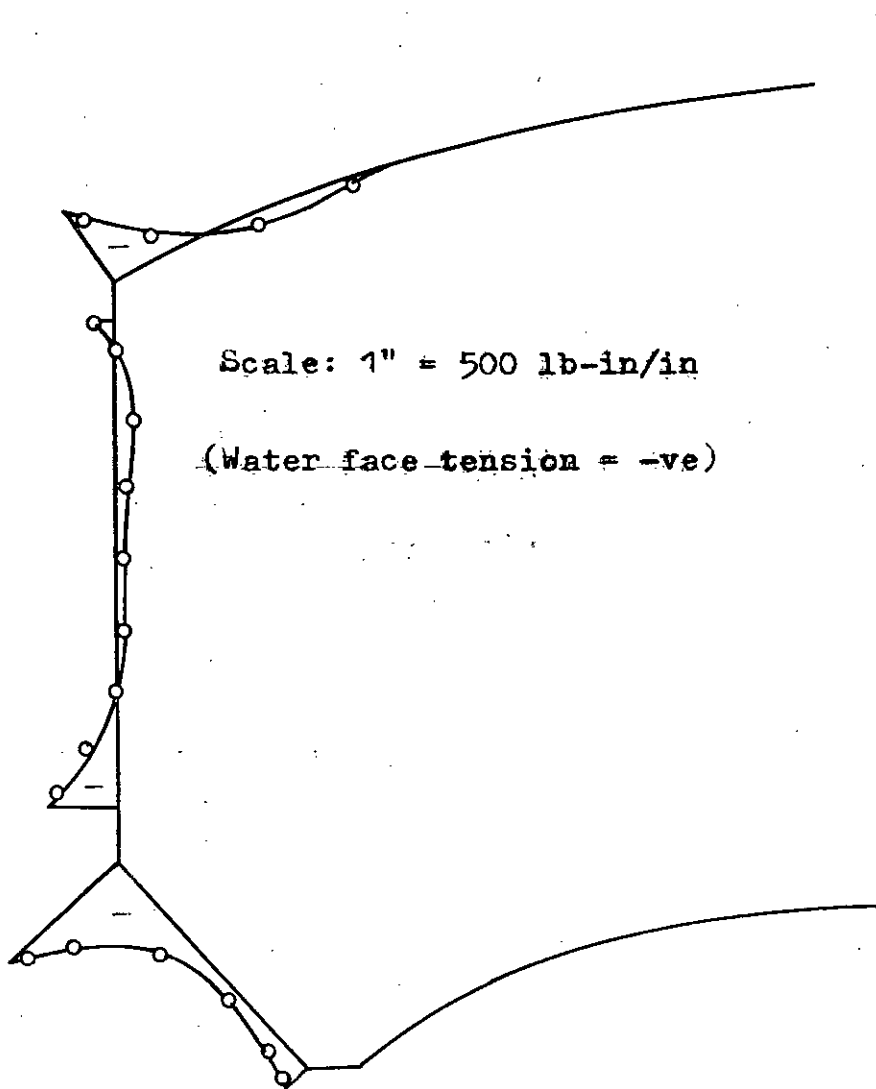


Fig. 4.65 Meridional moment for wind load
at $\theta = 75^\circ$.

8 Discussion

8.1 The Top Dome

The deflected shape and the stress pattern of the top dome indicate that membrane behaviour prevails almost throughout the shell as assumed in conventional analysis. However, a marked deviation from membrane behaviour is observed near the edge. Excepting a small peripheral ring 5 to 5 ft wide ($\approx D/10$) both the meridional and circumferential stresses are compressive in nature and are well below the allowable compressive stress in concrete. This means that a shell of nominal thickness provided with nominal meridional and circumferential reinforcements would be sufficient for the top dome except for a peripheral ring near the support. The outward radial movement of the top ring beam induces circumferential tension in this peripheral ring and calls for provision of adequate circumferential reinforcement to take care of the tension. On the other hand the partial restraint exerted by the ring beam on the dome edge develops mild meridional moment causing tension on the top face. As a result some additional meridional reinforcement should be provided near the edge of the dome for a length of about $D/10$ on the top face. In some cases slight thickening of the top dome near the edge may be advisable.

It may be noted that the stresses in the top dome are caused almost exclusively by its self-weight and surface load. The hydrostatic pressure against the cylindrical wall

has little effect on the stresses in the top dome. Also the effect of a moderate lantern load at the crown is negligible. Even the local stresses under the lantern do not warrant any special measure such as thickening of the shell near the crown.

4.8.2 The Top Ring Beam

This ring-beam is provided to take care of the hoop tension arising out of the inclined meridional thrust of the top dome. A study of the tables in Art. 4.5 shows that the actual hoop tension (T_{θ}) as obtained by Finite Element method is only 30 to 40 percent of that obtained by conventional methods. However, the value obtained by Jai and Jain's method (Phase II) appears to be even less than the Finite Element value ($\approx 75\%$). Thus, the top ring-beam may be designed for a hoop force not exceeding 40% of that obtained by conventional method. In this respect, an important observation is that if the size of the ring-beam is reduced it develops a still smaller hoop force, as seen from the results with modified dimensions. This is due to the redistribution of stresses, whereby the adjoining parts of the top dome and the cylindrical wall carry a larger share of the hoop force in the region.

4.8.3 The Cylindrical Wall

It appears from the stress resultants tabulated in Art. 4.5 for different case studies that in the design of

the cylindrical wall the prime concern is the circumferential tension (N_{θ}). The restraint moment (M_{ϕ}) at the base of the wall figures in secondary consideration only. The direct compression due to N_{ϕ} is of little concern other than the fact that it has a rather beneficial effect when considered in conjunction with the flexural stresses in as much as it acts as a sort of prestress to reduce the tension caused by flexure.

As regards the circumferential tension it is observed from the tables referred to above that the value of N_{θ} at the bottom of the wall obtained by Finite Element analysis is slightly less than (about 94 to 99% of) the values obtained by conventional methods. This assertion, however, is not true for case study 4 where N_{θ} has been calculated by Reissner's theory assuming a cylindrical wall fixed at the base which appears to be unacceptable in view of the results of Finite Element analysis.

It may be recalled that all the three conventional methods due to Gray & Manning, Sushil Kumar and Jai & Jain assume that the circumferential tension in the cylindrical wall is caused solely by the hydrostatic pressure against the wall and varies linearly from zero at the top to a maximum value at the bottom. The diagrams for hoop tension (N_{θ}) in Art. 4.4 obtained by FE analysis show marked deviations from the above assumption. Firstly, the maximum hoop tension occurs not exactly at the bottom but a small distance above the bottom. Secondly, N_{θ} is not zero at the top of the wall where it actually assumes some

tensile value due to the radially outward displacement of the top ring-beam caused mainly by the meridional thrust of the top dome. Thirdly, the variation of N_{θ} along the depth is anything but linear. In fact, the hoop tension in the wall is caused not only by the hydrostatic pressure but also by the gravity loads of the tank and the combined N_{θ} curve happens to look not like a straight line but more or less like the outline of a wide-mouth, flat-bottom pitcher.

Thus, it is quite apparent from the N_{θ} diagrams that it is needless and hence useless to provide a uniform thickness of the wall throughout. It is seen that a nominal wall thickness of 4" or 5" is sufficient at the top and it may be increased linearly (or in steps) to the required maximum thickness at the bottom. The maximum thickness required at the bottom may very well be estimated on the basis of the maximum hoop tension calculated by conventional method. Since the cylindrical wall is a major component of the Intze tank, use of a tapered section (trapezium) instead of a rectangular section would result in a considerable saving of concrete. This will have a beneficial effect on the design of the underlying parts due to reduction of dead load.

The meridional moment (M_{ϕ}) in the wall is found to be within the threshold of insignificance except at the bottom. But the striking fact is that, contrary to common ideas, the meridional moment at the base in most of the

cases is such as to cause compression on the water face although restraint moments would have just the opposite effect. As a matter of fact, the distorted shape due to hydrostatic pressure shows that the angle at the junction of the cylindrical wall and the cone tends to close, thereby developing compression on water face. Fortunately, however, the magnitude of the moment is rather small to cause much worry. Calculations show that nominal vertical reinforcements distributed equally on inner and outer faces suffice for the entire cylindrical wall except near the bottom, where a little additional reinforcement should be provided on the outer face.

4.8.4 The Bottom Ring Beam

It is observed that, in case studies 2 & 4, the hoop force in the bottom ring-beam, calculated by conventional methods, is in excellent agreement with that obtained by Finite Element analysis. On the other hand, in case studies 1 and 3, the Finite Element value is somewhat less than the conventional value (about 75 to 85%). This difference may be due to the effect of inclination of the conical dome. In case studies 1 & 3, the angle of inclination of the conical wall with the horizontal is less than 45° , whereas, in the other two cases, the angle is 45° . Thus the conventional calculation seems to give fairly reasonable value of the hoop force in the bottom ring beam for 45° inclination of the conical wall, but for smaller inclination the values are a little higher.

4.8.5 The Conical Wall

It may be recalled that the conventional membrane analysis gives more or less a constant value of hoop tension in the conical wall from top to bottom. However, the Phase II analysis of Jai & Jain reveals a different situation showing that the hoop force gradually vanishes towards the bottom of the conical wall and may even become compressive at the bottom as in case study-1. The hoop force diagrams drawn on the basis of Finite Element analysis indeed exhibit such a trend, although the magnitudes are not quite in agreement. According to FE analysis the combined hoop force (N_{θ}) for gravity and hydrostatic pressure at the bottom of the conical wall is compressive in case studies 1, 2 and 3 but tensile in case study-4, the magnitude being small, however. Thus, it is needless to provide the same amount of hoop reinforcement towards the bottom of the conical wall as at the top. And it would be apparent from the analyses for modified dimensions of all the cases that even the thickness of the conical wall may be somewhat reduced towards the bottom to save concrete.

As regards bending moments in the conical wall, the FE analysis shows that considerable bending moments do develop at the bottom of the conical wall due to rotational restraint at the joint. The moment towards the top of the wall is however of opposite sign causing tension on outer face, the magnitude being of the order of 40% to 80% of the moments at the bottom.

4.8.6 The Bottom Circular Beam

The Finite Element analysis using axi-symmetric shell elements is not capable of providing any useful information regarding the stress condition of the bottom circular beam. Conventionally this beam is designed for positive and negative bending moments, twisting moments and shear. None of these quantities are available from the FE program. In fact the program has no scope to deal with discrete supports as provided by the columns. Rather it assumes an idealised support condition wherein the beam is supposed to have a continuous support along the whole length of its periphery which is necessary for the sake of analysis using axi-symmetric shell elements.

Due to the above inherent limitation of the program it is not possible to suggest any improvement in the design of the bottom circular beam. The conventional method of analysis and design is, therefore, recommended for this part of the structure.

4.8.7 The Bottom Dome

As in the top dome, membrane behaviour prevails in the bottom dome as well except at the edge. Meridional bending moment of moderate intensity develops at the edge due to end effect. To take care of this moment flexural reinforcements must be provided on the top surface of the dome near the junction with the bottom circular beam. It

may be desirable to thicken the dome near the edge. In some cases circumferential tension may develop in a small peripheral ring if the bottom circular beam is in hoop tension. These points need to be considered during the design of the bottom dome.

CHAPTER 5

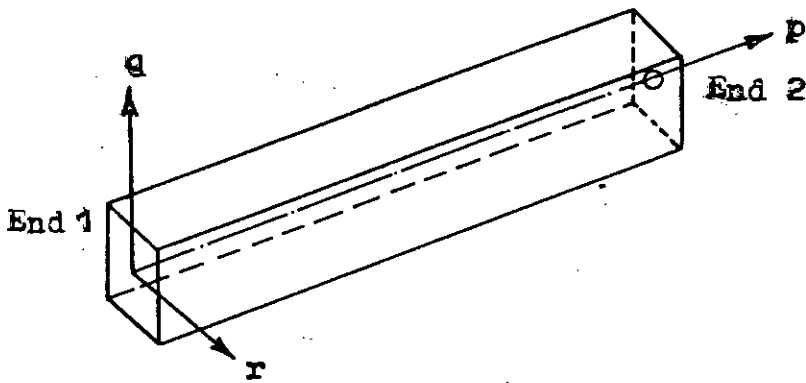
SPACE FRAME ANALYSIS OF THE TOWER

5.1 Introduction

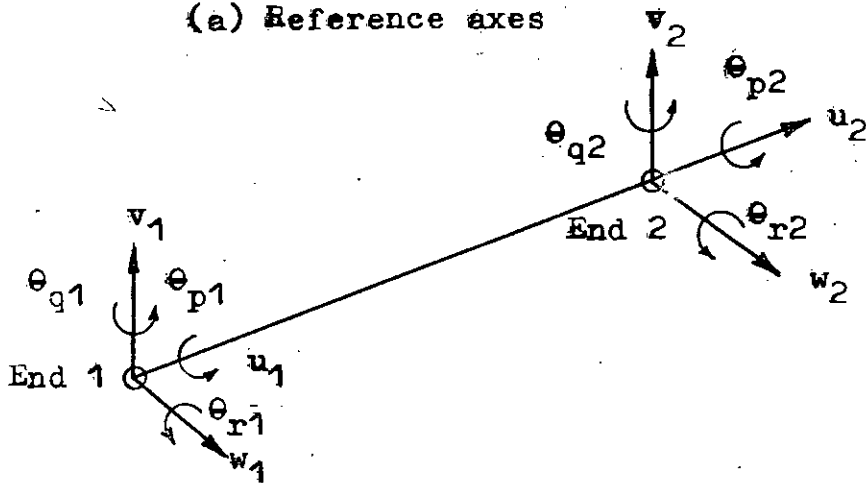
As stated in Chapter 3, the supporting tower of Intze tanks calls for a space frame analysis for rational design. To assess the degree of justifiability of the conventional methods of analysis which vary widely in their approach, the towers designed on the basis of conventional analysis in Chapter 3, have been subjected to computer analysis using a space-frame program due to Rahman⁽⁶⁾. In a bid to rationalise the design of the tower, the effect of a few basic parameters have been studied to some extent. The results of this study are presented and discussed in the last few articles of this chapter. Some important observations have been made from the investigation.

5.2 The Space-Frame Program

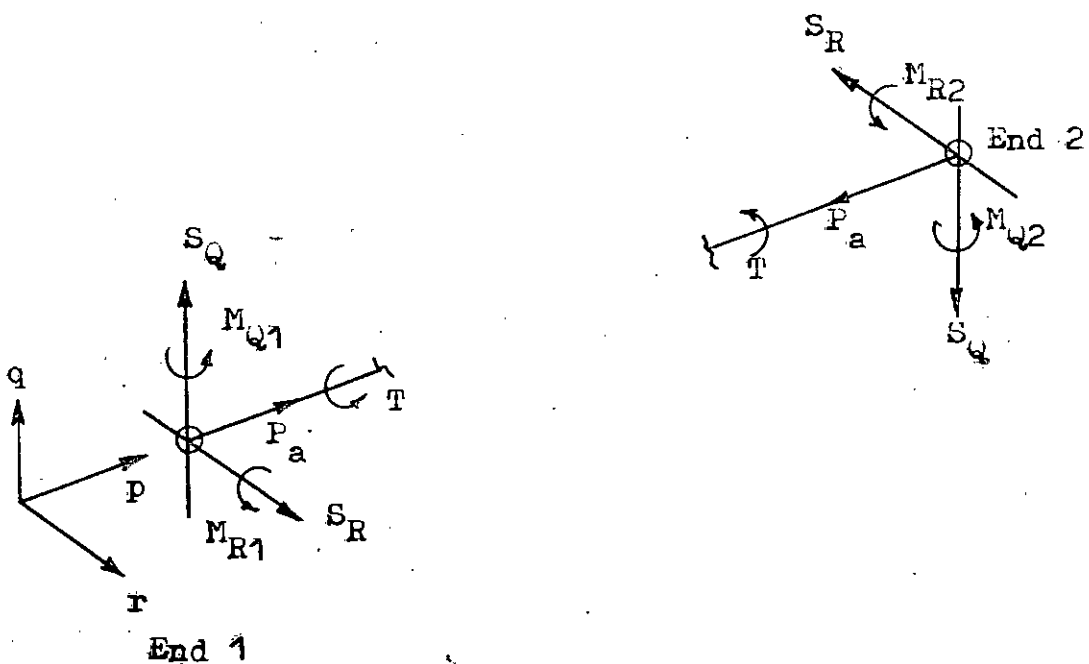
A general space-frame program developed by Rahman⁽⁶⁾ has been adapted with some modifications for the analysis of water towers. The original program being general in nature, required a considerable volume of input data such as the joint co-ordinates, member-joint connectivity, applied joint loads, material properties, fixity conditions etc. In order to reduce the volume of input data, a subroutine was written to generate the bulk of the data from a nominal input such as the height of tower, inclination of columns, no. of columns and bracings etc. The complete program is listed in a separate report with user instructions.



(a) Reference axes



(b) Nodal displacements



(c) Forces and moments

Fig. 5.1 Space frame member element.

The space frame member element used in the finite element formulation is shown in Fig. 5.1(a), in which the direction of the p-axis is always from end 1 (lower joint) to end 2 (higher joint). Each end of the member can have three translations and three rotations as shown in Fig. 5.1(b). The eight possible member forces and moments are shown in Fig. 5.1(c). These are the axial force P_a , two shear forces S_R and S_Q , torque T and the moment at the two ends about q and r axes M_{Q1} , M_{Q2} , M_{R1} and M_{R2} . The computer output gives the above eight quantities for each member directly.

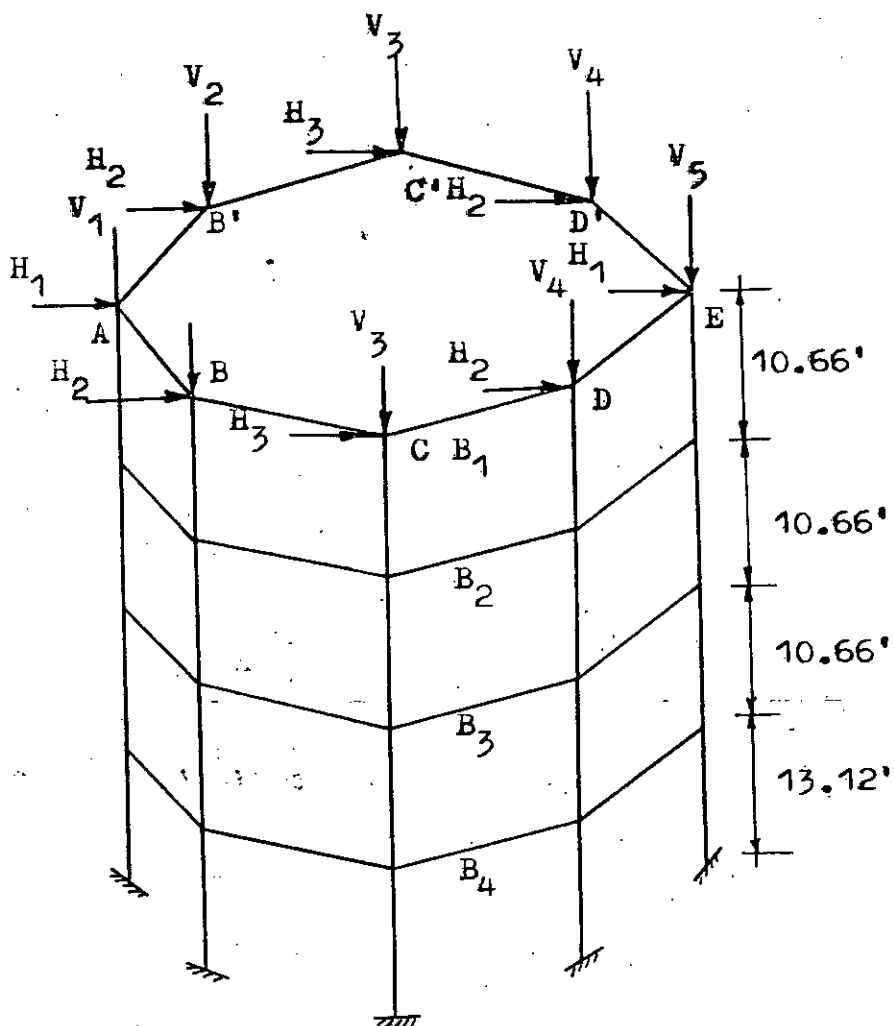
5.3 Case Studies

The results of finite element analysis (using space frame member elements) of the water tank towers designed in Chapter 3, are presented in graphical/tabular form in the following sub-articles.

5.3.1 Case Study 1

Fig. 5.2 shows the geometrical features of the tower and the joint loads applied at the top. The vertical loads V_1 , V_2 etc. at the column tops are the combined forces due to

- a) the weight of the tank (and water) above and
- b) the vertical forces induced at the column tops by the wind acting on the tank.



Columns = 19.69" dia.
 B₁ = 15.7"x26.6"
 B₂, B₃, B₄ = 10"x14.5"
 Dia. of col. circle
 = 29.53'

Fig. 5.2 Assumed distribution of wind load and dead load at column tops. Joint loads due to wind and dead-load of members applied at other joints not shown.

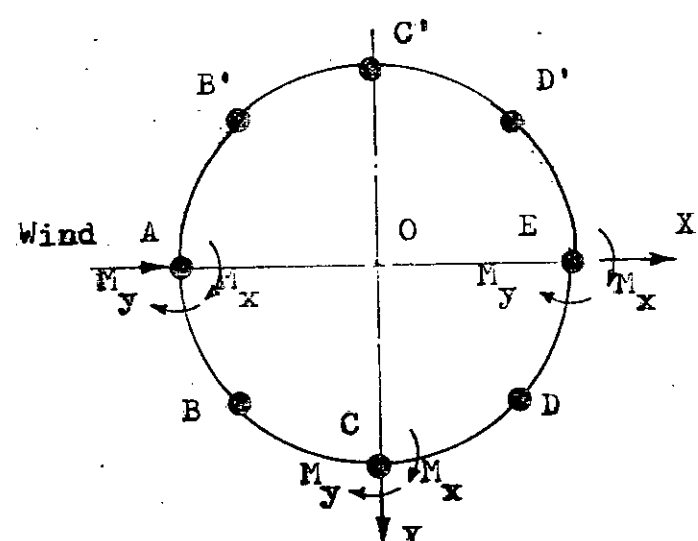
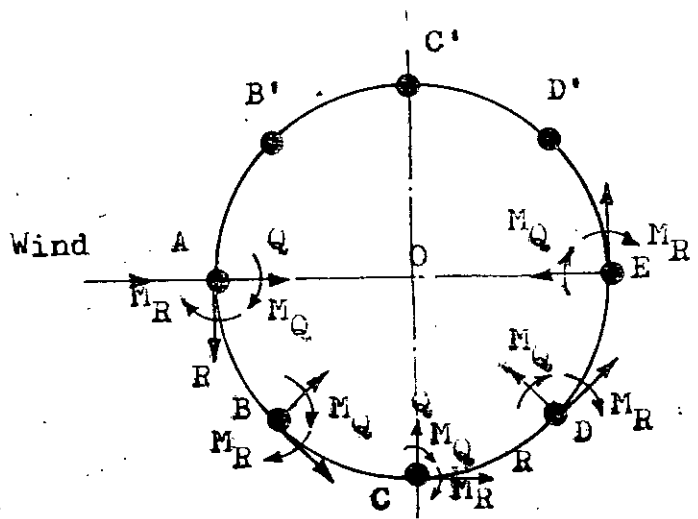


Fig. 5.3 Positive sense of M_Q and M_R . M_Q = Moment about radial axis. M_R = Moment about tangential axis.
 Fig. 5.4 Positive sense of M_x and M_y .

The horizontal forces H_1 , H_2 etc. are the shares of the total horizontal wind force acting on the tank attributed to the columns. The joint loads acting at other joints due to the weight of the columns and bracings, and the wind acting on their surface are computed inside the program and therefore not shown in the diagram.

Fig. 5.3 shows the positive sense of the column end moments M_Q and M_R with respect to member axes that are obtained as direct outputs from the computer. These may be reorganised with necessary conversion of signs and magnitudes to give the column end moments as M_x and M_y (Fig. 5.4) in global coordinates if desired.

The tower in case-study-1 has been analysed for two different distributions of the horizontal forces H_1, H_2 etc. at the column tops, the sum of the forces remaining the same in both the cases. In Case 1(a) $H_1 = H_2 = H_3$ i.e. $H_1:H_2:H_3 = 1:1:1$, while in Case 1(b) $H_1:H_2:H_3 = 0:1:2$.

The diagrams for column moments M_Q and M_R for the two cases are shown in Figs. 5.5 through 5.8 which reveal some important features:

(i) The column moments remain virtually the same whether the horizontal wind force acting on the tank is distributed equally or unequally among the columns at their top.

(ii) The extreme windward and leeward columns (columns A & E) develop large M_R but negligible M_Q , while for the

Case 1(a)

Vertical loads

$V_1 = 217.705$ kips

$V_2 = 218.944$ "

$V_3 = 221.936$ "

$V_4 = 224.927$ "

$V_5 = 226.166$ "

Lateral loads

$H_1 = 2.38$ kips

$H_2 = 2.38$ "

$H_3 = 2.38$ "

i.e. $H_1:H_2:H_3 = 1:1:1$

Geometry as shown in Fig. 5.2

Scale: 1" = 1000 k" = 83.33 k'

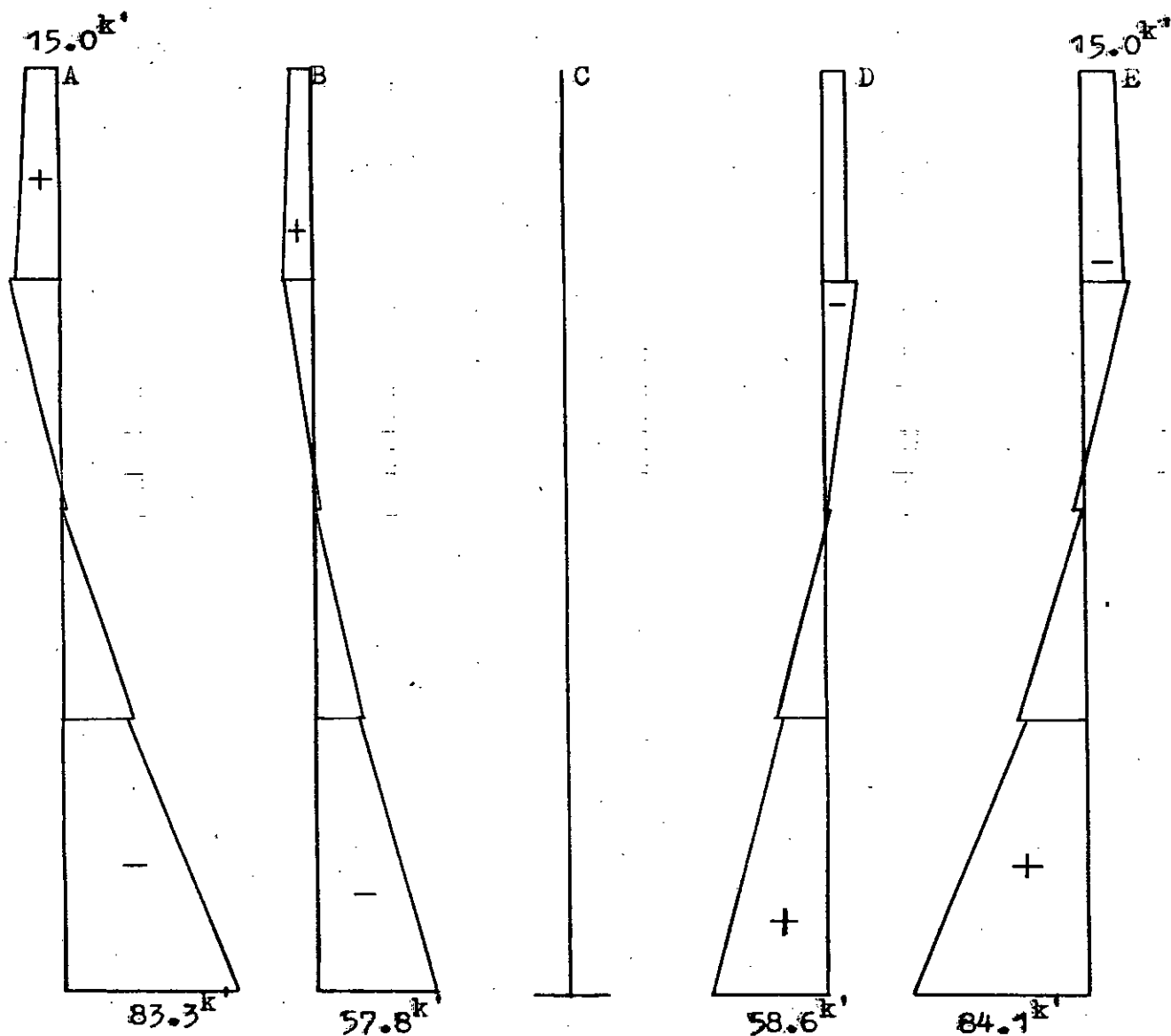


Fig. 5.5 Column moment M_R (+ve sense of M_R shown in Fig. 5.3)

Case 1(a)

Scale: $1'' = 1000 k'' = 83.33 k'$

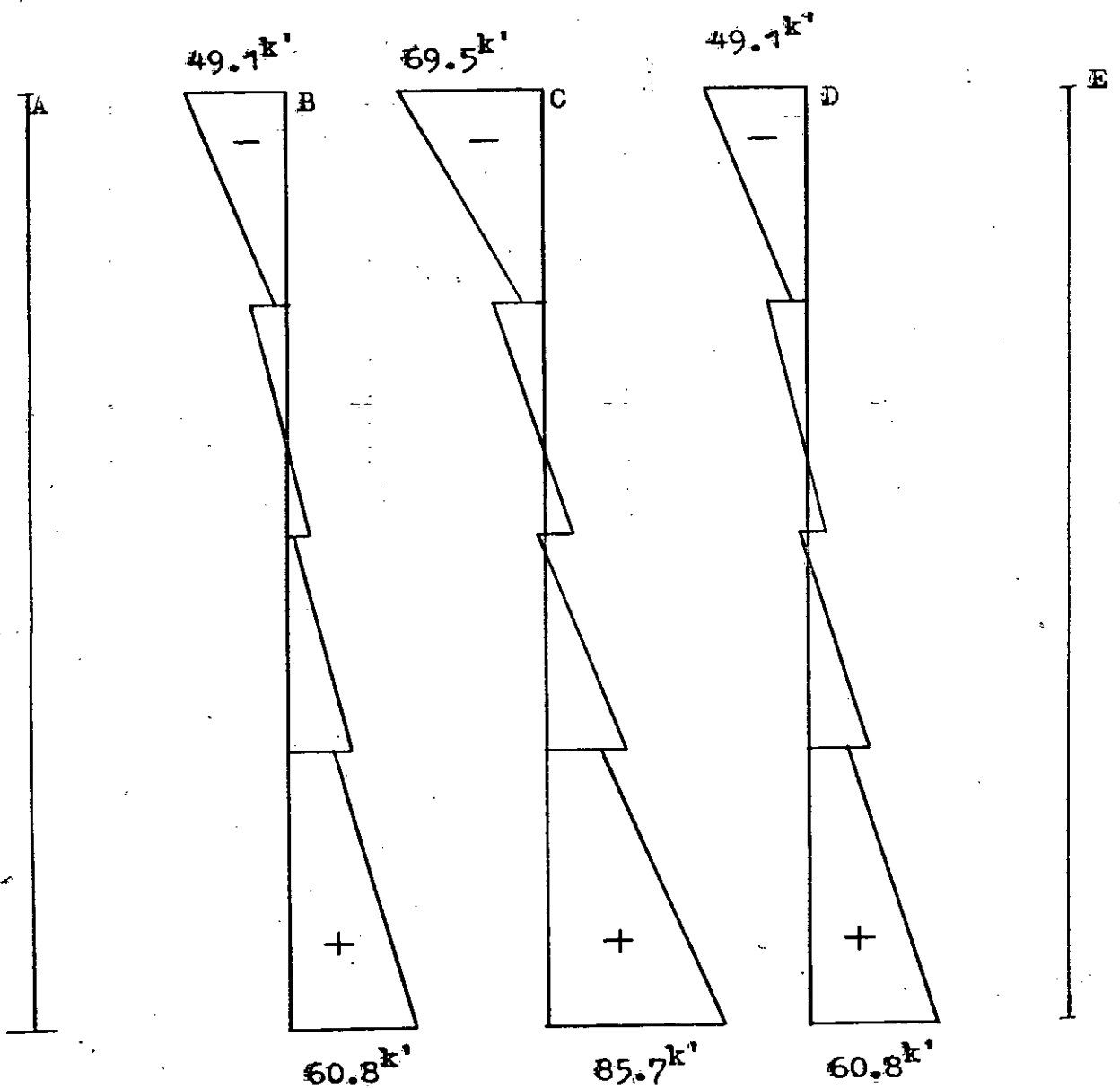


Fig. 5.6 Column moment M_c (+ve sense of M_c shown in Fig. 5.3)

Case 1(b)

Vertical loads
as in case 1(a).

Lateral loads

$$H_1 = 0.0 \text{ kips}$$

$$H_2 = 2.38 \text{ "}$$

$$H_3 = 4.76 \text{ "}$$

$$\text{i.e. } H_1:H_2:H_3 = 0:1:2$$

Geometry as in 1(a).

Scale: 1" = 1000k" = 83.33k'

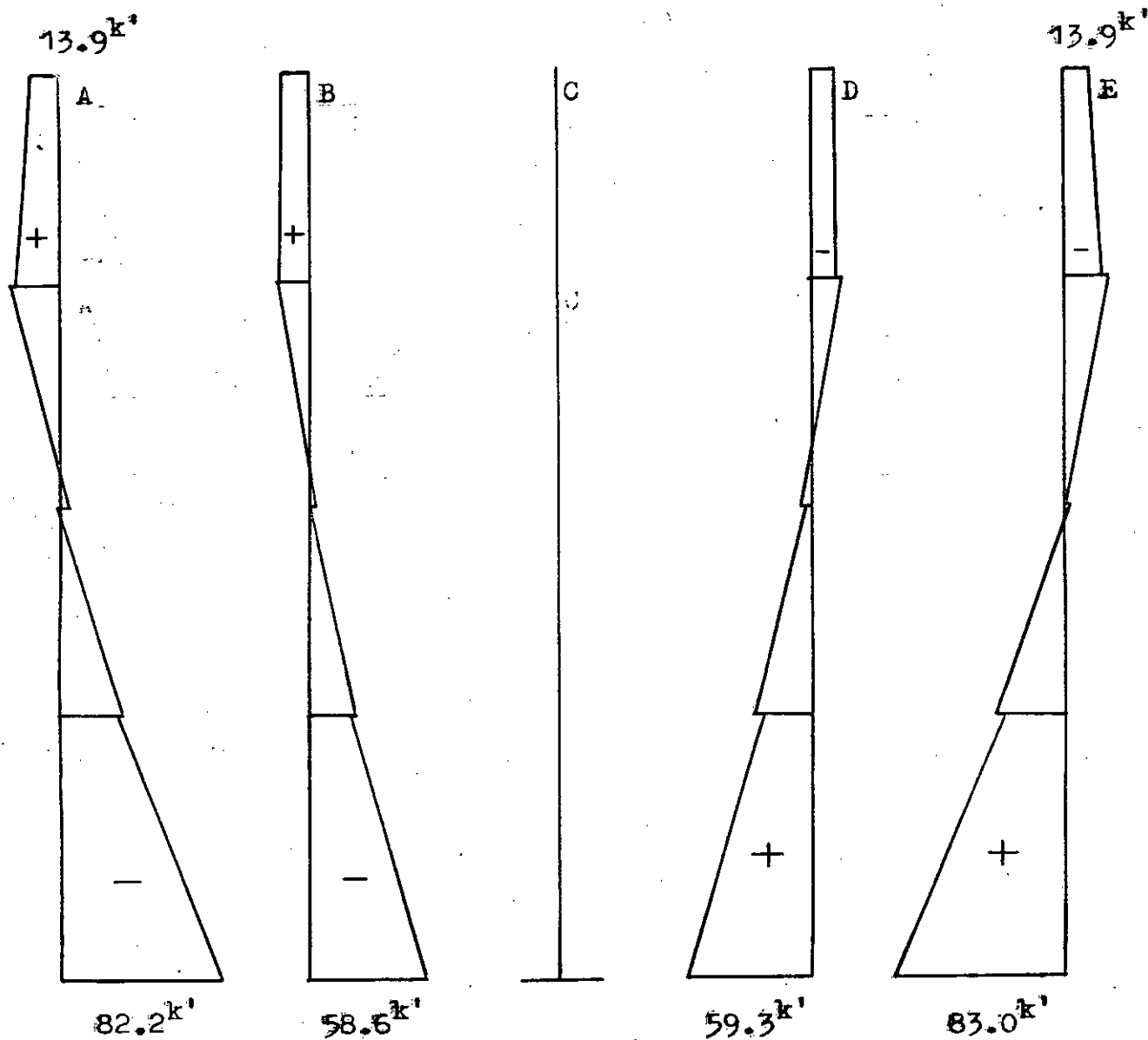


Fig. 5.7 Column moment M_R .

Case 1(b)

Scale: 1" = 1000 k-in = 83.33 k'

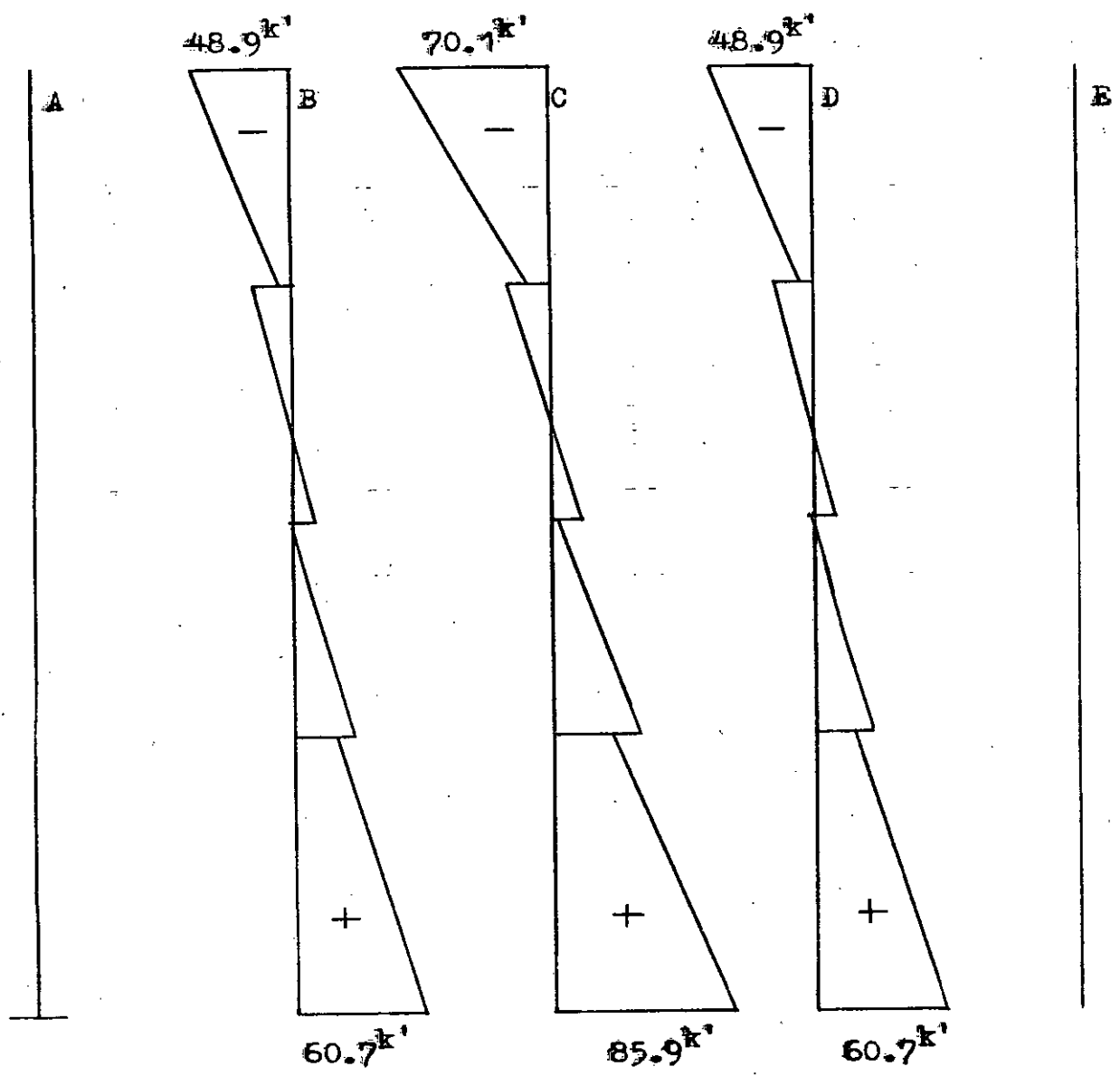


Fig. 5.8 Column moment M_c .

columns lying on the bending axis (columns C and C') the case is just the reverse. Moreover, the values of M_R in columns A and E are nearly equal in magnitude at any level of the tower. While at the base of the tower the moment M_R in column A or E also approximately equals the moment M_Q in column C or C'. In other columns M_Q and M_R have intermediate values but interestingly their resultant is of the same order as M_R in column A or M_Q in column C.

(iii) Points of contraflexure do not occur at the midheights of the column panels as has been assumed in the conventional analysis. This means that the bracings used in the design are not sufficiently stiff compared to the columns ($K_{Br} : K_{col} = 1:3.1$), to force the columns develop points of contraflexure at the mid-heights of their panels.

(iv) The bracings are most effective (although not sufficiently) for columns lying on the bending axis and least effective for the extreme windward and leeward columns as evident from the jumps in the moment diagrams of the columns at the joints.

(v) The twisting moments in the bracings are negligible.

In view of the observation (ii) above, it appears that if the column moments M_Q and M_R (Fig. 5.3) are replaced by M_x and M_y (Fig. 5.4) then it would be sufficient to plot only the column moment M_y for all the columns in single diagrams as in Figs. 5.9 and 5.10 for Cases 1(a) and 1(b) respectively. The bracing moments (M_B) are also plotted on the same diagrams. In addition the axial forces in the columns at the bottom are shown as reactions. The bracings

Case 1(a)

Scale: $1'' = 1000k'' = 83.33k'$

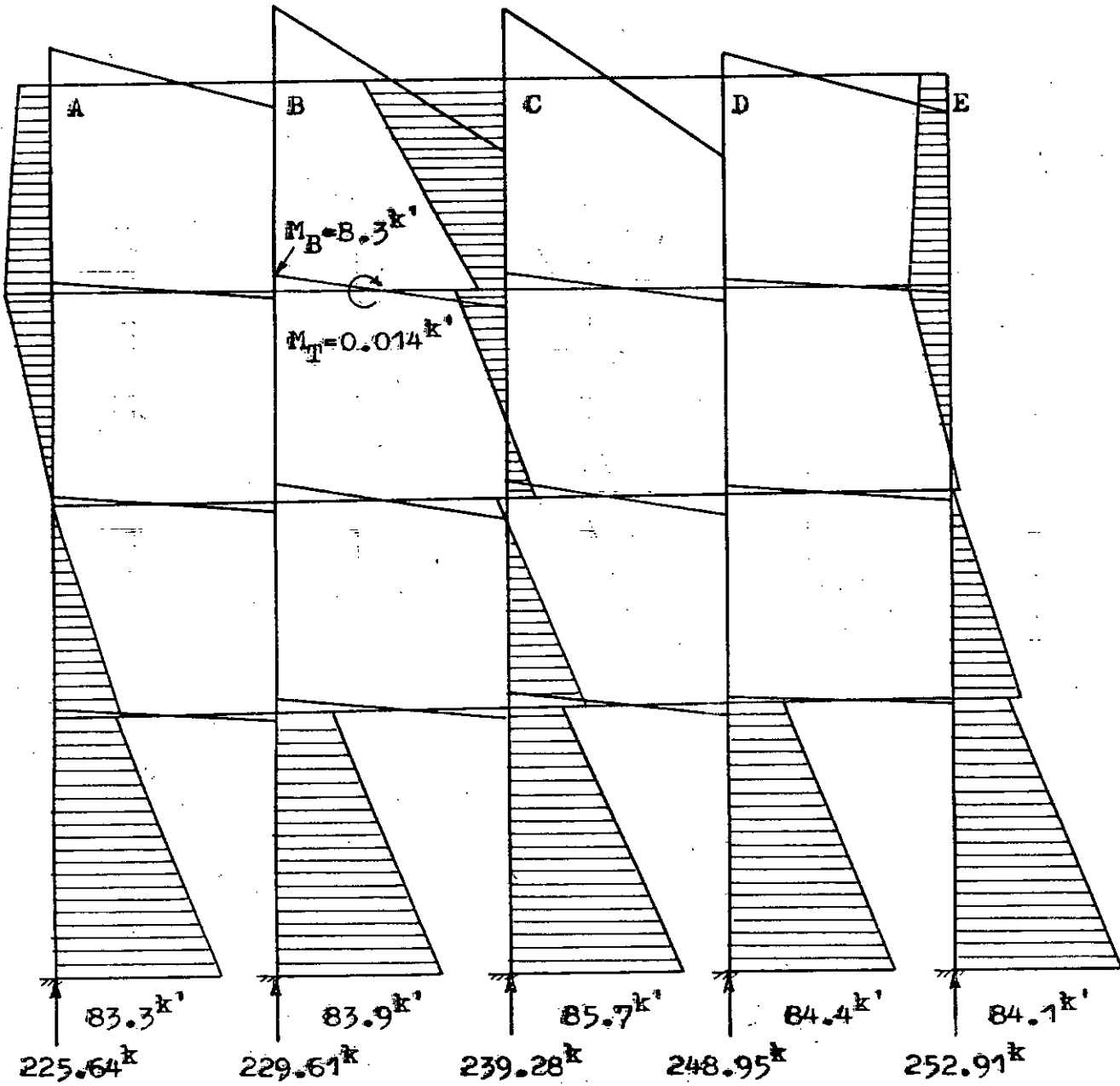


Fig. 5.9 Column moment M_y and bracing moment M_B .

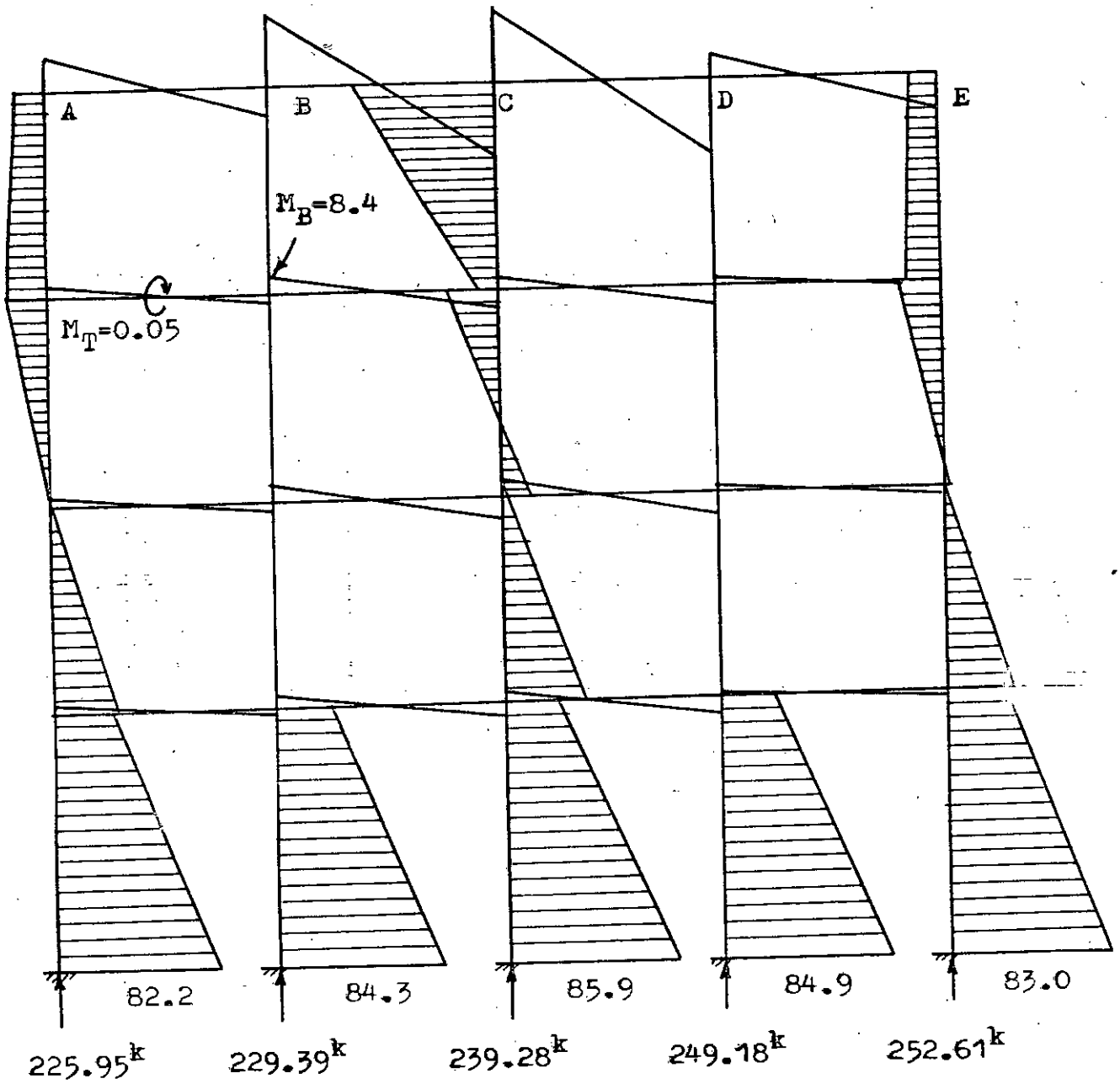
Case 1(b)

Fig. 5.10 Column moment M_y and bracing moment M_B .
Scale: $1'' = 83.33^k'$

which develop the maximum bending moment M_B and the maximum twisting moment M_T are identified in the diagrams by writing the values of M_B and M_T in the corresponding braces.

It will be observed that complete moment diagrams have not been drawn for the intermediate columns B and D. This has been done advertently because M_y for these columns have to be calculated manually from M_Q and M_R whereas it appears to be of little use for design purposes.

The values of M_y , M_B , M_T and the axial forces in the columns (AF) at critical locations are tabulated in Table 5.1 for both the Cases 1(a) & 1(b) alongside the corresponding values calculated by the conventional method due to Jai and Jain for direct comparison.

TABLE 5.1

Cases		1(a)	1(b)	Jai & Jains
Forces & Moments				
Column A (Bottom)	AF(kips)	225.64	225.95	222.09
	M_y (K')	83.3	82.2	0.0
Column E (Bottom)	AF(kips)	252.92	252.61	262.35
	M_y (K')	84.1	83.0	0.0
Column C (Bottom)	AF(kips)	239.28	239.28	242.22
	M_y (K')	85.7	85.9	47.7
Bracing	M_B (K')	8.3	8.4	68.35
	M_T (K')	0.014	0.05	3.42
	SF(kips)	1.64	1.66	13.27

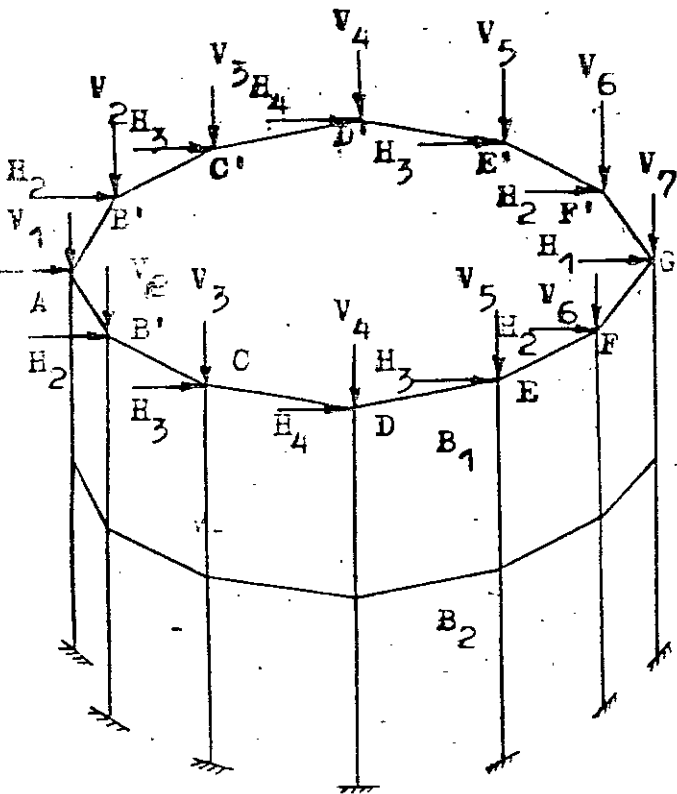
5.3.2 Case Study 2

In the light of observation (i) of Case study-1, the tower in case study 2 is analysed only for equal distribution of horizontal wind load at the column tops as shown in Fig. 5.11. The resulting bending moments M_y and M_B in the columns and bracings, the maximum twisting moment M_T in the bracing as well as the vertical reactions at the bases of the columns are shown in Fig. 5.12 and the critical values tabulated in Table 5.2. The following points are observed in this case study:

(i) The moments (M_y) in the columns A, B, C and D are in the ratio of 1:1.11:1.33:1.44 at the bottom ends and 1:1.43:2.27:2.70 at the top ends. It is worthwhile to note that the ratio assumed by Gray & Manning is 3:4:5:6 (Art. 3.2.3) which is equivalent to 1:1.33:1.67:2.0.

(ii) The bracings appear to be more or less adequate in this case in restraining the columns ($K_{br} : K_{col} \approx 1:1.1$).

(iii) The twisting moment (M_T) in the bracings is of the order of 4% of the bending moment (M_B).



Geometry

Column size = 18" square

Top bracing, $B_1 = 18" \times 30"$

Other bracing, $B_2 = 12" \times 16"$

Diameter of col. circle = 40'

Height of tower = 40'

No. of columns = 12

Loads

$$H_1 = H_2 = H_3 = H_4 = 2.0^k$$

$$V_1 = 162.47^k$$

$$V_2 = 162.76^k$$

$$V_3 = 163.51^k$$

$$V_4 = 164.50^k$$

$$V_5 = 165.49^k$$

$$V_6 = 166.24^k$$

$$V_7 = 166.53^k$$

Fig. 5.11 Tower of case study 2.

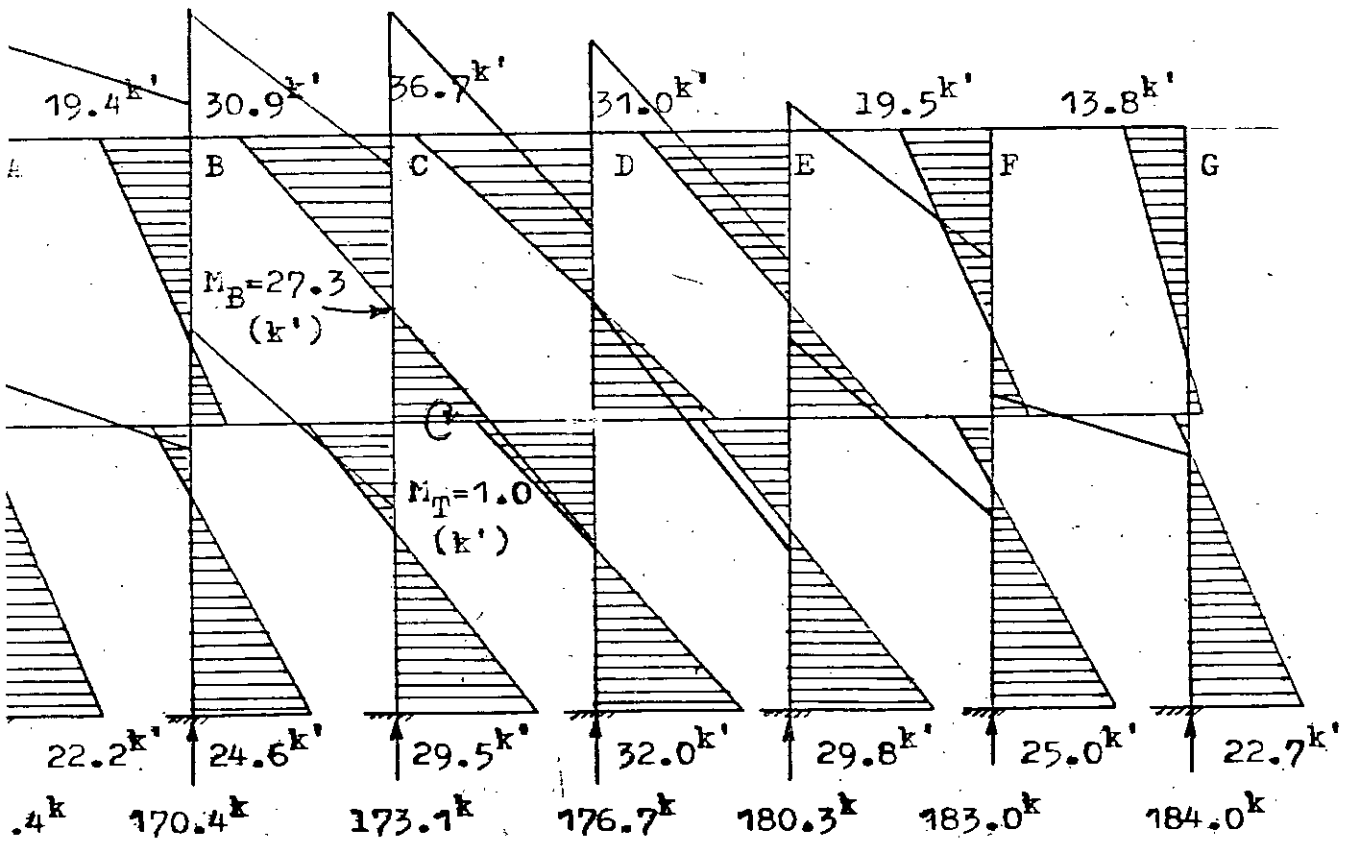


Fig. 5.12 Column moment M_T and bracing moment M_B .

(Scale: 1" = 41.67 k')

TABLE 5.2

Cases		2	Gray & Manning
Forces & Moments			
Column A (Bottom)	AF	169.4	171.89
	M_y	22.2	20.0
Column G (Bottom)	AF	184.0	188.1
	M_y	22.7	20.0
Column D (Bottom)	AF	176.7	180.0
	M_y	32.0	34.3
Bracing	M_B	27.3	34.3
	M_T	1.03	0.0
	SF	5.17	6.86

5.3.3 Case Study 3

The space frame analysis of the tower in this case (Fig. 5.13) also has been carried out assuming the wind load on the tank to be distributed equally to the eight joints at the top of the tower. Just as in case study 2, the results are shown diagrammatically in Fig. 5.14 and tabulated in Table 5.3. The salient features in this case are as follows:

(i) The proportion of the moments at the bottom of the columns A, B and C is about 1:1.02:1.05.

(ii) The bracings do not seem to have adequate stiffness compared to that of the columns ($K_{br} : K_{col} \approx 1:1.72$).

(iii) The twisting moments in the bracings are negligible.

TABLE 5.3

Cases		3	Sushil Kumar
Forces & Moments			
Column A (Bottom)	AF M_y	437.34 127.4	443.0 31.83
Column E (Bottom)	AF M_y	512.25 129.8	509.74 31.83
Column C (Bottom)	AF M_y	474.79 133.9	476.37 31.83
Bracing	M_B	20.6	89.83
	M_T	0.05	0.0
	SF	3.27	14.37

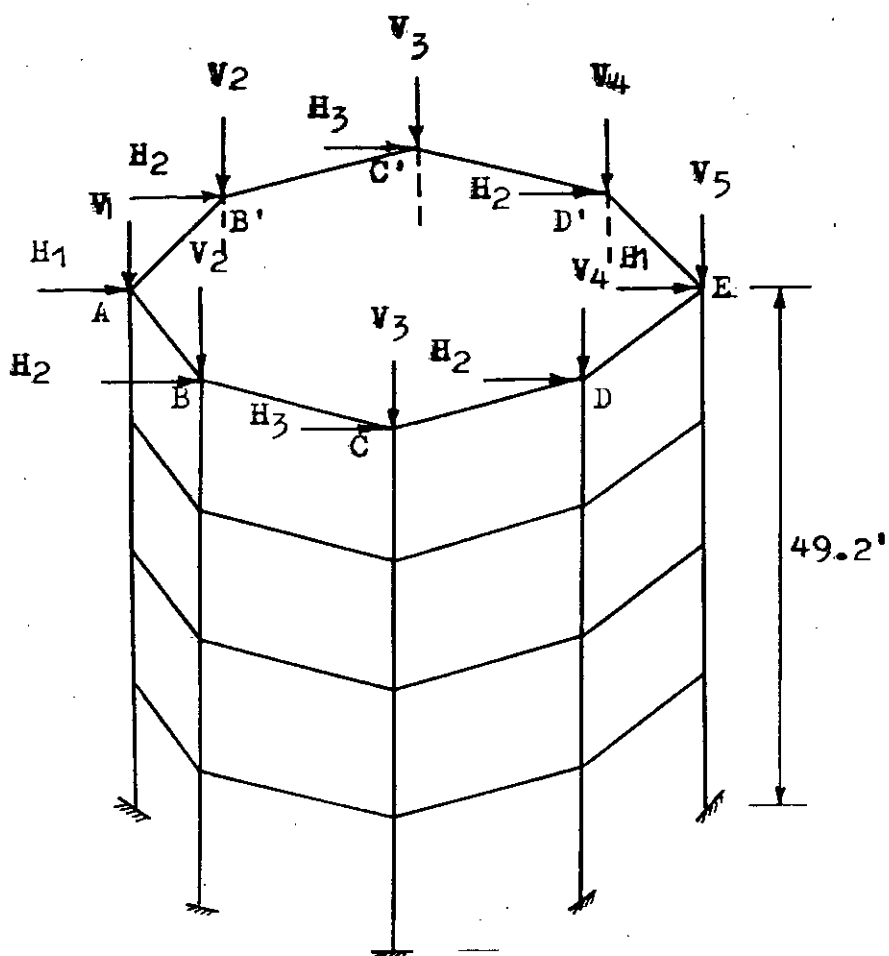


Fig. 5.13 The tower of case study 2.

Case Study 3

Z-loads

$V_1 = 414.799$ kips
 $V_2 = 421.157$ "
 $V_3 = 436.507$ "
 $V_4 = 451.858$ "
 $V_5 = 458.216$ "

X-loads

$H_1 = 3.720$ kips
 $H_2 = 3.720$ "
 $H_3 = 3.720$ "
 i.e $H_1:H_2:H_3=1:1:1$

Geometry

Height tower = 49.2 ft.
 Diameter = 32.8 ft.
 Column size = 25.6" dia.
 Top bracing = 25.6"x47.2"
 other bracings=19.69"x19.69"
 (3 layers equally spaced)

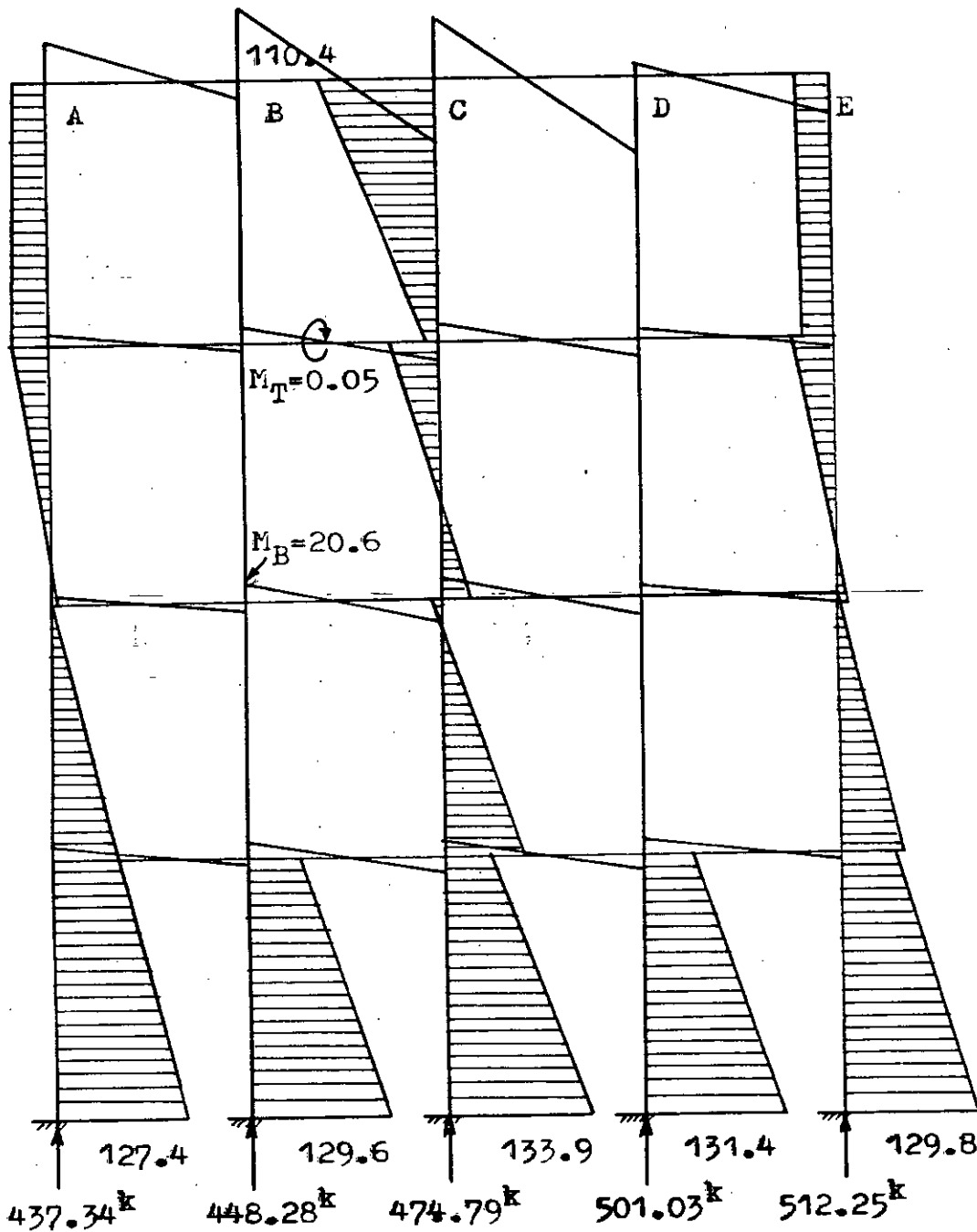


Fig. 5.14 Column moment M_y and bracing moment M_B .
 Scale: 1" = 166.67^{k'}

5.3.4 Case Study 4

Fig. 5.15 shows the tower and the loads applied at the top. This tower is analysed for an earthquake force of 218^k (vide Art. 3.3.4) assumed to act at a height 78' from ground level i.e. 8' above the top of the tower. The joint loads $H_1, H_2, \dots, V_1, V_2$ etc. are accordingly calculated taking into consideration the dead loads as well. As in Case study-1, this tower is also analysed for two different distributions of the lateral forces H_1, H_2 etc. to the column tops. In case 4(a) $H_1:H_2:H_3 = 1:1:1$ while in Case 4(b) $H_1:H_2:H_3 = 0:1:2$. Other conditions are the same for both the cases. It may be noted here that the geometry of this tower has some basic differences with that of the other cases. The columns of this tower are battered at an approximate ratio of 1 horizontal to 11.55 vertical. In addition, the section of the columns is rectangular with the sides $CQ = 30''$ in the radial direction and $CR = 18''$ in the tangential direction with respect to the circle of columns (Fig. 5.16). The results of analysis for the two cases, 4(a) and 4(b), are shown in Figs. 5.17 and 5.18 respectively and tabulated in Table 5.4 along with the results of conventional analysis. The following points are observed in this case study:

- (i) Equal or unequal distribution of the horizontal forces H_1, H_2, \dots etc. at the column tops does not affect the results significantly.

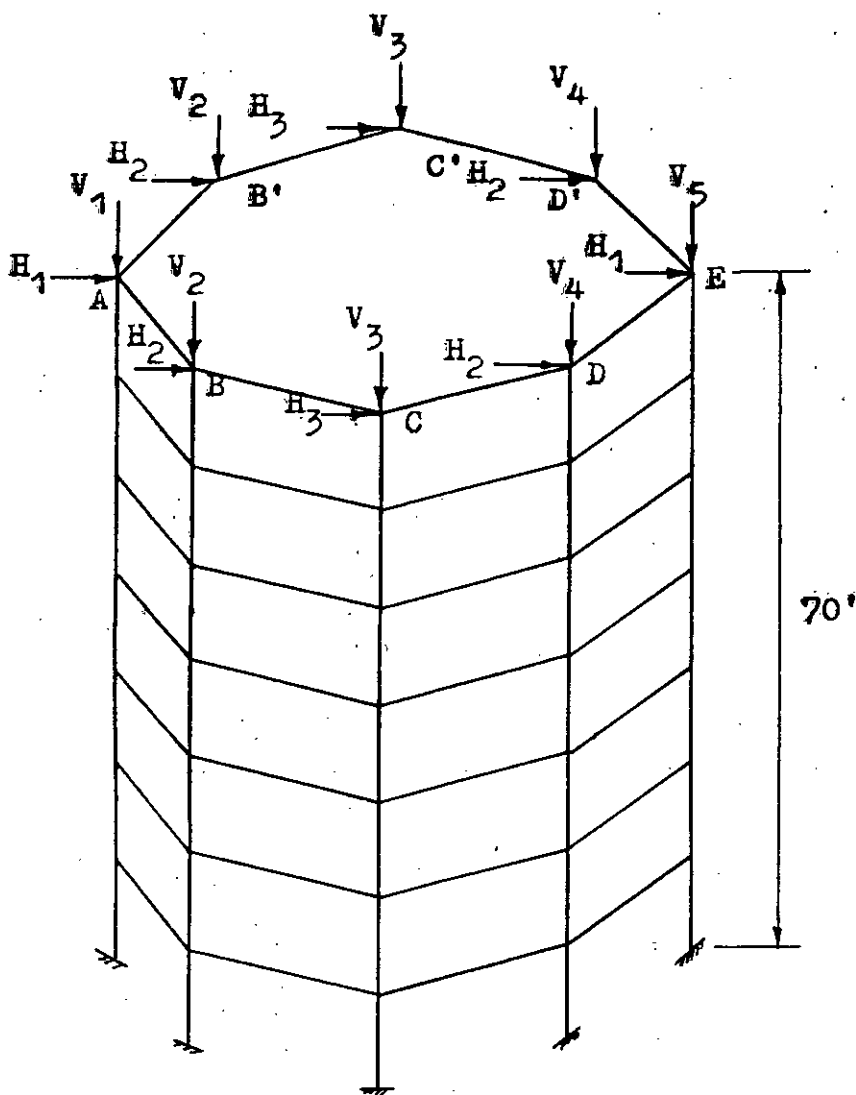


Fig. 5.15 Intze tank tower of case study 4.

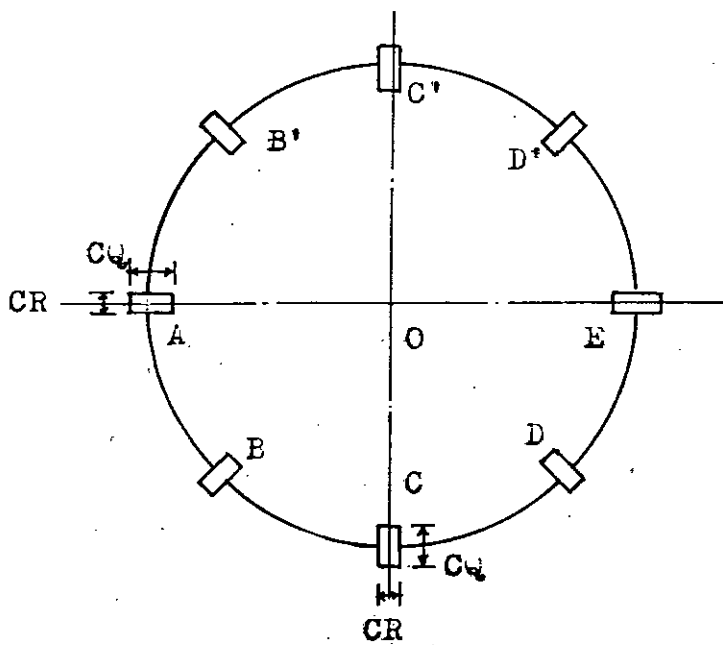


Fig. 5.16 Section of Tower.

Case 4(a)

Z-loads at top

$V_1 = 243.180$ kips
 $V_2 = 253.379$ "
 $V_3 = 278.000$ "
 $V_4 = 302.621$ "
 $V_5 = 312.821$ "

X-loads at top

$H_1 = 27.25$ kips
 $H_2 = 27.25$ "
 $H_3 = 27.25$ "
 i.e $H_1:H_2:H_3=1:1:1$

Geometry

Height of tower = 70.0'
 Diameter = 30.0' at top
 and 42.1' at bottom
 Batter of columns=1:11.55
 Column size:GR=18",CG=30"
 Top bracing=20"x40"
 Other bracings=15"x31"
 (6 equidistant layers)

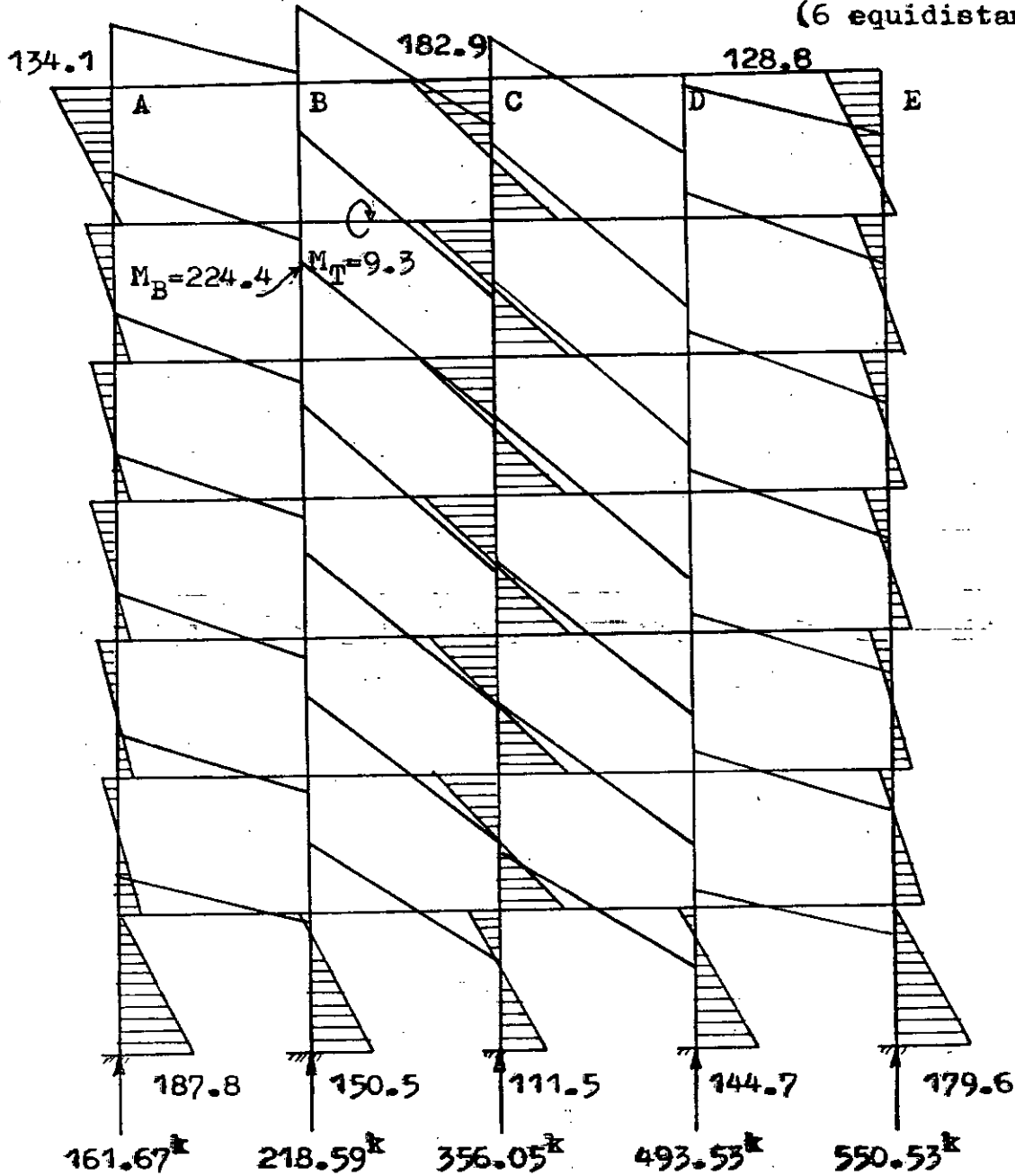


Fig. 5.17 Column moment M_y and bracing moment M_B .

Scale: 1" = 416.67k'

Case 4(b)

Z-loads at top: as in case 4(a).

X-loads at top: $H_1 = 0.0$ kips. $H_2 = 27.25$ " $H_3 = 54.50$ "i.e. $H_1:H_2:H_3 = 0:1:2$ Geometry

Same as in case 4(a)

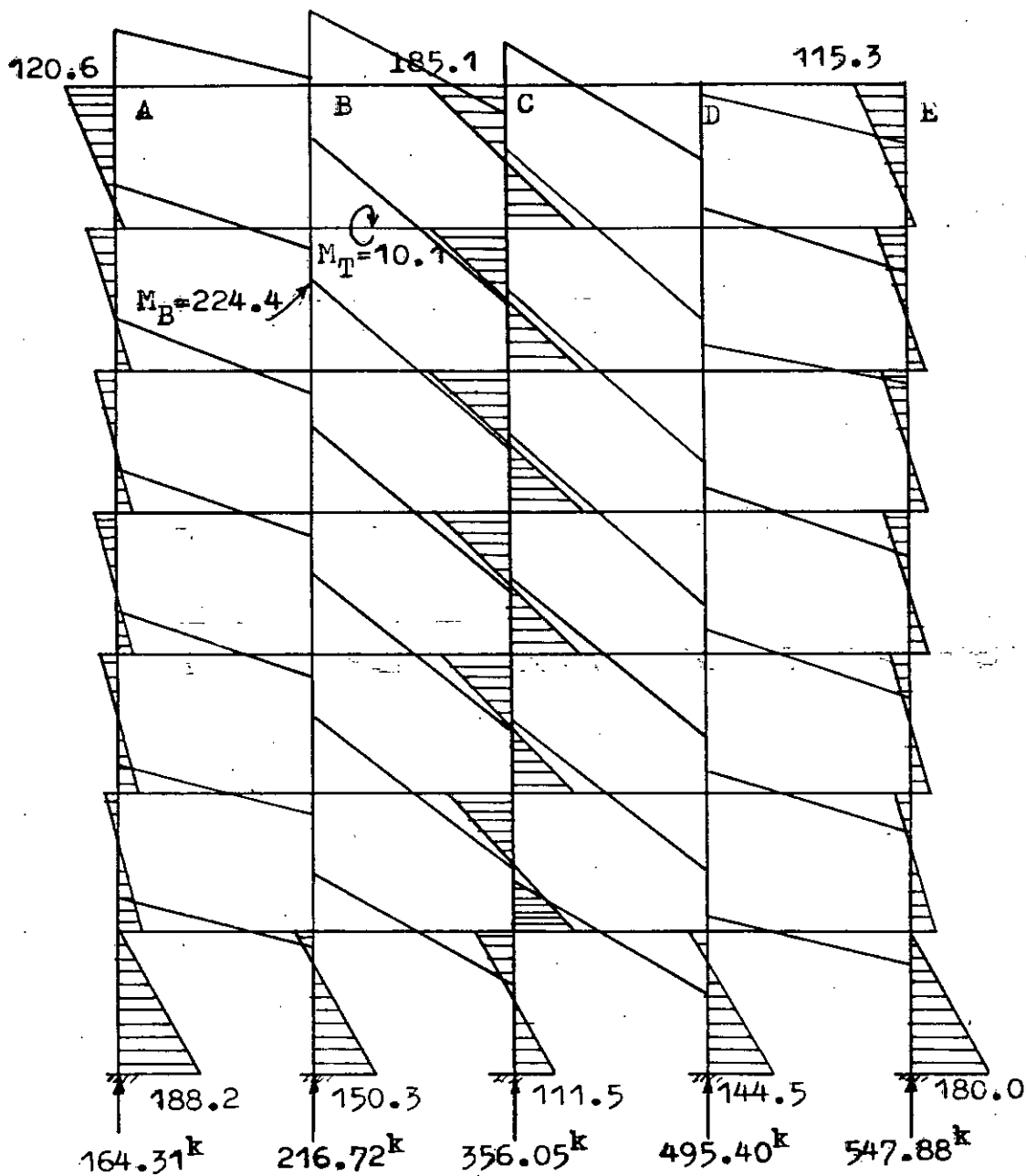


Fig. 5.18 Column moment M_y and bracing moment M_B
(Scale: 1" = 416.67^k)

TABLE 5.4

		Cases	4(a)	4(b)	BRTC	
		Forces & Moments				
Bottom	Column A	AF	161.67	164.31	148.0	
	M_y	M_y	187.8	188.2	136.0	
	Column E	AF	550.53	547.88	550.0	
	M_y	M_y	179.6	180.0	136.0	
	Column E	AF	356.09	356.05	349.0	
	M_y	M_y	111.5	111.5	136.0	
Top	Column A	AF	243.18	243.18	-	
	M_y	M_y	134.1	120.6	-	
	Column E	AF	312.82	312.82	-	
	M_y	M_y	128.8	115.3	-	
	Bracing	M_B		224.4	224.4	365.0
		M_x		9.3	10.1	0.0
SI			33.1	33.4	61.0	

- (ii) The bracings are quite effective in constraining the columns ($K_{br}:K_{col} = 1.85:1$).
- (iii) The moments (M_y) in the columns A, B and C are in the ratio of about 1:0.8:0.6 at the bottom, 1:1.2:1.4 at the top and 1:2.3:3.6 at intermediate panel ends.
- (iv) The column moments at intermediate panels are considerably lower than those at top or bottom panels for all columns except those on bending axis for which the moments are more or less uniform from top to bottom.
- (v) The twisting moments (M_T) in the bracings are of the order of 4% of the bending moments (M_B) in the bracings.
- (vi) Excepting top and bottom panels, in general, M_y is largest for columns lying on the bending axis (col. C or C') for which I_y is smallest, whereas M_y is smallest for columns lying on the extreme windward or leeward side for which I_y is largest.

5.4 Study of Parameters

The parameters studied to some extent to determine the response of the tower to variations of the parameters are as follows:

- (i) distribution of horizontal force to the columns at their top,
- (ii) the orientation of column section w.r. to the circle of columns,
- (iii) the inclination or batter of columns, and
- (iv) the stiffness of braces.

In addition to considering the results of the foregoing case studies, the tower of case study-4 is specially considered for further analysis for the sake of investigation. The tower is supposed to be acted upon by a horizontal force $F_{EQ} = 218^k$ due to earthquake in the positive x-direction at a height of 8.0' from the top of the tower. This horizontal force may conventionally be distributed to the column tops in various proportions, maintaining symmetry about x-axis. the axial force induced in any column is assumed to be proportional to its distance from the axis of bending. This force is added algebraically to the column loads due to dead load of the tank and water. The joint loads and fixed-end-moments due to the weight of bracings and columns are computed and applied at the joints by the data generation sub-routine. These are not shown in Fig. 5.15. The results of the investigation of the parameters are presented and discussed one by one in the following sub-articles.

5.4.1 Distribution of Horizontal Force to the Columns at Their Top

On the basis of the observation (i) in both case study-1 and case study-4 it can be inferred that equal or unequal distribution of horizontal forces to the column tops due to the effect of the wind or earthquake acting on the tank has no appreciable effect on the bending moments etc. in the columns or bracings, so long as the loads applied in say x-direction are symmetrical about x-axis. This means that the column moments etc. are actually governed by the total magnitude of the horizontal force and are virtually unaffected by the ratio in which the force is assumed to be distributed to the column tops. As a result subsequent analyses are based on equal distribution of the lateral force to the columns.

5.4.2 Orientation of Column Section

It has been observed that most of the conventional methods directly or indirectly recommend the use of column sections that have more or less equal moments of inertia about all axes through the centre such as circular, Octagonal (regular) or square sections. However, it might be noticed that in case study-4, a rectangular column section (18"x30") has been used with its longer side in the radial direction and shorter side in the tangential direction with respect to the circle of columns, i.e. CR = 18" and CQ = 30" (Fig. 5.16). The column section could also

have been aligned the other way making CR = 30" and CQ = 18". In order to determine which orientation is preferable from the point of view of efficiency and hence economy, three cases have been considered 4(c), 4(d) and 4(e). In all these cases the sectional area of the column as also the other conditions have been kept the same, while the relative values of CR and CQ have been changed as follows:

$$4(c) \text{ CR} = 18", \text{ CQ} = 30"$$

$$4(d) \text{ CR} = 23.24", \text{ CQ} = 23.24" \text{ (square section)}$$

$$4(e) \text{ CR} = 30", \text{ CQ} = 18"$$

The deflected shape of the tower (considering x and z displacements only) for the three cases are shown in Figs. 5.19, 5.20 and 5.21 respectively while the bending moments etc. in the columns and bracings are shown in Figs. 5.22, 5.23 and 5.24 respectively. If the x-displacement of the top of the tower Δ_x be considered as an index of the stiffness of the tower as a whole, then it would be apparent from the deflected shapes that the stiffness increases in the order 4(c) \rightarrow 4(d) \rightarrow 4(e) as Δ_x decreases in that order from 1.05" \rightarrow 0.877" \rightarrow 0.759".

This may be explained as follows. The horizontal force applied parallel to the x-axis develops bending moments in the columns about y-axis (M_y), the moments about x-axis being negligible. In restraining the columns against M_y , the bracings are most effective for columns C and C' lying on the bending axis and least effective for columns A & E.

Loads as in case 4(a).

Geometry also as in case 4(a) except: batter of columns = 1:11

Column size : CR = 18", CQ = 30"

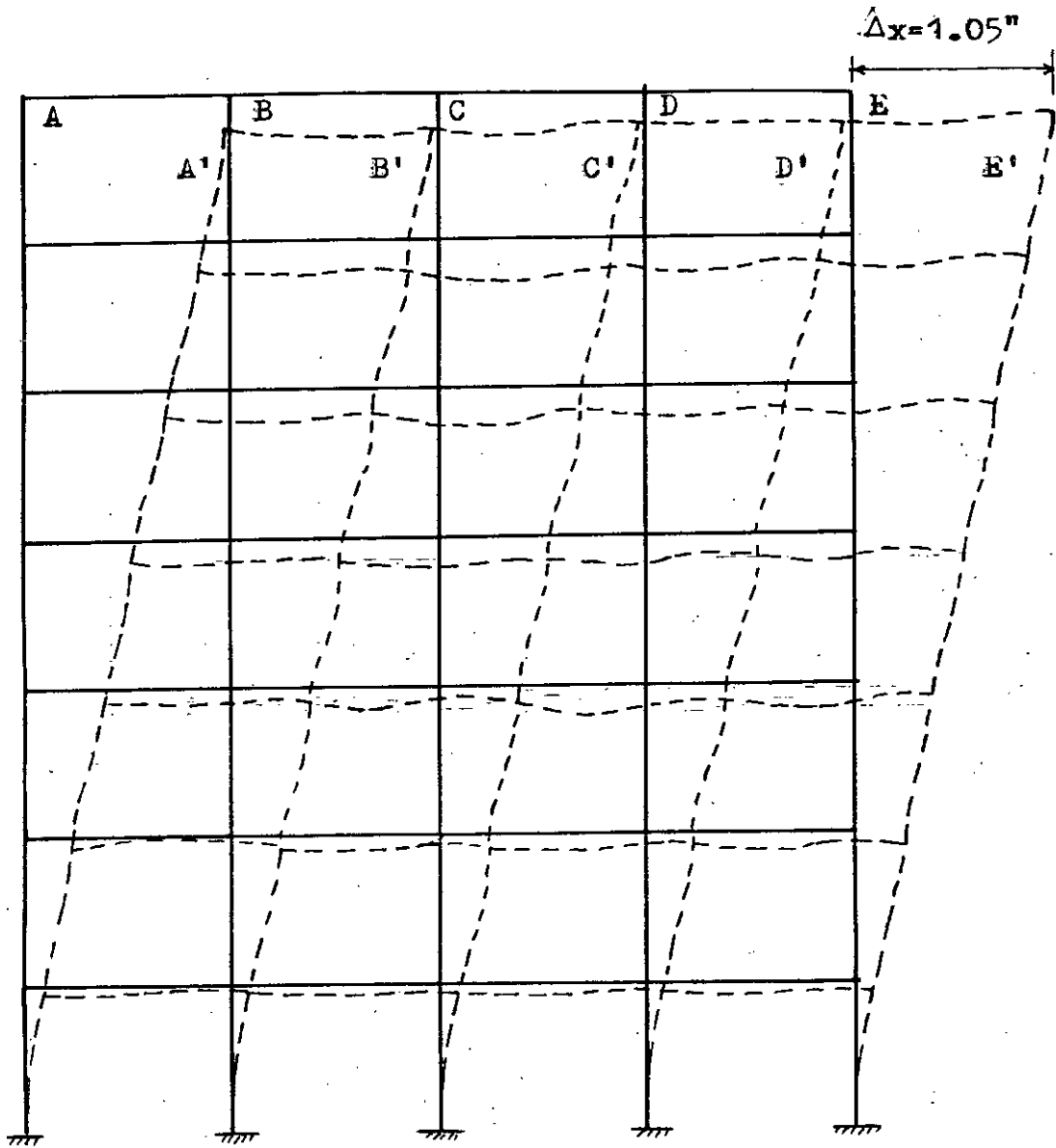


Fig. 5.19 x and z displacements for tower of case 4(c). (Scale: 1"=1")

Case 4(d)

Loads as in case 4(a)

Geometry also as in case 4(a) except: batter of columns = 1:11
 and Col. size CR = 23.24", CQ = 23.24"

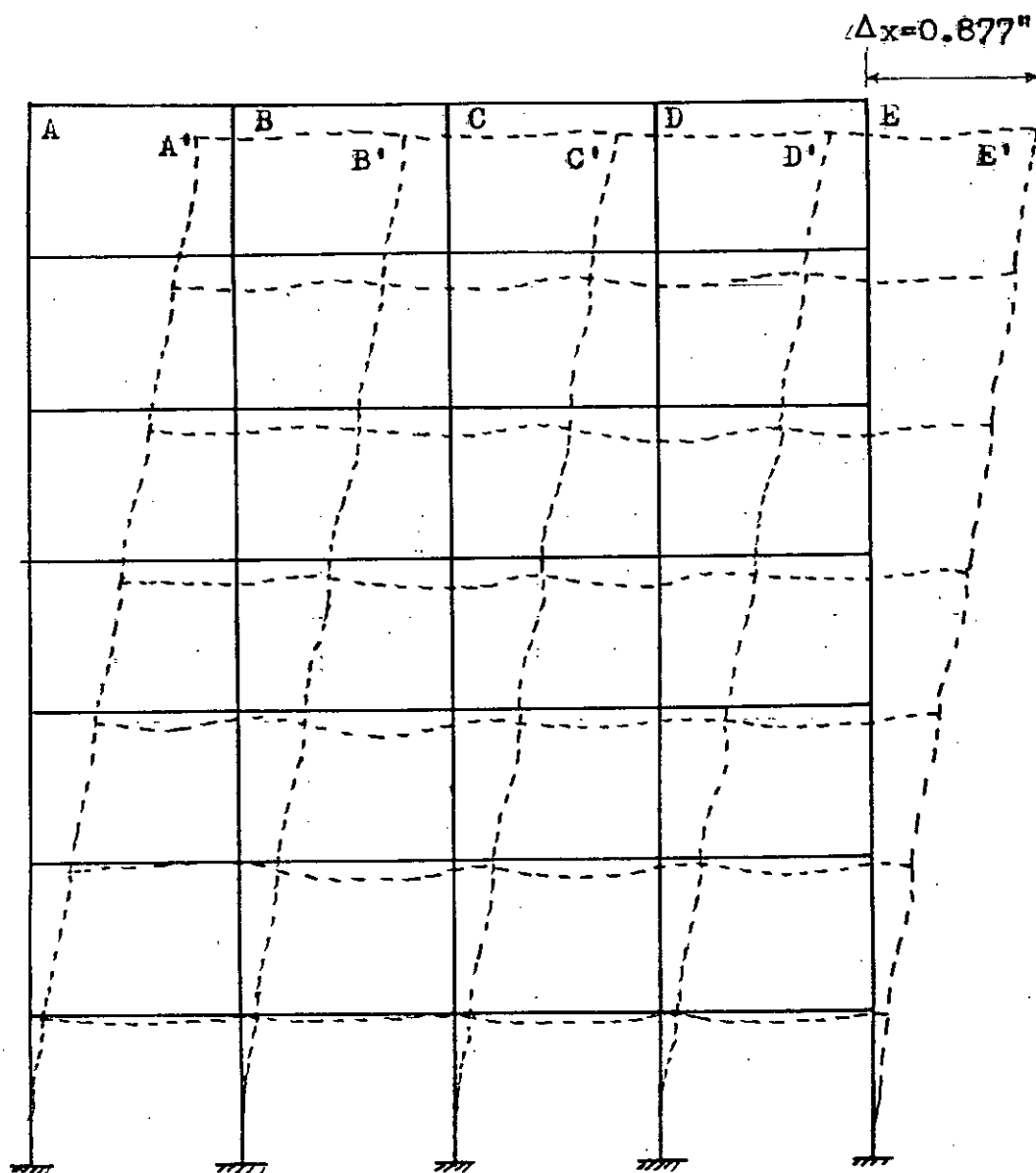


Fig. 5.20 x and z displacements.

(Scale: 1" = 1")

Case 4(e)

Loads as in case 4(a)

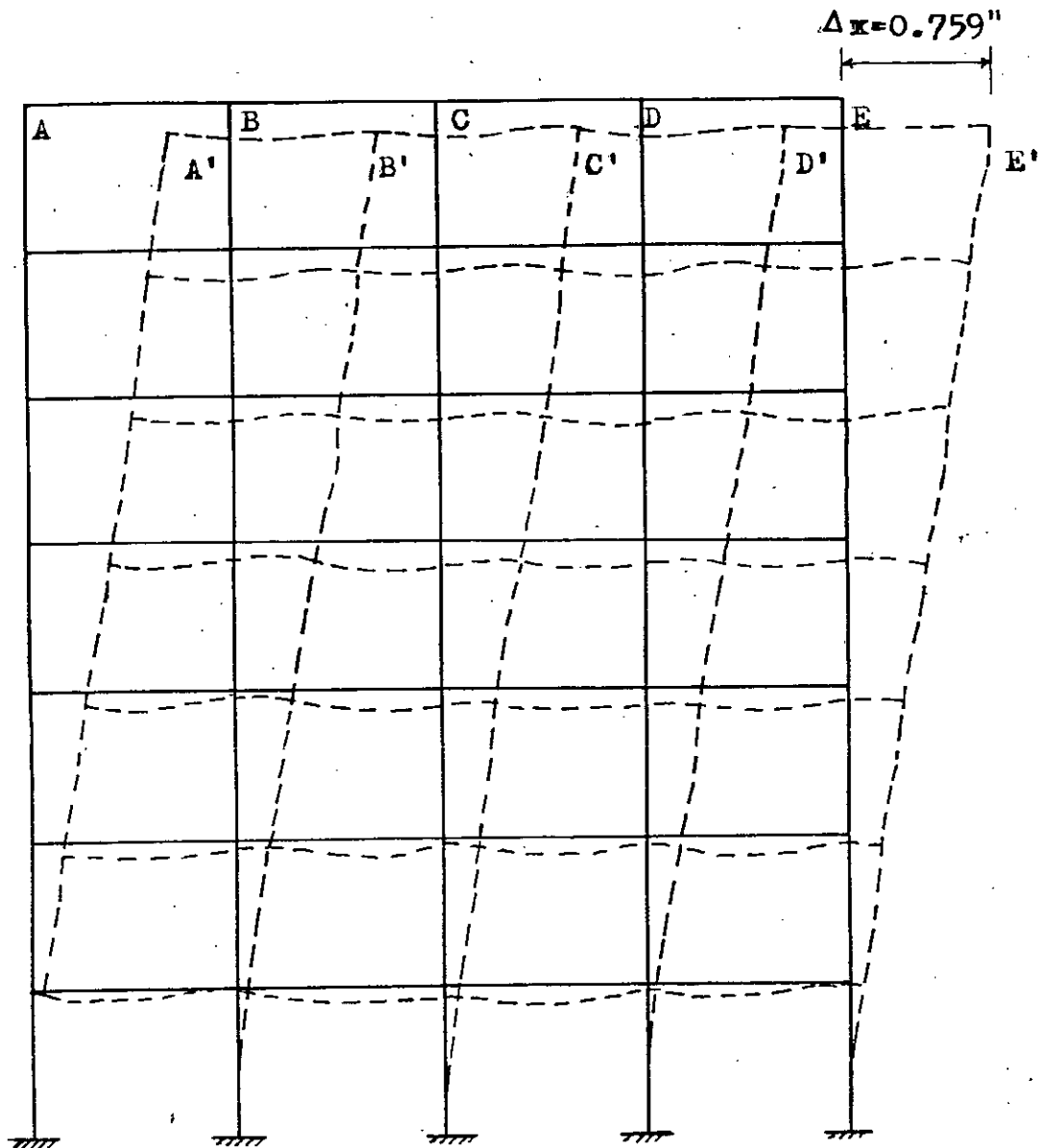
Geometry also as in case 4(a) except: batter of columns = 1:11
and Col. size: CR = 30", CQ = 18"

Fig. 5.21 x and z displacements for tower of case study 4(e). (Scale: 1"=1")

Case 4(c)

Loads as in case 4(a).

Geometry also as in case 4(a) except: batter of columns = 1:11
column size: CR = 18", CQ = 30".

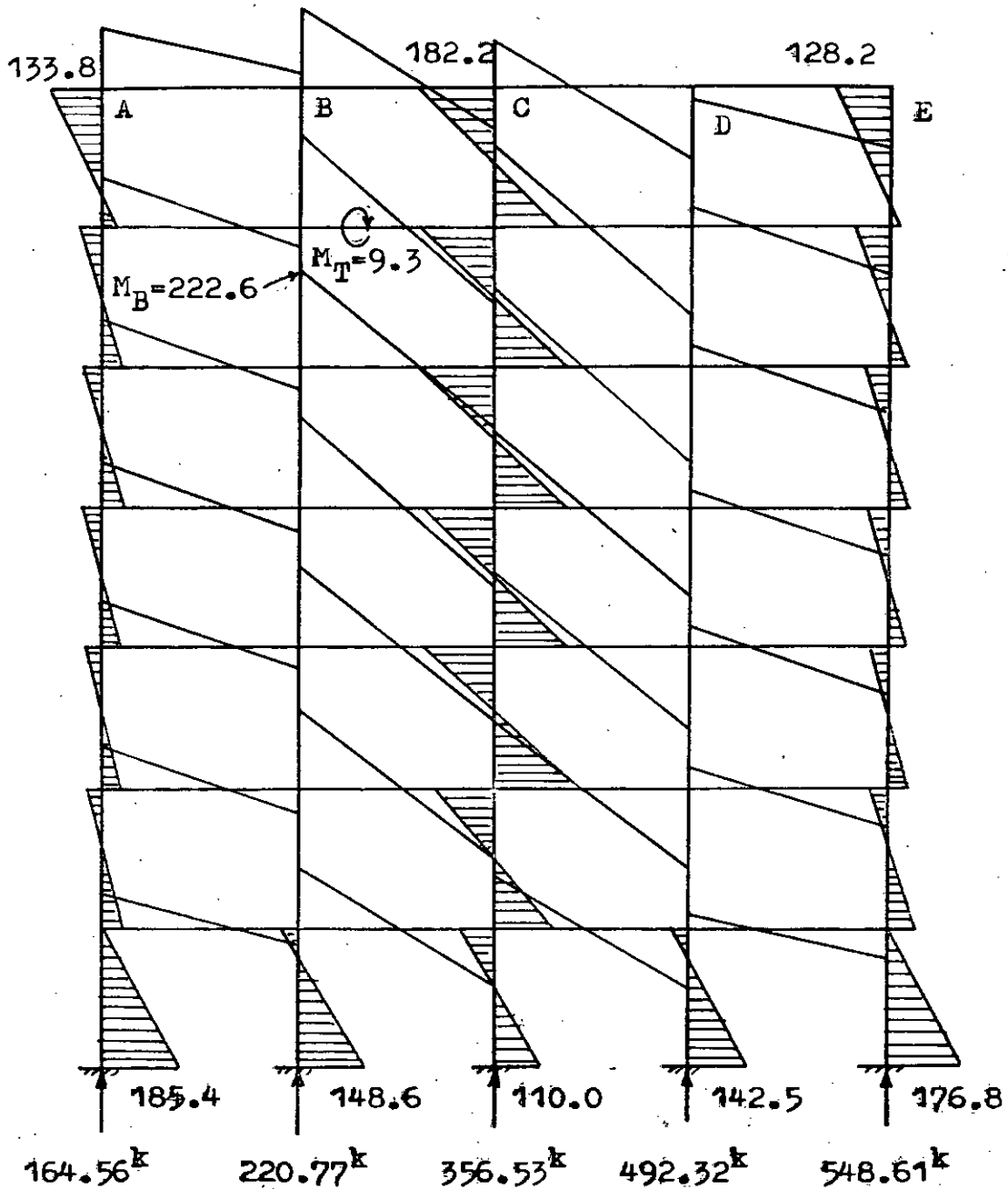


Fig. 5.22 Column moment M_y and bracing moment M_B

Scale: 1" = 416.67^k

Case 4(d)

Loads as in case 4(a)

Geometry also as in case 4(a) except: batter of columns = 1:11
and column size = 23.24" x 23.24"

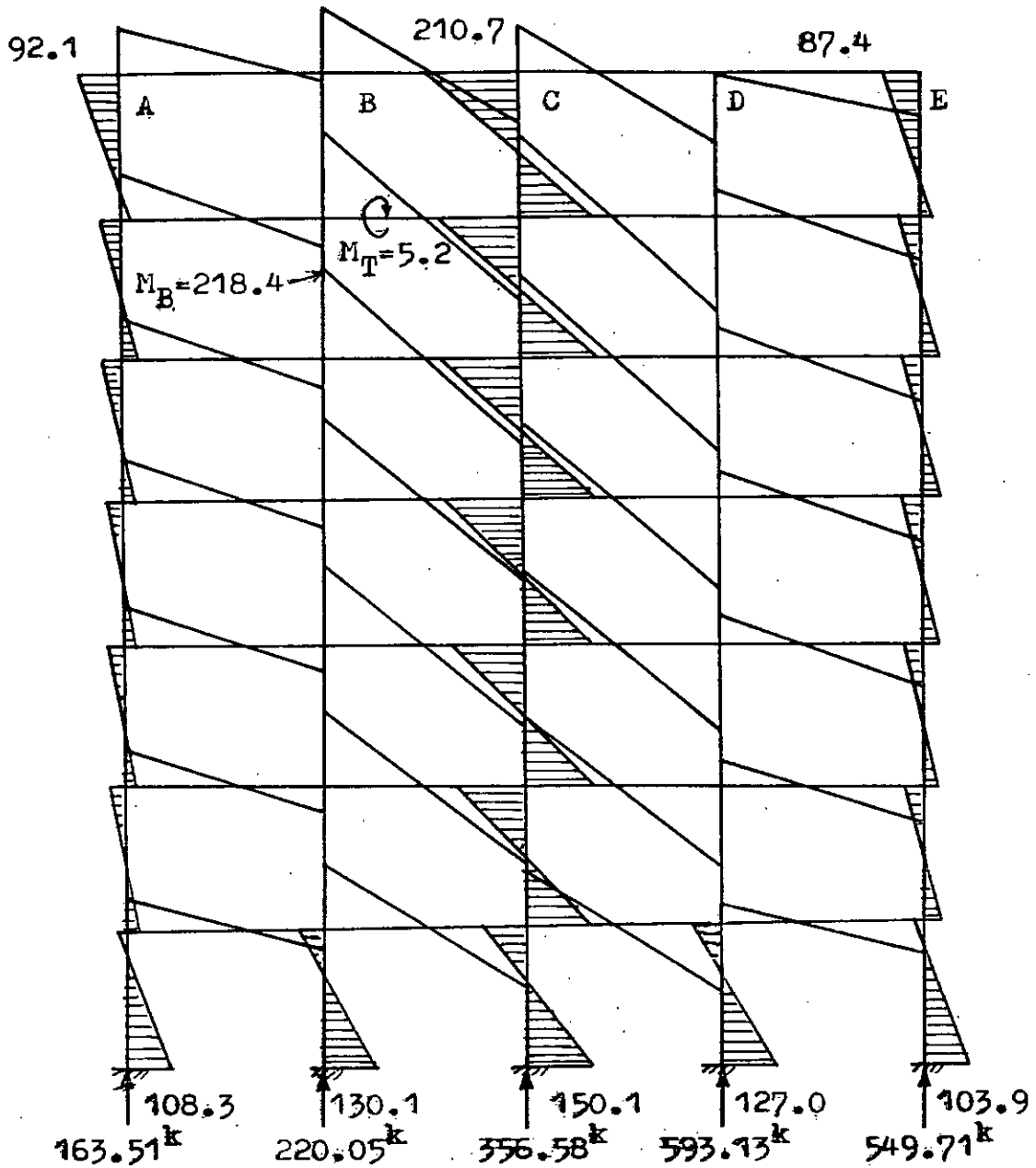


Fig. 5.23 Column moment M_y and bracing moment M_B .
Scale: 1" = 416.67 k'

Case 4(a)

Loads as in case 4(a)

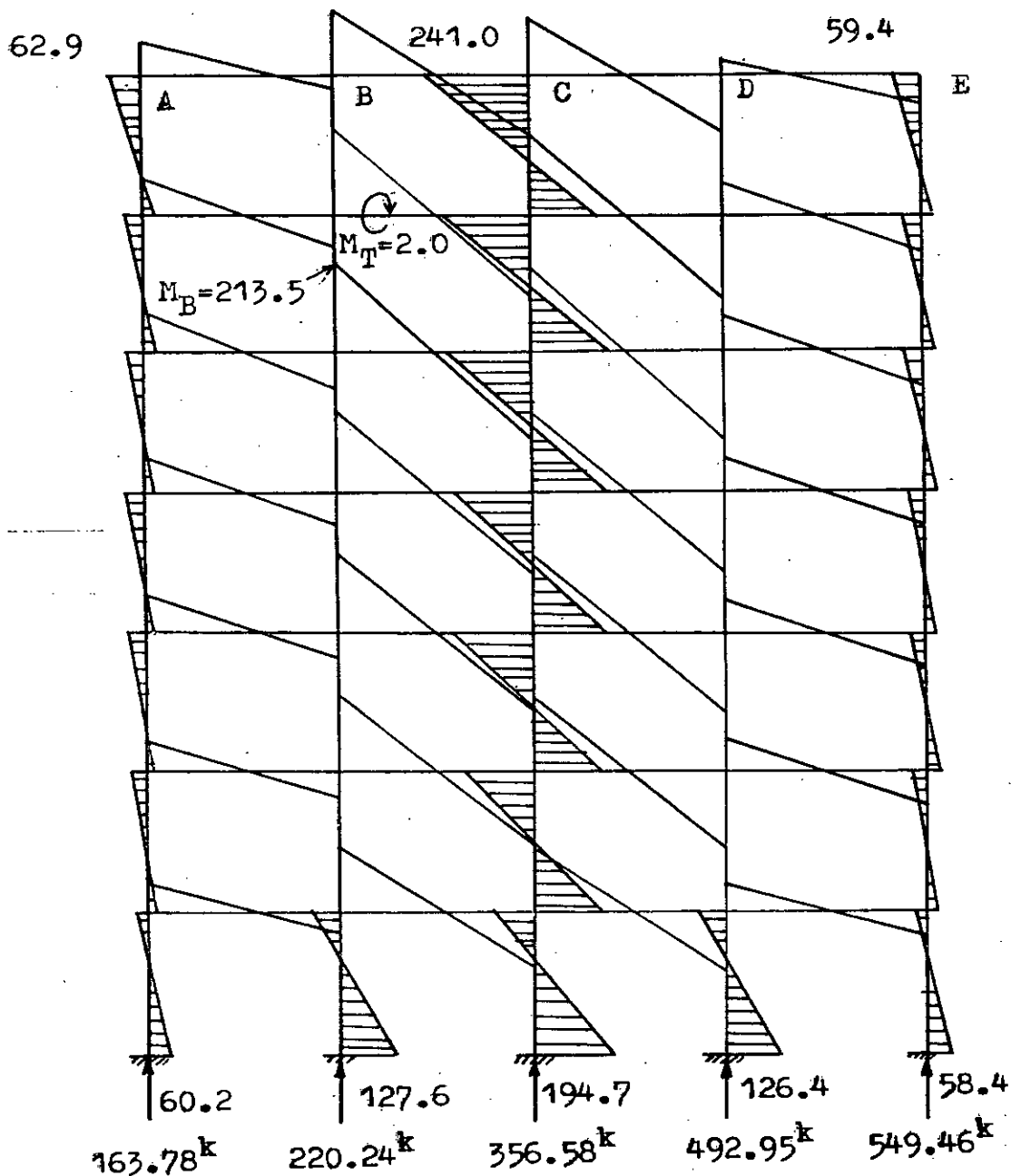
Geometry also as in case 4(a) except : batter of columns = 1:11
and column size = 30" x 18"

Fig. 5.24 Column moment M_y and bracing moment M_B .
Scale: 1" = 416.67k'

lying farthest away from the bending axis. As a result columns C & C' develop larger M_y than columns A or E. Therefore, it is quite logical that if the columns that develop larger M_y are provided with larger section modulus (S_y) or moment of inertia (I_y), the structure would withstand the load more effectively and undergo lesser deflection. The orientation of column section in case 4(e) conform with this requirement and hence the deflection Δ_x is least in this case. Fig. 5.22 shows that with the column orientation of case 4(c), the bending moments M_y at the base of columns A or E are very nearly equal to the bending moment (M_y) at the top of column C (or C'). But the moment of inertia I_y of column C (or C') is much less than that of column A (or E). If column A is just safe for a given M_y , then obviously column C will not be safe for the same M_y . Now taking into account the very fact that M_y for columns A and C are more or less equal, one may be tempted to provide a square section that would give the same I_y for both A & C as in Case 4(d). However, an inspection of column moments as portrayed in Fig. 5.23 for Case 4(d) unveils a new dimension of the problem. It is observed that the moment M_y in column C is now about twice as much as that in column A. This is not unexpected however. Because by making the columns square, the stiffness (about y-axis) of column C has been increased while that of column A has been decreased.

As a result column C now draws a larger share (about 15% more in this case) of the moment while column A draws

a smaller share compared to Case 4(c). Thus it is evident that square sections ($CQ=CR$) are more desirable than rectangular sections with $CQ > CR$. In fact it may be more rational to use a rectangular section with its longer side in the tangential direction ($CR > CQ$) as in case 4(e). This makes column C(or C') even stiffer (because of larger I_y) and hence it draws an even larger moment ($\approx 15\%$) as evident from Fig. 5.24. But considering the column moments in the three cases 4(c), 4(d) and 4(e) the orientation in Case 4(e) seems to be more reasonable than in the other two cases. As is obvious, however, an iterative process would have to be performed in order to arrive at the optimum ratio of CR to CQ that might result in the most economical design.

5.4.3 Batter of Columns

The effect of batter of columns on the column moments and forces may be noticed in Figs. 5.25, 5.23 and 5.26 {Cases 4(f), 4(d) and 4(g) respectively}. In these three cases, the column and bracing sections as well as the loads (at top) are the same. Only the inclination (or batter) of columns has been changed as follows:

Case	Inclination
4(f)	1.5:22
4(d)	2.0:22
4(g)	2.5:22

It is observed from the corresponding figures that, as the

Case 4(f)

Loads as in case 4(a)

Geometry also as in case 4(a) except: batter of columns = 1.5:22
 i.e. 1:14.67
 and column size = 23.24" x 23.24" .

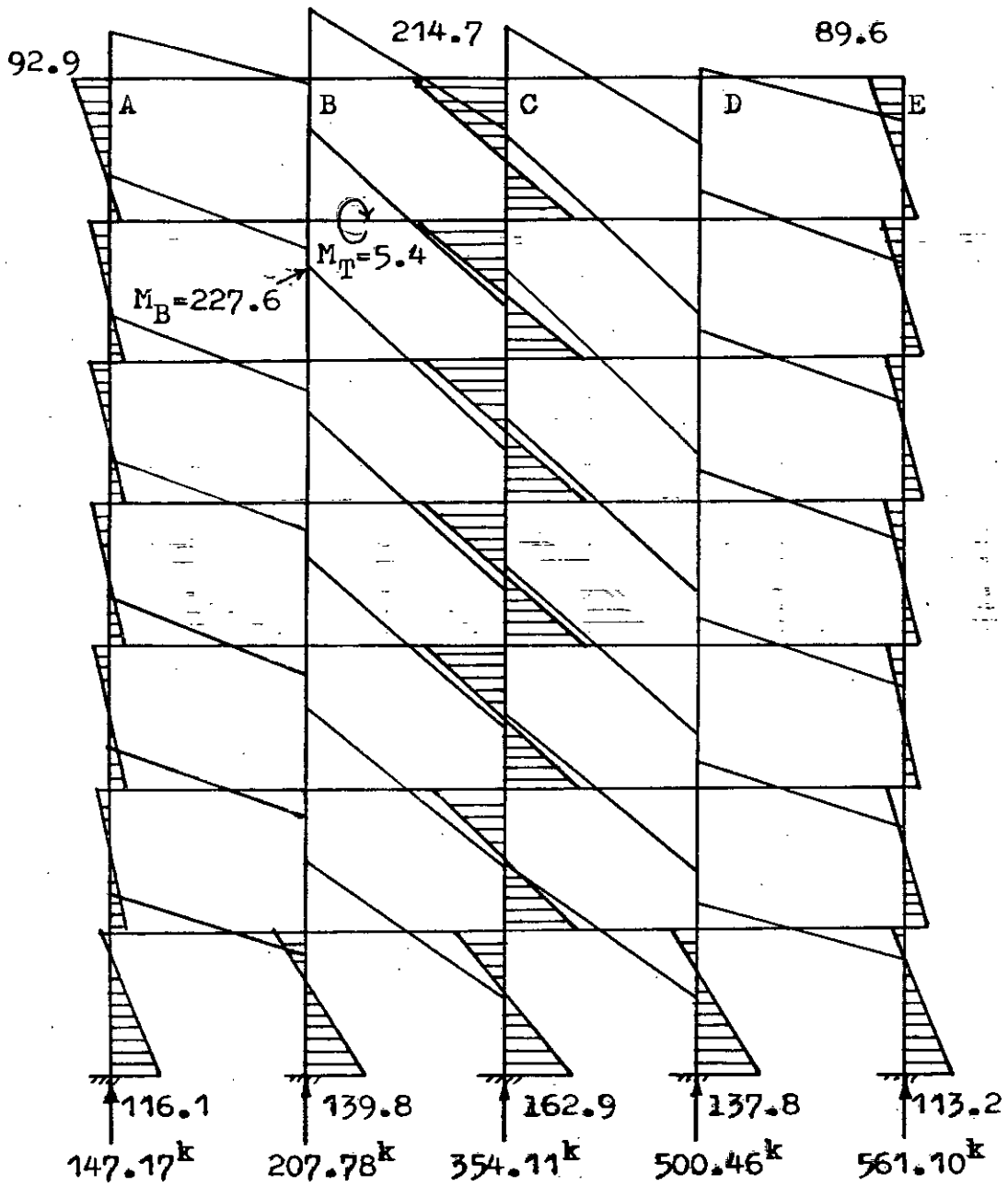


Fig. 5.25 Column moment M_y and bracing moment M_B .
 Scale: 1" = 416.67^{k'}

Case 4(g)

Loads as in case 4(a).

Column size = 23.24"x23.24"

Batter of columns = 2.5:22 i.e. 1:8.8

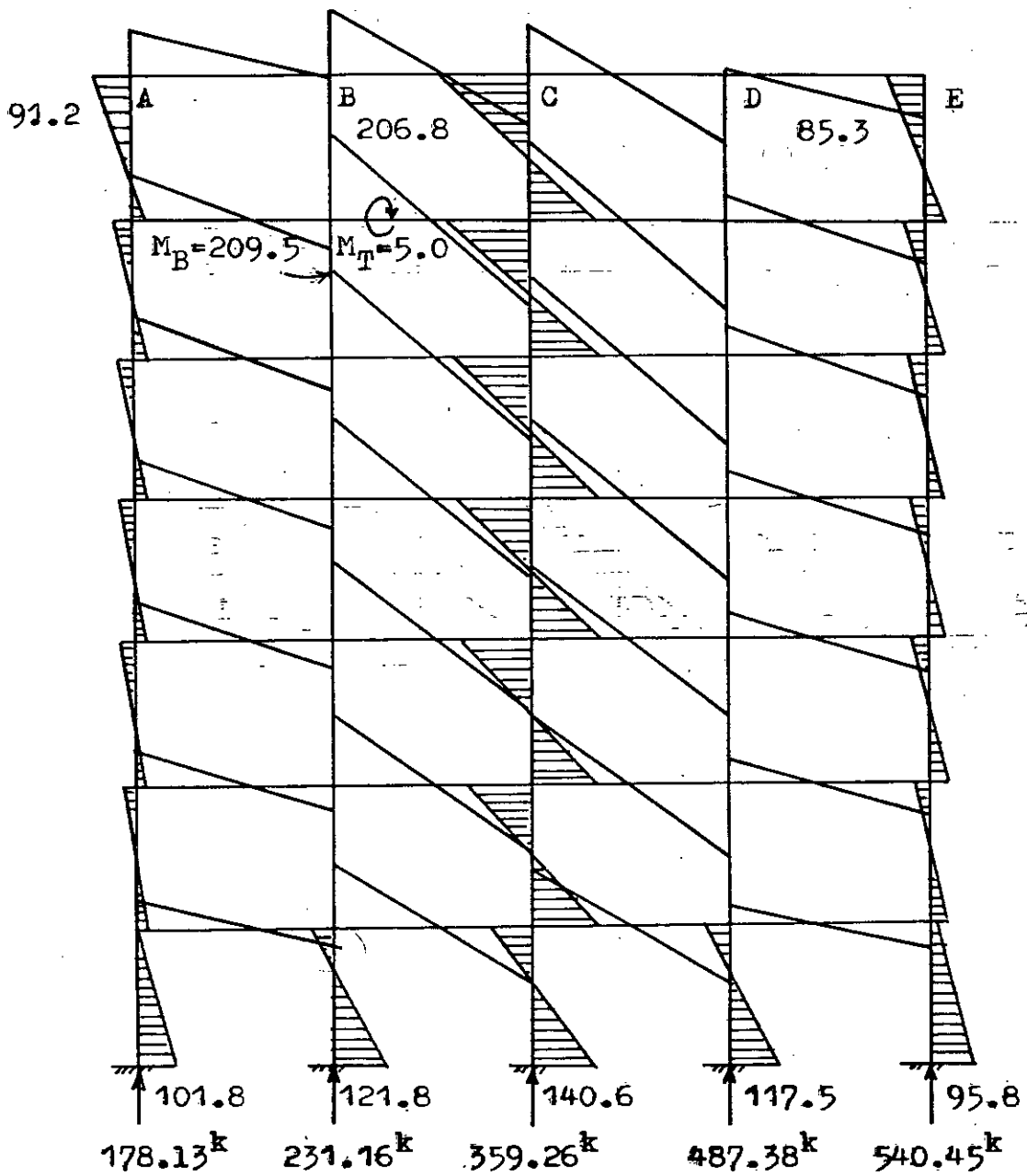
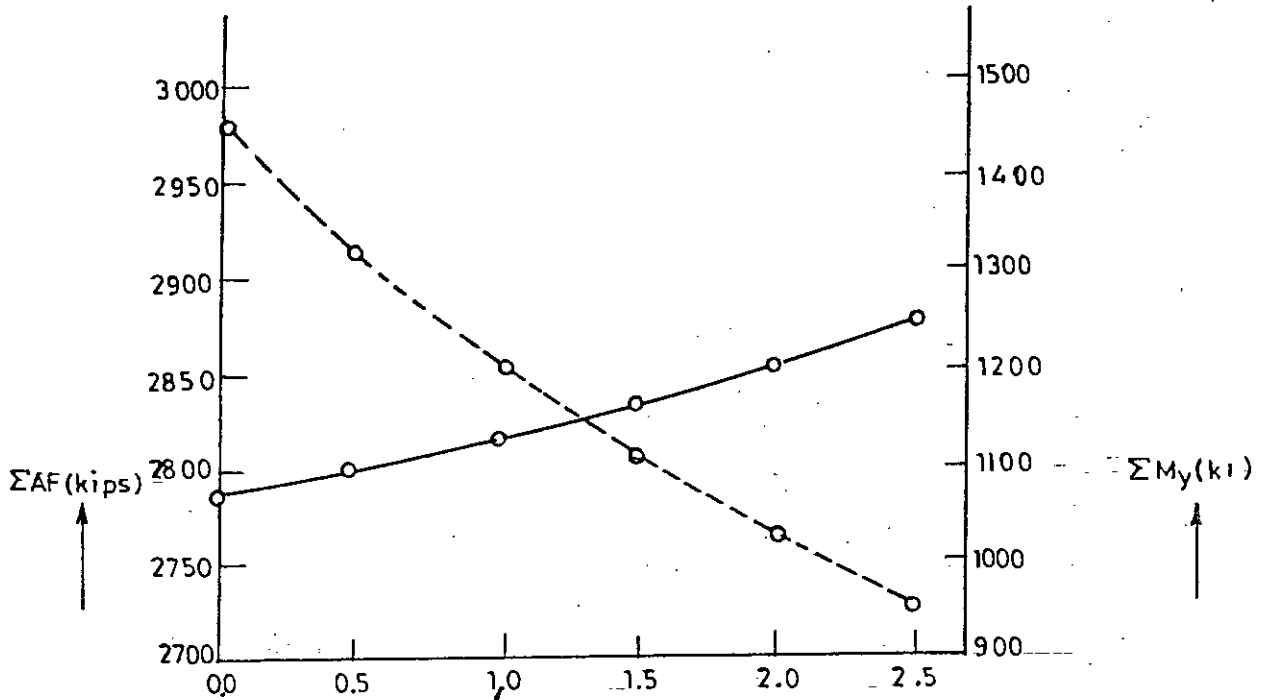


Fig. 5.26 Column moment M_y and bracing moment M_B
Scale: 1" = 416.67^k

batter of columns increases, the sum of the moments in the columns slowly decreases but the sum of the axial forces of the columns increases. This increase of axial force is due to the increased lengths of bracings and columns. It is therefore apparent that increasing the splay of columns beyond some optimum value would turn out to be uneconomical; because the gain attainable in the design of column section due to reduction of moment will be offset by the increased volume of material due to increased lengths of the bracings and columns. The increase in the lengths of the bracings due to the splay of columns may be quite considerable for tall towers. However, slight battering of columns (of the order of 1:15) are found to be economical, because with gradual increase of splay beginning from zero, the column moments at first decrease rapidly and then the trend gradually flattens down (Fig. 5.27). But it appears that the 1:11 inclination of the columns as used by BRTC is slightly excessive.

5.4.4 Stiffness of Braces

The effectiveness or for that matter the stiffness of the bracings is a factor of primary importance. The assumption that points of contraflexure occur at the mid-heights of column panels would be void if the bracings are not effective enough. It is observed from the moment diagrams that the performance of the bracings in case studies 1 and 3 is highly unsatisfactory as reflected in Figs. 5.9



→ Batter, x (as parts of 22 i.e. x:22)

----- = ΣM_y i.e. sum of moments at the bottom of all the columns.

———— = ΣAF i.e. sum of axial forces at the bottom of all the columns.

Fig. 5.27 Variation of ΣM_y and ΣAF with batter of columns.

(or 5.10) and 5.14, though in case study-2 the situation is slightly better (Fig. 5.12). In all the case studies it is, however, observed that the bracings are more effective for columns lying on or near the bending axis and far less effective for extreme windward and leeward columns.

It is, therefore, apparent that in order that the bracings may stand up to their purpose they must be made much more stiff than they have been in the above three cases. The required stiffness of the bracings would obviously be influenced by the stiffness of the columns; the stiffer the columns are, the stiffer must the bracings be. In case study-4 the bracings appear to be strong enough to stand up to their purpose as displayed in Figs. 5.17 or 5.18. It will be observed from these figures that due to desirable performance of the bracings the columns do develop points of contraflexure at about midheights of the panels excepting the bottom and topmost panels. It may be observed that in the bottom panel the points of contraflexure move upwards especially for the columns A & E. This is due to total fixity of the columns at the base and ineffectiveness of the bracings for columns A & E. Similar effect is observed in the uppermost panel due to high stiffness of the top bracing which is substituted for the bottom circular beam of the tank atop the columns. It is observed that the restraint moment M_y in columns A or E in top and bottom panels is about twice as much as

the end moments in the columns in other (intermediate) panels. In column C however the moment M_y remains almost the same from top panel to bottom panel.

CHAPTER 6

CONCLUSION

6.1 Findings from the Investigation

6.1.1 Introduction

The conventional methods of analysis of Intze tanks and the supporting towers differ so widely in their approach that designers find it difficult to determine which method is more rational and as such which one to follow. The differences between the various methods have been investigated, pointed out and reflected through appropriate case studies in the early stage (Chapter 2 and 3) of this researchwork. In the second phase the same problems as considered in the case studies have been analysed by sophisticated Finite Element programs using axi-symmetric shell elements for the tank itself and space frame elements for the supporting tower. The results of this computer analysis have been presented in Chapters 4 and 5 for the tank and the tower respectively. This investigation clearly indicates that the conventional methods often lead to uneconomical designs in certain respects and what may, in fact, be fatal, to unsafe designs in other respects. This would be clear when the findings of this research as summarised below are compared with the assumptions of the conventional methods. The conclusions arrived at on the basis of the computer analysis of the tank and the tower are presented in the following two articles.

6.1.2 Conclusions from the Analysis of the Tank

The conclusions stemming from the results of Finite Element analysis of the Intze tank are as follows:

(i) Membrane analysis holds good for the top and bottom domes except for a small peripheral ring (about one-fifth of the radius of the corresponding dome). This peripheral ring needs to be designed for bending moment in both top and bottom domes and for hoop tension in the top dome. Sometimes hoop tension may also develop in the peripheral ring of the bottom dome depending on the relative geometrical proportions of the cone and the bottom dome.

(ii) The hoop force in the top ring beam is about 30 to 40 percent of that obtained by conventional method.

(iii) The cylindrical wall is to be designed primarily for hoop tension which happens to be maximum at or near the bottom. Taking into account the variation of hoop force in the vertical direction, considerable saving of material can be achieved by making the section of the wall tapered towards the top. The bending moment in the wall remains so small that practically no flexural reinforcement is necessary except for the mild sagging moment at the base of the wall.

(iv) The design of the bottom ring beam by conventional method appears to be quite reasonable. The hoop force in this ring beam as calculated by conventional method is in fair agreement with that obtained by Finite Element analysis.

(v) The conical wall must be designed for both hoop tension and meridional moment. The hoop force is maximum at

the top and decreases almost linearly to a small positive or negative value at the lower end of the conical wall. Paradoxically, therefore, the conical wall may be made thinner towards the bottom as the hoop tension almost vanishes at the bottom. The thickness of the wall is in fact governed by hoop tension at the top end and meridional moment at the bottom end.

(vi) Finite Element analysis using axi-symmetric shell elements gives no idea about the stress conditions in the bottom circular beam; as such conventional methods may be followed for its analysis which appear to be quite conservative.

(vii) As regards the effect of wind load on the tank body it is observed that the stresses caused by wind are very small compared to those due to gravity or hydrostatic pressure. In view of the fact that 33% overstressing is allowed when the effect of wind is considered, the wind stresses may be neglected during design.

5.1.3 Conclusions from the Analysis of the Tower

The conclusions arrived at on the basis of the space frame analysis of the supporting tower are as follows:

(i) The bracings are most effective for columns lying on the bending axis and least effective for those lying on the extreme windward and leeward columns. The torsional resistance of the bracings is negligible.

(ii) Due to the above behaviour of the bracings the columns on the bending axis develop much larger moments than the extreme windward and leeward columns do. As such rectangular column sections with the longer side in the tangential direction are found to be more effective and economical.

(iii) For tall towers slight battering of columns (of the order 1:15) results in economy.

(iv) Effectiveness of the bracings is very essential to ensure that points of contraflexure in the columns occur at about the midheights of the panels between layers of bracings. The bracings are found to be more or less effective when the flexural stiffness of the bracing about horizontal axis of the section is nearly the same as that of the column about the radial axis of its section.

(v) Due to total fixity of the columns at the base, the point of contraflexure in the bottom panel tends to move upwards especially for the columns lying away from the bending axis. Similar effect is observed in the top panel as well where the point of contraflexure moves downward. This point must be borne in mind while designing the columns.

6.7 Scope for Further Research

This researchwork has been limited to the study of the stress conditions in the various parts of the Intze tank and the supporting tower. No effort could have been

made towards proportioning the component parts of the Intze tank for optimum design. Attempts may be made to develop charts/tables giving coefficients for calculating moment, hoop tension, meridional stress etc. in the component shells/ring beams. The height/diameter ratio of the cylindrical portion of the tank, depth and inclination of the conical wall, thickness of the various shells and size of the ring beams may be considered as parameters in developing such charts. As regards the supporting tower, it would be very useful if the bending moments in the columns about either axis could be related to the column sections and orientation, stiffness and spacing of bracings etc. giving empirical relations to aid designs without going for computer analysis.

REFERENCES

1. Gray, W.S., and Manning, G.P:
"Concrete Water Towers, Bunkers, Silos and other Elevated Structures", Concrete Publications Ltd. London, Fourth Edition (1964).
2. Jai Krishna and Jain, O.P.:
"Plain and Reinforced Concrete" Vol. 2, New Chand and Bros., Roorkee (1968).
3. Irons, B.M., and Ahmad, S:
"Techniques of Finite Elements"
Ellis Horwood Limited, a division of John Wiley & Sons, (1980).
4. Zienkiewicz, O.C.:
"The Finite Element Method",
McGraw-Hill Book Company (U.K.) Limited, Third Edition.
5. Ahmad, S.:
"Axi-symmetric Thick-Shell Element Program (Non-symmetric Loading)", Computer Program Report, Dept. of Civil Engg., University of Wales, Swansea, No. 22 (October 1969).
6. Rahman, A.:
"Program Developed for Analysis of General Space Frame Structures", Personal Communication.
7. Sushil Kumar:
"Treasure of R.C.C. Designs", Standard Book House, Dheli, Sixth Edition (1977).
8. Ramaswamy G.S.:
"Design and Construction of Concrete Shell Roofs", Tata-McGrawhill Publishing Company Ltd., New Delhi, TMH Edition (1971).
9. Jain O.P. and Sing, K.K.:
"Computer Analysis of Intze Tanks", The Indian Concrete Journal Vol. 51 (Aug. 1977).
10. Arya, A.S.:
"Data for Analysis and Design of Circular Shell Structures", Part 1 to 5. The Indian Concrete Journal, Vol. 42 (Aug. 1969), Vol. 44 (Jain. 1970, Feb. 1970, June 1970), Vol. 45, (Dec. 1971).
11. Singh, Prakash and Jain:
"Finite Element Analysis of Intze Tanks", Indian Concrete Journal.
12. BRTC (Bureau of Research, Testing and Consultation):
"A Departmental Report on the Design of an Intze Tank", Dept. of Civil Engg., BUET, (1982).
13. Ahmad S., Irons B.M. and Zienkiewicz, O.C.:
"Analysis of Thick and Thin Shell Structures by General Curved Elements with Special Reference to Arch Dams", Research Report No. C/R/99/69, Civil Engg., Dept., University of Wales, Swansea (1969).

